Louisiana State University
LSU Digital Commons

LSU Historical Dissertations and Theses | Graduate School

1989

The Evolution of Tertiary St. Croix.

Ivan Ponce Gill
Louisiana State University and Agricultural & Mechanical College

Follow this and additional works at: https://digitalcommons.lsu.edu/gradschool_disstheses

Recommended Citation
Gill, Ivan Ponce, "The Evolution of Tertiary St. Croix." (1989). *LSU Historical Dissertations and Theses*. 4844.
https://digitalcommons.lsu.edu/gradschool_disstheses/4844

This Dissertation is brought to you for free and open access by the Graduate School at LSU Digital Commons. It has been accepted for inclusion in LSU Historical Dissertations and Theses by an authorized administrator of LSU Digital Commons. For more information, please contact gradetd@lsu.edu.

INFORMATION TO USERS

The most advanced technology has been used to photograph and reproduce this manuscript from the microfilm master. UMI films the text directly from the original or copy submitted. Thus, some thesis and dissertation copies are in typewriter face, while others may be from any type of computer printer.

The quality of this reproduction is dependent upon the quality of the copy submitted. Broken or indistinct print, colored or poor quality illustrations and photographs, print bleedthrough, substandard margins, and improper alignment can adversely affect reproduction.

In the unlikely event that the author did not send UMI a complete manuscript and there are missing pages, these will be noted. Also, if unauthorized copyright material had to be removed, a note will indicate the deletion.

Oversize materials (e.g., maps, drawings, charts) are reproduced by sectioning the original, beginning at the upper left-hand corner and continuing from left to right in equal sections with small overlaps. Each original is also photographed in one exposure and is included in reduced form at the back of the book.

Photographs included in the original manuscript have been reproduced xerographically in this copy. Higher quality 6" x 9" black and white photographic prints are available for any photographs or illustrations appearing in this copy for an additional charge. Contact UMI directly to order.

U·M·I

University Microfilms International
A Bell & Howell Information Company
300 North Zeeb Road, Ann Arbor, MI 48106-1346 USA
313/761-4700 800/521-0600

Reproduced with permission of the copyright owner. Further reproduction prohibited without permission.

Reproduced with permission of the copyright owner. Further reproduction prohibited without permission.

Order Number 9025305

The evolution of tertiary St. Croix

Gill, Ivan Ponce, Ph.D.

The Louisiana State University and Agricultural and Mechanical Col., 1989

Copyright ©1990 by Gill, Ivan Ponce. All rights reserved.

U·M·I
300 N. Zeeb Rd.
Ann Arbor, MI 48106

Reproduced with permission of the copyright owner. Further reproduction prohibited without permission.

Reproduced with permission of the copyright owner. Further reproduction prohibited without permission.

The Evolution of Tertiary St. Croix

A Dissertation

Submitted to the Graduate Faculty of the Louisiana State University and Agricultural and Mechanical College in partial fulfillment of the requirements for the degree of Doctor of Philosophy

in

The Department of Geology and Geophysics

by
Ivan Gill

B.A., The University of Rochester, 1979
M.S., The University of Rochester, 1983
December, 1989

Reproduced with permission of the copyright owner. Further reproduction prohibited without permission.

ACKNOWLEDGEMENTS

Many people have assisted throughout the duration of this project, and I would like to express my gratitude for their help. Clyde Moore served as major advisor, and I appreciate his unstinting support, encouragement, field work and advice throughout a long tenure. Jeff Hanor served as minor advisor, and his teaching and guidance extend beyond geochemistry. The members of the committee have all supplied enthusiasm and expertise to a project that tapped many of their interests. Their critical discussions, support and encouragement throughout the project have been invaluable: Paul Aharon, Wim van den Bold, Dennis Hubbard, Lynton Land, Kam Liu, Dag Nummedal and Barun Sen Gupta. Paul Aharon has been generous with his time, equipment and advice in the stable isotope lab.

Dennis Hubbard has been a source of freely discussed ideas throughout the project, and has supported the project from its inception. Dave Eby is thanked for his encouragement and generous support throughout the project, and for his encouragement to start the project. Dick Koepnick and Mobil Research Lab supplied the strontium isotopic analyses that are central to the geochemical portion of the project, and freely discussed the results. The project would not have been possible without the interest and cooperation of Ken Eastman and Caribbean Drilling Services.

Numerous members of the faculty of the Geology Department have lent guidance: Gary Byerly, Rex Pilger, Joe Hazel, Jeff Nunn and Ajoy Baksi. Special thanks to Lui Chan for meticulous lab advice and isotopic discussions, to Mike Simms for the generous sharing of equipment and ideas, and to Tony Dickson for acute observations and patient teaching.

Reproduced with permission of the copyright owner. Further reproduction prohibited without permission.

Stan Frost, Don Thorstenson, Fernando Gomez and the San Juan Office of the U.S. Geological Survey and Barbara Lidz are thanked for their assistance at various stages of the project. Laboratory work would have been impossible without the competence of Wanda LaBlanc, Ron Snelling, Paul Carpenter and Feng Jiang Hua. Sam Reed single-handedly kept the rock labs going and produced numerous high quality thin sections.

Fellow grad students and colleagues at LSU are thanked for their help and humor. Art Saller and Jay Banner have been generous throughout with advice and guidance, and I thank them as well as Steve Moshier, Ezat Heydari, Brian and Kris Carter, Bo and Ellen Tye, Rick and Marilyn Huff, Rowdy Lemoine, Pete McLaughlin and Amitava Roy (the author of the Assymptotic Dissertation Model) for their friendship and help. The willingness of Pete McLaughlin to contribute time and expertise to the paleontological aspects was gratifying and produced a substantially better project.

Special thanks to Louis Nichols, Barbara Delaville, Cheri Weber, Marlene Moore and Faye Couvillon. I am grateful to the staff of the West Indies Laboratory for assistance throughout the field portion of the project. Numerous agencies on St. Croix lent invaluable cooperation and support: the Virgin Islands Planning Office, the Department of Public Works, the V.I. Water and Power Authority, the Martin Marietta Corporation, the Hess Oil Virgin Islands Corporation, the Office of the Tax Assessor, the Department of Natural Resources, the Coastal Zone Management Division, the Women's Coalition of St. Croix and the National Park Service. Many individuals have contributed as well: Tom Sedgewick, the Berg brothers, the late Martha Hubbard, Dan Hendrix, L. McGinnis, R. Bowen, O. Schuster, Y. Bordeaux, B. Carter, K. Carter, T. Poche, K. Myers, N. Martinez, T. and L. Gill, and many others whose contributions are greatly appreciated.

Reproduced with permission of the copyright owner. Further reproduction prohibited without permission.

Support for the project from SOHIO, Shell Oil, Chevron, Union Pacific, D. Eby, the American Association of Petroleum Geologists, the Geological Society of America, the Virgin Islands Water Resources Research Center, the Basin Research Institute and the Department of Geology and Geophysics is gratefully acknowledged. Fellowship support from the Louisiana State University Alumni Federation, the Department of Geology, and from the Applied Carbonate Research Program provided the freedom to do the research. Moon: wahine ilikea o ka mahinahina, mahalo.

Reproduced with permission of the copyright owner. Further reproduction prohibited without permission.

FOREWORD

In the last five centuries, St. Croix has witnessed a spectrum of humanity. It has been the home for the farming communities of the Arawaks, and later served as base for the warrior Caribs, migrating through the Antilles arc. Columbus landed here on his second voyage, and initiated European domination that was to last through the flags of seven nations.

St. Croix served as an agricultural locus of the slave-sugar-rum triangle that brought Africans to the sugar plantations, swelling the population and earning Danish St. Croix the nickname "Emerald of the Caribbean". Organized uprisings secured emancipation two decades before the American Civil War. Now, the lime ruins of plantations and windmills decay in the fields, and serve as witness to the dissipation of an era. But the roads and estates still owe their names and shapes to the surveyers and planters of the Danish Crown, and the right angle bends around estate corners are more suited to the donkey cart than the automobile.

The geological history is no less revealing. This study was initiated as a detailed look at dolomitization in localized Tertiary strata, perhaps part of a regional pattern of Caribbean dolomitization. It has since burst whatever topical constraints it had, and has spread into a study of the sedimentologic evolution of St. Croix. In part, this is a result of the samples brought back by the drilling project. Subsurface data showed that the existing story of Tertiary development needed modification. This dissertation looks at the development of St. Croix during the Neogene, with the intention of understanding the factors leading to St. Croix's present shape, location, and mineralogy.

Reproduced with permission of the copyright owner. Further reproduction prohibited without permission.

The dissertation is broken into three chapters that cover:

1) the biostratigraphy and microfauna of Neogene section of St.Croix;
2) the sedimentology and evolution of St. Croix in the Tertiary;
3) dolomitization and diagenesis as the final products of St. Croix development.

The first chapter attempts to tie together the biostatigraphic work on the outcrops with new subsurface data, as well as critically reviewing previous interpretations of St. Croix biostratigraphy. This chapter was written in collaboration with Peter McLaughlin and Wim van den Bold and serves as the biostratigraphic framework for the dissertation. Barun Sen Gupta and Dag Nummedal contributed numerous ideas and suggestions for improvements. It is Peter McLaughlin's and my intention to publish this chapter as a separate paper, with McLaughlin as the senior author.

The second chapter outlines the development of the Tertiary basin on St. Croix based on new subsurface data, and discusses the differences between this dissertation and previously published basin models. In addition, the second chapter evaluates present models of tectonic development in the northeastern Caribbean from the perspective of St. Croix geology. A number of the ideas in this section have been developed during discussions with Clyde Moore, Peter McLaughlin, Dag Nummedal and others. In particular, freely critical discussions with Dennis Hubbard over a period of several years produced and clarified many of the ideas presented here.

Because the sedimentary development and tectonic development of St. Croix are closely related, they are joined into a single article to share introductory material. Two sedimentological technical reports that served as way points in the subsurface study are

Reproduced with permission of the copyright owner. Further reproduction prohibited without permission.

cited, with the most important information revised and included in the text of the first and second sections. Drilling logs are contained in the Appendix.

The third and final chapter combines petrographic data, isotopic data, and hydrogeologic information in a study of St. Croix dolomitization. Groundwater geochemical information relevant to dolomitization is included in the third chapter. Additional information on St. Croix groundwater geochemistry is contained in a technical report released in 1986. Information in this report extends beyond material pertinent to dolomitization, and is cited in the dolomitization section. Paul Aharon, Jeff Hanor, Lynton Land and Clyde Moore all contributed ideas and critical reviews regarding dolomitization and groundwater geochemistry, but not all agree with the interpretations presented here.

Reproduced with permission of the copyright owner. Further reproduction prohibited without permission.

TABLE OF CONTENTS

Reproduced with permission of the copyright owner. Further reproduction prohibited without permission.

Reproduced with permission of the copyright owner. Further reproduction prohibited without permission.

Reproduced with permission of the copyright owner. Further reproduction prohibited without permission.

Reproduced with permission of the copyright owner. Further reproduction prohibited without permission.

Reproduced with permission of the copyright owner. Further reproduction prohibited without permission.

Reproduced with permission of the copyright owner. Further reproduction prohibited without permission.

Reproduced with permission of the copyright owner. Further reproduction prohibited without permission.

LIST OF TABLES

Reproduced with permission of the copyright owner. Further reproduction prohibited without permission.

Reproduced with permission of the copyright owner. Further reproduction prohibited without permission.

LIST OF FIGURES

Reproduced with permission of the copyright owner. Further reproduction prohibited without permission.

Chapter 3.

Reproduced with permission of the copyright owner. Further reproduction prohibited without permission.

Reproduced with permission of the copyright owner. Further reproduction prohibited without permission.

Reproduced with permission of the copyright owner. Further reproduction prohibited without permission.

Reproduced with permission of the copyright owner. Further reproduction prohibited without permission.

LIST OF PLATES

Chapter 1.

Reproduced with permission of the copyright owner. Further reproduction prohibited without permission.

ABSTRACT

St. Croix is a sedimentary island at the juncture of two northeastern Caribbean tectonic provinces. For this reason, the sedimentary development of St. Croix is of considerable importance to regional tectonic reconstruction. This dissertation utilizes evidence from outcrops and samples from an extensive drilling program on St. Croix, and addresses three major subjects: 1) the biostratigraphy and correlation of the Tertiary section, 2) the sedimentological and tectonic development of the Tertiary basin, and 3) the diagenesis and dolomitization of the St. Croix carbonates.

Previous models of the late Tertiary development of St. Croix presume a static, isolated land mass, with a self-contained sediment source. These models also suggest that parts of the lower Neogene carbonate section were deposited in shallow water. However, subsurface evidence requires significant modification of previous models of basin evolution on St. Croix.

Benthic-foraminiferal faunas collected during drilling suggest that the lower Neogene section of St. Croix was deposited at depths of 600 to 800 m; there is no indication that any part of the present basin was deposited in shallow water. Furthermore, the subsurface evidence indicates that portions of the Neogene section were deposited prior to graben formation, and that faulting began no earlier than the middle Miocene. Therefore, a sediment source external to the present structural basin is required to deposit the pre-graben strata. It appears likely that St. Croix has migrated and was uplifted in the late Neogene, with motion dominated by oblique left-lateral slip accompanied by block faulting.

The localized distribution of St. Croix dolomite suggests that dolomitization was restricted to a relict Tertiary lagoon. The isotopic composition of the dolomite is enriched in ^{18}O, and depleted in ^{87}Sr relative to unaltered Pliocene or younger seawater. In

Reproduced with permission of the copyright owner. Further reproduction prohibited without permission.

addition, the strontium isotopic composition is incompatible with the Pliocene age of the dolomitic host rock. In order to account for the geochemistry and geologic distribution of the dolomites I suggest that dolomitization took place from fluids that were produced from a mixture of evaporated seawater and groundwater similar to that on St. Croix today.

Reproduced with permission of the copyright owner. Further reproduction prohibited without permission.

CHAPTER 1

SURFACE AND SUBSURFACE BIOSTRATIGRAPHY OF THE ST. CROIX NEOGENE SECTION

Reproduced with permission of the copyright owner. Further reproduction prohibited without permission.

ABSTRACT

Planktonic foraminifera from four cored wells, two water wells, and three outcrop sections in the central plain of St. Croix permit the determination of a precise biostratigraphic zonation within the subsurface Tertiary sequence. In addition, these data allow the re-evaluation of the age and correlation of outcropping strata. This sequence is known to be at least 700 m (2300 ft) thick, and exhibits a clear upward-shoaling trend. Dark, planktonic foraminifera-rich marls of the subsurface Jealousy Formation, comprise the lower part of the sequence. The conformably overlying Kingshill Limestone is characterized by buff pelagic limestones and marls and shelf-derived sediment flows. Shallow-marine debris increases upsection, reflecting a transition from deep-marine to slope conditions. A disconformity separates the Kingshill Limestone from the stratigraphically higher, shallow-marine carbonates referred to here as the Mannings Bay Member of the Kingshill Limestone and the Blessing Formation. These units include a platform-slope facies rich in larger foraminifera and a reef-lagoon facies, respectively. Of the two, only the Mannings Bay Member contains enough planktonic foraminifera to be considered in this zonation.

The St. Croix Tertiary sequence extends from the lower Miocene to the uppermost Miocene or lower Pliocene. The lowest Jealousy Formation strata sampled are assigned to the lower Miocene *Praeorbulina glomerosa* zone. The boundary between the Jealousy Formation and the overlying Kingshill Limestone is diachronous, ranging from the *P. glomerosa* zone to the middle Miocene *Globorotalia fohsi fohsi* zone. Deposition of the Kingshill Limestone continued to near the Miocene - Pliocene boundary, with its uppermost strata placed in the upper part of the *Globorotalia humerosa* chronozone. The Mannings Bay Member is generally poor in planktonic

Reproduced with permission of the copyright owner. Further reproduction prohibited without permission.

foraminifera, with samples lying between the upper part of the *Globorotalia humerosa* chronozone and the top of the lower Pliocene *Globorotalia margaritae* zone.

Reproduced with permission of the copyright owner. Further reproduction prohibited without permission.

INTRODUCTION

St. Croix is located in the northeastern corner of the Caribbean Sea between the Greater Antilles and Lesser Antilles geologic provinces. It lies inside the northwestern edge of the Lesser Antilles arc, approximately 176 km southeast of San Juan, Puerto Rico (Fig. 1.1). The island is 39 km long, 9 km at its widest, and covers a total of 207 sq. km. St. Croix lies upon a nearly east-west oriented submarine platform that is separated from Puerto Rico and the Virgin Islands Platform by the Virgin Islands Basin and the Anegada Passage (Fig. 1.1).

Because St. Croix contains a thick, uninterupted Tertiary sequence, information on the geological development of St. Croix can provide important constraints on the timing and nature of the tectonic development of the northeastern Caribbean. In this context, the objectives of this paper are:

1) to outline the surface and subsurface Tertiary stratigraphy of St. Croix;
2) to constrain the age of the sedimentary sequence using planktonic foraminiferal biostratigraphy
3) to compare previous biostratigraphic work with the results from this project.

To date, stratigraphic work on St. Croix has been restricted primarily to outcrop (Vaughan, 1923; Gerhard and others, 1978; Lidz, 1982; Andreieff and others, 1986). These studies were limited by the difficulty in correlating between exposures, and the lack of subsurface data. Previous subsurface work has been based on well-cuttings taken in the 1930s, which suffer from a lack of depth control and from possible down-hole contamination. The samples have subsequently been lost and cannot be re-examined in light of modern taxonomic conventions.

Reproduced with permission of the copyright owner. Further reproduction prohibited without permission.

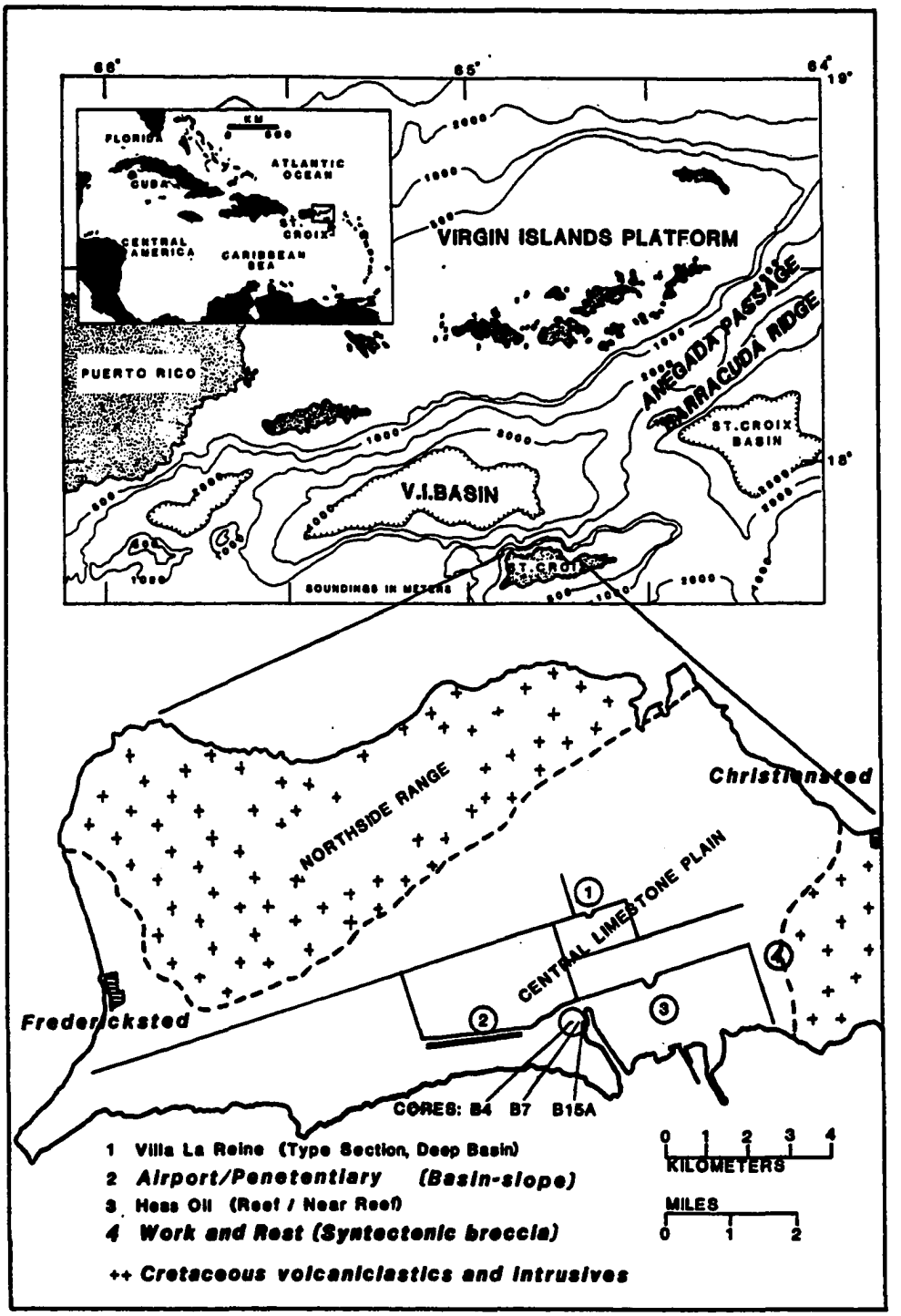

Figure 1.1. St. Croix: location map and study area.

Reproduced with permission of the copyright owner. Further reproduction prohibited without permission.

This paper adds new information to previous biostratigraphic work on St. Croix and extends the knowledge of lithostratigraphy and biostratigraphy into the subsurface. Our study of the planktonic foraminifera in drill samples from the central plain of the island allows a precise biostratigraphy to be established for the Jealousy Formation and the subsurface Kingshill Limestone.

Cores and split spoon samples were collected during a systematic drilling program around St. Croix, and provide contamination-free samples taken at well-controlled depths. Combined with outcrop samples, the core samples permit correlation across the breadth of the Tertiary section of St. Croix and allow a precise biostratigraphic framework to be established for the Jealousy Formation, the Kingshill Limestone, the Mannings Bay Member , and the Blessing Formation, (Fig. 1.2). A more precise depositional history of these units is important not only to the understanding of the development of St. Croix, but of the evolution of the northeastern Caribbean in the Neogene.

Reproduced with permission of the copyright owner. Further reproduction prohibited without permission.

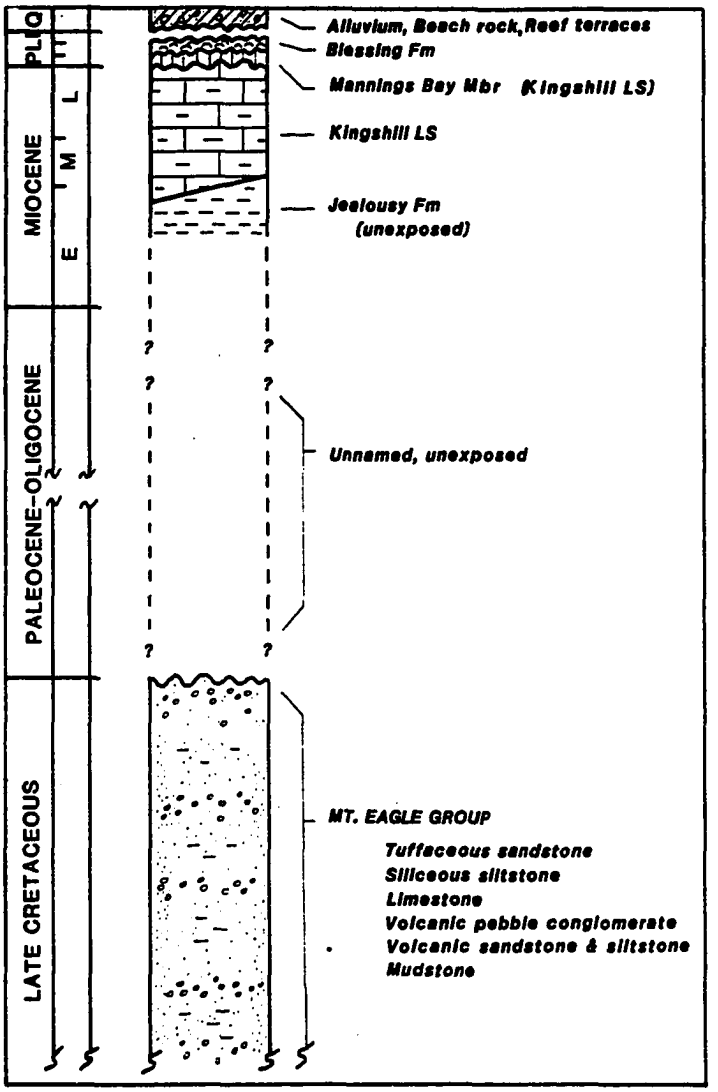

Figure 1.2. Generalized stratigraphic section for St. Croix.

Reproduced with permission of the copyright owner. Further reproduction prohibited without permission.

GEOLOGIC SETTING AND STRATIGRAPHY

St. Croix is dominated by a northeast-southwest trending graben structure that forms the central plain of the island (Gerhard and others, 1978; Whetten, 1966). The central graben is bounded by blocks that form the mountainous eastern and western ends of the island (Figs. 1.3 and 1.4a). These blocks are generally composed of well-lithified siliciclastic rocks of Cretaceous age, predominantly tuffaceous and volcaniclastic material deposited in basinal depths (Whetten, 1966). Mafic intrusives cut this sedimentary material at several points on the island, and have been dated by hornblende potassium-argon to range in the late Cretaceous from ca. 75 to 66 Ma (Speed and others, 1979).

The central graben is filled by alluvium and by Tertiary carbonate units, the interpreted age of which has ranged from the middle Oligocene (Vaughan, 1923) to early Pliocene (Lidz, 1982)(Fig. 1.2). The major carbonate units in the graben include:

1) upper Miocene to Pliocene reef, lagoon and bank carbonates at the top of the sequence that will be referred to here as the Mannings Bay Member of the Kingshill Limestone and the Blessing Formation. The Mannings Bay Member of this paper comprises the benthic foraminiferal wackestone and grainstone facies of the Kingshill Limestone as originally described by Gerhard and others (1978). These strata were included within the "post-Kingshill" limestones by Lidz (1982) and Andreieff (1986).
2) the Miocene Kingshill Limestone, a rhythmically bedded basinal unit composed of marls and limestones rich in planktonic foraminifera, alternating with flows of terrigenous and shelf-derived sediments.

Reproduced with permission of the copyright owner. Further reproduction prohibited without permission.

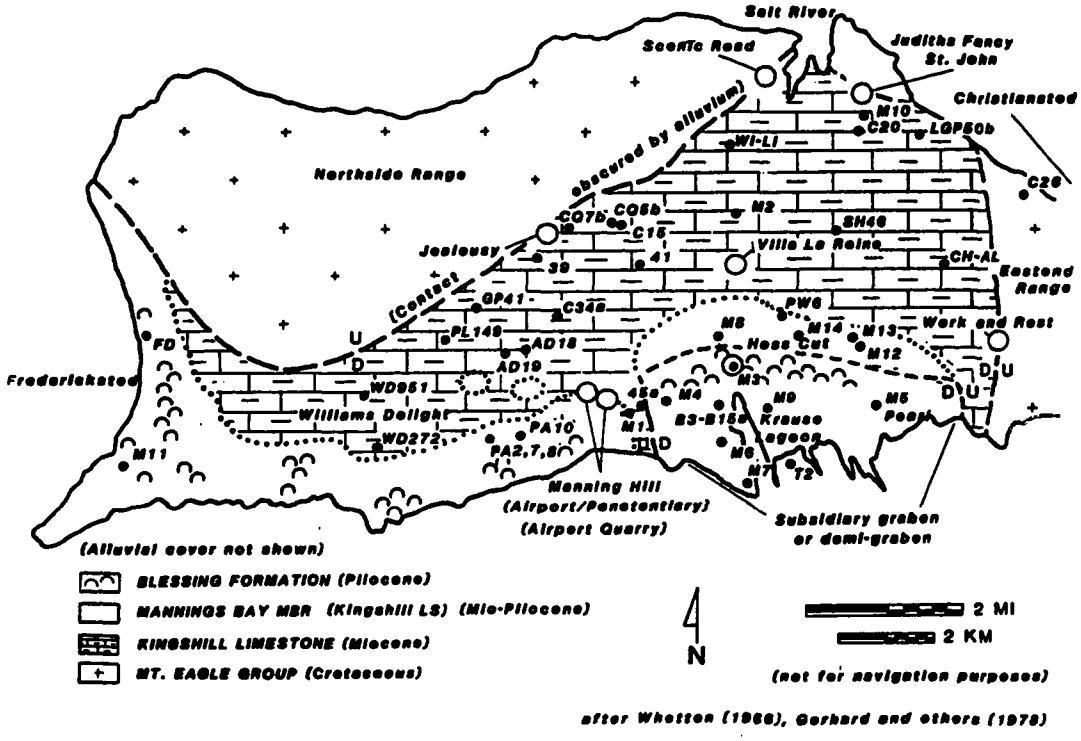

Figure 1.3. Generalized geologic map of St. Croix, with locations of test holes and stratigraphic sections. Kingshill Limestone/Mt. Eagle contact is well-exposed on the eastern graben boundary (Work and Rest) and poorly exposed along the northwestern boundary (Northside Range). The subsidiary graben in the southeastern portion of the central plain is well-defined by drilling only along its western border.

3) the Miocene Jealousy Formation, comprised of blue-grey marls rich in planktonic foraminifera. Deep drilling in the 1930s established the presence of a number of conglomeratic beds and thin layers of limestone at depth (Cederstrom, 1950).

The fault boundary along the eastern border of the graben is mappable at the surface (Fig. 1.3). Tertiary sediments along this border contain angular clasts of reworked terrigenous material, and dip more steeply than those found in the central basin (Gill and Hubbard, 1986, 1987). The western boundary of the basin is obscured by

Reproduced with permission of the copyright owner. Further reproduction prohibited without permission.

alluvium, except in the northern section in the Northside range where an abrupt, angular contact abuts against the Cretaceous rocks, and chaotic, steeply dipping beds are occasionally exposed (Gill and Hubbard, 1986). On the basis of this evidence, Gerhard and others (1978) suggested that the central graben could be "hinged" along the western boundary, with the largest fault displacement occurring in the southeast.

A subsidiary graben block within the main basin exists on the southern coast of the island (Figs. 1.3 and 1.4b), and contains Blessing Formation, Mannings Bay Member, and presumably Kingshill Limestone strata. The western fault boundary of this block is well-documented by drilling (Gill and Hubbard, 1986; 1987;), whereas the other boundaries remain speculative (Chapt. 2, this dissertation). Based on core data (Fig. 1.4b), the western boundary fault cuts through Pliocene material, with a minimum displacement of 50 m. If correlation to nearby outcrops is accurate, the fault displacement may approach 80 m (Gill and Hubbard, 1986). In either case, this data extends the timing of faulting in the St. Croix graben system at least into the Pliocene (Gill and Hubbard, 1986; 1987; Chapt. 2, this dissertation).

Reproduced with permission of the copyright owner. Further reproduction prohibited without permission.

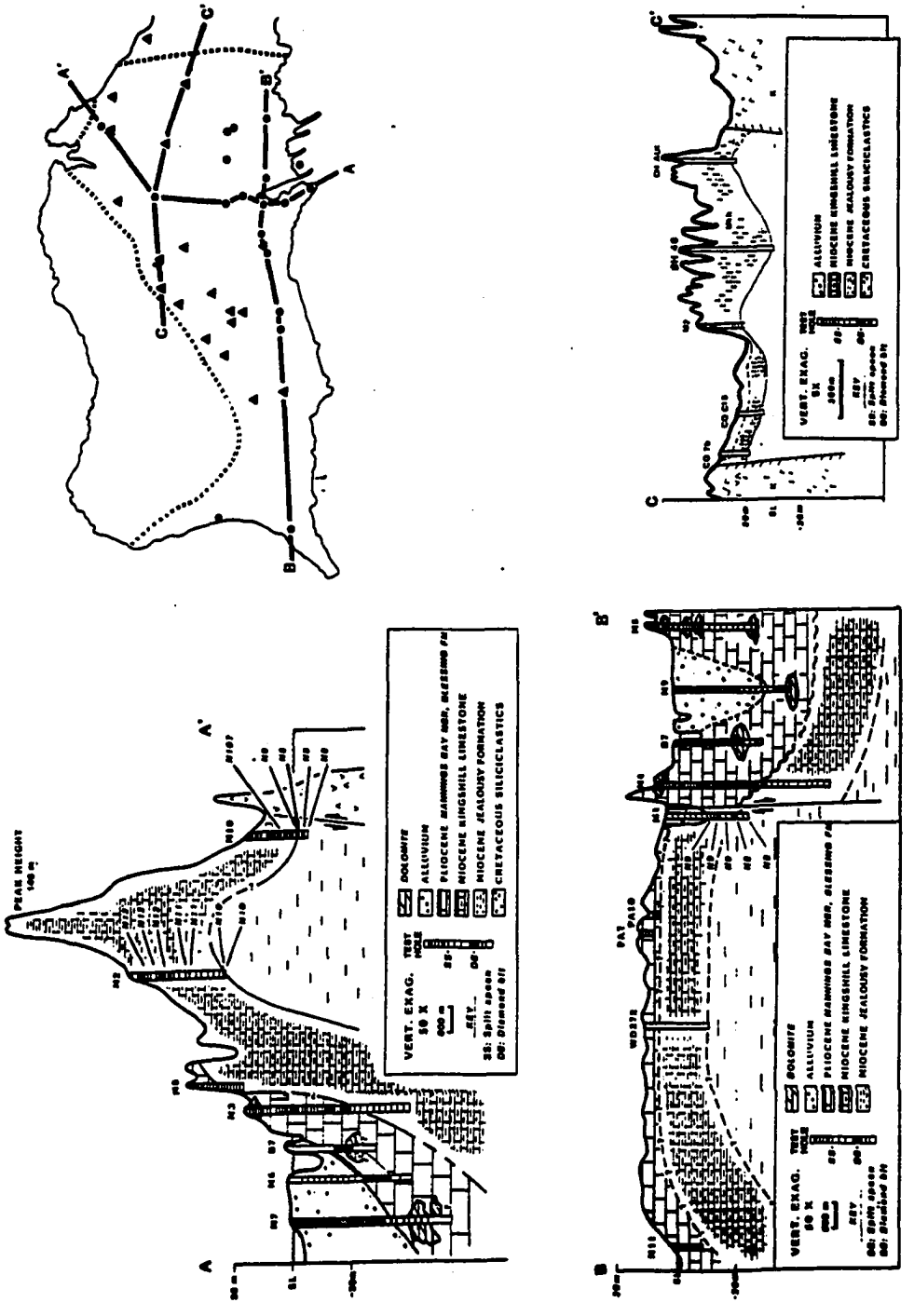

Figure 1.4. Generalized geologic cross sections of the Tertiary basin of St. Croix.

Reproduced with permission of the copyright owner. Further reproduction prohibited without permission.

PREVIOUS WORK

The first studies focussing on the stratigraphy and paleontology of the Tertiary strata of St. Croix were conducted by T.W. Vaughan in the early part of the century. Outcrops just east of Fredriksted (Fig. 1.1) were assigned a middle Oligocene age based on corals and larger foraminifera (Vaughan, 1923). Kemp (1926) included these and all other Tertiary strata on St. Croix in the "Kingshill Series".

Knowledge of the Tertiary sequence was expanded by subsurface drilling conducted by the Civilian Conservation Corps and the National Park Service between 1930 and 1950. In particular, Well 41, Well 39, and Well 45a (In Todd and Low, 1976, these are designated as Test Wells No. 1, No. 2, and No. 3, respectively) provided important data used in later refinement of stratigraphic nomenclature by Cederstrom (1950; see also Jordan, 1975). Blue clays with conglomeratic intercalations found in the deeper parts of several of the wells were named the Jealousy Formation, with a type section designated in Well 41. The benthic foraminifera in these wells were studied by Cushman (1946) and interpreted as Miocene faunas, with some Oligocene in the deepest part of well 41.

The name "Kingshill Marls" was applied to the stratigraphically higher buff limestones and marls. This name was formally changed to "Kingshill Limestone" by Gerhard and others (1978) in recognition of the varied lithology of the unit. Reef and shelf limestones overlying the Kingshill were studied by Behrens (1976), and are referred to here as the Blessing Formation.

Studies since 1950 have greatly refined the biostratigraphy of the St. Croix Tertiary sequence, but again have mostly focussed on data from outcrops (Table 1.1). Planktonic foraminifera have been studied by Bold (1970), Todd and Low (1976; subsurface), Multer and others (1977), Lidz (1982), and Andreieff and others (1986).

Reproduced with permission of the copyright owner. Further reproduction prohibited without permission.

Larger foraminifera were examined by T.W. Vaughan and F.G. Henbest for Cederstrom (1950) and by Andreieff and others (1986, 1987). Nannofossil determinations have been made by W.W. Hay for Multer and others (1977) and the biostratigraphic significance of the ostracode fauna was reported by Bold (1970).

Reproduced with permission of the copyright owner. Further reproduction prohibited without permission.

METHODS AND MATERIALS

Core material examined for this study was collected during a drilling program undertaken from 1984 to 1986 (Gill and Hubbard, 1986). The holes were drilled with a rotary rig capable of sampling to several hundred feet. Friable or unconsolidated sediments were sampled at five or ten foot intervals with a split-spoon sampler, and well-lithified material was collected with a diamond-bit core barrel. Samples were disaggregated by soaking in Calgon solution, washed in a 63 micron sieve, and the residue examined for microfossils. Well locations are shown in Figure 1.2.

Forty-four species or subspecies of planktonic foraminifera were recovered from samples of the Jealousy Formation and Kingshill Limestone (Table 1.2; Plates 1.1-1.3.) Biostratigraphic zones of Table 1.2 are based primarily on the zonation scheme and corresponding species ranges of Bolli and Saunders (1985). The nearest, but not necessarily equivalent, zones of Blow (1969, 1979) are given in parentheses based on the correlations provided by Bolli and Saunders (1985). Zone terminology conforms to the rules of the North American Stratigraphic Code, with biozones recognized only where the defining species-datum planes are noted (Table 1.3). Where defining datum planes are not evident, the biozone cannot be technically recognized, but the presence or absence of other stratigraphically useful species may suggest time-equivalence to the biozone. In this case the strata are referred to the biochronozone of the same name.

Discussion of the paleoenvironmental significance of the foraminifera concentrates mainly on the occurrences of seventeen types of benthic foraminifera of relatively well-understood bathymetric significance (Table 1.4). Their ranges within the well sections are used to resolve the paleobathymetry of the subsurface strata. Percentages, where cited, are based on sample counts of approximately 300 specimens.

Reproduced with permission of the copyright owner. Further reproduction prohibited without permission.

RESULTS

Jealousy Formation

The Jealousy Formation type section was formally defined by Cederstrom (1950) in Well 41, near Bethlehem and Fredensborg (Fig. 1.3). The description is as follows (p.19):

> "...1,398 ft of dark clayey strata lying below the Kingshill marl were penetrated, the lowest strata consists of 305 ft of gray clay in which a few streaks of limestone, not more than a few inches in thickness, are present. Five feet of calcareous conglomerate overlies the gray clay. The conglomerate is made up of rounded and subangular boulders of Mount Eagle volcanics (Cretaceous) in a limy matrix. Eighty-five feet of gray clay overlies the conglomerate, and above that 16 feet of calcareous conglomerate is present. A core of the conglomerate showed that soft clayey partings were present. Above the upper conglomerate stratum 987 feet of greenish gray clay is present. As in the deepest clay stratum, thin streaks of limestone are found, but in this stratum the limestone streaks do not occur throughout the thickness but are localized within a zone 293 to 387 feet from the bottom of the stratum."

The foraminifera in cuttings from this well and wells 39 and 45a were studied by Cushman (1946) and by Todd and Low (1976), but the samples have since been lost.. Apparently, the drilling program of Gill and Hubbard (1986) provides the only samples of the Jealousy Formation presently available for analysis.

Reproduced with permission of the copyright owner. Further reproduction prohibited without permission.

Lithostratigraphy

In all of the samples collected for this project, the Jealousy Formation is remarkably uniform, consisting of blue-grey foraminiferal marls. The Jealousy Formation was reached during drilling of wells M1, M2 and M10 (Figs. 1.3, 1.4). In addition, samples were taken from recently drilled water wells in Grove Place and Plessen, samples GP-41 and PL-149, respectively (Fig. 1.3).

In all cases during the drilling for this project, the Jealousy Formation was unconsolidated and was sampled below the water table. The lithofacies present in the well sections examined in this study are summarized in the Appendix. No bedding or grading of any sort was noted in the samples. The samples average 89 (+/- 5)% silt and clay size sediment, with the sand fraction of each sample dominantly composed of planktonic foraminiferal tests (89 +/-8%). Non-carbonate components ranged from 1 to 19 percent within the sand -size fraction.

The Jealousy Formation sediments underlie the Kingshill Limestone and alluvium throughout the central plain of St. Croix and exceed 450 m (1400 ft) in thickness (Cederstrom, 1950). Although the base of the Jealousy Formation has never been reached, Shurbet and others (1956) estimated a total thickness of over 1800 m (6000 ft) based on gravity surveys.

The contact between the Jealousy Formation and the underlying Cretaceous Mt. Eagle Series was noted by Cederstrom (1950) to have been reached in Well 39 close to the northwestern boundary of the basin near Jealousy (Fig. 1.3). The contact is unconformable and slopes south-southeastward at 33 degrees (Cederstrom, 1950; Whetten, 1966).

The contact between the Kingshill Limestone and the Jealousy Formation has not been observed in outcrop, and information on the contact is entirely from drilling. In core, the contact is abrupt and is used by local well drillers as an easily recognized

Reproduced with permission of the copyright owner. Further reproduction prohibited without permission.

stratigraphic marker. Furthermore, the Jealousy Formation / Kingshill Limestone contact is not planar, but shows considerable regional relief, bowing upward in the carbonate highlands and warping downward towards the coastlines (Fig. 1.4a).

Biostratigraphy

The biostratigraphy of the Jealousy Formation is based on the study of rich planktonic foraminiferal faunas. Strata studied range from upper lower Miocene to lower upper Miocene (Table 1.5).

Well M1.-- The Jealousy Formation in well M1 spans the lower Miocene / middle Miocene boundary. The lowest two core samples, 41.6 and 44.2 m (136.5 and 145 ft) are placed in the lower Miocene *Praeorbulina glomerosa* zone (N8) based on the co-occurrence of *Globigerinatella insueta* and *Praeorbulina glomerosa curva.* This is supported by the presence of *Clavatorella bermudezi, Praeorbulina sicana, Globigerinoides bisphaericus,* and *Sphaeroidinellopsis disjuncta* . The highest Jealousy Formation sample, at 38 m (125 ft), contains the first occurrences of *Orbulina universa* and primitive *Globorotalia fohsi peripheroacuta,* suggesting equivalence of these strata to the *Globorotalia fohsi peripheroronda* zone (N9). The lower Miocene / middle Miocene boundary is placed at approximately 10 ft (3 m) below the top of the Jealousy Formation.

Well M2.-- Well M2 penetrated only the uppermost 0.3 m (1 ft) of the Jealousy Formation, and the planktonic foraminifera present indicate the same zonal placement as the lower part of the overlying Kingshill Limestone, in the middle Miocene *G. fohsi fohsi* zone (N10). This determination is based on the presence of the nominative taxa of the zone and the position of this sample before the first-occurrence of *Globorotalia fohsi lobata* .

Reproduced with permission of the copyright owner. Further reproduction prohibited without permission.

Well M10.-- The three samples from Well M10 in the Jealousy Formation, from 26.5, 30.5, and 32.0 m (87, 100, and 105 ft), contain faunas indicating equivalence to the upper part of the lower Miocene *Praeorbulina glomerosa* zone (N8). This determination is based on the presence of *Praeorbulina glomerosa circularis* and *Orbulina suturalis* at the bottom of the interval and *Globigerinatella insueta* at the top. Also characteristic of the *Praeorbulina glomerosa* zone are the occurrences of *Praeorbulina sicana, P. transitoria,* and *Globigerinoides bisphaericus* in this interval.

Water wells.-- Samples of the Jealousy Formation from the bottom of two water wells, holes GP-41 and PL-149, yield upper lower Miocene planktonic foraminiferal faunas. The presence of *Globigerinatella insueta* and *Globigerinoides obliquus obliquus* and the absence of *Orbulina universa* in the base of GP-41 (32m / 105 ft) indicates equivalence to the *Praeorbulina glomerosa* zone (N8). Seven and one-half meters (25 ft) below the top of the Jealousy Formation in PL-149, a cutting sample from the bottom (24.4 m / 80 ft) contains planktonic foraminifera diagnostic of the upper part of the lower Miocene. The co-occurrence of *Praeorbulina glomerosa glomerosa* and *Globigerinatella insueta* places it in the *Praeorbulina glomerosa* zone (Table 1.3).

Ostracodes.-- The ostracode faunas from a number of upper Jealousy Formation corehole samples are lower and middle Miocene types and are clearly of deep-marine character (Table 1.4). These forms have been described from various parts of the Antilles, including the Montpelier Formation of Jamaica (Steineck, 1981), the Cipero Formation of Trinidad (Bold, 1972), and the Kingshill Limestone of St. Croix (Bold, 1970). The presence of *Krithe reversa* in the upper Jealousy strata suggests that this part of the formation was deposited in depths below 1000 m. Shallow-water species are

Reproduced with permission of the copyright owner. Further reproduction prohibited without permission.

completely absent in this interval. It should be noted that these forms suggest a totally different environment than those reported from outcropping "Jealousy" strata by Bold (1970). Those strata are now placed in the Kingshill Limestone, as will be discussed later in the paper.

Benthic foraminifera

The Jealousy Formation contains benthic foraminiferal species generally associated with both middle and upper bathyal environments. Four species present are suggestive of a middle bathyal setting: *Cibicides wuellerstorfi, Cibicides bradyi, Cibicides robertsonianus,* and *Osangularia culter. Cibicides wuellerstorfi,* which is most common at depths of 1000 m or more but found up to 500 m (Parker, 1954; Phleger, 1951), occurs in low percentages (0.4 to 2.4%) in several samples. *Osangularia culter* is an uncommon species in several Jealousy Formation samples and has an upper depth limit (UDL) of approximately 600 m in the Gulf of Mexico (Phleger, 1951). *Cibicides bradyi* and *Cibicides robertsonianus* are both also present and have occurrences below 450 m in the Gulf of Mexico (Pflum and Frerichs, 1976).

Pullenia bulloides and stilostomellids such as *Stilostomella* and *Siphonodosaria* are present in our samples from the Jealousy Formation. In modern studies, these forms are most abundant at middle to lower bathyal depths but range upward to above the top of the bathyal zone. *Pullenia bulloides* is rare, never comprising more than 0.5% of the fauna. Stilostomellids, typical of middle and lower bathyal depths (Bandy and Rodolfo, 1964; Begggren and Haq, 1976), are common in the lower Miocene of Wells M1, M10, and PL-149, comprising up to 17% of the fauna, but are less significant constituents (<1%) of the middle Miocene Jealousy Formation strata of Well M2.

Reproduced with permission of the copyright owner. Further reproduction prohibited without permission.

A number of species indicative of upper bathyal and greater depths are also present in the Jealousy Formation (Table 1.4): *Bulimina alazanensis, Cassidulina subglobosa, Cibicides renzi, Episominella sp. cf. E. exigua, Laticarinina pauperata, Oridorsalis umbonatus, Rectuvigerina multicostata,* and *Siphonina tenuicarinata.* All are uncommon in the samples, with the exception of *Cassidulina subglobosa* and *Epistominella sp. cf. E. exigua.* Pflum and Frerichs (1976) note that *E. exigua* increases in abundance below the top of the middle bathyal zone, reaching values of over 2%.

From this faunal data, the Jealousy Formation strata sampled in our drilling program reflect deposition in the upper part of the middle bathyal zone (600-800 m). The fauna is dominated by forms typical of upper bathyal and greater depths and includes several species not commonly found above the middle bathyal zone.

Kingshill Limestone

The Kingshill Limestone is characterized in outcrop by alternating beds of pelagic carbonates and sediment gravity flows of shallow-marine derived carbonate debris. The formation is exposed throughout the northern and central portions of St. Croix's central plain and is overlain on the southern and western coastlines by Pliocene Blessing Formation shallow-water facies (Fig. 1.3). Although the name "Kingshill" has been applied to these strata since early in this century (Kemp, 1926), the unit was not formally described until 1978 by Gerhard and others.

The Kingshill Limestone ranges up to 180 m (600 ft) in thickness (Cederstrom, 1950). The actual documented maximum thickness of the formation is closer to 140 m

Reproduced with permission of the copyright owner. Further reproduction prohibited without permission.

(450 ft) in the highland areas referred to by Cederstrom, but may approach or exceed this estimate in the southeastern areas where younger carbonates overlie it.

Lithostratigraphy

The Kingshill Limestone includes a variety of sedimentary facies. In the subsurface, the lower part of the formation is dominated by packstone, predominantly planktonic foraminifera-rich clays with lithic grains or pebbles occurring at some levels. Less common are lithic-pebble or foraminifera-rich wackestones (Table 1.7).

Outcrop lithofacies at the Kingshill Limestone type section at Villa La Reine are characterized as polymictic packstones (Gerhard and others, 1978), including beds of foraminiferal chalk, soft marly interbeds and debris flows of coral and terrigenous debris. The debris flow beds often have erosional bases and include cobble- to boulder-size clasts, primarily coral heads. In most cases, the corals are well-cemented and replaced by calcite, but may still be recognized by morphologic type and in some cases to the genus and species level.

A section at Estate Work and Rest (Fig. 1.3), approximately 5 km (3 mi) to the east, displays similar lithologies (Gerhard and others, 1978). Interbedded with the foraminifera-rich beds, however, are beds composed predominantly of terrigenous breccia presumably derived from Cretaceous Mt. Eagle Series rock.

The stratigraphically highest Kingshill Limestone strata studied are exposed in the Airport/Penetentiary section along the Melvin Evans Highway (Fig. 1.3) The outcrop can be divided into two parts, separated by a disconformity. The lower part, characterized by regularly bedded intercalations of softer, planktonic foram-rich beds and more indurated shelf-derived debris beds. The upper part of the outcrop is characterized by channelled beds of shelf-derived carbonate debris, including sediment flows of larger foraminifera interbedded with softer beds containing poorly preserved

Reproduced with permission of the copyright owner. Further reproduction prohibited without permission.

planktonic foraminifera (foraminiferal wackestone facies of Gerhard and others, 1978). The upper part of the outcrop, above the disconformity was included in the "post-Kingshill" limestones by Lidz (1982) and Andreieff and others (1986) but was included in the Kingshill Limestone by Gerhard and others (1978). It is discussed later in this chapter, and in Chapter 2, as the Mannings Bay Member of the Kingshill Limestone.

The contact between the lower Kingshill Limestone and the Mannings Bay Member is distinct in outcrop, but difficult to locate in cores (Gill and Hubbard 1986; 1987). The lower contact between the Kingshill Limestone and the Jealousy Formation is abrupt, distinguished by a marked color change from a buff limestone in the former, to blue-grey in the latter. However, the Kingshill Limestone and the Jealousy Formation are indistinguishable on the basis of textural characteristics and bulk x-ray diffractograms (Chapt. 2, this dissertation).

Biostratigraphy

Planktonic foraminifera are abundant and well-preserved in core samples from the lower Kingshill Limestone, and permit clear biostratigraphic assignment (Table 1.5). Outcrop samples in the upper part of the formation contain less-rich, less-well preserved faunas, but are nevertheless useful. The lower Kingshill Limestone extends from the upper part of the lower Miocene *Praeorbulina glomerosa* zone to the upper part of the upper Miocene *Globorotalia humerosa* chronozone.

Well M1.-- The Kingshill Limestone section in Well M1 is placed in the lower middle Miocene. Samples at 32.0 and 35.1 m (105 and 115 ft), contain *Orbulina universa* and primitive *Globorotalia fohsi peripheroacuta,* suggesting stratigraphic placement in the *Globorotalia fohsi peripheroronda* zone (N9).

Reproduced with permission of the copyright owner. Further reproduction prohibited without permission.

Well M2.-- An upcore transition from *Globorotalia fohsi fohsi* to *G. fohsi robusta* indicates a middle Miocene age for the samples in well M2 (Table 1.5). Three intervals are recognized:

1) *Globorotalia fohsi fohsi* zone (N10), from the base of the Kingshill Limestone (50.7 m / 166.5 ft) to 50.3 m (165 ft), where the first occurrence of *G. fohsi praefohsi* is noted;

2) *Globorotalia fohsi lobata* zone (N11), from the first occurrence of the nominative taxon at 30.9 m (101.5 ft) to 21.8 m (71.5 ft);

3) lower part of the *Globorotalia fohsi robusta* zone (N12), from the first occurrence of the nominative taxon at 11.3 m (37 ft) to the highest fossiliferous sample (3.4 m / 11 ft), with *Globorotalia menardii* absent.

Reworked specimens are mixed in with younger forms in several of the samples. At 36.5, 37, and 75 feet (11.1, 11.3, 22.9 m) in the cores, more primitive forms of *Globorotalia fohsi* are present (*G. f. fohsi, G. f. peripheroacuta,* and *G. f. peripheroronda,* respectively) in later middle Miocene samples. These suggest that, during middle middle Miocene times, submarine erosion reworked lower middle Miocene pelagic sediments.

Well M10.-- The Kingshill Limestone section in Well M10 spans the lower Miocene / middle Miocene boundary. The lowest sample, from 26.5 m (87 ft), contains a fauna characteristic of the *Praeorbulina glomerosa* zone (N8). Stratigraphically important species present include *Praeorbulina glomerosa curva* and *Globigerinatella insueta.* The upper part of the well section is placed in the middle Miocene *Globorotalia fohsi peripheroronda* zone (N9) based on the first occurrences of *Orbulina universa* and

Reproduced with permission of the copyright owner. Further reproduction prohibited without permission.

Globorotalia peripheroacuta at 24.7 m (81 ft) and the absence of species of *Praeorbulina.*

Ostracodes.-- Twelve shallow-marine ostracode species occur in the lower part of the Kingshill Limestone , 6 of which are also found in the "Jealousy" conglomerate (Table 1.7). The similarities between the lower Kingshill and the exposed "Jealousy" conglomerate are discussed in a later section, and suggest that some of the lower Kingshill sediments are redeposited. The absence of *Loxoconcha runa* in the lower Kingshill (latest occurrence in N9) supports the planktonic foraminiferal assignment of these strata to Blow's zone N10-N12.

Kingshill Limestone type section, Villa La Reine. -- Five samples from the Villa la Reine outcrop (Fig. 1.3) yielded rich, middle Miocene planktonic foraminiferal faunas. Large *Orbulina universa* and *Globoquadrina altispira* are especially conspicuous in the samples, with *Globigerinoides trilobus* subspp. and *Globigerinoides obliquus obliquus* also abundant. *Globorotalia mayeri* is present in two samples in the.section (D and H, Table 1.5) and *Globorotalia menardii* is present throughout the section. These occurrences, combined with the absence of *Globorotalia acostaensis* (pre-appearance), indicate that this section belongs in the *Globorotalia mayeri* zone (N14), possibly extending into the *Globorotalia menardii* zone (N15) towards the top.

Estate Work and Rest section..-- Poor preservation of planktonic foraminifera the outcrop at Estate Work and Rest (Fig. 1.3) makes zonal placement of this part of the section imprecise. *Globigerina nepenthes* is evident in the one usable sample recovered, indicating a position in the middle Miocene *Globorotalia mayeri* zone

Reproduced with permission of the copyright owner. Further reproduction prohibited without permission.

(N14) or higher. The presence of *Sphaeroidinellopsis multiloba* is evidence for an upper limit at the top of the *Globorotalia acostaensis* zone (N16). The lack of *Globorotalia mayeri* and of *Globorotalia acostaensis* suggest placement in the *Globorotalia menardii* zone (N15), but this placement is tentative due to possible diagenetic control on absences in this poorly preserved sample.

Airport/Penetentiary section.-- A disconformity in the Airport/Penetentiary section (Fig. 1.3) separates distinctly bedded Kingshill Limestone in the lower part of the outcrop from less evenly bedded Mannings Bay member in the upper part of the outcrop. Planktonic foraminifera identified in our study indicate that this section spans, or lies just under, the Miocene/Pliocene boundary:

1) below the disconformity, in lithologies corresponding to lower Kingshill Limestone, the planktonic foraminiferal fauna corresponds to the upper part of the upper Miocene *Globorotalia humerosa* zone (upper N17);
2) above the disconformity in the Mannings Bay member, the planktonic foraminifera suggest a stratigraphic position in the upper part of the *Globorotalia humerosa* chronozone (upper N17) or in the lower Pliocene *Globorotalia margaritae* chronozone (N18 or 19).

The uppermost Miocene placement of the Kingshill Limestone interval is based on the presence of the zonal marker *Globorotalia humerosa* and of *Candeina nitida*, and on the lack of Pliocene marker species such as *Globorotalia margaritae* and *Sphaeroidinella dehiscens*. Several lines of evidence suggest that these absences are of biostratigraphic rather than ecologic or diagenetic significance: the planktonic foraminiferal fauna is rich and diverse, including both shallow-dwelling forms, such as *Globigerinoides*, and deep-dwelling forms, such as *Globorotalia* and *Sphaeroidinellopsis* (Bé, 1977; Keller,

Reproduced with permission of the copyright owner. Further reproduction prohibited without permission.

1985); and preservation of the fauna is good to fair, indicating only minor diagenetic effects.

Benthic foraminifera

The benthic foraminiferal faunas of the Kingshill Limestone in Wells M1, M2, and M10 differ little from those of the underlying Jealousy Formation. *Melonis pompilioides* and *Sphaeroidina bulloides* are found in the Kingshill Limestone but have not been noted in the underlying Jealousy strata. *Cibicides robertsonianus* and *Cibicides renzi* are present in the Jealousy Formation but are absent in the Kingshill Limestone samples. These minor faunal differences do not reflect any significant environmental shifts from the setting of the Jealousy Formation. *Melonis pompilioides* was probably most typical of upper bathyal settings in the Miocene (Hasegawa, 1984), and *Sphaeroidina bulloides* is most common at middle and upper bathyal depths (Morkhoven and others, 1986). Therefore, the Kingshill Limestone sampled in this study appear to have been deposited in the upper part of the middle bathyal zone (Table 1.4).

Reproduced with permission of the copyright owner. Further reproduction prohibited without permission.

The Mannings Bay Member and the Blessing Formation

The Mannings Bay member and Blessing Formation strata unconformably overlie the Kingshill Limestone proper, and represent shallower carbonate depositional environments. They constitute reef, lagoon, and shallow-marine carbonate facies that extend from the southern coastline of the central plain to the western coastline of the island. The greatest thickness of Mannings Bay and Blessing Formation accumulation is preserved in a subsidiary graben block on the south-central coastline, where total thickness may exceed 91.5 m (Gill and Hubbard, 1986).

Lithostratigraphy

Planktonic foraminiferal strata of the Mannings Bay member were studied above the unconformity at the Airport/Penetentiary cut and in Well M4. The strata at the Airport/Penetentiary section are characterized by discontinuous, irregular beds of shelf-derived carbonate debris, with thin intercalations of softer planktonic foraminiferal deposits. Most notable in these deposits are sediment flows of the larger foraminifera *Operculinoides* and *Paraspiroclypeus* (Andreieff and others, 1986; Andreieff and others, 1987; Gerhard and others, 1978). The Mannings Bay and Blessing Formation strata in Well M4 are bioclastic packstones, composed in the lower part of the well of larger foraminifera and in the upper part of the well of coral, coralline algae, and molluscs.

Biostratigraphy

Planktonic foraminifera were recovered in Well M4 and at the Airport Penetentiary section. The zonation of this interval is based only on species present. Species absences are unreliable since they may be due to either unfavorable ecological or diagenetic

Reproduced with permission of the copyright owner. Further reproduction prohibited without permission.

factors, as suggested both by the abundance of shallow-marine larger foraminifera, and the poor state of preservation of the planktonic foraminifera.

The interval above the unconformity in the Airport/Penetentiary section (Fig. 1.3) lies between the uppermost Miocene, in the top of the *Globorotalia humerosa* chronozone (upper N17), and the top of the lower Pliocene *Globorotalia margaritae* chronozone (top N19). The upper limit is derived from the presence of *Globigerina nepenthes*. The lower stratigraphic limit is set by the position of this interval above the first occurrence of *Candeina nitida*.

The biostratigraphic significance of samples from well M4 is less clear and tentatively defined. One of the samples (21.8 m / 71.5 ft) includes a poor fauna consisting of 6 species. Specimens of *Globoquadrina altispira, Globigerinoides trilobus* subspp., and *Globigerinoides obliquus extremus* appear to be autochthonous and suggest placement near the Miocene / Pliocene boundary, between the base of the upper Miocene *Globorotalia humerosa* chronozone (N17) and the middle of the Pliocene *Globorotalia miocenica* chronozone (top of *Globigerinoides trilobus fistulosus* subchronozone, N20). If tentative identification of one small menardiform specimen as *Globorotalia tumida* is correct, the sample may lie in the Pliocene portion of this interval. *Globorotalia fohsi peripheroronda* is present, reworked from middle Miocene strata.

Reproduced with permission of the copyright owner. Further reproduction prohibited without permission.

DISCUSSION

Biostratigraphy

The biostratigraphic results presented here help revise a number of previous age interpretations of the Jealousy Formation and Kingshill Limestone (Table 1.1). Differences with older studies, notably Vaughan (1923) and Cushman (1946), can be attributed to changes in the interpretation of stratigraphic boundaries or revisions of the taxonomy and ranges of stratigraphically important species. Differences with more recent studies, such as Lidz (1982), are shown here to be based primarily on difficulties in separating morphologically similar forms.

Previous subsurface studies.

In a study of the benthic smaller foraminifera in cuttings from Wells 41, 39, and 34a (Test Wells No. 1, No. 2, and No.3), Cushman (1946) proposed that all three wells penetrated Miocene strata, with Test Well No. 1 extending down to strata inferred to be of Oligocene age. These "Oligocene" strata were subsequently included in the lower part of the type section of the Jealousy Formation by Cederstrom (1950). The larger foraminifera were identified for Cederstrom (1950) as Oligocene forms by T.W. Vaughan and F.G. Henbest.

The planktonic foraminifera of these wells were later studied by Todd and Low (1976), who reported two faunal associations in the subsurface section:

(1) in the lower part of the wells, which includes the Jealousy and lower Kingshill, a fauna assigned to the lower part of the middle Miocene (N9 to N11); and

(2) in the Kingshill strata of the upper part of the wells, a fauna assigned to the middle part of the middle Miocene (N12 or N13).

Reproduced with permission of the copyright owner. Further reproduction prohibited without permission.

Re-evaluation of their identifications and consideration of the reported highest stratigraphic occurrences of various species allows a rezonation of the wells.

Well 41 (Test Well No. 1) -- This well section is interpretedas lower Miocene (*Praeorbulina glomerosa* zone / N8 or lower) to middle Miocene (*Globorotalia fohsi lobata* zone / N11) based on the following criteria:

1) *Globorotalia fohsi lobata* is present from the top of the well downward and *Globorotalia menardii* is absent, indicating that the strata in the top of the well are equivalent to the *Globorotalia fohsi lobata* zone (N11);

2) the top of *Globigerinatella insueta* at approximately 152.4 m (500 ft) indicates that below this level, the well section is equivalent to the lower Miocene *Praeorbulina glomerosa* zone (N8) and lower. This is supported by a sudden downhole increase in abundance of *Globigerinoides bisphaericus* and *Praeorbulina transitoria* at the same depth.

Given the 22.9 m (75 ft) maximum thickness of the *Globorotalia fohsi lobata* zone in well M2 of our study, the Jealousy Formation / Kingshill Limestone boundary in well 41 probably lies in.the *Globorotalia fohsi fohsi* chronozone (N10).

Well 39 (Test Well No. 2) -- This well penetrates lower and middle Miocene strata, from the *Praeorbulina glomerosa* zone (N8) to the *Globorotalia fohsi peripheroronda* (N9) or *G. f. fohsi* (N10) zones. The following points were considered:

1) the top of *Globigerinatella insueta* lies at about 27.4 m (90 ft) in well 39, suggesting that most of this borehole penetrates lower Miocene strata;

2) *Globorotalia fohsi* is noted in scattered samples in the well. Since the form in the figures of Todd and Low (1976; their Plate 12, Figure 4) has no keel, this name

Reproduced with permission of the copyright owner. Further reproduction prohibited without permission.

probably includes both *Globorotalia fohsi fohsi* and *G. fohsi peripheroacuta*. It is assumed that the form present in this hole is *G. fohsi peripheroacuta*, due to faunal associations, and that it is present throughout the well as a contaminant from the uppermost part .*Globorotalia fohsi peripheroronda* is also present, reported and figured (their Plate 12, Figures 1 and 2) as *Globorotalia acostaensis* by Todd and Low (1976);

3) Specimens reported as *Orbulina suturalis* in this well, which generally would indicate a middle Miocene age, are suspected to include the lower Miocene species *Praeorbulina glomerosa* (see Todd and Low, 1976, Plate 11and Figure 12).
Given that Jealousy Formation / Kingshill Limestone boundary is at 27.7 m (91 ft) depth in this well, these data suggest that all of, or the upper part of, the Kingshill section lies in the lower middle Miocene, equivalent to the *Globorotalia fohsi peripheroronda* (N9) or *Globorotalia fohsi fohsi* (N10) zones. The Jealousy interval may be correlated to the upper lower Miocene *Praeorbulina glomerosa* zone (N8), possibly extending lower.

Well 45a (Test Well No. 3) -- This interval is interpreted as lying between the base of the Globorotalia fohsi fohsi zone (N10) and the middle of the *Globorotalia fohsi robusta* zone (N12) from the following occurrences:

1) *Globorotalia archeomenardii* is reported throughout the cuttings from Well 45a, a form which, from their figures (their Plate 12, Figure 5), appears to include *Globorotalia praemenardii*. Combined with the apparent absence of *Globorotalia menardii*, the presence of *Globorotalia praemenardii* would indicate an upper limit in the middle of the *Globorotalia fohsi robusta* zone (N12) for the strata in this well.

2) the presence of *Globorotalia fohsi fohsi* sets a lower limit for the well section at the base of the *Globorotalia fohsi fohsi* zone (N10).

3) *Globorotalia fohsi lobata* is noted at approximately 30.5 m (100 ft), suggesting that the *G. fohsi lobata* zone (N11) is represented in part of the cored interval.

Reproduced with permission of the copyright owner. Further reproduction prohibited without permission.

Although the well penetrated Jealousy Formation blue clays, depths given by Todd and Low (1976) suggest that all of the samples they studied from this borehole were from the Kingshill Limestone.

The larger foraminifera in these wells were determined by Vaughan and Henbest (in Cederstrom, 1950) to be of Oligocene age. However, re-evaluation of the biostratigraphy of these forms by Andreieff (Andreieff and others, 1987) has shown them to be characteristic of the upper part of the lower Miocene, in his *"Operculinoides" panamensis* zone.

Previous outcrop studies

A wide range of ages has also been cited for outcropping Neogene strata on St. Croix. These range from Oligocene in studies from the early part of the century to early Pliocene in more recent studies.

"Jealousy Formation" conglomerate -- Samples were collected in 1966 by Bold from outcrops believed to be Jealousy Formation in the Salt River Valley, about 200 m west of the junction of Scenic Road with Northcoast Road (Fig. 1.3). The strata were composed of lenses of greenish clay interbedded with conglomerate. The clay contained an ostracode fauna including *Cytherella* sp. aff. *C. gracilis, Paracypris* sp., *Bairdia condylus, Paranesidea antillea, Perissocytheridea alata, Procythereis? deformis, Quadracythere sparsa, Loxoconcha (Loxocorniculum) antillea, Loxoconcha runa,* and *Sclerochilus* sp. (Table 1.8) (Bold, 1970).

The fauna is very similar to that of the Anguilla Formation of Anguilla and the Lowlands Formation of St. Martin, but significantly lacks *Hemicyprideis* and *Peratocytheridea*, indicating a shallow-marine, probably reefal environment instead of the lagoonal environment in Anguilla. The foraminiferal fauna is dominated by *Archaias* and

Reproduced with permission of the copyright owner. Further reproduction prohibited without permission.

miliolids and is similar to that of Recent Caribbean reefs. The ostracode fauna is completely different from that of the subsurface Jealousy Formation, but contains several species in common with the lower Kingshill Limestone collected in the drilling program.

The stratigraphic range of some of the ostracode species in the conglomerate is sufficiently known to restrict the age of this sample between Blow's zones N7 and N9, earliest middle or latest early Miocene. The same age interval is indicated for the Anguilla Formation. As only shallow-water species are found, no comment can be given on the assumed redeposited nature of the conglomerate based on fauna alone. However, 1) the presence of the same or similar shallow-water species in the Kingshill Limestone, and 2) comparison to equivalent section in nearby Well M2, suggests that the green-clay ostracode fauna is allochthonous, and is associated with surrounding debris-flow deposits.

The question is, where did these flows originate? The ostracode fauna suggests that the clay was deposited under rather similar conditions and probably not very far away from the Anguilla Formation, which is certainly autochthonous. Near the lower-middle Miocene boundary this area may have been to the south or southwest of Puerto Rico. However, sediments of a similar age are lacking in southern Puerto Rico with the exception of a thin sand with *Globigerinatella insueta* between the Angola limestone (N 4 and ?N5) and the Ponce Formation (N17 and younger; Bold, written comm., 1989).

Kingshill Limestone, southwestern and central St. Croix -- Outcrops of the Kingshill Limestone east of Fredriksted near the Wheel of Fortune estate were placed in the middle Oligocene by Vaughan (1923). However, Multer and others (1977) pointed out that this determination may have been primarily based on misidentification of Miocene scleractinian coral species as similar Oligocene forms. Placement of these strata within the Kingshill Limestone is not confirmed. In central St. Croix, the ostracodes

Reproduced with permission of the copyright owner. Further reproduction prohibited without permission.

and planktonic foraminifera in Kingshill Limestone outcrop samples were studied by Bold (1970), who reported a middle Miocene age with samples ranging from the *Globorotalia fohsi fohsi* zone to the *Globorotalia fohsi robusta* zone.

Kingshill Limestone type section, Villa La Reine -- A variety of biostratigraphic determinations have been made for the Kingshill Limestone type section at Villa La Reine. Recently, Andreieff and others (1986) reported a late middle Miocene fauna, in contrast to a previous late Miocene interpretation of Lidz (1982). The results presented here agree most closely with those of the Andreieff study, which assigns the lower one-third of the section to zone N14 and the upper two-thirds to zone N15.

Our data do not support the upper Miocene determination (N17) of Lidz (1982). This may be explained by likely difficulties in the identification of two key species used in the determination:

1) *Globorotalia humerosa.* Juvenile specimens of *Globoquadrina altispira* may resemble *Globorotalia humerosa*, as appears to be the case for the specimens identified as *G. humerosa* in Figures 57 to 59 of the Lidz study. The aperture on the figured specimen appears to be umbilical with a small tooth, in contrast to the narrow umbilical-extraumbilical aperture typical of *G. humerosa.*

2) *Globorotalia plesiotumida.* This species may be difficult to differentiate from other menardiform species. Members of the *Globorotalia merotumida - plesiotumida* group were noted by Banner and Blow (1965a) as being more convex and tumid than *Globorotalia menardii,* but juvenile middle and Late Miocene specimens of *Globorotalia menardii* "A" are usually much more convex and tumid than their adult forms.

Calcareous nannoplankton determinations by Hay (in Multer and others, 1977) suggest an early Miocene age for the Villa La Reine section, in the *Discoaster druggi* and *Sphenolithus belemnos* zones. This is considerably older than our planktonic

Reproduced with permission of the copyright owner. Further reproduction prohibited without permission.

foraminiferal determinations indicate, or than those of Multer and others (1977), Lidz (1982) and Andreieff and others (1986). It is possible that the nannoplankton reflect the diagenesis evident in these strata, with calcite overgrowths on forms like discoasters altering their appearances to more like those of older species. In addition, some reworking of older early and middle Miocene planktonic foraminifera is evident in this section, and the more easily transported calcareous nannoplankton should be more strongly affected.

Airport/Penetentiary section -- Earlier studies of the Airport/Penetentiary section (referred to as the Evans Highway section in Lidz, 1982; and Andreieff and others, 1986) report results similar to those presented here. However, their interpretations diifer from ours on three points:

1) *Globorotalia tumida* and *Globigerinoides ruber*, species not identified in our study nor in that of Andreieff and others, were noted from below the unconformity in the Kingshill strata in the Lidz study. In the zonation of Bolli and Saunders (1985), these forms would indicate a lower Pliocene position; however, the recognition of *Globorotalia tumida* in the lower part of its stratigraphic range can be difficult and is considered by Stainforth and others (1974) as "too tenuous to be reliable in zonation."

2) Both the Lidz and Andreieff studies assign the strata above the unconformity to the lower Pliocene based on the disappearance of *Globoquadrina dehiscens* . We also note the absence of *G. dehiscens* in these strata, but differ in the interpretation of its stratigraphic significance. According to Bolli and Saunders (1985), the last-appearance datum (LAD) of this species, lies above the basal Pliocene FAD of *Globorotalia margaritae* and is placed at the top of the *Globorotalia margaritae margaritae* subzone (top of N18). Therefore, we consider it possible that these strata could lie in the uppermost Miocene.

Reproduced with permission of the copyright owner. Further reproduction prohibited without permission.

3) Andreieff and others (1986) also note the presence of *Globigerinoides conglobatus* above the unconformity as diagnostic of the lower Pliocene (see also Andreieff and others, 1987). However, the fact that early Pliocene examples of *Globigerinoides conglobatus* may exhibit characteristics intermediate between late Miocene *"Globigerinoides canimarensis"* -type forms and more typical Pleistocene and Recent specimens makes the use of the FAD of this species as a Miocene / Pliocene boundary marker difficult.

The larger foraminifera *Paraspiroclypeus chawneri* and *"Operculinoides" cojimarensis* are also present in the "post-Kingshill Limestone" (Andreieff and others, 1986). Andreieff and others (1987) indicate that the co-occurrence of these two species is diagnostic of a Pliocene age.

Species Ranges

Several differences over species ranges among different planktonic foraminiferal zonations can be resolved in the St. Croix Tertiary section. Disagreement on the biostratigraphic significance of the first-appearance datum (FAD) of the genus *Sphaeroidinellopsis* can be resolved through consideration of the Jealousy Formation fauna well M1. Bolli and Saunders (1985) set the FAD of the first species of this genus, *S. disjuncta,* at the base of the *Globorotalia fohsi peripheroronda* zone (N9). However, its occurrence with *Globigerinatella insueta* in the lowest part of well M1 supports its FAD in lower Miocene zone N7 (approximately equal to the *G. insueta* zone) by Kennett and Srinivasan (1983).

Globigerinoides mitra is characterized in Bolli and Saunders (1985) as appearing at the base of the middle Miocene *Globorotalia fohsi peripheroronda* zone (N9). However, the presence of this species in the lower Miocene fauna at 26.5 m (87 ft) in

Reproduced with permission of the copyright owner. Further reproduction prohibited without permission.

well M10 supports an earlier FAD for *G. mitra* , in zone N7 (approximately the *Globigerinatella insueta* zone) as reported by Kennett and Srinivasan (1983).

Lithostratigraphy

The data presented here permit resolution of a number of important points on the Mio-Pliocene lithostratigraphy of St. Croix.

Jealousy Formation

The Jealousy Formation appears to be a completely subsurface unit. Cederstrom (1950) and Whetten (1966) both mapped extensive outcrop areas of Jealousy Formation on the lower slopes of the northside range. The strata are lithic and bioclastic conglomerates cemented with carbonate mud and were correlated to conglomerates encountered in the Jealousy Formation in well 41 and well 39. However, the exposures are entirely unlike the pelagic, microfossil-rich blue clays of the Jealousy Formation sampled during our drilling program. The lithologies are more consistent with those of the Kingshill Limestone, which includes numerous conglomeratic deposits. Therefore, outcropping strata previously described as Jealousy Formation are placed in the Kingshill Limestone, in agreement with Gerhard and others (1978) and Gill and Hubbard (1986; 1987).

Kingshill Limestone

Related to these "Jealousy Formation" outcrops are conglomerates cropping out near Judith Fancy and Salt River composed of shallow-marine macrofossils and rounded pebbles of Cretaceous rock. Gerhard and others (1978) interpreted these as shallow lagoonal / strandline deposits lying at the base of the Kingshill Limestone. However,

Reproduced with permission of the copyright owner. Further reproduction prohibited without permission.

this limited outcrop interval can be correlated to the nearby, more complete section of Well M10. There the Kingshill Limestone section is dominated by limestones and marls rich in planktonic foraminifera. Comparison of the sections yields two points:

1) the outcropping strata are deep marine deposits of reworked shelf-derived material rather than strandline deposits;

2) the outcrops do not lie at the base of the Kingshill Limestone.

The Kingshill Limestone reflects a transition from deep-marine deposition to shallow-marine carbonate and peripheral slope sedimentation. It does not appear that any significant environmental change accompanies the color change across the Jealousy Formation / Kingshill Limestone boundary. However, starting from the deep-basinal carbonate deposits of the lower Kingshill Limestone, the influence of transported, shallow-marine constituents increases upward through the outcrops at Villa La Reine, Estate Work and Rest, and Evans Highway.

Mannings Bay member and Blessing Formation

These limestones have been discussed in general terms in a number of stratigraphic and sedimentologic studies (Andreieff and others, 1986 and 1987; Gerhard and others, 1978; Lidz, 1982, 1984, 1988). For the purposes of this paper, two subdivisions are suggested:

1) an upper Kingshill member (Mannings Bay member) consisting of larger foraminifera debris flow facies lower in the section, characterized by irregularly bedded, channelled deposits of transported *Operculinoides* and *Paraspiroclypeus* (Andreieff and others, 1986; Andreieff and others, 1987; Gerhard and others, 1978);

2) a "post-Kingshill" unit (Blessing Formation) consisting of reef and lagoon facies higher in the section, characterized by massive shallow-marine limestones with well-developed moldic porosity and patchy dolomitization. It has been previously

Reproduced with permission of the copyright owner. Further reproduction prohibited without permission.

suggested that the Blessing strata as described here should be subdivided into two separate formations (Behrens, 1976; S. Frost, pers. comm., 1986). However, the suggested subdivisions are not mappable and are best represented as individual facies rather than formations (Chapt. 2, this dissertation). Detailed descriptions of the post-Kingshill strata can be found in Behrens (1976), Gill and Hubbard (1986; 1987), and Chapter 2 (this dissertation).

Benthic environment.

The subsurface samples of the Jealousy Formation and Kingshill Limestone of wells M1, M2, and M10 are notably rich in Bolivina. The percentage ranges from a low of 14% in the Jealousy Formation to a high of 38% in the Kingshill Limestone. Overall, *Bolivina* is most abundant in the middle Miocene (N10-N11) sedimentary rocks in test Well M2, averaging 31.5% of the fauna. In the upper lower Miocene (N8) and the lower middle Miocene (N9) portion of the Jealousy Formation - Kingshill Limestone sequence, higher *Bolivina* percentages are noted in the southern part of St. Croix than in the northern part, averaging 30% in Well M1 versus 21% in M10. High proportions of *Bolivina* are known in low oxygen environments (Boltovskoy and Wright, 1976; Phleger and Soutar, 1973) and nutrient-enriched settings associated with upwelling (Sen Gupta, Lee, and May, 1981). This suggests that low-oxygen or upwelling conditions may have prevailed around the time of the early Miocene - middle Miocene transition in the southern part of the island and in the middle Miocene in the central part of the island.

The faunas of the three wells differ in other notable aspects. *Epistominella sp. cf. E. exigua, Cassidulina subglobosa,* and the stilostomellids are significant components of the upper lower Miocene (N8) and lowermost middle Miocene (N9) deposits of wells M1 and M10, but are generally much less common in the higher middle Miocene strata (N10-

Reproduced with permission of the copyright owner. Further reproduction prohibited without permission.

N11) of well M2. This trend may reflect temporal oceanographic changes. *Epistominella exigua* is a species with strong water mass preferences, most closely with the lower North Atlantic Deep Water (Schnitker, 1980) in Recent faunas. A significant drop in bottom water temperatures in the early part of the middle Miocene (Savin and others, 1975) may have caused oceanographic changes responsible for this faunal shift.

Reproduced with permission of the copyright owner. Further reproduction prohibited without permission.

CONCLUSIONS

The drilling program conducted for this dissertation between 1984 and 1986 provides new information on the subsurface geology of the island. Data from these cores provide a more complete biostratigraphic framework for the Jealousy Formation and the lower part of the Kingshill Limestone than has previously been possible. These data also allow the refinement of previous biostratigraphic interpretations for outcrops of the Kingshill Limestone and allow the resolution of several problems in stratigraphic correlation.

These data, and a re-examination of older data, indicate that the biostratigraphy of the Neogene formations can be summarized as follows (Table 1.5):

(1) Jealousy Formation - The oldest strata recovered in our boreholes are stratigraphically equivalent to the upper lower Miocene *Praeorbulina glomerosa* zone (N8). The top of the formation is diachronous, ranging from within the *P. glomerosa* chronozone (N8) in well M10 to the lower part of the lower middle Miocene *Globorotalia fohsi fohsi* chronozone (N10) in wells M1 and M2.

(2) Kingshill Limestone - Judged by the ages of the Jealousy Formation / Kingshill Limestone boundary, this unit extends to near the top of the uppermost Miocene *Globorotalia humerosa* zone (N17) below the unconformity in the Evans Highway section.

(3) "upper Kingshill" limestones - These shallow-marine limestones are exposed above the disconformity in the Airport/Penetentiary section, where poor planktonic foraminiferal faunas indicate placement between the upper part of the upper Miocene *Globorotalia humerosa* zone (upper N17) and the top of the lower Pliocene *Globorotalia margaritae* zone (top N19). Larger foraminifera present suggest a Pliocene age (Andreieff and others, 1986).

Reproduced with permission of the copyright owner. Further reproduction prohibited without permission.

The new subsurface geologic data resolve the following points on stratigraphic correlation:

(1) The Jealousy Formation is an entirely subsurface unit of deep-marine sediments. Comparison of material recovered from the Jealousy Formation in our cores to reported exposures of Jealousy strata reveals little in common lithologically. The outcrop material is compatible with the range of lithologies included in the Kingshill Limestone, and field relationships suggest correlation to surrounding Kingshill subsurface sections.

(2) The boundary between the Jealousy Formation and the Kingshill Limestone is distinct and abrupt; with blue marls of the former unit capped by tan marls of the latter. However, this boundary is diachronous, ranging from the upper part of the lower Miocene in Well M10 (*Praeorbulina glomerosa* zone / N8) to the middle Miocene in Wells M1 and M2 (*Globorotalia fohsi fohsi* zone / N10). The boundary does not appear to indicate any significant paleoenvironmental change.

(3) Shallow-marine Pliocene limestones that lie at the top of the St. Croix carbonate sequence may be differentiated from the Miocene basinal deposits of the Kingshill Limestone. These are referred to here as "post-Kingshill" limestones and reflect significant shallowing of the basin. Lithologies range from deposits of transported larger foraminifera to reefal limestones.

Reproduced with permission of the copyright owner. Further reproduction prohibited without permission.

TABLES

Reproduced with permission of the copyright owner. Further reproduction prohibited without permission.

Table 1.1 Summary of the results of previous biostratigraphic studies on St. Croix. The age determinations given are either those of the respective authors, or are interpreted from their publications, and do not necessarily agree with this study.

Author	Study	Fossil Type	Kingshill LS Mannings Bay Mbr*	Kingshill LS	Jealousy Fm
Vaughan (1923)	outcrop	corals, molluscs, larger foraminifera	—	middle Oligocene	—
Cushman (1946)	subsurface	smaller foraminifera	—	Miocene	Oligocene to Miocene
Bold (1970)	outcrop	ostracodes, planktonic foraminifera	—	Middle Miocene (*G. fohsi fohsi* to *G. fohsi robusta* zone)	late early Miocene
Todd and Low (1976)	subsurface	planktonic foraminifera	-	lower middle Miocene (N9 to N11) to middle middle Miocene (N12 or N13)	lower middle Miocene (N9 to N11)
Multer and others (1977)	outcrop	planktonic foraminifera	—	middle Miocene (*G. fohsi fohsi* zone)	—
Multer and others (1977) by W. W. Hay	outcrop	calcareous nannoplankton	—	middle lower Miocene (*Discoaster druggi* and *Sphenolithus belemnos* zones)	—
Lidz (1982)	outcrop foraminifera	planktonic	lower Pliocene (upper N18 and N19)	middle to upper Miocene (N10 to lower N18)	—
Andreieff and others (1986)	outcrop	planktonic foraminifera	lower Pliocene (N18-19)	middle to upper Miocene (N12 to N17; also, N9 to N11?)	—
Andreieff and others (1986 and 1987)	outcrop	larger foraminifera	lower Pliocene (*Paraspiroclypeus chawneri* zone)	—	—

*referred to as the "post-Kingshill" limestones in Lidz (1982) and Andreieff and others (1986)

Reproduced with permission of the copyright owner. Further reproduction prohibited without permission.

Table 1.2. Planktonic foraminiferal zonation in the subsurface sections discussed in this study.

Zone	Foraminiferal Event *			Test Well / Sample depth M1	M2	M10
G. fohsi robusta zone	top	LO	*G. fohsi robusta*		11 ft	
	base	FO	*G. fohsi robusta*		51.5 ft	
G. fohsi lobata zone	top	FO	*G. fohsi robusta*		51.5 ft	
	base	FO	*G. fohsi lobata*		91.5 ft	
G. fohsi fohsi zone	top	FO	*G. fohsi lobata*		91.5 ft	
	base	FO	*G. fohsi fohsi*		166.5 ft	
G. fohsi peripheroronda zone	top	FO	*G. fohsi fohsi*	105 ft **		55 ft **
	base	FO	*G. insueta*	136.5 ft		85 ft
Praeorbulina glomerosa zone	top	LO	*G. insueta*	136.5 ft		85 ft
	base	FO	*P. glomerosa*	145 ft		105 ft

Numbers refer to the sample depth within the test well, as measured from land surface.

* FO = First occurrence of diagnostic species
LO = Last occurrence of diagnostic species

** Occurrence of *G. fohsi fohsi* not observed due to replacement of marine section by alluvium at depth noted.

Reproduced with permission of the copyright owner. Further reproduction prohibited without permission.

Table 1.3. Planktonic foraminiferal criteria used in the zonation of the St. Croix Tertiary sequence.

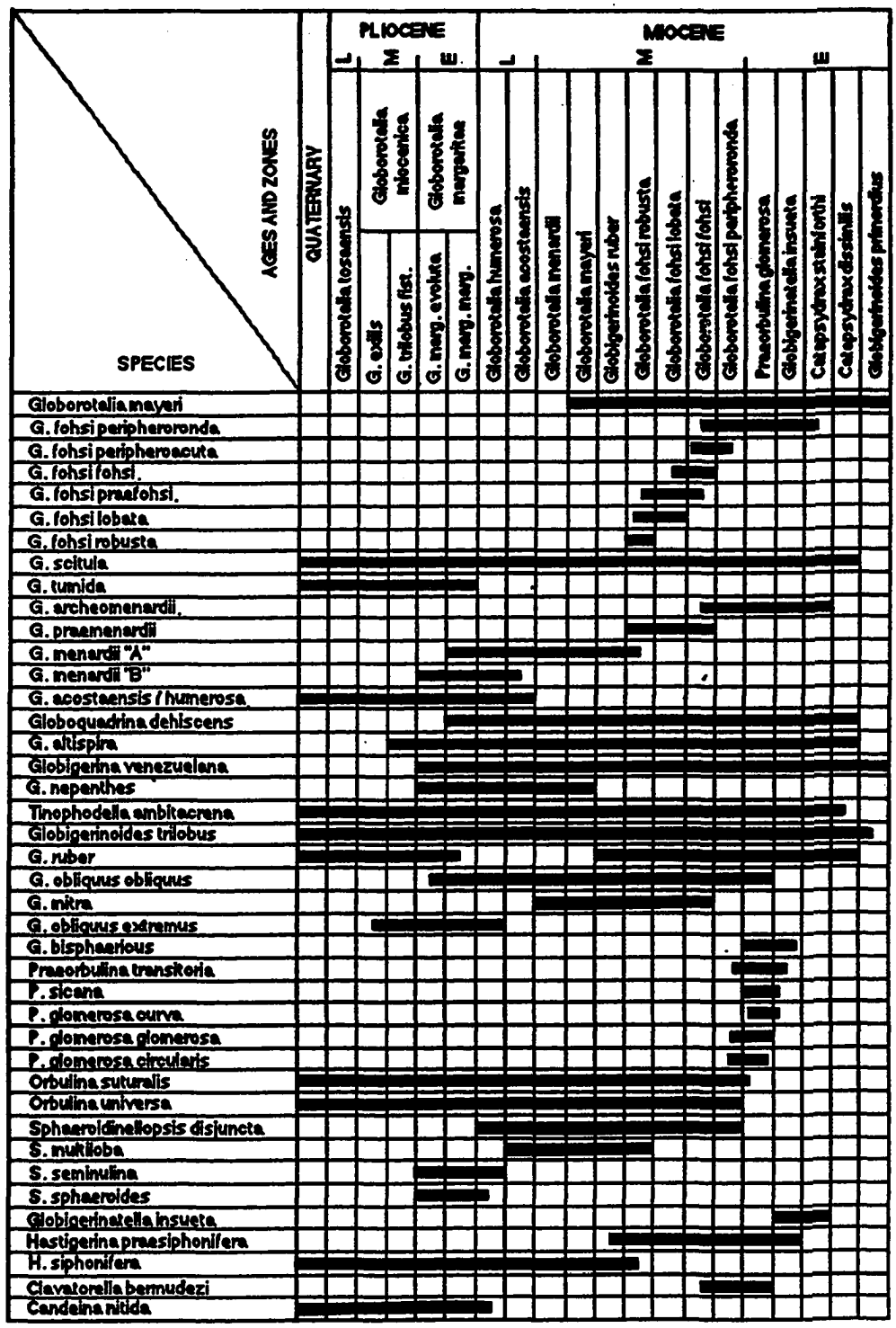

Reproduced with permission of the copyright owner. Further reproduction prohibited without permission.

Table 1.4. Benthic foraminifera used in the bathymetric interpretation of the Kingshill/Jealousy Basin.

Taxon	Bathymetry and remarks
1. Stilostomellids	Significant numbers (>5%) of *Stilostomella* noted typical of lower bathyal depths (1, 3); ornamented forms have been associated with the lower middle bathyal - middle bathyal transition..
2. *Bolivina* spp.	Abundant Bolivina are often associated with nutrient-enriched or low-oxygen environments which may be related to upwelling (2, 5, 14, 15).
3. *Bolivina alazanensis*	Ranges from the upper bathyal zone to abyssal depths, most common between 500 and 100m (10, 11, 12).
4. *Pullenia bulloides*	Predominantly middle-lower bathyal; > 65m in Gulf of Mexico (12); > 150m in the North Atlantic, mostly 500-2500m (3, 4, 13); >175m off California, 2000-2600m in Catalina Channel (9), mostly 1200-3500m (3,4); found below 1300m off Panama (2) and El Salvador (16).
5. *Cassidulina subglobosa*	Wide ranging bathymetry, found up to 75 m, more common and larger @>200m (11) in the Gulf of Mexico; characteristic of >130m, mostly 500-700m, in the Pacific off Central America (16).
6. *Cibicides bradyi*	Inhabits >450 m in the Gulf of Mexico (11).
7. *Cibicides renzi*	Characterized as an upper bathyal species in Tertiary deposits of the Caribbean region (8).
8. *Cibicides robertsonianus*	Reported >450 m in the Gulf of Mexico (12); specimens noted in this study are transitional towards *Cibicides bradyi,* generally with 9 chambers in the last whorl.
9. *Cibicides wuellerstorfi*	Reported >500m (10) and 700m (12), but most common below 3000m; >630m in the North Atlantic (3, 4, 14).
10. *Episominella* sp. cf. E.*exigua*	*E. exigua* is characterized as occurring below 180 m and most common near 500 m (>2%) in the Gulf of Mexico (10, 11). Reported in 30 - 60 m deep water off the coast of El Salvador (16). Specimens noted in this study are nearly identical with *E. exigua* but are very small (~0.1mm).

Reproduced with permission of the copyright owner. Further reproduction prohibited without permission.

Table 1.4. Cont.

11. *Laticarinina pauperata*	Reported from >205m (12) and 300m (10), most common in lower bathyal zone, in the Gulf of Mexico; middle and lower bathyal forms are larger (~3mm) than the specimens noted here (11); >200m, mostly 550-3000m in North Atlantic (3,4,14); >200m, mostly 1200-3500 m off California (3,4).
12. *Melonis pompilioides*	Specimens identified are inflated *M. pompilioides (=soldanii)* of Morkhoven et al. (1986), closer to forma *sphareoides* than to the compressed *M. barleeanum* form; they probably inhabited the upper bathyal zone in the Miocene (6) rather than the greater depths it characterizes today.
13. *Osangularia culter*	Found at >600m in the Gulf of Mexico (12).
14. *Oridorsalis umbonatus*	In the Gulf of Mexico, >65m, mostly >80m (12); in the North Atlantic, > 60m, predominantly 1500-3500m (3, 4, 14); characterizes 1300-3200m range off El Salvador (16).
15. *Rectuvigerina multicostata*	Characterized as a bathyal species (8).
16. *Siphonina tenuicarinata*	Characterized as outer neritic to middle bathyal, most commonly bathyal, UDL estimated at about 100m (8). Similar to modern carinate *Siphonina bradyana* which is found at 45-700m in the Gulf of Mexico (13).
17. *Sphaeroidina bulloides*	Small specimens up to ~100m in Gulf of Mexico and North Atlantic, most commonly middle-upper bathyal (8).

Reproduced with permission of the copyright owner. Further reproduction prohibited without permission.

Table 1.4. Cont.

Key to References

1. Bandy and Rodolfo (1964)
2. Bandy and Arnal (1957)
3. Berggren and Haq (1976)
4. Berggren and others (1976)
5. Boltovskoy and Wright (1976)
6. Hasegawa (1984)
7. Ingle (1980)
8. Morkoven and others (1986)
9. Natland (1933)
10. Parker (1954)
11. Pflum and Frerichs (1976)
12. Phleger (1951)
13. Phleger, Parker and Peirson (1953)
14. Phleger and Soutar (1973)
15. Sen Gupta, Lee and May (1981)
16. Smith (1964)

Reproduced with permission of the copyright owner. Further reproduction prohibited without permission.

Table 1.5. Planktonic foraminiferal occurrences in the well and outcrop sections of this study. Core sections represent those that penetrated the Jealousy Formation; numerical sample numbers represent sample depth in feet below land surface. "R" = reworked; "?"= questionable identification.

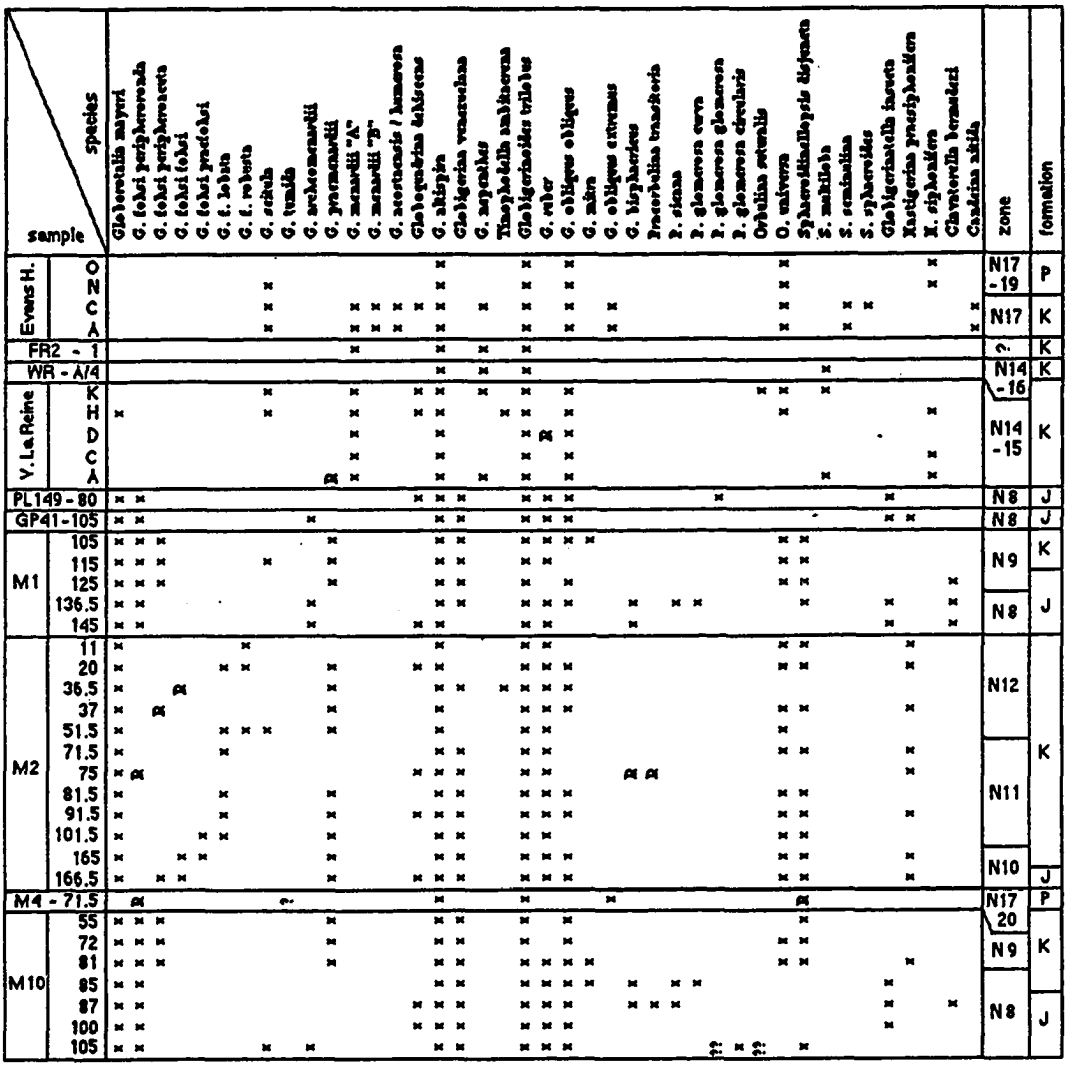

Reproduced with permission of the copyright owner. Further reproduction prohibited without permission.

Table 1.6. Ostracodes recovered from core samples of the upper Jealousy Formation. Test holes M1, M2 and M10. Shallow-water species are completely absent in the sampled Jealousy sediments

Cytherella sp. aff. *C. vulgata* Ruggieri, *C.* sp. 1 Steineck

Cardobairdia glabra Bold

Argilloecia suavis Lubimova and Sanchez, A. sp. 2, Bold, 1971

Bairdia oarion Bold

Krithe lambi Bold, *K. morkhoveni* Bold, *K. prolixa* Bold, *K. reversa* Bold*,
K. vandenboldi Steineck

Messinella jamaicensis Bold

Procythereis ?calhounensis (Smith)

Agrenocythere hazelae (Bold)

Trachyleberidea mammidentata (Bold)

Henryhowella ex gr. *asperrima* (Reuss)

Ambocythere sp. aff. *A. caudata* Bold

Bradleya johnsoni Benson

*The presence of *Krithe reversa* in the upper Jealousy suggests that this part of the formation was deposited in depths below 1000 m.

Reproduced with permission of the copyright owner. Further reproduction prohibited without permission.

Table 1.7. Ostracode fauna from the lower Kingshill Limestone drill samples (Blow's Zone 10-12)

Cytherella sp. 1, Steineck

Argilloecia suavis Lubimova and Sanchez, *A.* sp. 1, Bold, 1971, *A.* sp. 2, Bold, 1971, *A.* sp. 3, Bold, 1971, *A.* sp. Bold, 1970

Abyssocypris tipica Bold, *A. pykna* (Bold)

Bythocypris sp. cf. *B. bosquetiana* (Brady)

Bairdia sp., Bold, 1970 *

Bairdoppilata cassida (Bold)

Paranesidea antillea (Bold) **

Krithe lambi Bold, *K. morkhoveni* Bold, *K. prolixa* Bold, *K. reversa* Bold, *K. trinidadensis* Bold, *K. vandenboldi* Steineck.

Parakrithe vermunti (Bold)

Procythereis ?deformis (Reuss)**, *P ? calhounensis* (Smith)

Orionina vaughani (Ulrich and Bassler)**

Caudites nipeensis Bold*, *Caudites sacer* Bold*

Quadracythere antillea (Bold)**, *Q. sparsa* Bold**

Puriana gatunensis (Coryell and Fields)*

Trachyleberidea mammidentata (Bold)

Thalassocythere bermudezi crebripustulosa (Bold)

Costa cubana Bold

Neocaudites macertus (Stephenson)*

Agrenocythere hazelae (Bold)

Loxoconcha (Loxoconcha) sp. aff. *L. (L.) forda* Bold

Loxoconcha (Loxocorniculum) antillea Bold**

Reproduced with permission of the copyright owner. Further reproduction prohibited without permission.

Loxoconcha (Palmoconcha) banesensis Bold

Paracytheridea tschoppi Bold*

* shallow marine species occurring in the lower part of the Kingshill Limestone,

6 of which are also found in the "Jealousy" Formation conglomerate.

Note absence of *Loxoconcha runa* in the Kingshill, latest occurrence in N9.

Reproduced with permission of the copyright owner. Further reproduction prohibited without permission.

Table 1.8.

Ostracode fauna recovered from the "Jealousy" Formation conglomerate (Bold, 1970)

Cytherella sp. aff. *C. gracilis* Lienenklaus

Propontocyspris sp., Bold, 1970

Paracupris sp. B, Bold, 1970

Bairdia condylus Bold

Paranesidae antillea (Bold)

Perissocytheridea alata Bold

Procythereis ? *deformis* (Reuss)

Orionina vaughani (Ulrich and Bassler)

Quadracythere antillea (Bold), *Quadracythere sparsa* Bold

Loxoconcha runa Bold

Loxoconcha (Loxocorniculum) antillea Bold

Sclerochilus sp., Bold, 1970

Xestoleberis sp. E, Bold, 1946 = X. sp. B, Bold, 1970

(Note the absence of *Puriana gatunensis* in the conglomerate,

earliest occurrence in zone N9)

Reproduced with permission of the copyright owner. Further reproduction prohibited without permission.

PLATES

All photos 100x unless otherwise noted.

Reproduced with permission of the copyright owner. Further reproduction prohibited without permission.

Plate 1.1.

1. *Globigerina venezuelana*, dorsal view.
2. *Globigerina nepenthes*, ventral view.
3, 4. *Globoquadrina dehiscens*:: 3. dorsal view, 4. ventral view.
5. *Globoquadrina altispira*, side view.
6. *Globigerinatella insueta*, side view.
7. *Candeina nitida*, dorsal view.
8. *Globigerinita naparimaensis*, ventral view
9, 10. *Globigerinoides ruber*:: 9. dorsal view, 10. ventral view.
11, 12. *Globigerinoides obliquus obliquus*:: 11. ventral view, 12. dorsal view.
13, 14. *Globigerinoides obliquus extremus*:: 13. ventral view, 14. dorsal view.
15. *Globigerinoides mitra*, side view.
16. *Globigerinoides trilobus forma immaturus*, dorsal view.
17. *Globigerinoides bisphericus*, ventral view.
18. *Praeorbulina transitoria*, side view.

Reproduced with permission of the copyright owner. Further reproduction prohibited without permission.

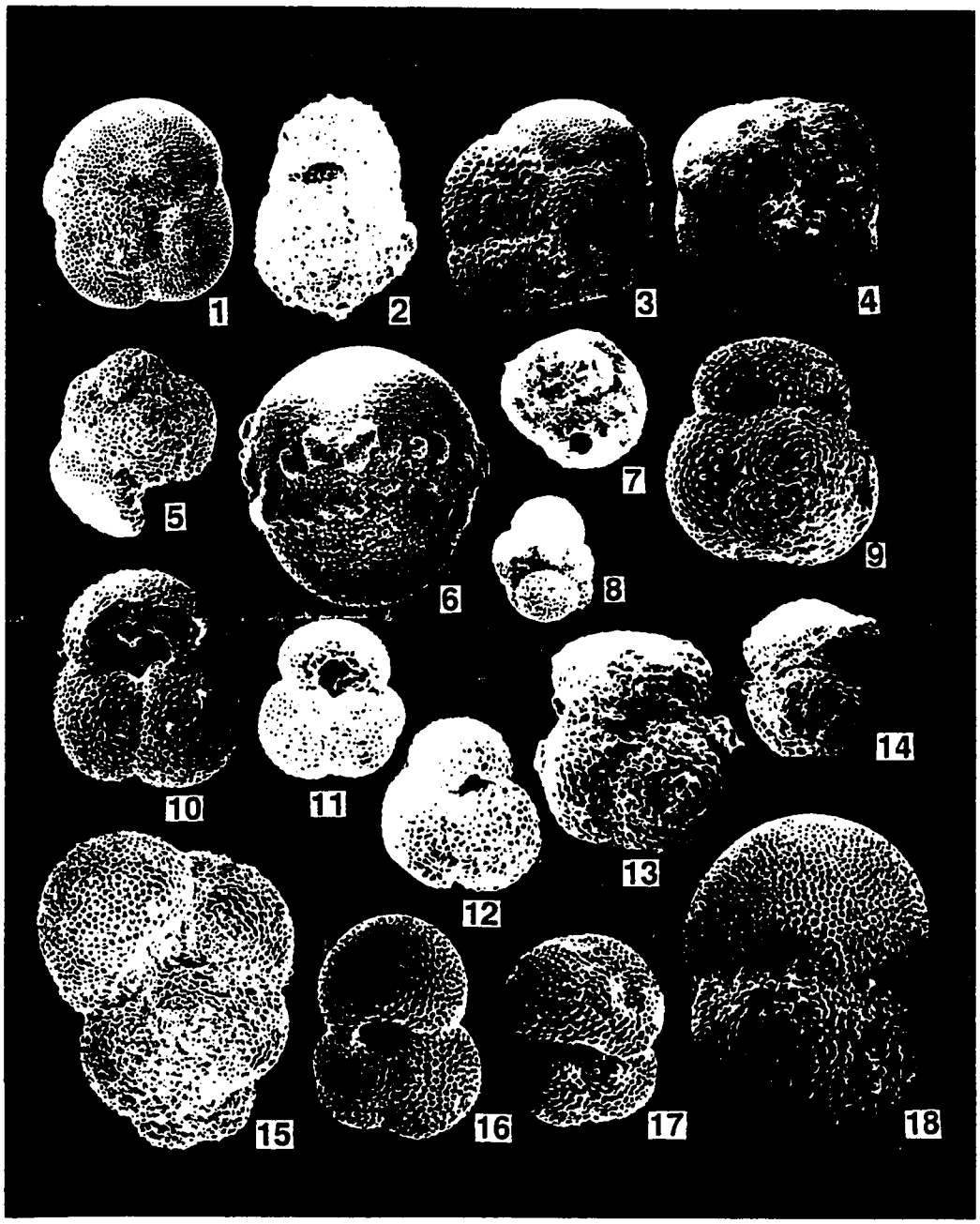

Reproduced with permission of the copyright owner. Further reproduction prohibited without permission.

Plate 1.2.

1. *Praeorbulina sicana*, side view.

2, 3. *Praeorbulina glomerosa curva*:: 2. side view, 3. bottom view.

4, 5. *Praeorbulina glomerosa glomerosa*:: 4. bottom view, 5. side view.

6. *Praeorbulina glomerosa circularis*, bottom view.

7. *Orbulina universa.*

8. *Orbulina suturalis.*

9, 10. *Globorotalia humerosa*:: 9. ventral view, 10. dorsal view.

11, 12. *Globorotalia mayeri*:: 11. dorsal view, 12. ventral view.

13, 14, 15. *Globorotalia fohsi peripheroronda*:: 13. dorsal view, 14. side view, 15. ventral view.

16, 17, 18. *Globorotalia fohsi peripheroacuta*:: 16. dorsal view, 17. side view, 18. ventral view.

19, 20, 21. *Globorotalia fohsi fohsi*: : 19. ventral view, 20. side view, 21. dorsal view.

Reproduced with permission of the copyright owner. Further reproduction prohibited without permission.

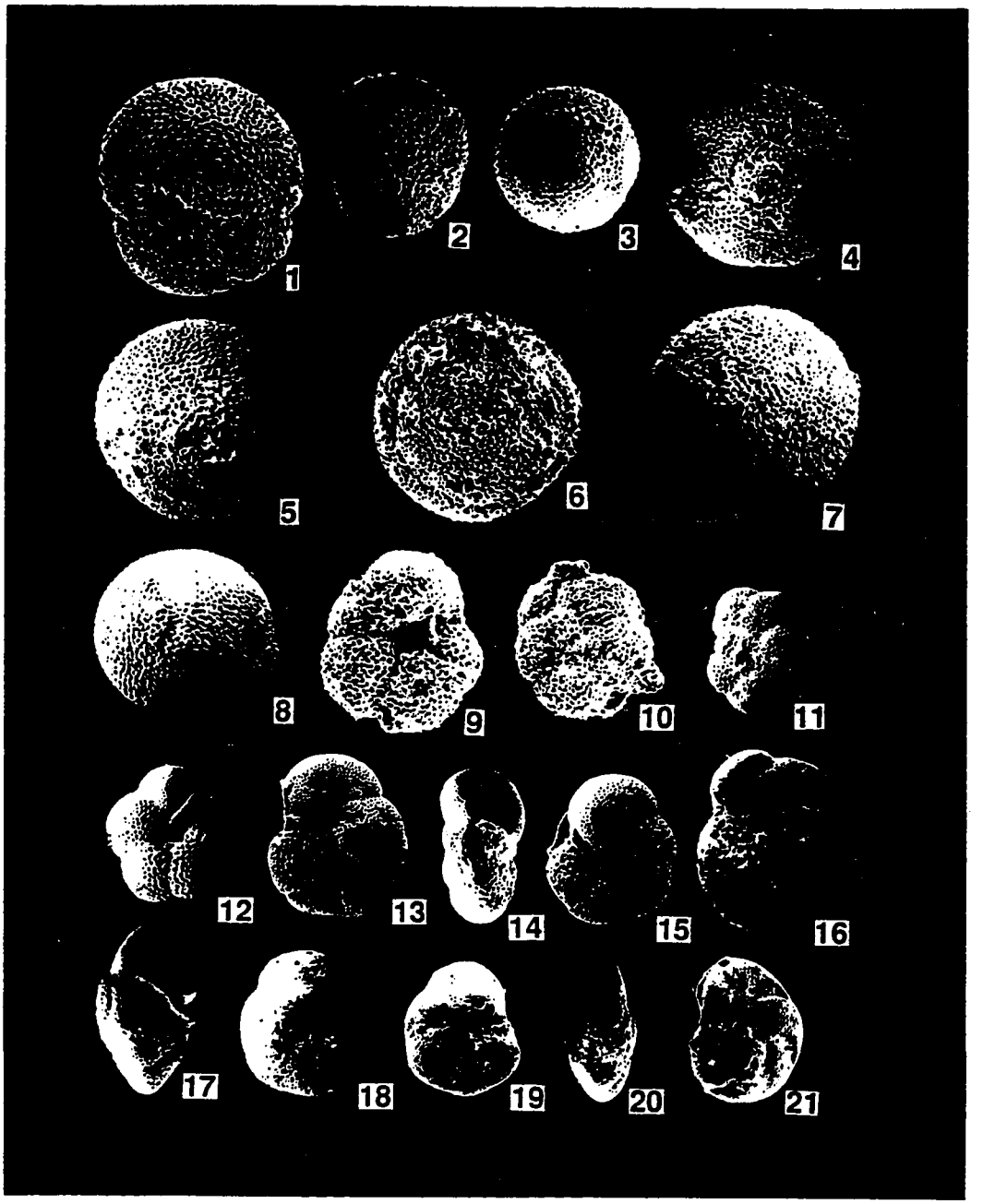

Reproduced with permission of the copyright owner. Further reproduction prohibited without permission.

Plate 1.3.

1, 2, 3. *Globorotalia fohsi praefohsi*:: 1. ventral view, 2. side view, 3. dorsal view.
4, 5, 6. *Globorotalia fohsi lobata*:: 4. ventral view, 5. side view, 6. dorsal view.
7, 8, 9. *Globorotalia fohsi robusta*:: 7. ventral view, 8. side view, 9. dorsal view.
10, 11, 12. *Globorotalia archaeomenardii*:: 10. ventral view, 11. dorsal view, 12. side view.
13, 14, 15. *Globorotalia praemenardii*:: 13. ventral view, 14. side view, 15. dorsal view.
16, 17. *Globorotalia menardii* forma "A": 16. dorsal view, 17. ventral view.

Reproduced with permission of the copyright owner. Further reproduction prohibited without permission.

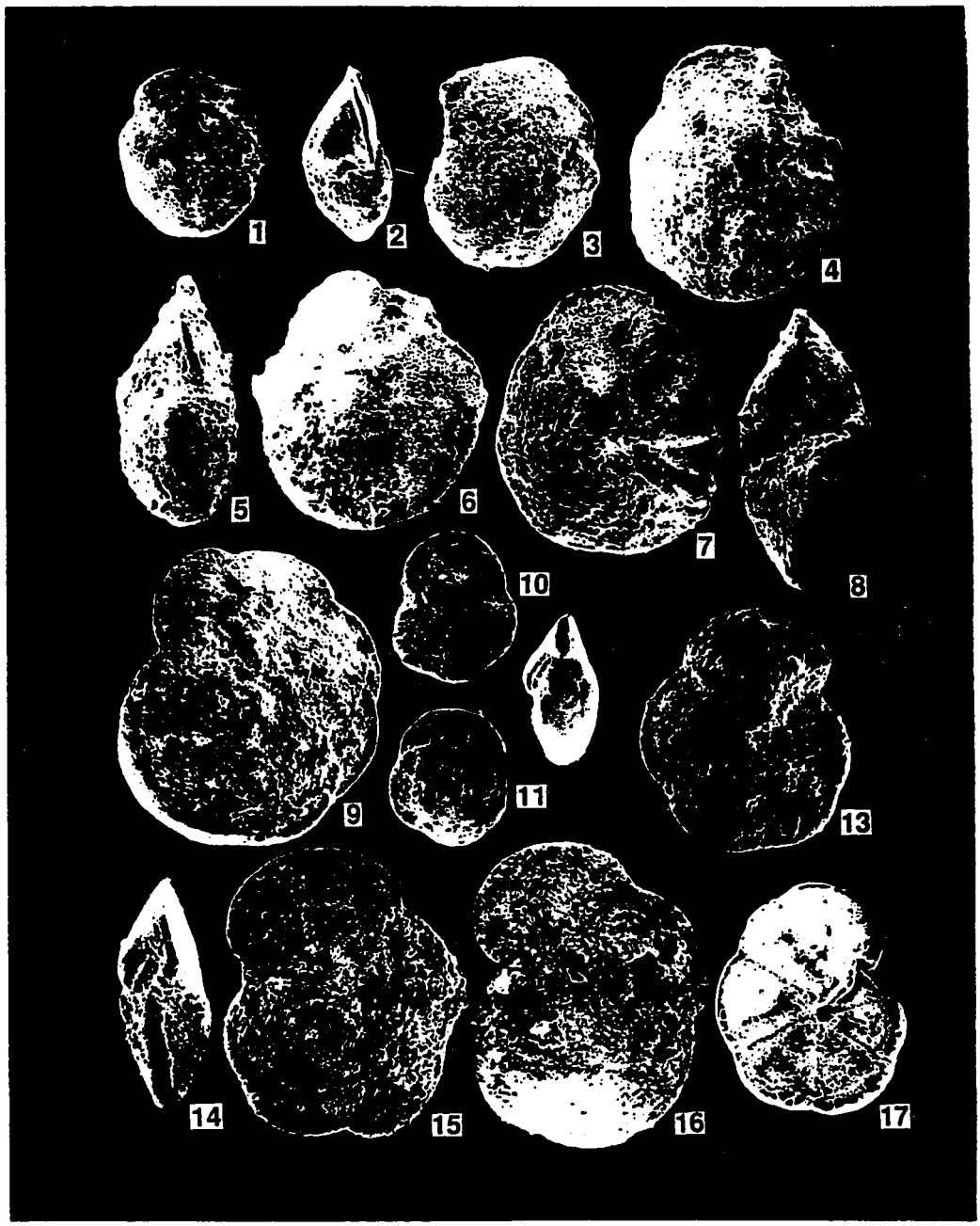

Reproduced with permission of the copyright owner. Further reproduction prohibited without permission.

Plate 1.4.

1, 2. *Globorotalia menardii* forma "B": 1. dorsal view, 2. ventral view.
3, 4. *Globorotalia scitula*:: 3. dorsal view, 4. ventral view.
5, 6, 7. *Globorotalia miozea*:: 5. ventral view, 6. side view, 7. dorsal view.
8, 9. *Sphaeroidinellopsis multiloba*:: 8. ventral view, 9. dorsal view.
10. *Sphaeroidinellopsis seminulina*, ventral view.
11. *Sphaeroidinellopsis sphaeroides*, ventral view.
12, 13. *Hastigerina siphonifera*:: 12. front view, 13. side view.
14, 15. *Hastigerina praesiphonifera*:: 14. front view, 15. side view.
16. *Clavatorella bermudezi*:, front view.

Reproduced with permission of the copyright owner. Further reproduction prohibited without permission.

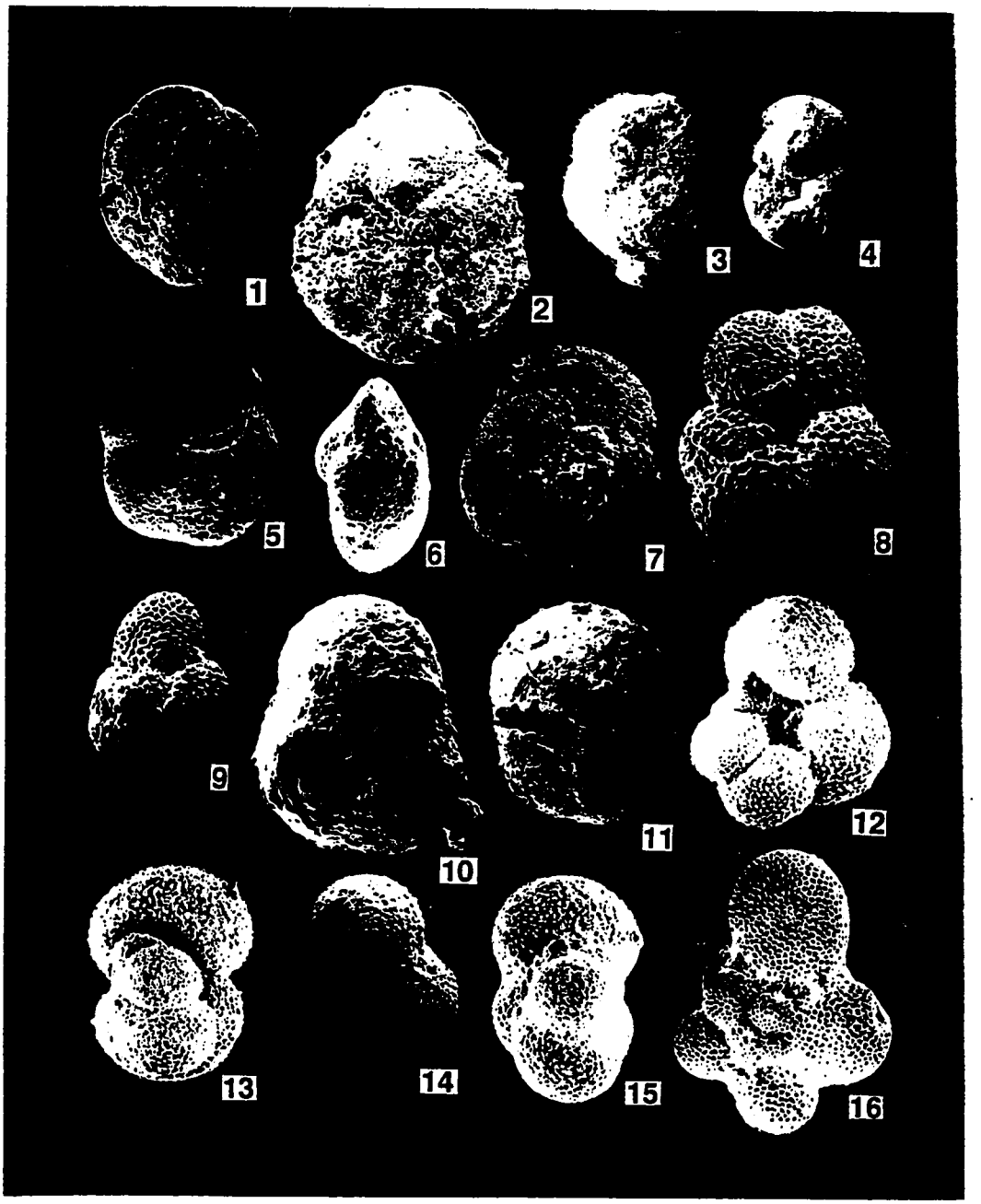

Reproduced with permission of the copyright owner. Further reproduction prohibited without permission.

CHAPTER 2.

SEDIMENTOLOGICAL AND TECTONIC EVOLUTION OF TERTIARY ST. CROIX

Reproduced with permission of the copyright owner. Further reproduction prohibited without permission.

ABSTRACT

St. Croix is a sedimentary island at the juncture of two northeastern Caribbean tectonic provinces. For this reason, the sedimentary development of St. Croix is of considerable importance to regional tectonic reconstruction. Previous models of the late Tertiary development of St. Croix assume either that the carbonate sediments were deposited in shallow water or that they were basinal sediments deposited entirely within the confines of an insular graben system. Both models presume a static, isolated land mass, with a self-contained sediment source. Evidence from a systematic drilling program on St. Croix requires significant modification of both models of basin evolution.

Benthic-forminiferal faunas from drill samples suggest that most of the lower Neogene section reached by drilling was deposited in 600 to 800 m of water in the middle bathyal zone. Pronounced shallowing occurred during the latest Miocene to early Pliocene, culminating in the establishment of a Pliocene reef tract that rimmed the southern and western coasts of the island. The western side of the basin shows no evidence for the existence of the graben-bounding fault zone, or for any associated land mass during the early Miocene. However, coarse clastic debris in Kingshill Limestone exposures along the eastern fault zone indicates that faulting and graben formation may have begun prior to the latest middle Miocene (N15) during deposition of the Kingshill Limestone.

This evidence indicates that the Jealousy Formation and portions of the Kingshill Limestone were deposited prior to graben formation, and that faulting began in the middle Miocene, between zones N8 and N15. A source external to the present

Reproduced with permission of the copyright owner. Further reproduction prohibited without permission.

structural basin is required to produce the pre-graben, shelf-derived carbonate components; I suggest source areas either 1) to the northwest on Puerto Rico or the Virgin Islands Platform, or 2) to the east near Anguilla and Saba Bank. It appears likely that St. Croix has migrated and was uplifted due to the opening of the Virgin Islands Basin and Anegada Passage in the late Neogene. The creation of these seismically active features was probably dominated by transtensional movement with a significant left-lateral component of slip.

Other recent tectonic models propose that the opening of the Virgin Islands Basin and Anegada Passage was accomplished by right-lateral faulting in the Pliocene or the Quaternary. These models cannot be disproved by the structural and sedimentological evidence presented here, providing that the reversal in plate motion occurred after the range of depositional record on St. Croix. However, a right-lateral model is not supported by the orientation of faults through St. Croix strata deposited as recently as the Pliocene. In addition, incorporating such a model into known plate movements in the northeastern Caribbean requires several complicating assumptions that are not supported by seismic evidence.

I suggest that the present position of St. Croix was achieved by oblique sinistral faulting along the present Anegada Passage leading to the formation of the Virgin Islands Basin as a strike-slip basin. Assuming a constant rate of migration from a position directly south of Vieques, the migration rate for St. Croix would be approximately 6 to 7 mm/yr, with a total range of migration rates between 1 and 20 mm/yr.

Reproduced with permission of the copyright owner. Further reproduction prohibited without permission.

INTRODUCTION

St. Croix is a sedimentary island located inside the sweep of the Lesser Antilles arc. It is geographically separated from Puerto Rico and the Lesser Antilles by the 4500 m deep Virgin Islands Basin, the Anegada Passage and the St. Croix Basin (Fig. 2.1). However, St. Croix's thick sequence of Tertiary carbonates provides a record of Tertiary deposition and uplift at the juncture of the Lesser Antilles geologic provinces. The tectonics of this area are complicated, and at this point, remain controversial.

To this point, the Tertiary section of St. Croix has been viewed as a self-contained product of an isolated graben system. In the most recent interpretations (Whetten, 1966; Multer and others, 1977; Gerhard and others, 1978), the Tertiary section is either not tied to regional tectonics, or is interpreted to be solely the product of vertical tectonics. Based on outcrop evidence alone, these interpretations offer the simplest reasonable explanations of the development of St. Croix in the Neogene.

A drilling program undertaken in the past several years furnishes some constraints on the motion and timing of faulting on St. Croix, and provides a more detailed picture of St.Croix's sedimentary evolution during the Tertiary. This subsurface information, in conjunction with outcrop data, furnishes structural, sedimentological and paleontological information that allows the testing of several models of basin development. As a result, it is suggested here that St. Croix was not a static, isolated land mass during the Neogene, and instead required an external source of sediment during much of its development. The details of Neogene basin development bear both

Reproduced with permission of the copyright owner. Further reproduction prohibited without permission.

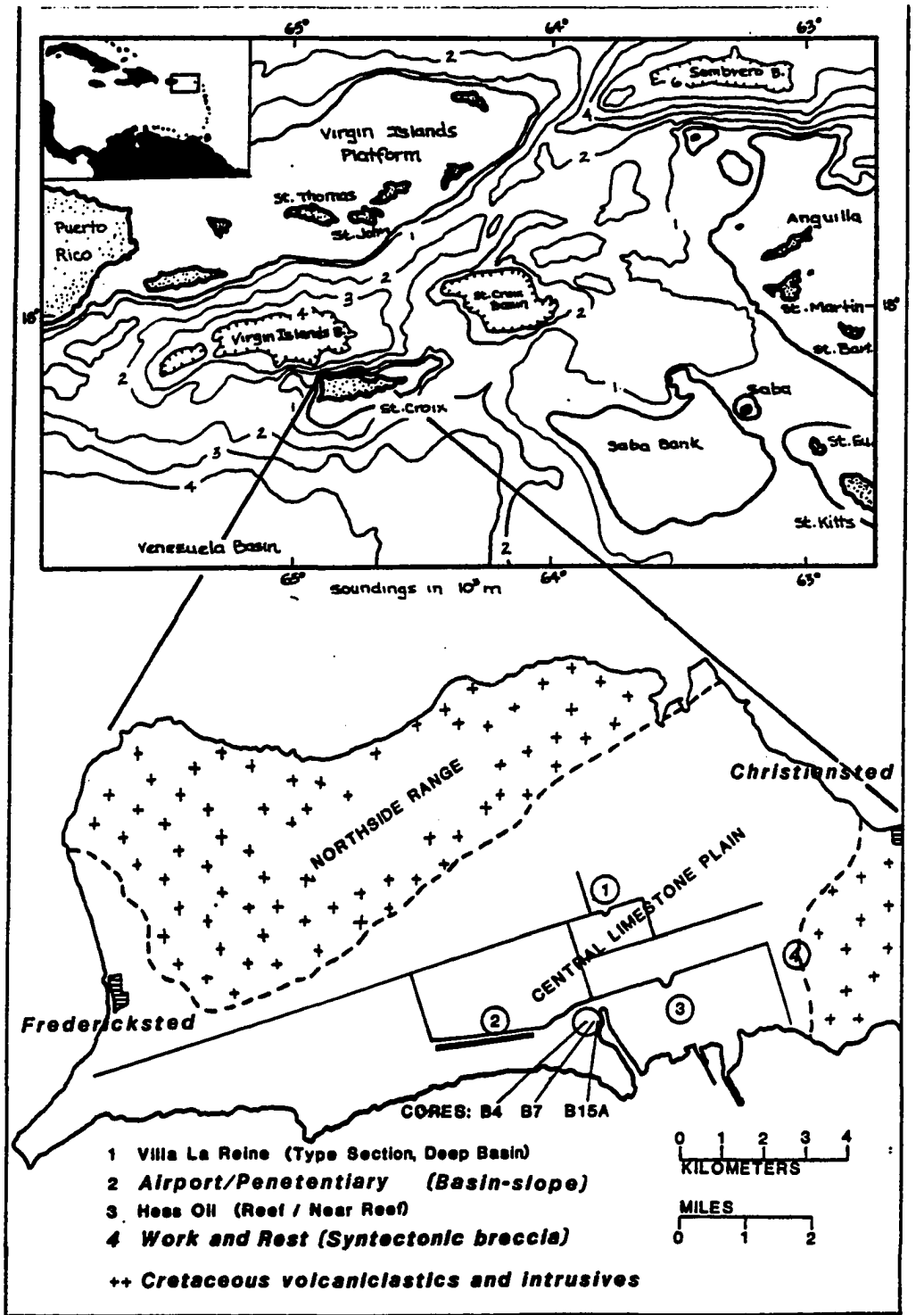

Figure 2.1. St. Croix location map and study area.

Reproduced with permission of the copyright owner. Further reproduction prohibited without permission.

directly and indirectly on the tectonics of the region, and these details are discussed in the following portions of this chapter.

Reproduced with permission of the copyright owner. Further reproduction prohibited without permission.

GEOLOGIC SETTING

St. Croix lies at the northwestern edge of the Lesser Antilles arc, approximately 176 km southeast of San Juan, Puerto Rico (Fig. 2.1). At its widest points, the island is 39 km long and 9 km wide, and covers a total of 207 sq. km. St. Croix is tectonically and geologically distinct from the majority of the primarily igneous islands of the Lesser Antilles.

The central plain of the island is formed by deposits of alluvium and exposures of the underlying Tertiary carbonate rocks (Fig. 2.2), and lies between the mountainous Eastend and Northside Ranges composed of Cretaceous siliciclastic and intrusive rocks of the Mt. Eagle Group. The Tertiary carbonates are contained within a graben that we will refer to as the *Kingshill-Jealousy Basin.* The rock units dealt with in this paper are (Figs. 2.3 and 2.4):

1) the Cretaceous *Mt. Eagle Group* that brackets the basin to the east and west, and presumably floors the graben;
2) the Miocene *Jealousy Formation*, consisting of grey-blue, planktonic foram-rich clays.
3) the Miocene *Kingshill Limestone*;
4) Carbonate units that overlie the Kingshill Limestone along the southern coast that will be referred to here as the *post-Kingshill limestones.* We subdivide this section into the *Mannings Bay Member* and the *Blessing Formation* (Figs. 2.3, 2.4).

Reproduced with permission of the copyright owner. Further reproduction prohibited without permission.

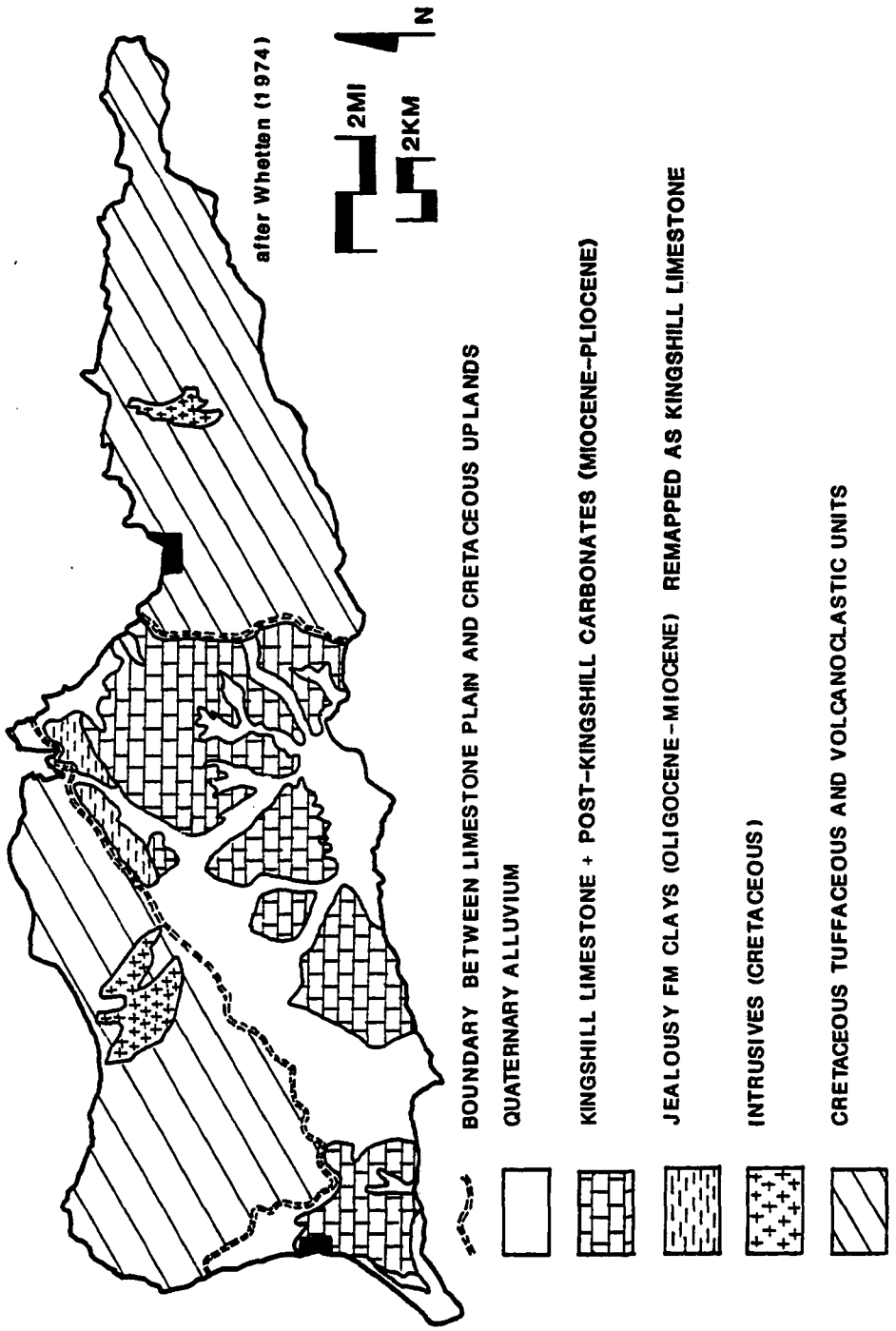

Figure 2.2. Generalized geologic map of St. Croix. Exposed strata mapped as Jealousy Formation by Whetten (1966) are re-mapped as Kingshill Limestone in this dissertation.

Reproduced with permission of the copyright owner. Further reproduction prohibited without permission.

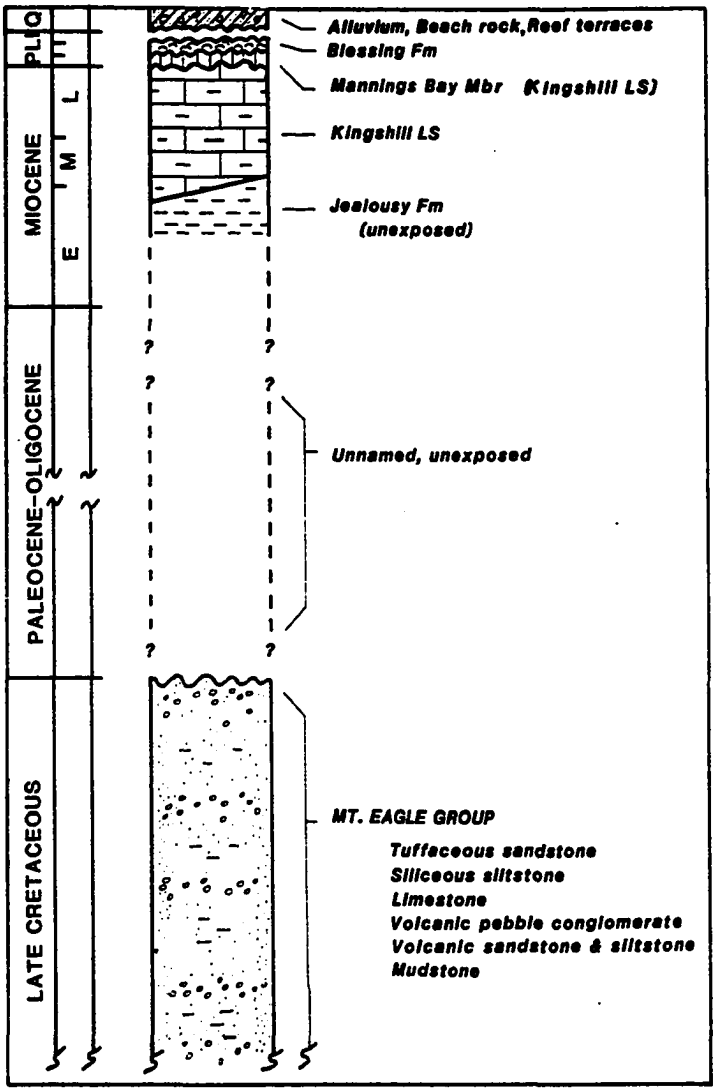

Figure 2.3. Generalized stratigraphic column including the underlying Cretaceous section; intrusives not shown. Due to its potential thickness, the Jealousy Formation may extend into the Paleogene. However, no samples earlier than the Miocene have been recovered from the Jealousy Formation.

The maximum known thickness of the Kingshill Limestone is close to 140 m in the carbonate highlands along the north coast of St. Croix. The total thickness of the combined carbonate section in the south coast area is unknown, but exceeds 90 m, the maximum drilling penetration for this project. The underlying sediments of the Jealousy Formation are at least 427 m thick based on drilling completed in 1939 (Cushman, 1946;

Reproduced with permission of the copyright owner. Further reproduction prohibited without permission.

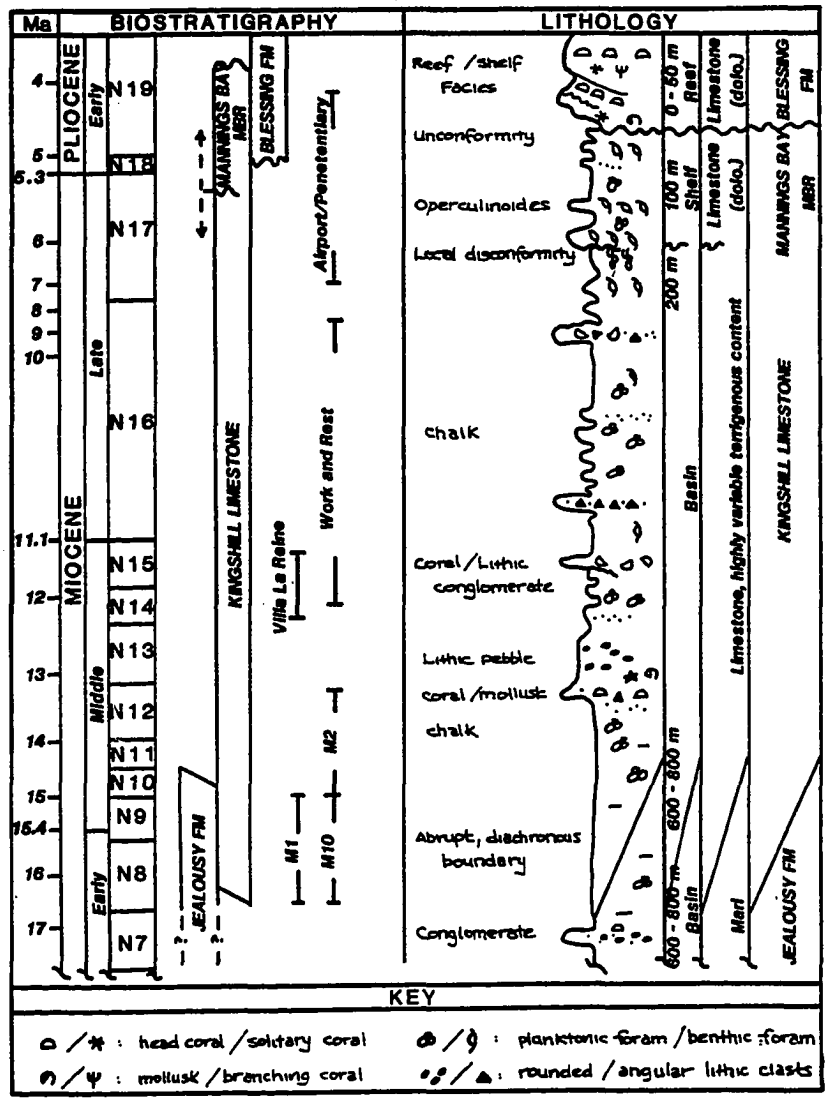

Figure 2.4. Expanded stratigraphic column showing the St. Croix Tertiary section, including chronologic, biostratigraphic and lithologic characteristics.

Cederstrom, 1950), and are estimated to be as much as 2000 m thick on the basis of gravity-anomaly surveys (Shurbet and others, 1956).

Although previous papers do not segregate the post-Kingshill carbonates from the Kingshill Limestone, we do so here because these strata are mappable, lithologically

Reproduced with permission of the copyright owner. Further reproduction prohibited without permission.

distinct from those of the Kingshill Limestone, and represent significantly different depositional environments.

Geologic Nomenclature

The nomenclature of the carbonate units on St. Croix has changed over the years and a short note will help to clarify matters. The name "Kingshill Series" was used by Kemp (1926) to describe the entire Tertiary section of St. Croix. Cederstrom (1950) used the terms "Kingshill Marl" to differentiate the carbonates from the underlying clays of the Jealousy Formation discovered during the deep drilling of 1938-39. Whetten (1966, 1974) followed the usage of Cederstrom (1950) as did Multer and others (1977), whereas Bold (1970) referred to the unit as the "Kingshill Formation". Gerhard and others (1978) formalized the name "Kingshill Limestone", and designated the type section at Villa La Reine (Outcrop 1, Fig. 2.1). This formalized usage has been adopted for this paper.

Reproduced with permission of the copyright owner. Further reproduction prohibited without permission.

METHODS

The cross-sections in this paper are based on borings drilled between 1984 and 1986, outcrop work, as well as water-well drilling logs and records from previous reports and government files. Records from these latter reports and drilling logs are summarized and described in Gill and Hubbard (1986; Appendix). The contact between the Kingshill Limestone and the underlying "blue clay" of the Jealousy Formation was selected as a stratigraphic marker due to its abruptness, presumed geologic importance, and ease of identification by untrained loggers.

Sampling

Test holes were drilled with a rotary drilling rig capable of sampling to 100 m. Friable or unconsolidated sediments were sampled at 1.5 or 3 m (5 or 10 ft) intervals with a split-spoon sampler and well-lithified material was collected with a diamond-bit core barrel. Core material from pre-existing test holes provides additional data on the carbonate units underlying the southeastern portion of the central plain.

Unconsolidated sediments were sieved into gravel-, sand- and mud size fractions. Further size analyses were not undertaken due to aggregation of carbonate grains and other diagenetic alteration. Whole-grain counts and mineralogical analysis by X-ray diffraction provide data on grain origin and composition. Thin sections were prepared from consolidated material and loose grain mounts, and were used for mineralogical and facies analysis.

Reproduced with permission of the copyright owner. Further reproduction prohibited without permission.

Logging

Test holes were geophysically logged with a portable gamma logging unit; in cases where hole collapse did not interfere, the test holes were also logged with a portable spontaneous potential and resistivity unit. The majority of the gamma logging was done through the steel auger that served as casing during the drilling process.

Biostratigraphy and micropaleontology

Micropaleontological work was done on the sand fraction (>63 μm) of relatively unaltered material. Disaggregation of the sediments was accomplished by soaking in Calgon solution. The planktonic foraminiferal biostratigraphy is detailed in Chapt. 1 (this dissertation). The zones are those of Bolli and Saunders (1985), with the "N-zones" of Blow (1979) also provided. A reference table of the species ranges used for these determinations is presented in Chapt. 1.

Discussion of the paleoenvironmental significance of the foraminifera relies chiefly on the occurrences of seventeen types of benthic foraminifera whose bathymetric significance is relatively well-understood. Their ranges within the well sections are used to resolve the paleobathymetry of the subsurface strata. A more detailed discussion of the paleobathymetry and benthic foraminifera can be found in Chapt. 1 (this dissertation).

Reproduced with permission of the copyright owner. Further reproduction prohibited without permission.

RESULTS

Summary of Test Hole Sampling

The term "test hole" refers to a drilled hole from which geologic samples or information have been retrieved and is distinguished from wells drilled specifically for water.

Fourteen test holes were drilled to a maximum depth of 91 m with the cumulative depth of drilling exceeding 580 m. Two additional samples from the Jealousy Formation (GP-41 and PL-149) were taken from hollow-stem auger cuttings from private water wells. In addition, samples from several engineering test holes were provided by Caribbean Drilling Services and TAMS Inc. The locations of wells used for the construction of cross-sections can be found in Figure. 2.5. Drilling records for each hole, as well as detailed descriptions of lithology are appended.

Jealousy Formation

The Jealousy Formation underlies the Central Plain of St. Croix, and can be considered the hydrologic basement. The downward transition from yellowish carbonates and marls of the Kingshill Limestone to the blueish carbonates and marls of the Jealousy Formation is marked and abrupt. Well drillers almost invariably stop after reaching the Jealousy Formation, colloquially called the "blue clay", and the boundary is well marked on their drill logs. The Jealousy Formation contains a rich planktonic-foraminiferal assemblage that allows both paleoenvironmental analysis and biostratigraphic correlation.

Reproduced with permission of the copyright owner. Further reproduction prohibited without permission.

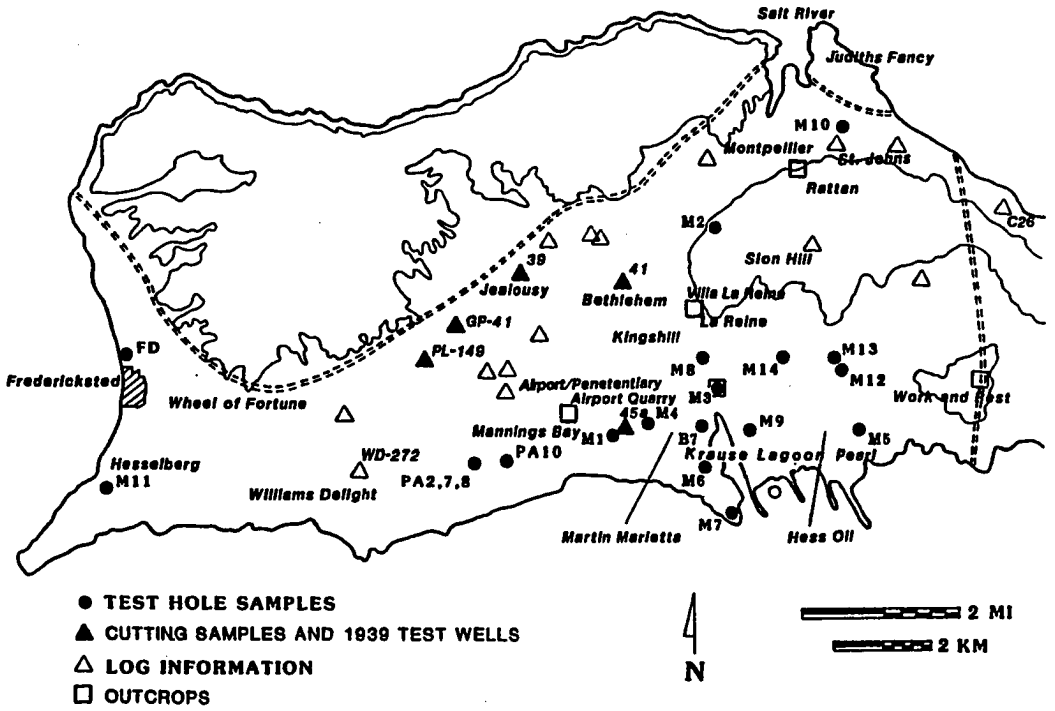

Figure 2.5. Locations of outcrops, test holes and water wells used in the stratigraphic cross sections.

The type section for the Jealousy Formation is defined as the interval from the deepest penetrating test well drilled by the Civilian Conservation Corps in 1939 (Test well 41, Figs. 2.5, 2.6). This well penetrated more than 426 m of Jealousy Formation sediments (Cederstrom, 1950), which gravity surveys indicate may be as much as 2000 m thick (Shurbet and others, 1956).

Conglomeratic deposits are noted at various depths in the Jealousy Formation (Cederstrom, 1950) but were not encountered in the holes drilled for this project. However, none of the test holes drilled for this project penetrated more than 8 m of Jealousy Formation clays (Figs. 2.6, 2.7).

Reproduced with permission of the copyright owner. Further reproduction prohibited without permission.

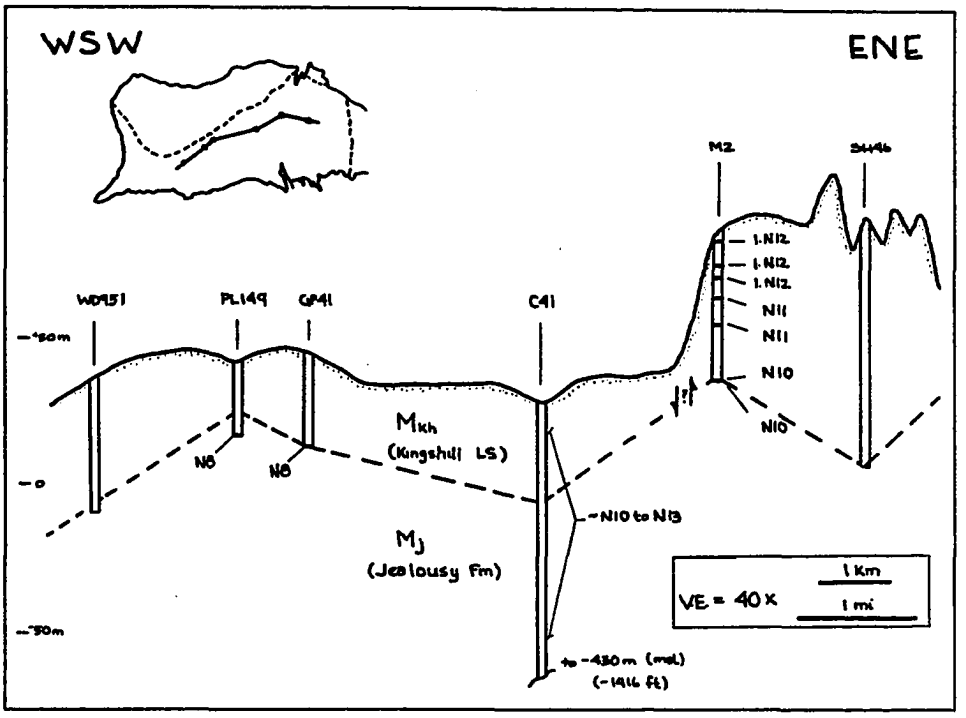

Figure 2.6. East-west biostratigraphic cross section. N-zones of Blow (1979) determined on core samples as shown.

Biostratigraphy and Lithology.

Samples from the Jealousy Formation range from upper lower Miocene (N8) to lower middle Miocene (N10). Since no documented Jealousy Formation strata extend beyond the early Miocene, the Jealousy Formation is accurately referred to as a *Miocene* and not an *Oligocene* unit (Chapt. 1, this dissertation). It is possible that the Jealousy Formation extends into the Oligocene or earlier, however, given a potential thickness of 1800 m (Shurbet and others, 1956),

Samples taken for this project were uniformly fine-grained planktonic-foraminiferal muds. However, Cederstrom (1950) notes that the Jealousy Formation extends beyond the reach of the drill as a blue or grey "clay" formation interrupted by conglomerate or thin limestone layers. Because the conglomeratic layers are bracketed

Reproduced with permission of the copyright owner. Further reproduction prohibited without permission.

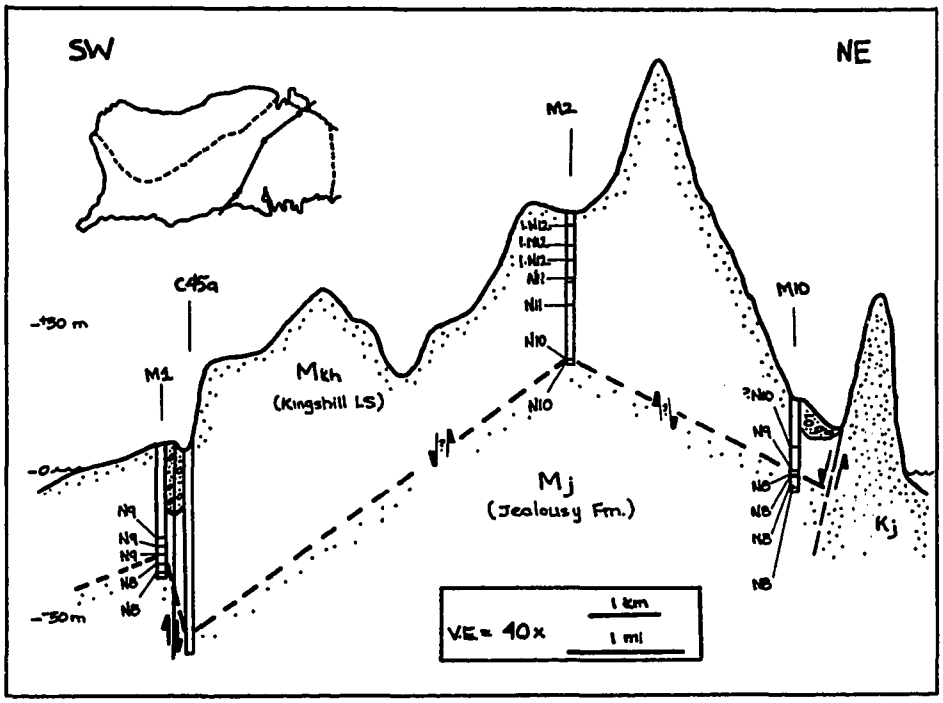

Figure 2.7. North-south biostratigraphic cross section. N-zones of Blow (1979) determined for test hole samples as shown.

both above and below by the pelagic blue clays, they are best interpreted as allochthonous deposits, and must therefore be derived from some nearby sediment source.

In all of our samples, Jealousy Formation sediments are dominantly calcite, with significant components of quartz, feldspars and clay minerals. The sand fraction is composed almost entirely of planktonic foraminifera. Insoluble residues from the Jealousy Formation range from 30 to 51%, and powder-mount x-ray diffractograms from the Jealousy Formation are indistinguishable from diffractograms from the immediately overlying Kingshill Limestone, described below.

Reproduced with permission of the copyright owner. Further reproduction prohibited without permission.

Based on preliminary data, the mineralogy of the Jealousy Formation does not change within the basin, or within the stratigraphic section sampled. No samples of the Jealousy Formation from previous reports are presently available, so no comment can be made on the mineralogy at greater depths.

Biofacies.

All samples collected from the Jealousy Formation contain benthic foraminiferal species generally associated with middle and upper bathyal environments and includes species not commonly found above the middle bathyal zone (Chapt. 1, this dissertation).

This foraminiferal fauna indicates that the Jealousy Formation was deposited in a marine setting in 600 to 800 m of water, rather than in an estuarine setting as previously interpreted (cf. Bold, 1970; Multer and others, 1977; Lidz, 1982). In addition, the fauna does not indicate shallowing anywhere within the Kingshill-Jealousy basin, even toward the extreme basin margins. This finding is difficult to reconcile with the notion of 1) a steep, fault-sided basin which should contain a substantial debris apron, or 2) a basin with substantial estuarine environments along its edges.

Structure.

The surface of the Jealousy Formation is characterized by three general trends (Figs. 2.8, 2.9, 2.10):

1) a marked upbowing of the surface beneath the highlands in the northern section of the central plain;
2) gentle dip toward the northern and southern coasts of St. Croix;

Reproduced with permission of the copyright owner. Further reproduction prohibited without permission.

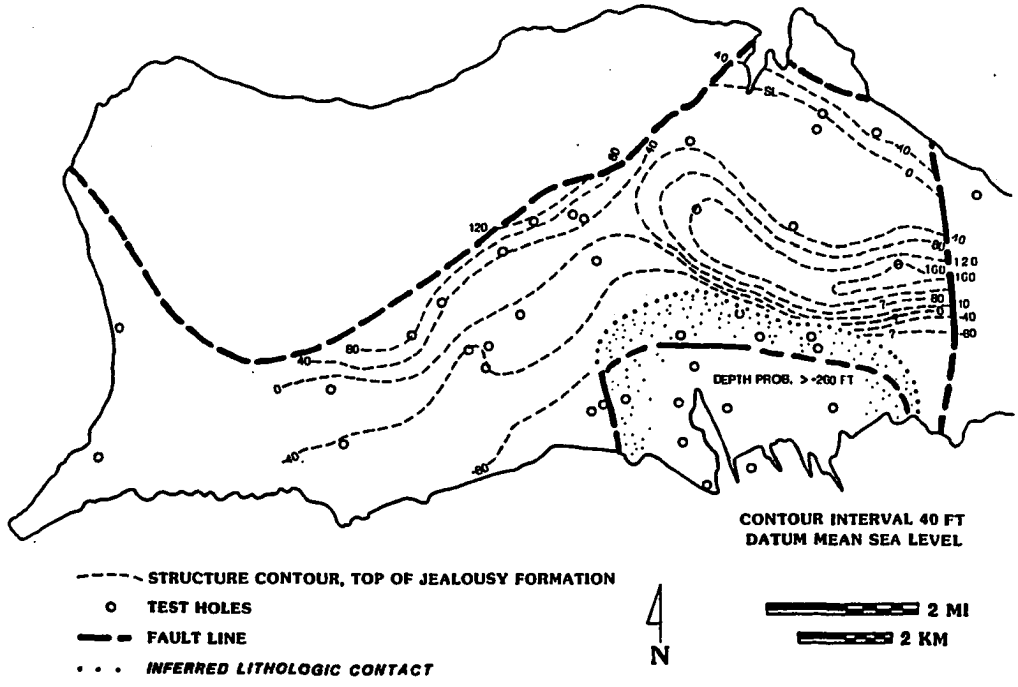

Figure 2.8. Structure map: top of the Jealousy Formation. Well control is sparse along the eastern fault boundary of the Tertiary limestones. No Jealousy Formation sediments were encountered within the southeastern coastal section of the Central Plain, which is a graben or demi-graben structure. Depth to Jealousy Formation sediments in this area exceeds 80 m.

3) a pronounced rise of the Jealousy Formation surface close to the fault boundary imposed by the Northside Range (Figs. 2.8, 2.9).

The depth to the Jealousy Formation surface close to the eastern fault boundary is unknown because of poor well control (Fig. 2.8). Similarly, the depth to the Jealousy Formation surface in the southeastern coastal section is not known due to local faulting, which places the upper surface of the Jealousy Formation beyond 80 m, the maximum penetration of the drill (Fig.2.10).

The rise of the Jealousy Formation surface close to the northwestern fault boundary is produced by block faulting on the Kingshill-Jealousy basin margins, and

Reproduced with permission of the copyright owner. Further reproduction prohibited without permission.

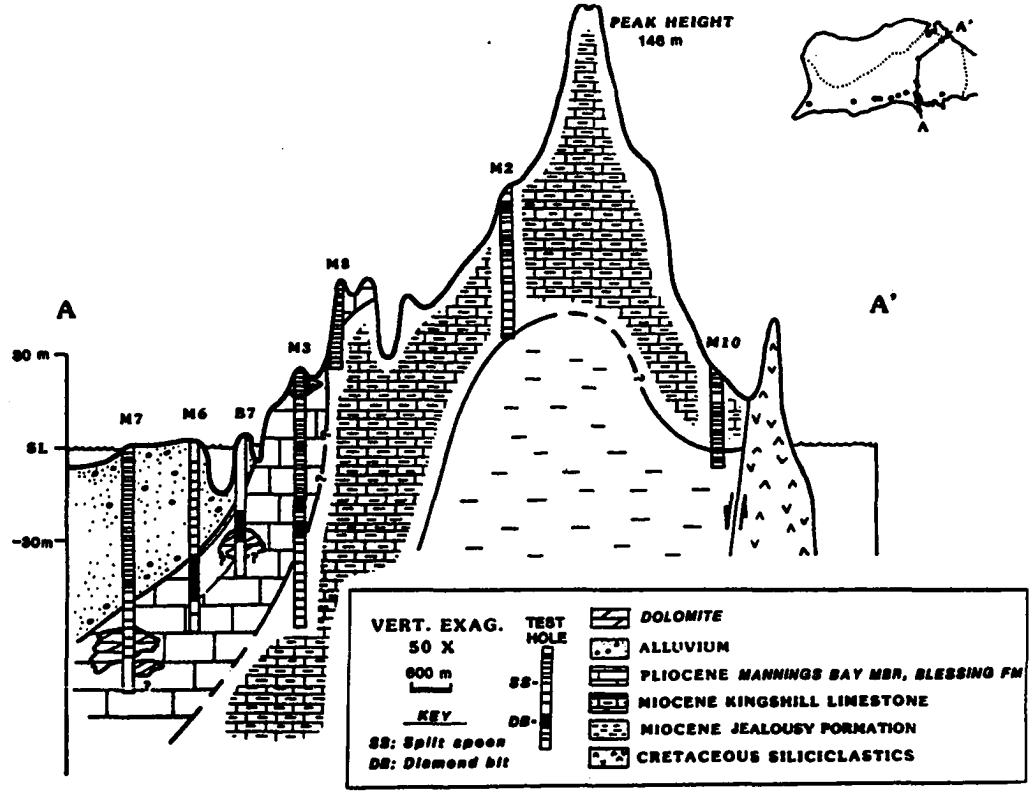

Figure 2.9. Cross section A-A': Krause Lagoon to Judiths Fancy. Note that the Jealousy Formation surface roughly follows the topography of the Kingshill Limestone. Sample depths are shown for each test hole.

indicates that faulting started or continued after the deposition of the Jealousy Formation in this area (Fig. 2.8). It is more difficult to interpret the other trends of the Jealousy Formation surface since it is not clear what causes the marked color change between the Jealousy Formation and the overlying Kingshill Limestone. This is discussed further in the following section.

Distribution.

The Jealousy Formation is found in the subsurface throughout the Central Plains region as documented both by our drilling program and by Cederstrom (1950) and Robison (1972). In addition to the subsurface occurrences, Cederstrom (1950) mapped

Reproduced with permission of the copyright owner. Further reproduction prohibited without permission.

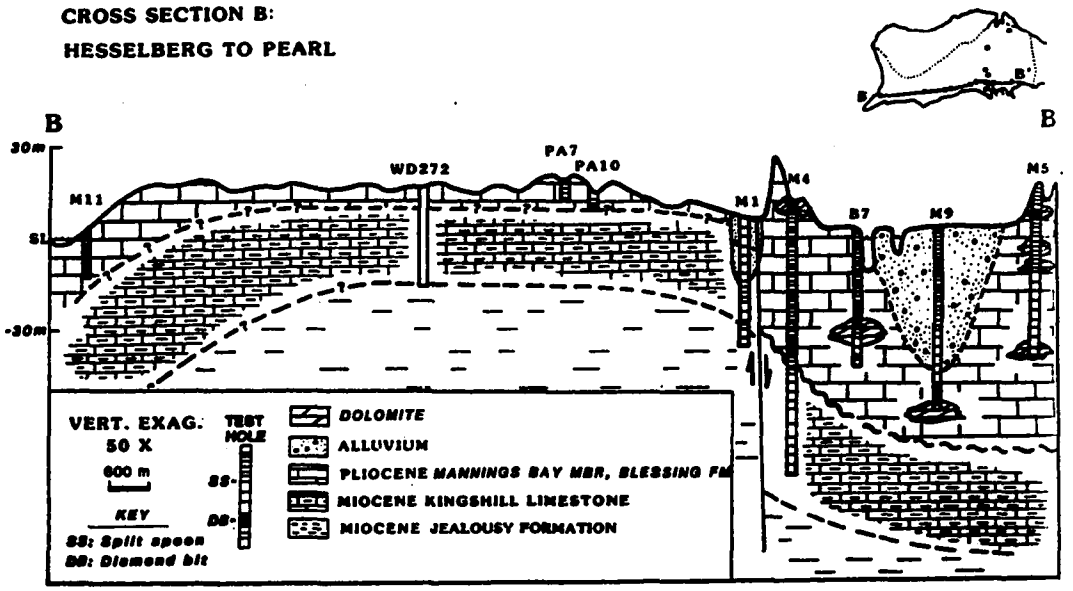

Figure 2.10. Cross section B-B': Estate Hesselberg to Pearl. A normal fault forming the western boundary of the subsidiary graben block occurs between test holes M1 and M4. The Jealousy Formation was not reached the east of this fault.

several areas in the Northside Range as Jealousy Formation, correlating the calcareous conglomerate he found there with the basal conglomerate he encountered in Test well 39 (Fig. 2.5).

Whetten (1966) extended this interpretation by mapping extensive areas of calcareous conglomerates and marls in the Northside Range and Judith Fancy areas as Jealousy Formation. We suggest that these strata are more correctly mapped as Kingshill Limestone, following the suggestion of Gerhard and others (1978). The reasoning for this is based on the following:

1) the exposed units in the Northside Range bear no resemblance to the Jealousy Formation sediments recovered by drilling for this project (Gill and Hubbard, 1987);

Reproduced with permission of the copyright owner. Further reproduction prohibited without permission.

2) "weathered exposures show apparent conformity and gradational lithologies between the conglomerates and true Kingshill..." (Gerhard and others, 1978); the range of facies included in the Kingshill Limestone easily encompasses the conglomeratic beds referred to here.

3) The exposures in the Northside Range occur at similar altitudes, and contain similar lithologic facies as outcrops of Kingshill Limestone in the other parts of the island (Fig. 2.5).

4) the biostratigraphic age represented by these exposures is within the age range of Kingshill Limestone deposition (Bold, 1970; Bold *in* Gill and Hubbard, 1986; Chapt.1, this dissertation).

The Jealousy Formation was encountered outside the graben boundaries as well. Blue clay was penetrated about 18 m below sea level in Test well C26 to the east of the bounding fault (Fig. 2.5) and was tentatively identified as Jealousy Formation (Cederstrom, 1950). The presence of Jealousy Formation sediments outside of the structural basin boundaries indicates that the Jealousy Formation is not confined solely to the Kingshill-Jealousy Basin, and that Jealousy deposition preceded basinal faulting.

Kingshill Limestone

The Kingshill Limestone outcrops throughout the Central Plain region. Samples of the Kingshill Limestone were taken from outcrop as well as test holes,and display a range of facies from planktonic-foraminiferal oozes to shelf-derived coral debris

Reproduced with permission of the copyright owner. Further reproduction prohibited without permission.

(Gerhard and others, 1978). In general, the Kingshill Limestone has a gentle southerly dip, and the outcrops young to the south.

Biostratigraphy and Lithology.

Deposition of the Kingshill Limestone, including those portions exposed in outcrop, spans the range from the lower Miocene (N8) to close to the Mio-Pliocene boundary (N17). The subsurface section sampled in our drilling program spans a narrower range, from lower Miocene (N8) in Wells M1 and M10, to middle Miocene (N12) in the upper parts of Well M2.

The lithology of the lowermost Kingshill Limestone is not detectably different from that of the immediately underlying Jealousy Formation. The marked color contrast between the upper Jealousy Formation and the lowermost Kingshill Limestone does not reflect a significant change in either age, depositional pattern or mineralogy. The two units represent a continuous record of deposition, and the cause and significance of the color change between the Kingshill Limestone and the Jealousy Formation is unknown.

The lower Kingshill Limestone in the St. John/Judiths Fancy area has been interpreted by Gerhard and others (1978), Lidz (1982) and Andreieff and others (1986) as shelf and lagoon deposits. These interpretations were based on the presence of rounded terrigenous gravel, as well as shallow-water fauna that include echinoids and benthic forams. However, these deposits are bracketed above in outcrop, and below in Test Well M10 (Fig. 2.5), by pelagic and hemipelagic carbonates. For this reason, it is more reasonable to interpret these sediments as allochthonous, deposited in basinal conditions similar to those reflected elsewhere in the Kingshill Limestone.

Reproduced with permission of the copyright owner. Further reproduction prohibited without permission.

Deposition of the type-section at Villa la Reine occurred in the late middle Miocene, and is characterized by a variety of depositional styles in outcrop (Figs. 2.1, 2.11). Sediments of this age range were not recovered in our core samples, and we rely on outcrop samples for information on deposition during this time period. Our interpretation of the age of this outcrop agrees closely with Multer and others (1977) and Andreieff and others (1986), but differs from Lidz (1982). The biostratigraphy of the type section is described in more detail in Chapt. 1 (this dissertation).

Sediments in the type-section represent several lithologic facies types, and range from pelagic and hemipelagic layers to boulder-sized coral heads with accompanying shelf-derived lithic and carbonate debris. The environment of deposition, however, is similar to that of the strata previously described. Although the contribution of shallow-derived material is pronounced in the later strata of the Kingshill Limestone, the foraminiferal faunas in beds that over- and underlie the debris flows and turbidites closely resemble the faunas in earlier deposition. I agree with Multer and others (1977) in interpreting these outcrops as representing basinal accumulations and suggest that the water depths represented here are closely comparable to the middle bathyal depths of underlying strata.

Work and Rest Exposures.-- The outcrop exposures along the eastern fault contact between the Kingshill Limestone and Cretaceous Mt. Eagle Group rocks have been placed biostratigraphically between upper middle and lower upper Miocene (N14 to N16), and are most likely upper middle Miocene (N15; Chapt. 1, this dissertation). In these exposures, angular clasts of presumably Mt. Eagle Series rock form layers of breccia between beds of carbonate Kingshill Limestone. Similar beds are interpreted to

Reproduced with permission of the copyright owner. Further reproduction prohibited without permission.

Figure 2.11. Photograph of the Villa La Reine outcrop, type section of the Kingshill Limestone. Arnie Miller for scale.

represent a syntectonic breccia (Gerhard and others, 1978) in an outcrop that could not be located for this study. However, the fault contact in this area is sharp and well marked, and the contact zone is characterized by breakage of both Cretaceous and Kingshill strata. This indicates that at least a portion of the Kingshill Limestone was deposited before the formation of the basin boundary fault on the eastern border. Lacking more conclusive data, I suggest similar fault timing on the western basin fault as well.

Reproduced with permission of the copyright owner. Further reproduction prohibited without permission.

Late Kingshill deposition.-- Outcrops south of the Villa la Reine type section lie stratigraphically above the type section and express significantly different depositional character. In the Airport/Penetentiary Cut (Figs. 2.1, 2.12), the upper Kingshill strata show increasing incursions of shelf-derived carbonate sands as well as burrowing, indicating basin shallowing. Uppermost Kingshill Limestone strata are directly overlain by a disconformity surface that separates the Kingshill Limestone from the overlying Mannings Bay Member.

Strata in the Airport/Penetentiary exposure range from upper Miocene (N17) to lower Pliocene above the disconformity chosen as the upper boundary of the Kingshill Limestone (Gill and Hubbard, 1986; Chapt. 1, in prep.).

Biofacies.

The benthic foraminifera of the Kingshill Limestone in Test Wells M1, M2, and M10 differ little from those of the underlying Jealousy Formation (Table 2). The faunal differences that exist do not reflect any significant environmental shifts from the setting of the Jealousy Formation. Like the Jealousy Formation, the Kingshill Limestone was deposited in the upper part of the middle bathyal zone between 600 and 800 m. Significant basinal shallowing does not occur until close to the top of the formation at the Mannings Bay Member boundary. A more complete description of the benthic foraminiferal faunas can be found in Chapt. 1 (this dissertation).

Structure.

The contacts between the Kingshill Limestone and the Cretaceous rocks are interpreted as faults by Whetten (1966) and Multer and others, (1977). Biostratigraphic evidence from fault breccias in the eastern Kingshill Limestone/Cretaceous contact

Reproduced with permission of the copyright owner. Further reproduction prohibited without permission.

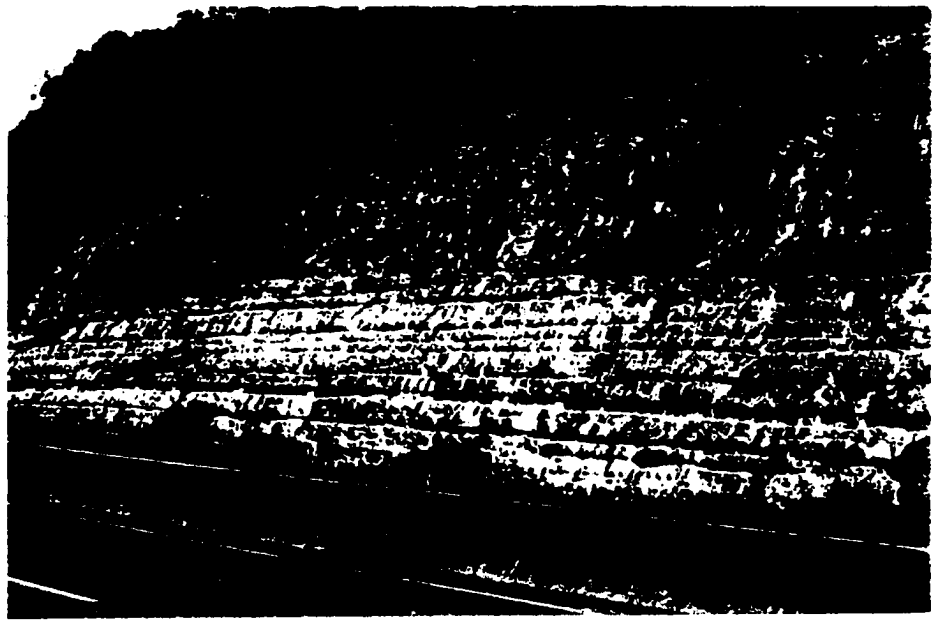

Figure 2.12. Photograph of the Airport/Penetentiary outcrop. Note the disconformity about midway up the outcrop (approx. 7 m above road level) corresponding to the lower Kingshill Limestone/Mannings Bay Member contact.

discussed above, indicates that basin faulting had occurred prior to late middle Miocene (outcrop 4, Fig. 2.1). The contact against the Northside Range is mostly obscured by alluvial cover (Fig.2.2). Gerhard and others (1978) suggest with some evidence that there was less displacement along this northern fault boundary than along the eastern basin margin. A north-south cross section through the island (Fig. 2.9) shows the marked upbowing of the Jealousy Formation and Kingshill Limestone strata under the highlands close to the northern coast.

Distribution.

The thickness of the Kingshill Limestone is reported by Cederstrom (1950) to range from 0 to 180 m, the larger figure referring to extrapolated thickness in the carbonate highlands of the Rattan Hill area. The maximum thickness of Kingshill

Reproduced with permission of the copyright owner. Further reproduction prohibited without permission.

Limestone encountered during this project is about 140 m (Fig. 2.9). Isopach patterns of the Kingshill Limestone are shown in Figure 2.13, and reveal three major trends:

1) pinching out toward the north and northwest margins of the basin;
2) pronounced thickening in the carbonate highlands close to the northern coast of St. Croix;
3) gentle thickening toward the south of the basin, interrupted by post-depositional faulting along the south coast (Fig. 2.13).

Well control for the Kingshill Limestone section is poorest within the faulted section of post-Kingshill carbonates on the south coast, and to the west of Estate Williams Delight (Fig. 2.5). In general, Kingshill Limestone thickness patterns follow the trends shown by the Jealousy Formation structure map (Fig. 2.8). If deformation is ignored, the Kingshill Limestone isopach patterns imply a basin opening to the south but deepest in the section presently occupied by the carbonate highlands.

It should be noted that only three of the 14 test holes drilled for this project completely penetrated the Kingshill Limestone and encountered Jealousy Formation muds (Test Holes M1, M2 and M10 at Fairplain, Bonne Esperance and St. John respectively, Fig. 2.5). The other holes, drilled for the most part on the southern coast, penetrate extensive thicknesses of limestone. The majority of this limestone is Mannings Bay Member and Blessing Formation carbonate deposition and therefore the total thickness of Kingshill Limestone in the southeastern region is unknown.

These stratigraphic relationships are illustrated in Figure 2.10. The Jealousy Formation underlies the Kingshill Limestone across most of the south coast of St.

Reproduced with permission of the copyright owner. Further reproduction prohibited without permission.

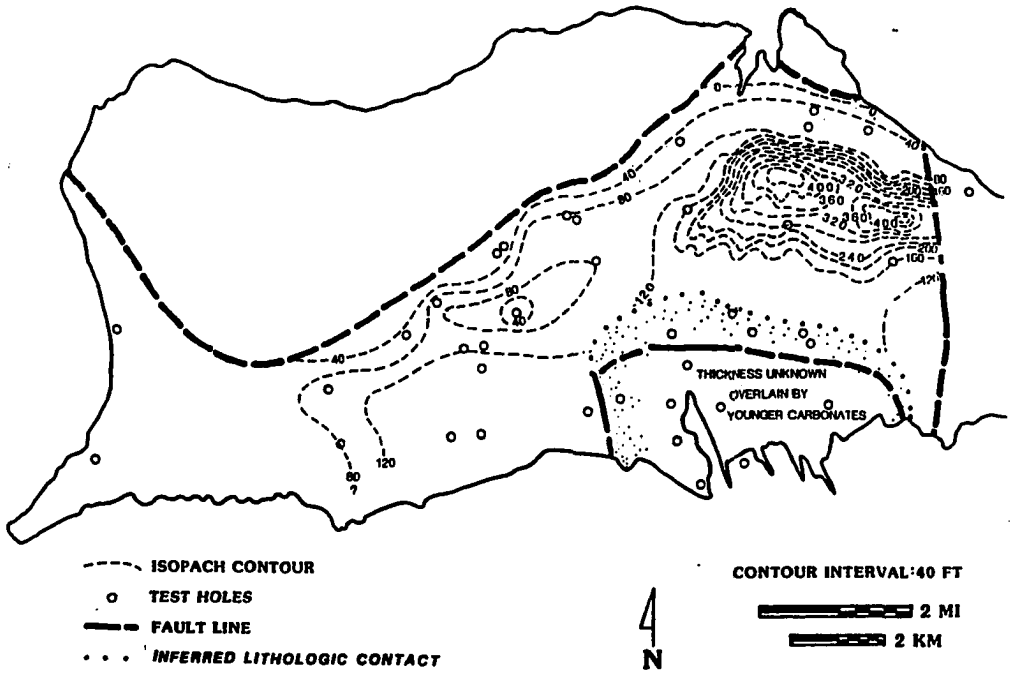

Figure 2.13. Isopach map of the Kingshill Limestone; the contoured area represents the Central Limestone Plain region. The thickest known areas of the Kingshill Limestone correspond with areas of high topographic relief. If the hilly limestone areas were produced structurally, they have not existed long enough to be planed down by erosion. Well data are sparse along the eastern fault boundary, and the Kingshill Limestone was not penetrated to its base within the subsidiary graben in the southeastern Central Plain.

Croix. The position of the Kingshill Limestone/Jealousy Formation contact is unknown west of Estate Williams Delight due to poor core control, and east of Estate Anguilla due to faulting within the Tertiary section between Test Holes M1 and M4 (Figs. 2.5, 2.10).

Mannings Bay Member

The Mio-Pliocene Mannings Bay Member of the Kingshill Limestone is characterized by sediment-gravity flows of larger benthic foraminifera. These rocks were included in the Kingshill Limestone by Gerhard and others (1978) but are described here

Reproduced with permission of the copyright owner. Further reproduction prohibited without permission.

as a separate member. The Mannings Bay Member is exposed in outcrop along portions of Evans Highway, primarily in the Airport/Penetentiary cut (Figs. 2.1, 2.12), and in a quarry on the southeastern side of Mannings Hill that we suggest as a type section (Figs. 2.1, 2.14). Subsurface Mannings Bay Member strata were also encountered in several of the test wells drilled for this project.

Biostratigraphy and Lithology.

The possible stratigraphic range of the Mannings Bay Member is between the top of the upper Miocene (upper N17) and the top of the lower Pliocene (upper N19; Chapt. 1, this dissertation). It is not possible to further refine stratigraphic placement due to extensive diagenetic alteration.

However, the onset of deposits of larger foraminifera signals the establishment of an environment that does not have an analog in modern carbonate enviroments. The assemblage includes, and is dominated in places by the nummulitid forams *Operculinoides cojimarensis* and *Paraspiroclypeus chawneri* (Behrens, 1976; S. Frost, pers. comm., 1986; Gerhard and others, 1978). These larger forams sometimes show signs of transport or reworking, such as fracturing, abrasion, and imbrication. In foraminiferal wackestone strata the matrix also includes significant quantities of planktonic foraminifera, including the ubiquitous *Orbulina universa* and *Globigerina* spp.

Larger forams such as *Operculinoides* and *Paraspiroclypeus* were more than likely photic zone forms (Frost, pers. comm. 1986) and temporarily dominated St. Croix shallow carbonate environments. Other bioclasts that contribute significantly to the facies are coralline algal crusts and rhodoliths, shallow benthic foraminifera such as

Reproduced with permission of the copyright owner. Further reproduction prohibited without permission.

Figure 2.14. Photograph of the Airport Quarry outcrop. The unconformity at the top of the photo marks the Mannings Bay/Blessing Formation contact.

Archaeis and *Amphistigina*, and echinoid spines and plate fragments. Minor coral fragments and molluscan debris are also part of the assemblage, but are represented mostly by external molds and pore space in the cores.

Biofacies.

The bioclast assemblage in the Mannings Bay Member is described above, and was analyzed from thin sections. Whole-test benthic foraminiferal assemblages were not analyzed due to extensive diagenetic alteration. However, the presence of both shallow and poorly developed deep-water planktonic foraminifera suggests deposition in approximately 100 m of water (Chapt. 1, this dissertation).

Reproduced with permission of the copyright owner. Further reproduction prohibited without permission.

Structure.

The western margin of the Mannings Bay and Blessing carbonates lies against a fault contact near Fairplain. Test Hole M1 at Fairplain reaches Jealousy Formation clays at -29 m msl (Fig.2.15). Test hole M4, less than 180 m to the east, does not contact Jealousy Formation material despite penetration to 80 m below sea level. Similarly, Test hole 45a, drilled 60 m to the east of M1 (Fig. 2.5), strikes Jealousy Formation sediments more than 24 m deeper, indicating a steeply dipping fault zone.

The presence of a fault at this location is supported by surface displacements as well. Strata in the Evan's Highway outcrop to the west of Well M1 (Fig. 2.1) dip toward the fault line, and the Kingshill/Mannings Bay Member contact is elevated 24 m above sea level. In Well M4, this contact is not reached until approximately 55 m below sea level, setting a minimum fault displacement of 79 m. In addition, River and Bethlehem Guts, two ephemeral streams, run along the presumed line of the fault close to the coastline (Fig. 2.5).

Faulting through these strata indicates significant tectonic activity after deposition of both the Kingshill Limestone and post-Kingshill carbonates, and therefore extends the time of fault activity into the Pliocene. However, it is not obvious how far, and in what direction the Fairplain fault continues. Some indication is given by disrupted stream flow patterns to the east of Test Hole M1.

Stream flow along a line between Holes M8 and M3, extending from River Gut eastward to Hole M5, is oriented parallel to the coastline rather than north-south and directly into the sea. The area of stream diversion also corresponds to the lateral extent of the exposed reef facies. We suggest that the topography in this area is partly the

Reproduced with permission of the copyright owner. Further reproduction prohibited without permission.

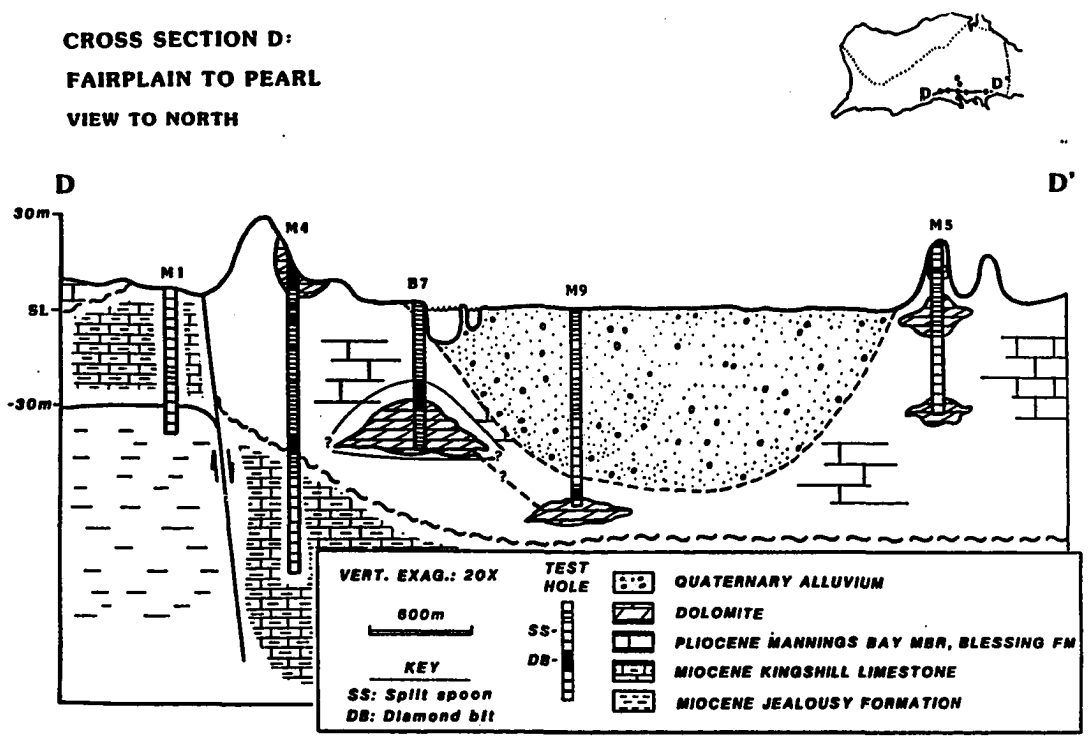

Figure 2.15. Cross section D-D': Estate Fairplain to Pearl. The normal fault between Test wells M1 and M4 displaces Jealousy Formation, Kingshill Limestone and post-Kingshill strata. The age of the faulting therefore probably extends into the Pliocene.

result of reef development patterns, but also marks the location of the hingeline of a half-graben or graben block that contains most of the post-Kingshill sediments (Fig.2.16).

Distribution.

The Mannings Bay Member overlies the disconformity in the Airport/Penetentiary exposure, discussed in the last section, and underlies the reef and lagoon facies that comprise the Blessing Formation. Large thicknesses of the Mannings Bay Member are preserved in a small down-dropped block just discussed (Gill and Hubbard, 1986, 1987).

Reproduced with permission of the copyright owner. Further reproduction prohibited without permission.

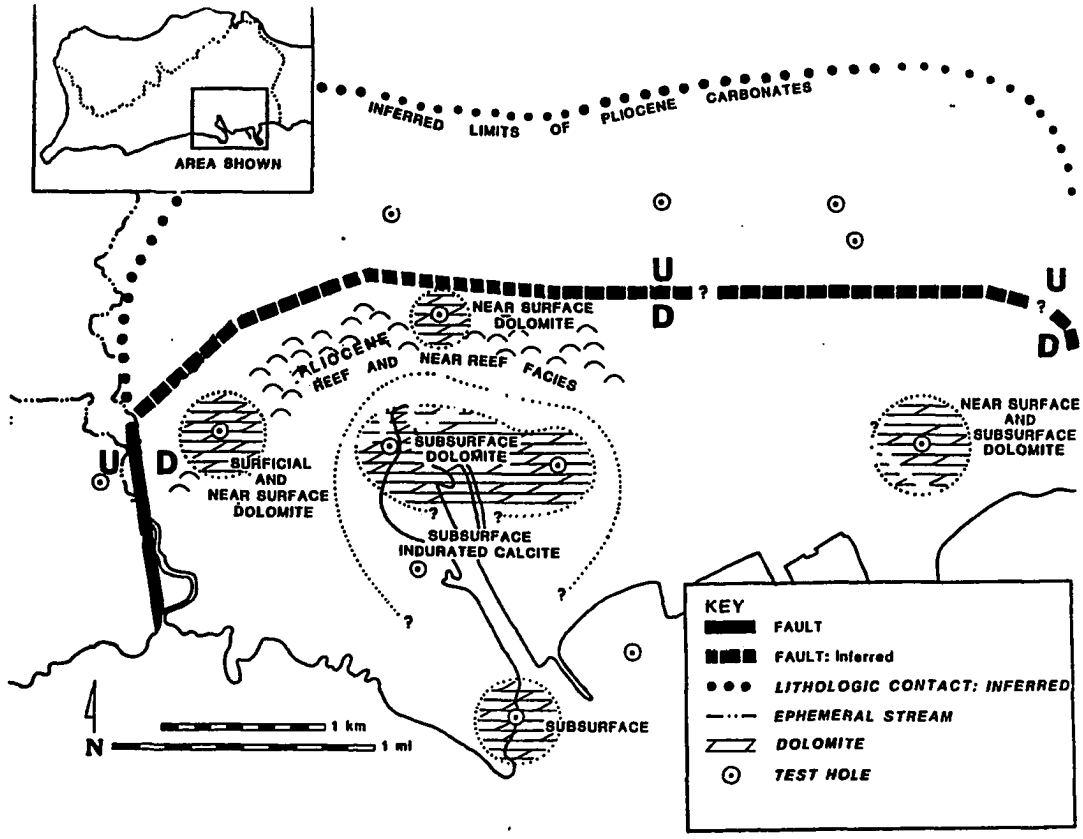

Figure 2.16. Facies map: south coast industrial area. Dolomite in the vadose zone or exposed in outcrop is patchily distributed in an arcuate region following the Pliocene reef trend. Dolomite presently in the phreatic zone is found in off-shore facies. The western boundary of the subsidiary graben is well-defined by a normal fault. The northern and eastern boundaries are poorly known.

Based on our core material, we assign the lower boundary of the post-Kingshill facies to 44 m below sea level in Test Hole M4 (Fig. 2.10). The transition is marked by a change in dominance from the deep-water planktic fauna of the Kingshill Limestone to the mixture of planktonic and shelf-derived benthic fauna of the Mannings Bay Member. The core material from Test Hole M4 indicates that the Mannings Bay Member extends for at least 56 m subsurface.

Reproduced with permission of the copyright owner. Further reproduction prohibited without permission.

Blessing Formation

The Blessing Formation represents a Pliocene reef and lagoon system that extended across the southern and western coastlines of St. Croix (Fig. 2.17), with the greatest exposure in the Hess Cut outcrop which we suggest as the type-section (Figs.2.1, 2.18). Like the Mannings Bay Member, the greatest thickness of the Blessing Formation is contained within a subsidiary graben block in the southeastern coastal section of the Central Plain region.

Stratigraphy and Lithology.

Deposition of the Blessing Formation occurred in the lower Pliocene (Andreieff and others,1986; Chapt. 1, this dissertation). This assignment is based on planktonic foraminifera and is further supported by stratigraphic position of the Blessing Formation relative to underlying units, and the occurrence of larger benthic forams and scleractinians.

Exposures and core samples of the Blessing Formation contain a macrofaunal assemblage represented by external molds of scleractinians, gastropods and pelecypods, as well as skeletal debris from forams, coralline algae and a wide variety of shallow-water invertebrates. The scleractinians include several extant genera (*Agaricia* , *Diploria*, *Montastrea* , *Siderastrea* , among others) as well as extinct solitary corals such as *Stylophora* spp., *Teliophyllia* sp. and *Thysanus* sp. In general, the different faunal assemblages within the Blessing Formation represent
co-existing reef, forereef, and lagoon environments that extended along the southern and western coastlines of St. Croix.

Reproduced with permission of the copyright owner. Further reproduction prohibited without permission.

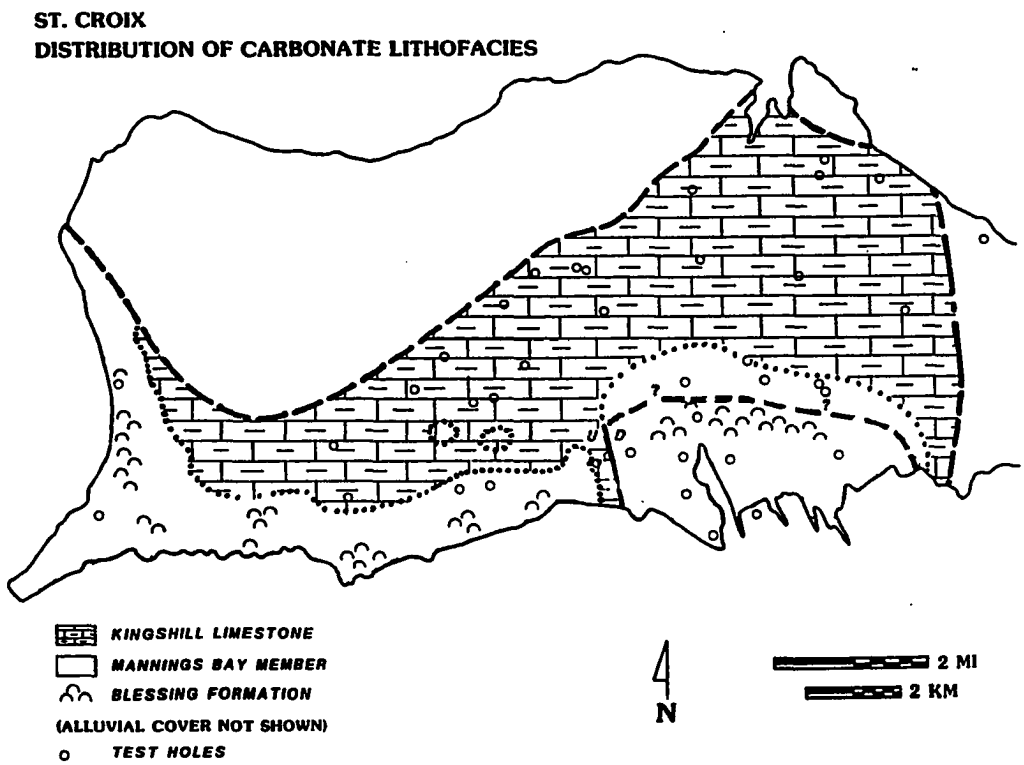

Figure 2.17. Distribution of carbonate lithofacies, St. Croix Central Plain. The greatest thickness of post-Kingshill carbonate accumulation occurs in the subsidiary graben block in the southeastern corner of the Central Plain. A thinner veneer of reefal material, presumably correlative with the accumulation in the graben, stretches around the southern and western coastlines of the island.

Structure.

The structure of both the Mannings Hill and the Blessing Formations is discussed in an earlier section. Fault displacement of Blessing Formation strata indicates continuing normal fault activity as recently as the lower Pliocene, and perhaps younger.

Distribution.

The greatest accumulation of Blessing Formation sediments, is found in the subsurface to the east of the Fairplain fault mentioned in a previous section. The thickness of the Blessing Formation in this area may reach 30 m and indicates that the

Reproduced with permission of the copyright owner. Further reproduction prohibited without permission.

Figure 2.18 Photographs of the Hess Cut outcrop.

Upper photo: oblique view looking north-northwest, rent a wreck for scale. Apparent "bedding" dipping from upper left to lower right is actually bulldozer scarring.

Lower photo: Hardground and exposure surfaces in the Blessing Formation reef tract. Rock hammer and field book for scale.

Reproduced with permission of the copyright owner. Further reproduction prohibited without permission.

fault activity controlled both the accumulation and preservation of reef facies. It should be noted that towards the western end of St. Croix, core control is poor and outcrop exposures are sparse. For this reason the age and nature of the reef facies in this area are speculative. Test hole locations are shown in Figure 2.5, and outcrops west of the Airport/Penetentiary outcrop are limited to scattered exposures along the highway, around Fredericksted, and a reef exposure described by Gerhard and others (1978) The maximum thickness of the Blessing Formation west of the fault at Fairplain is estimated to be between 10 and 20 m.

Dolomitization and diagenesis.

The Pliocene carbonates show patchy areas of dolomitization both in the surface and subsurface (Fig. 2.16). No dolomite has been detected anywhere else on St. Croix. Based on its stratigraphic position, the dolomitization occurred during or following the Pliocene, and is discussed in more detail in Chapt. 3 (this dissertation).

Subsurface dissolution, reflected in voids encountered during drilling, occurs in the post-Kingshill carbonates but have not been encountered in the Kingshill Limestone. Adequate permeability for significant dissolution of post-Kingshill strata exists today, since flowing artesian conditions were encountered during the drilling of Test Hole M7 (Fig. 2.5).

Well-cemented, undulating layers within the Hess outcrop (Fig. 2.1) correspond to marked light stable-isotopic excursions and karsting, and indicate subaerial exposure. The pattern of exposure surfaces in the Blessing Formation strata indicates that the southern shoreline was exposed several times during the Pliocene. The exact chronology of the exposures is uncertain.

Reproduced with permission of the copyright owner. Further reproduction prohibited without permission.

DISCUSSION: EVOLUTION OF THE KINGSHILL BASIN

Previous models for the evolution of St. Croix call for a static, insular land mass during the deposition of the Tertiary section. Whetten (1966) suggested that the Tertiary section was deposited in a graben in the central part of the island, and that the carbonate rocks were reefal and estuarine deposits. He concluded that there was no significant evidence for strike-slip motion north of St. Croix, and that the Tertiary section was affected only by vertical tectonics.

More recent interpretations, (e.g. Multer and others, 1977; Gerhard and others, 1978), suggest instead that the Kingshill Limestone was deposited in a trough-shaped seaway. The seaway was open to the northeast and southwest, and basin conditions were similar to deep marine settings north of the present island of St. Croix. The structural context outlined by Whetten (1966) has been accepted by later workers, but the interpretation of the Kingshill Limestone was changed from a reef environment to deep marine conditions between 500 and 750 m. More recent studies of St. Croix geology build from this framework (e.g. Lidz, 1982), but do not materially change the basic outline of basin development.

Earlier studies also suggest that the Tertiary section of St. Croix is the product of a general sea level rise between the Oligocene and the middle Miocene (Gerhard and others, 1978). The Jealousy has been interpreted as an Oligocene estuarine deposit (Multer and others, 1977), primarily on the basis of biostratigraphic assignments by Cushman (1946) and Vaughn and Henbest in Cederstrom (1950) and.ostracode ecological affinities as interpreted by Bold (1970).

Reproduced with permission of the copyright owner. Further reproduction prohibited without permission.

I suggest instead that the Kingshill-Jealousy Basin formed much later, during or after deposition of the Kingshill Limestone, and that the horst blocks that bracketed the basin were not available as a sediment source for the Jealousy Formation. The implications of this are that the Kingshill-Jealousy Basin required an external sediment source, and that St. Croix could not have been in its present location in order to receive these sediments. In addition, the Jealousy Formation appears everywhere in our samples to be a basinal Miocene unit, rather than an estuarine unit, and is dominated by a foraminiferal assemblage indicative of bathyal water depths (Chapt. 1, this dissertation).

In the following sections, we will discuss the development of Neogene St. Croix starting with the Jealousy Formation and ending with a discussion of the tectonic implications of the subsurface data and basin evolution model.

Deposition of the Jealousy Formation

Environment of deposition.

We differ from previous interpretations of the Jealousy Formation in several ways. In particular, the Jealousy Formation represents deep basinal accumulation throughout its sampled extent. The depth of the basin during the deposition of the Jealousy Formation apparently did not change 1) over the period of time represented by our samples; 2) over the geographic range from the western boundary of the present basin to the center; or 3) along a transect from the southern to the northern coastline.

Reproduced with permission of the copyright owner. Further reproduction prohibited without permission.

These conclusions are based on 1) the bathyal affinities of the benthic foraminiferal fauna, 2) the dominance of planktonic foraminifera, and 3) the fact that all conglomeratic layers are bracketed above and below by pelagic sediments.

Timing of graben formation.

Previous workers suggest that the Kingshill-Jealousy Basin formed in the Oligocene as a result of vertical tectonic movement. In particular, Whetten (1966) suggested that the central lowlands on St. Croix sank in a subsiding graben during the Oligocene, following a period of low-rank metamorphism, faulting, folding, igneous intrusion and uplift.

In contrast, we suggest that the present graben boundaries could not have been formed before the end of the early Miocene because:

1) Jealousy Formation sediments close to the Northside Range do not show evidence of basinal shallowing.
2) Jealousy Formation sediments exist outside of the confines of the graben.
3) Jealousy Formation sediments are Miocene, not Oligocene in age.

Regarding the first point, above, if bathyal Jealousy Formation sediments were deposited in a graben with a minimum depth of 600 m, the basin slope would exceed 45 degrees. These calculations use the measured distance from the test hole samples to the basin margin, and assume that the edges of the basin were subaerially exposed. This slope angle is comparable to that of the present St. Croix island slope, which shows marked trends of shallowing and shelf-derived sedimentation (Hubbard and others, 1983; Gill, 1983) as well as contributions from reef foraminifera such as *Amphistigina*

Reproduced with permission of the copyright owner. Further reproduction prohibited without permission.

(B. Sen Gupta and S. Lukert, pers. comm., 1984). Neither of these effects is seen in the Jealousy Formation near the northwestern basin boundary.

Regarding the second point above, the existence of Jealousy Formation sediments in Test Well C-26 .outside the graben boundary suggests that Jealousy deposition was not confined to the graben, and may have preceded basin faulting. In contrast, Lidz (1988) places the basin boundary fault to the east of Well C-26, presumably to place Well C-26 within the graben system. However, her placement of the fault line is not supported by field evidence, and is outside the Kingshill/Cretaceous contact mapped by Cederstrom (1950), Whetten (1966), and Gill and Hubbard (1986).

In summary, the Jealousy Formation was deposited in 600 to 800 m of water, and represents deep-marine depositional conditions. On the basis of the evidence discussed above, the graben block which now forms the Kingshill-Jealousy basin could not have been active before the early Miocene (Fig. 2.19a). The timing of basin formation is discussed further in a later section on the deposition of the Kingshill Limestone.

Tectonic Implications of Jealousy Formation deposition.

The points discussed above are relevant to the tectonics of the region as well. If the Kingshill-Jealousy Basin did not form before the middle Miocene, then the shelf-derived sediments in the Jealousy Formation must be derived from outside of the present island of St. Croix. Multer and others (1977) envisioned the Northside Range and the Eastend Range hills as subaerially exposed horst blocks, providing both terrigenous sediments and shelf-derived carbonates. For the reasons discussed above, these horst

Reproduced with permission of the copyright owner. Further reproduction prohibited without permission.

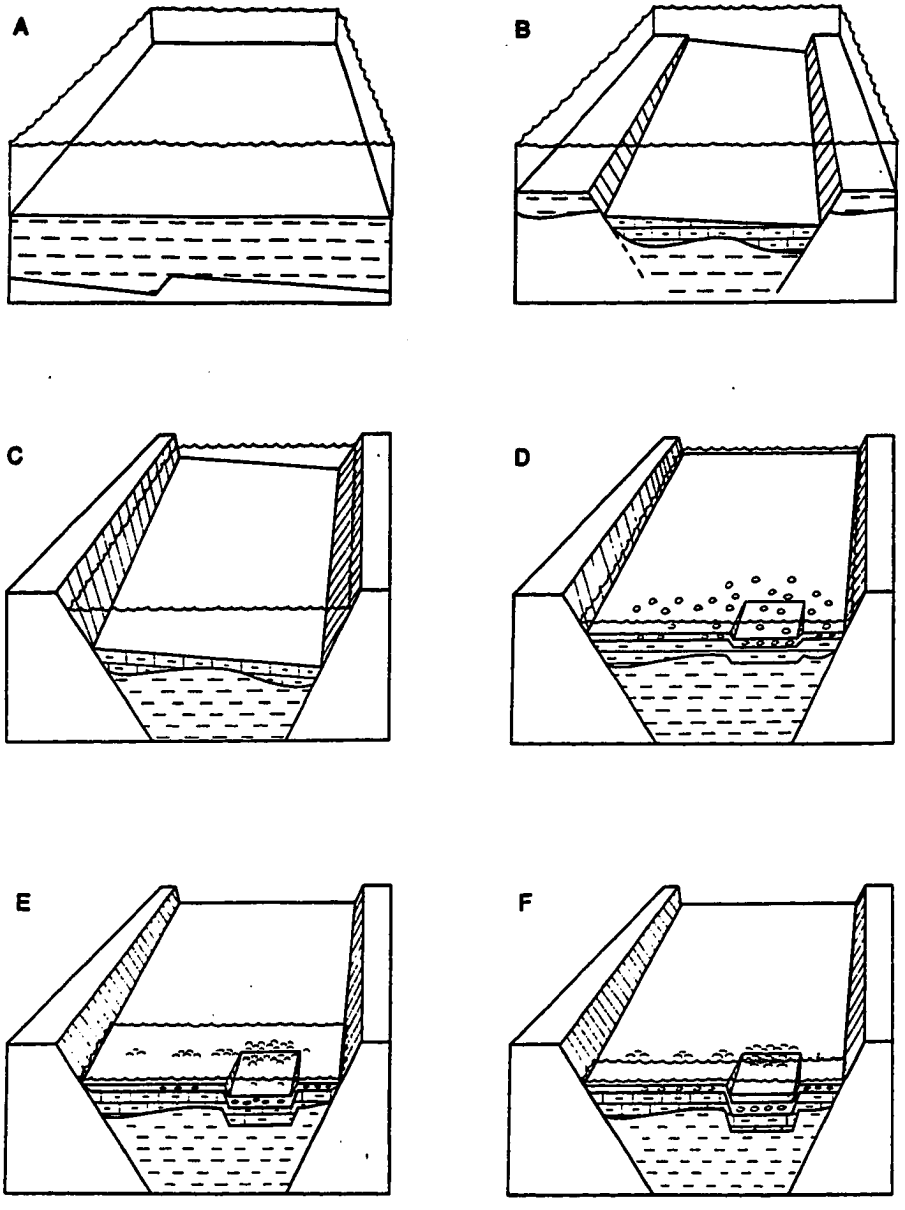

Figure. 2.19. Block models of St. Croix during the early Miocene.
A) Deposition of the Jealousy Formation in the early Miocene prior to formation of the graben system..
B) Deposition of the lower Kingshill Limestone in the latest early Miocene shortly after initiation of graben faulting. Note Jealousy Formation sediments on the horst blocks.
C) Deposition of the Kingshill Limestone in the middle Miocene.
D) Deposition of the Mannings Bay Member foraminiferal banks in the latest Miocene to early Pliocene and initiation of faulting in the subsidiary graben along the southern coastline..
E) Establishment of the Blessing Formation Reef Tract, early Pliocene.
F) Emergence and resubmergence of the Blessing Formation reefs.

Reproduced with permission of the copyright owner. Further reproduction prohibited without permission.

blocks could not have been emergent during the deposition of the lower Jealousy Formation (Fig. 2.19a), and therefore St. Croix :

1) must have been close to a land mass capable of supporting reef growth and supplying clastic materials, and
2) must have been deep enough to accumulate pelagic sediment.

We feel that Puerto Rico and the Virgin Islands Platform, to the northwest of St. Croix, and Anguilla and Saba, to the northeast, are possible source areas. Either source area requires significant lateral translation of the St. Croix platform.

Deposition of the Kingshill Limestone

The lowermost strata of the Kingshill Limestone were deposited in the same bathyal conditions as the immediately underlying strata of the Jealousy Formation (Fig. 2.19b). There are no changes in sediment character, and no changes in basin depth. Tectonic or eustatic changes, if they occurred in this period, either were not substantial enough to be detectable, or cancelled each other out. The origin of the sharp color change between the two formations remains undetermined, but may reflect differences in detrital or authigenic clays, or diagenetic effects.

Upsection, the dominance of shelf-derived sediments in outcrop may suggest an increase in shelf-derived sedimentation. This increase may reflect the onset of basinal faulting and the initial exposure of the Northside and Eastend ranges as horst blocks (Fig. 2.19c), providing deposits in the Work and Rest area are correctly interpreted as syntectonic breccias.

Reproduced with permission of the copyright owner. Further reproduction prohibited without permission.

Lidz (1982), Gerhard (1978) and Andreieff and others (1986) called for extensive shallow-water environments to prevail during deposition of Kingshill sediments in the St. John and Salt river areas (Fig. 2.5). Because these sediments contain rounded terrigenous gravel and abundant shallow-water fauna, a shelf environment of deposition is a reasonable interpretation. However, we disagree with a shallow-water interpretation for the following reasons:

1) these sediments are over- and underlain by basinal Kingshill sediments.
2) these sediments lie in close proximity to the edge of the graben, and to other obviously transported sediments along the fault in the Northside Range.

For these reasons, it is more reasonable to assume that the Kingshill Limestone deposits in the St. John/Salt River areas are allochthonous, and were deposited at bathyal depths. To interpret these outcrops as in-situ shelf accumulations (Lidz,1982; Gerhard and others, 1978) would require a 600 m shallowing from bathyal depths to shelf conditions, followed by a drop back to bathyal depths. This "basketball" tectonic history is complex, and is not documented anywhere else in the basin.

Shallowing of the Kingshill-Jealousy Basin only becomes apparent upsection at the southern edge of the Central Plain at the Airport/Penetentiary outcrop (Figs.2.1, 2.12). Here the Kingshill Limestone contains increasing quantities of shelf-derived sand, is burrowed, and is capped by a disconformity. The disconformity in this outcrop, which separates the Kingshill Limestone from the overlying Mannings Bay Member, was interpreted by Lidz (1984) as evidence of basinal shallowing caused by eustatic fall at the end of the Miocene. However, there is no evidence to interpret the

Reproduced with permission of the copyright owner. Further reproduction prohibited without permission.

unconformity as being caused by subaerial exposure (Lidz, 1984): no caliche, no karsting, and no terra rosa. Instead, the disconformity appears to be the result of submarine erosion caused by partly channelized flows of shelf-derived sediment. The amount of missing section represented by the disconformity may or may not be significant, and the corresponding hiatus is not resolveable by biostratigraphy (Chapt. 1, this dissertation). Due to the difficulties in resolving the biostratigraphic placement of the section, the timing of this disconformity cannot accurately be restricted to the Miocene/Pliocene boundary (Chapt. 1, this dissertation) let alone the Messinian eustatic drop.

Our interpretation of the disconformity is that the beds both below and above the disconformity surface represent tectonic shallowing and submarine erosion in the upper Miocene Kingshill-Jealousy Basin. The presence of a planktonic foraminiferal fauna that includes both shallow and deep water forms implies that the deposition of the uppermost Kingshill Limestone occurred in approximately 200 m of water (Chapt. 1, this dissertation).

Structural setting.

The fault relations between the Kingshill Limestone and the Cretaceous strata on the eastern boundary fault indicates that the Kingshill Limestone existed prior to and during basin faulting (Gill and Hubbard, 1986; 1987).

We suggest that initiation of the St. Croix fault system occurred no earlier than between the late early Miocene, on the basis of evidence discussed earlier, and the late middle Miocene (Fig. 2.19b), on the basis of the age of fault brecciation along the eastern edge of the basin. The Villa la Reine outcrop, as well as the rest of the exposed

Reproduced with permission of the copyright owner. Further reproduction prohibited without permission.

Kingshill Limestone section in the northern and central portions of the graben lies within this time range (Andreieff and others, 1986; Chapt. 1, this dissertation).

Tectonic Implications of Kingshill Limestone deposition.

The initiation of normal faulting during deposition of the Kingshill Limestone implies the onset of tensional tectonic stress oriented roughly along the long axis of St. Croix. Since prior deformation in the Cretaceous section appears to be dominantly compressional in nature, normal faulting in the Tertiary section represents a change in tectonic regime. One mechanism that could account for the change would be the onset of slippage along a major transcurrent fault north of St. Croix. These relationships are discussed in more detail in the section on tectonic development.

Reproduced with permission of the copyright owner. Further reproduction prohibited without permission.

Deposition of the Mannings Bay Member

The unconformable contact between the underlying Kingshill Limestone and the Mannings Bay Member signals both basin shallowing and the development of a shallow-water source of larger benthic forams, in particular *Operculinoides cojimarensis* and *Paraspiroclypeus chawneri*.. We agree with Gerhard and others (1978) in suggesting that extensive foraminiferal banks existed on St. Croix in the late Neogene (Fig. 2.19d).

The foraminiferal-coralline algal bank environment is not represented on St. Croix today and benthic forams may have replaced scleractinians as the dominant shelf carbonate producers during the Neogene. We suggest that local bathymetric controls may have played a major role in the control of community structure. During early basin shoaling, the Kingshill-Jealousy basin may have been at too great a depth to allow extensive coral reef growth because of limited light or reduced temperatures. The uplift of the basin left previously established reefs exposed to erosion, and hindered the establishment of new reef systems.

Alternatively, the relative lack of coral-derived carbonates could simply be the result of 1) the storage of reef debris upslope, with minor deposition only at sporadic intervals (e.g. Moore and others, 1976) or 2) changes in circulation patterns leading to nutrient or temperature conditions yielding competitive advantage to the foram-algal community.

Regardless of the cause, the nummulitid foram-algal facies marks a period of deposition when shallow-water carbonate production was dominated by benthic forams and coralline algae at the expense of scleractinian communities. The prominence of larger

Reproduced with permission of the copyright owner. Further reproduction prohibited without permission.

foraminifera-coralline algal communities in the Tertiary, and the lack of modern analogs, are points of interest outside the Caribbean region as well. More to the point of the Kingshill-Jealousy basin, these deposits mark basin shallowing from bathyal depths to outer platform or upper slope environments of around 100 m water depths (Fig. 2.19d).

Structural and tectonic setting.

The structural setting of the basin during the latest Miocene was quite similar to that of previous depositional periods. From a tectonic standpoint, the fault that cuts through the post-Kingshill units demonstrates that normal faulting, and therefore a tensional tectonic regime, extends into at least the Pliocene if not later. The orientation of this fault is roughly parallel to the orientation of the northeast-southwest trending main basin boundary faults, suggesting that the driving mechanism for the faulting is the same for both the basin boundary faults and the subsidiary "post-Kingshill" graben.

The fact that the greatest thickness of post-Kingshill facies is preserved in the graben implies that deposition was concentrated in this subsidiary depositional basin, or that the strata were preserved by down-faulting in the graben during island uplift. The former alternative suggests that topographic relief existed prior to and during deposition of the nummulitic facies, whereas the latter alternative requires only that post-depositional faulting occurred. We suggest that both alternatives are likely here, and that the subsidiary basin existed as an entity during and after the deposition of the nummulitid facies. The incorporation of reworked, cemented planktonic forams from the Kingshill Limestone in the post-Kingshill rocks demonstrates that erosion of the uplands area has removed significant section from the Kingshill Limestone and, by inference, the post-Kingshill rocks as well.

Reproduced with permission of the copyright owner. Further reproduction prohibited without permission.

The facies represented in the post-Kingshill rocks indicate that basinal shallowing had occurred by the latest-Miocene or early Pliocene. As discussed earlier, Lidz (1984) correlates this shallowing to the Messinian eustatic drop which occurred at approximately the same time. However, it is important to recognize that the majority of the shallowing in the Kingshill-Jealousy Basin was due to tectonic uplift. Neglecting eustatic variation, the Kingshill-Jealousy Basin shallowed from approximately 750 m of water depth in the middle Miocene to approximately 100 m water depth in the lower Pliocene (N17). The rate of uplift suggested by these estimates is 650 m of vertical movement over roughly 9 million years. This translates to a mimimum uplift of 72 m/Ma, or slightly less than 0.1 mm/y.

These calculations are based on the following assumptions:

1) the uplift took place evenly between the middle Miocene and the early Pliocene.
2) the foraminiferal biozones on St. Croix are equivalent to the biozones established elsewhere in the Caribbean;
3) the basin depth in the middle Miocene was between 600 and 800 m.

If these assumptions are correct, then the estimates correspond to a *minimum* estimate of uplift rate. If the actual uplift began later in the Neogene, the average rate of uplift would be higher. A *maximum* rate of uplift, calculated with uplift beginning in the uppermost Kingshill Limestone, would correspond to 650 m of vertical uplift over a time span of 3.5 million years (the approximate length of biozone N17), or 0.2 mm/y. This uplift culminated in the establishment of a Pliocene reef tract represented by the Blessing Formation.

Reproduced with permission of the copyright owner. Further reproduction prohibited without permission.

Deposition of the Blessing Formation

Continued shoaling of the Kingshill-Jealousy Basin resulted in the deposition of the Blessing Formation reef tract which apparently extended around the southern and western shorelines of St. Croix (Fig. 2.19e). The reef tract consisted of interspersed reefs and shelf systems similar to the arrangement of reefs around the southern coastlines of St. Croix today. The classic reef model with flanking fore- and back-reef beds does not appear to apply here. Reef facies on St. Croix apparently formed planar deposits with little topographic relief. This planar geometry is apparently common in Caribbean Tertiary reef deposits (S. Frost, pers. comm.).

Exposure and relative sealevel change.

The Blessing Formation contains several indications of exposure, as well as an on-lap surface near the Hess Oil Refinery. The conclusion to be drawn here is that during the deposition of the Blessing Formation, St. Croix experienced at least one period of Pliocene subaerial exposure along its southern coastline (Fig. 2.19f).

Structural setting.

The greatest thickness of reef growth occurred at what is now the industrial area on the south-central coastline, with the geographical distribution suggesting that faulting in the subsidiary graben affected sedimentation in the Blessing Formation as well as the Manning Hill Formation.. The arcuate distribution of reef and lagoonal facies in this area indicates that the area was an embayment during the establishment of the reefs (Fig. 2.16) with the size and shape of the embayment controlled by faulting in the Krause Lagoon area. The dominance of reef growth in the industrial area is not simply an

Reproduced with permission of the copyright owner. Further reproduction prohibited without permission.

artifact of the greater available outcrop exposure, but also represents a concentration of reef development in this area.

Tectonic implications.

Normal faulting of Blessing Formation sediments indicates that tectonic activity continued on St. Croix through the latest periods of Tertiary deposition, and therefore extended into the Pliocene or later. The fault orientation is poorly known, but appears to strike north-south at the location of test wells M1 and 45a (Fig. 2.5), which suggests that tensional tectonics continued throughout the period of Tertiary deposition on St. Croix.

Uplift continued during this time, and eustatic variation along with tectonic uplift account for the repeated exposure of Blessing Formation strata. Preferential uplift of the northern part of the island accounts for the more extensive erosion in the northern central plain, and the general southerly dip of Tertiary strata in the Kingshill-Jealousy Basin.

In summary, early Jealousy sedimentation preceded the development of the Kingshill-Jealousy Basin, and required an external sediment source. Subsequent Tertiary deposition records the formation of the graben and then shallowing from bathyal depths, culminating in a Pliocene reef tract that mimics the present shoreline. Faulting of the Pliocene reef deposits allowed accumulation of reef sediments during island uplift and eustatic changes, and indicates that tectonic activity has continued into the Pliocene and perhaps to the present.

The tectonic regime controlling faulting and deformation on St. Croix has remained relatively constant since the onset of graben formation in the Miocene

Reproduced with permission of the copyright owner. Further reproduction prohibited without permission.

Kingshill-Jealousy Basin. If transverse motion along the Anegada Fault zone and Virgin Islands Basin reversed itself in the Pliocene or Quaternary, as has been suggested by several recent workers, it is difficult to see how St. Croix strata could have escaped being marked by new patterns of structural deformation. This last point will be discussed in greater detail in the next section.

Reproduced with permission of the copyright owner. Further reproduction prohibited without permission.

DISCUSSION: TECTONIC IMPLICATIONS OF THE ST. CROIX SEDIMENTOLOGICAL MODEL

We propose that St. Croix was rifted away from a pre-existing mainland. This idea was suggested by Hess (1933, 1966) among others, but was rejected by Whetten, Hess' doctoral student, in his dissertation on the geology of St. Croix (Whetten, 1966). The idea is resurrected here because it best explains the characteristics of structure and sedimentation in the Tertiary section of St. Croix, and is far more consistent with regional tectonics and seismicity than a static basin model.

Several lines of evidence support the notion that St. Croix has not existed solely as an insular body in the Tertiary, and these arguments range from the geomorphological to the structural. This section outlines the evidence that rifting must have occurred, and then discusses several competing models from the context of the geologic record of St. Croix .

Evidence for rifting.

Geomorphologic arguments.

The northern shelf profile of St. Croix is rugged and quite steep, sloping between 23 and 45 degrees to the center of the Virgin Islands Basin and dropping off at near vertical angles near the shelf edge. The northwestern shoreline of the island is carved from cliffs of the Northside Range, and prompted Meyerhoff (1927) to suggest a relatively recent fault origin for this side of the island, probably no older than the Pliocene. The southern shelf and coastline of St. Croix are gentler, and are less suggestive of fault origins.

Reproduced with permission of the copyright owner. Further reproduction prohibited without permission.

On deep submersible dives in DSRV*Alvin* along the northern island slope, Dill (1977) encountered structures he interpreted as fault gouge in St. Croix basement rocks. In similar *Alvin* dives off the northwestern coast, a vertical escarpment greater than 10 m in height was observed at a depth of greater than 2600 m (Hubbard and others, 1983; Gill, 1983). The escarpment was composed of dark, terrigenous rock similar in appearance to the Cretaceous Mt. Eagle Group rocks that make up the eastern and western hills of St. Croix. If in-place, the sheer face of the escarpment suggests the possibility of a fault origin for the northern island slope of St. Croix.

Structural arguments.

On the northern wall of the Virgin Islands Basin, the islands of St. Thomas and St. John both show extensive faulting. Donnelly (1966) mapped a graben structure on both islands that strikes northeast-southwest, and displaces Cretaceous age rocks. Left-lateral strike-slip displacement of strata is apparent within the graben. These faults pre-date St. Croix strata, but show very similar orientation.

Seismologic arguments.

The geomorphologic and structural evidence suggests that both walls of the Virgin Islands Basin have been tectonically active. However, seismic activity today is detectable only in the shallow zones in the north wall from 0 to 50 km deep (Fig. 2.20; Frankel and others, 1980). These seismic events occur in swarms, and are generally less than magnitude 3.2 (Frankel and others, 1980). Historic records indicate that the potential exists for much larger earthquakes in the Virgin Islands Basin/Anegada Passage area. Two major earthquakes caused damage in both St. Croix and St. Thomas in 1867,

Reproduced with permission of the copyright owner. Further reproduction prohibited without permission.

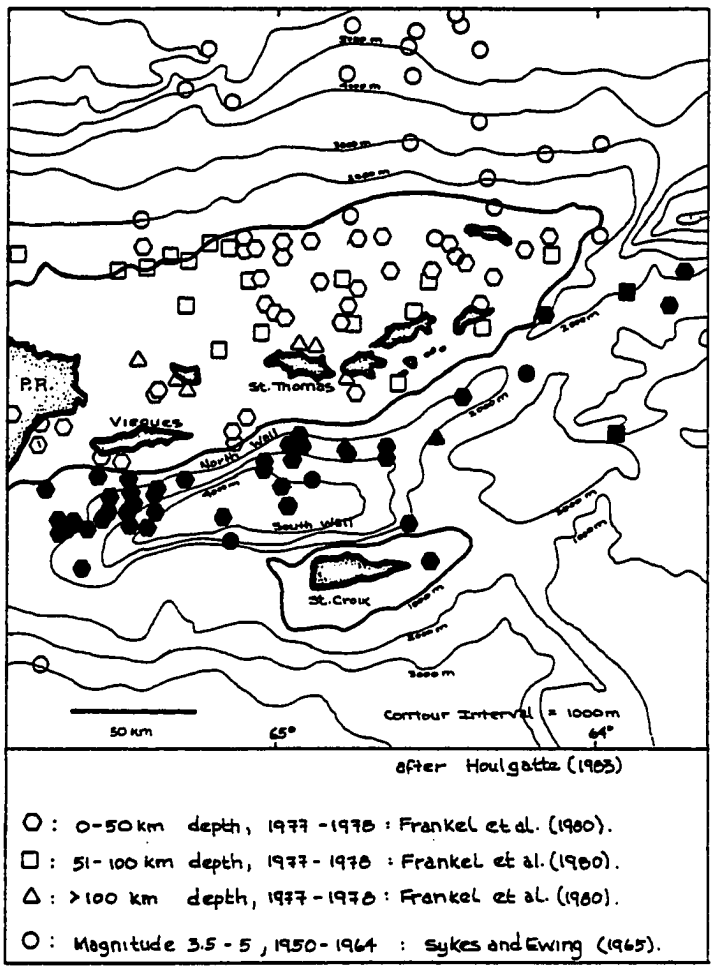

Figure 2.20. Seismicity in the Virgin Islands Platform area. Blackened symbols indicate seismic events occurring within the Virgin Islands Basin and Anegada Passage. Microseismic swarms (Frankel and others, 1980) occurred along the northern wall of the Virgin Islands Basin.

and were calculated on the basis of *tsunami* arrival times to have originated in the north wall of the Virgin Islands Basin (Reid and Tabor, 1920 in Frankel and others, 1980).

No fault-plane solutions exist for the seismicity in the Virgin Islands Basin area, and for that reason it is difficult to determine the orientation of fault movement. However, the seismic patterns make it clear that this area is seismically active today. If

Reproduced with permission of the copyright owner. Further reproduction prohibited without permission.

the geomorphological arguments are accepted, it is reasonable to assume that the southern wall of the Virgin Islands Basin has been active in the past as well.

Sedimentological arguments.

The Kingshill-Jealousy Basin did not form until the late early Miocene to middle Miocene. The evidence for this has been discussed earlier, and is based on the observations that:

1) Jealousy Formation sediments and foraminiferal faunas show no sign of shallowing toward the basin edges;
2) Jealousy Formation strata exist outside the confines of the basin faults.

Accepting this argument requires an external sediment source for the Kingshill-Jealousy basin, since significant quantities of conglomeratic deposits were noted in the type-section of the Jealousy Formation (Cederstrom, 1950), and the Jealousy Formation contains up to 50% non-carbonate material . Without upraised horst blocks to supply sediment, the shelf-derived conglomerates of the Kingshill-Jealousy Basin lack a sediment source.

A similar argument can be applied to the conglomeratic beds and rudistid-rich strata of the Cretaceous Judith Fancy formation that outcrops on the north and south coasts of St. Croix. Even with the vertical uplift of St. Croix removed, these boulder-sized materials would have had to traverse over 60 km (40 mi) of sea floor to reach St. Croix from the nearest potential sediment sources, Puerto Rico and the Virgin Islands Platform (Fig. 2.1).

Reproduced with permission of the copyright owner. Further reproduction prohibited without permission.

In summary, it is difficult to visualize St. Croix in its present location in either the Cretaceous or the Miocene, due to the long distances necessary to transport coarse detritus. The nearest and most likely sources for these materials are Puerto Rico and the Virgin Islands Platform to the northwest, and Anguilla and Saba Bank to the east and southeast.

The Left-Lateral Tectonic Model

We suggest that the present position of St. Croix is the result of uplift and left-lateral movement away from Puerto Rico and the Virgin Islands Platform. Any tectonic model designed to account for the original position of St. Croix must be consistent with the regional tectonic setting, and must account for the development of the area between the two rifted bodies. We suggest that St. Croix was rifted away from Puerto Rico by oblique left-lateral faulting, and that the Virgin Islands Basin is a strike-slip basin (Fig. 2.21).

Similar left-lateral faulting could have occurred between St. Croix and the Anguilla/Saba Bank area to the northeast. However, the structural and bathymetric relations in the St. Croix Basin (Fig. 2.1) are less clear than those in the Virgin Islands Basin. In the following sections we will concentrate on rifting between St. Croix and Puerto Rico because of the relative simplicity of the model and the larger body of data available.

Orientation of faults.

The graben faults on St. Croix strike in a northeast-southwest direction, and are oriented obliquely relative to the Virgin Islands Basin. All documented Tertiary faults on

Reproduced with permission of the copyright owner. Further reproduction prohibited without permission.

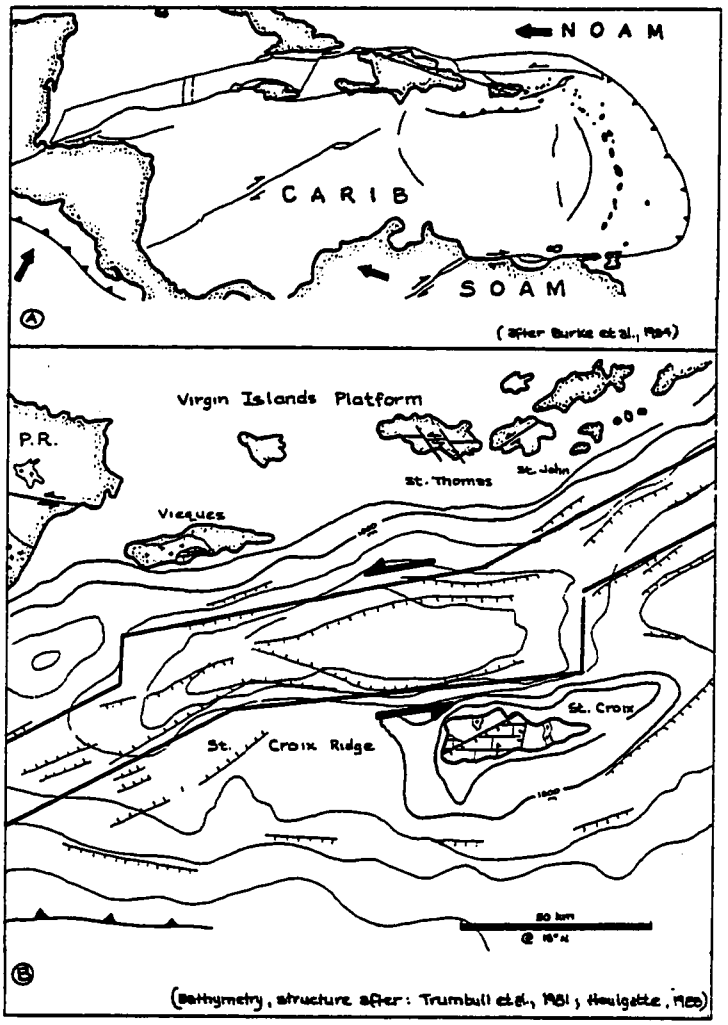

Figure 2.21. Left-lateral plate motion model.

A) NOAM= North American Plate; SOAM= South American Plate; CARIB= Caribbean Plate.

B) Oblique left-lateral model for St. Croix and the V. I. Basin. Note that major Tertiary faults on St. Croix are aligned at roughly 30 and 60 degrees to the orientation of the V. I. Basin. Normal faults on St. Croix Ridge parallel those on the island.

St. Croix are normal faults, and correspond roughly to the same orientation. On the St. Croix Ridge, bottom profiling and seismic observations indicate that the ridge is broken into a series of block fault "piano key" structures with the same northeast-southwest

Reproduced with permission of the copyright owner. Further reproduction prohibited without permission.

orientation as the St. Croix faults (Fig. 2.22). These structures are interpreted to be the products of normal faulting similar to that in the Tertiary section of St. Croix (Holcombe, 1979).

The northeast-southwest orientation of the apparently continuous set of tensional fractures is consistent with the type of deformation expected in a left-lateral wrench-fault zone aligned along the Anegada Passage. Such fractures tend to form parallel to the short axis of the strain ellipse in clay models (Wilcox and others, 1973). The northeast-southwest fault orientation is *not* consistent with right-lateral strike slip movement, which would produce normal faulting of the opposite orientation.

The consistent orientation of the St. Croix and St. Croix Ridge fracture system implies a tensional origin under a consistent tectonic regime (Fig. 2.22). The sharply defined walls of the Virgin Islands Basin, including the northern slope of St. Croix, suggest relatively recent tectonic activity along this area. Assuming that the origin of the faulting is connected to that of the Virgin Islands Basin/Anegada Passage, the orientation of the fault system on St. Croix suggests left-lateral wrench faulting north of St. Croix beginning between the middle and the late Miocene.

Sediment source.

As discussed above, the Kingshill/Jealousy Basin required an extrabasinal sediment source at least prior to the middle Miocene. The closest reasonable source for these sediments is the Virgin Islands Platform close to Puerto Rico. The southeastern section of Puerto Rico contains exposures of carbonate units of Tertiary age, and Tertiary carbonate units extend eastward of Puerto Rico only as far as the southern

Reproduced with permission of the copyright owner. Further reproduction prohibited without permission.

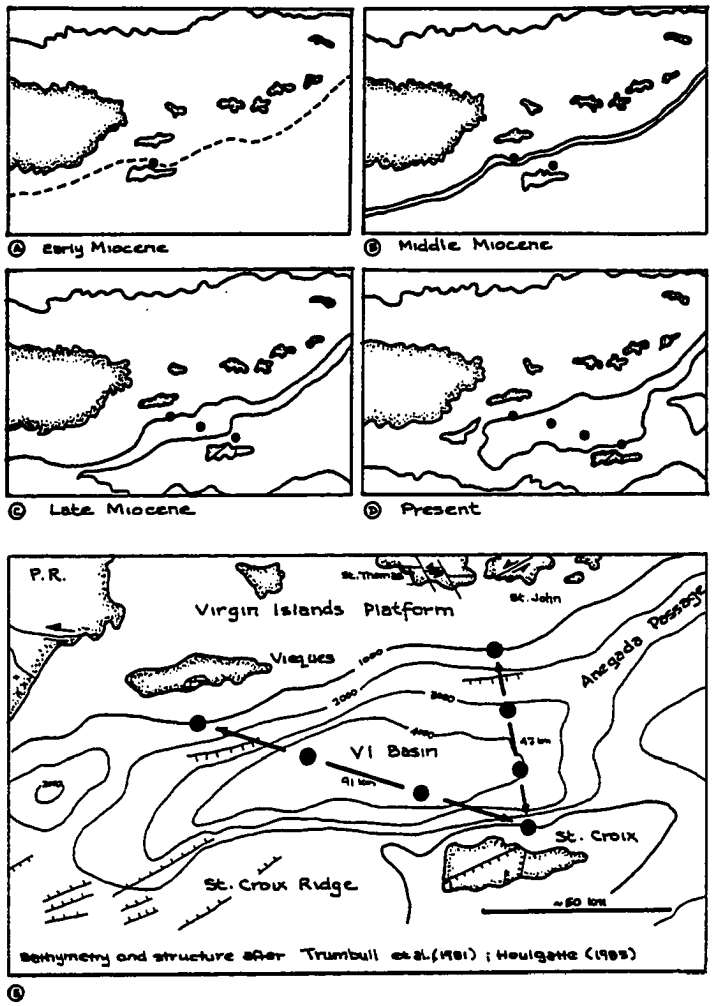

Figure 2.22 Migration model for Tertiary St. Croix. (A) through (D) show the hypothetical migration positions for St. Croix, assuming an initial position south of Vieques. (E) shows two possible migration paths discussed in the text.

coastline of Vieques island (Khudoley and Meyerhoff, 1971). These units are presently to the northwest of St. Croix, requiring left-lateral movement to place St. Croix in its present position.

A second potential sediment source is the Anguilla/Saba Bank area to the east. Shelf carbonates of the same age as the Jealousy Formation and the Kingshill Limestone

Reproduced with permission of the copyright owner. Further reproduction prohibited without permission.

exist in Anguilla (Bold, 1970; Chapt. 1, this dissertation) and contain very similar ostracode faunas. Saba Bank is underlain by rocks interpreted to be fluvio-deltaics of Eocene age, with a presumed sediment source on Puerto Rico (D. Hubbard, pers. comm.). If either of these areas were originally juxtaposed with St. Croix, assuming movement crudely parallel to the Anegada Passage, fault motion would again be left lateral. Lateral movement from Anguilla to the present location of St.Croix would require a greater travel distance than would movement from Puerto Rico. Unfortuately, information on the basins between St. Croix and Anguilla is too sparse to allow evaluation.

Seismicity.

No fault-plane solutions have been calculated for the seismic events currently taking place in the Virgin Islands Basin, and the seismicity is proof only that the basin is active today (Fig. 2.20). The direction of movement in the basin must therefore be based on other geologic evidence.

Geometry of the Virgin Islands Basin.

The steepest slopes in the Virgin Islands Basin are the southern wall of the basin formed by the St. Croix island slope, and the northern wall of the basin between Vieques and St. Thomas (Fig. 2.22). If the Virgin Islands Basin formed as a result of rifting, these slopes probably mark the scarps formed during the rifting event. If these scarps were initially juxtaposed, the present position of St. Croix could only have been achieved by St. Croix moving south and east relative to its initial position on the Virgin Islands Platform. This movement requires a combination of left-lateral movement and tensional separation which is consistent with the oblique left-lateral strike-slip motion we suggest for the formation of the Virgin Islands Basin.

Reproduced with permission of the copyright owner. Further reproduction prohibited without permission.

Plate motions in the northeastern Caribbean.

Active, documented subduction in the northeastern Caribbean is presently taking place only along the Lesser Antilles arc. At present, the Caribbean plate is interpreted as moving eastward relative to the North American plate, with slip and potentially compression occurring along the plate boundary close to the Puerto Rico Trench (Frankel and others, 1980; Burke and others, 1984). Large-scale plate motion is manifested by sinistral slip along the northern Caribbean Plate boundary, and by dextral slip zones along the southern boundary (Stephan and others, 1986).

The left-lateral model for the opening of the Virgin Islands Basin is consistent with the motion of the northern Caribbean Plate boundary. Given that sinistral motion occurs between the North American and the Caribbean plates, it is reasonable to predict that if decoupling did occur between the Virgin Islands Platform and St. Croix, the resulting transform motion would be left-lateral. The consistency and simplicity of this model is perhaps the reason that left lateral motion in the Anegada Passage was suggested by Hess (1933, *in* Whetten, 1966), Hess (1966), Burke and others (1984, table 7) and authors in Case and others (1984). Unfortunately, large-scale tectonic maps such as that of Burke and others (1984) generally don't trifle with petty features like the Anegada Passage (Fig. 2.21a), and detailed tectonic reconstructions are not available.

Is the hypothetical rate of migration, using a left-lateral model, consistent with accepted Caribbean plate motions? -- Assuming that St. Croix was separated from the Virgin Islands Platform by left-lateral transtensional faulting, the possible range of separation rates is between 3 and 21 mm/y. Minimum

Reproduced with permission of the copyright owner. Further reproduction prohibited without permission.

and maximum movement durations are 3.5 and 16 Ma, respectively, based on an earliest possible separation from the Virgin Islands Platform occurring at the beginning of the middle Miocene and a latest possible separation starting in the latest Miocene (ca. base of N17). Minimum and maximum assumed distances of lateral movement are 46 and 74 km respectively, based on the north slope of St. Croix being positioned against either the slopes of St. Thomas or Vieques (Fig. 2.22). Movement rates assuming Anguilla or Saba Bank as a sediment source would be somewhat higher.

Assuming that St. Croix was initially directly south of Vieques, and initiation of motion occurred in the late middle Miocene, the rate of lateral motion would be 6 km/Ma or 6 mm/y. Present movement along the Northern Boundary zone of the Caribbean Plate is estimated to be several times this estimate, between 20 and 40 mm/y (Golumbek, 1987). Thus the rates of lateral movement required by our model are within limits of presently known slip rates in the Caribbean. The fact that calculated slip rates for the movement of St. Croix are slower than movement along the Northern Plate Boundary Zone is consistent with the idea of Puerto Rico and the Virgin Islands Platform being decoupled, and moving eastward slightly more slowly than the Caribbean Plate (McCann and others, 1987).

The Right-Lateral Tectonic Model

An alternative model for the origin of the Virgin Islands Basin proposes that motion in the Virgin Islands Basin and Anegada Passage is right-lateral (Fig. 2.23; Houlgatte, 1983; Mauffret and others, 1986; Stephan and others, 1986; Jany and others, 1987). Mauffrey and others (1986) and Jany and others (1987) propose that motion along the Anegada Passage was originally sinistral, but has reversed itself since

Reproduced with permission of the copyright owner. Further reproduction prohibited without permission.

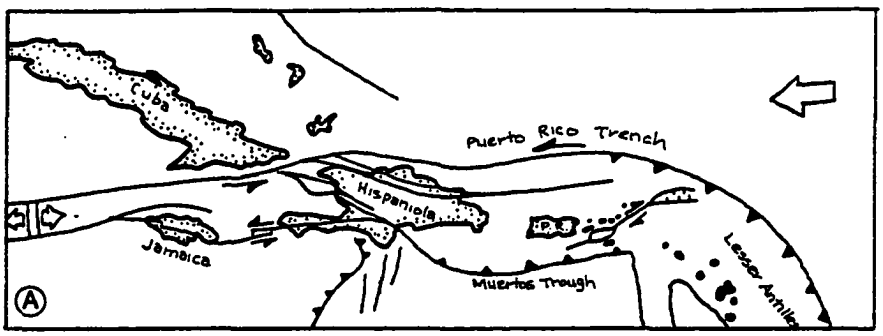

A) Plate tectonic model for the northern Caribbean with dextral slip in the Virgin Islands Basin/Anegada Passage via a "Puerto Rico Festoon". Note that documented sinistral faults through Puerto Rico are not noted on this diagram: from Stephan and others (1986).

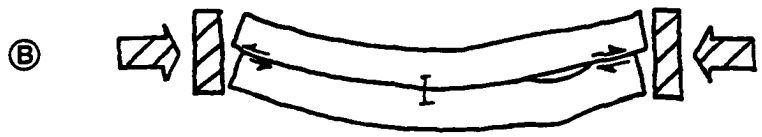

B) Mechanical analog for the formation of a "Puerto Rico Festoon" with dextral slip to the east, i.e., Virgin Islands Basin/Anegada Passage, and sinistral slip to the west: from Stephan and others (1986)

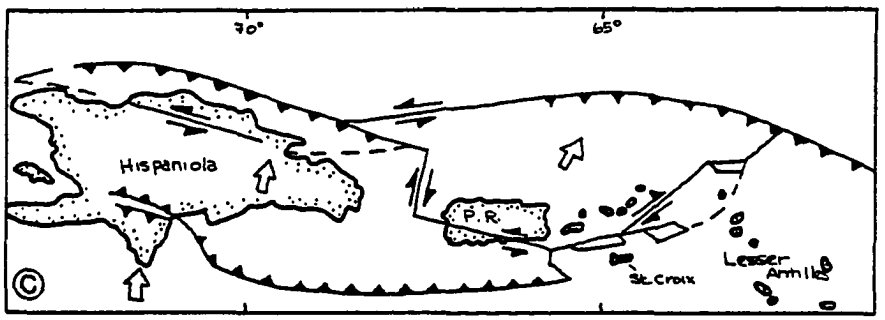

C) Plate tectonic model for the northern Caribbean with dextral slip in the Virgin Islands Basin/Anegada Passage. Note proposed triple junction to the southeast of Puerto Rico: from Jany and others (in press).

Figure 2.23. Right-lateral plate motion models.

Reproduced with permission of the copyright owner. Further reproduction prohibited without permission.

or during the Pliocene. The evidence for this model is based on geomorphology, seismic profiles and side-scan sonar traverses taken with the Seabeam and GLORIA systems, and is summarized below.

Basin geometry.

The "rhomboidal" morphology of the Virgin Islands Basin is suggested as evidence for dextral slip (Jany and others, in press). However, a rhomboidal shape by itself is diagnostic of neither dextral nor sinistral slip *per se,* rather, it is a likely shape for pull-apart basins in general.

Dextral or sinistral slip in pull-apart basins is indicated by the morphology of the basin, and the relationship of the basin to the strike-slip fault that generates the rifting. A left-stepping sinistral strike-slip fault would produce a "lazy-S" shaped basin, and a right-stepping dextral fault would produce a "lazy-Z" shaped basin (Fig. 2.24; Mann and others, 1983). The geometry of the Virgin Islands Basin is as easily interpreted as a product of left-lateral slip as right-lateral slip.

Seismic reflection.

Mauffrey and others (1986) show a seismic profile oriented NE-SW across the Virgin Islands Basin with low-angle reverse faulting (Fig. 2.25a). They interpret this structure as a product of right-lateral slip in the Virgin Islands Basin. However, right-lateral slip would produce tension rather than compression along a NE-SW line in the Virgin Islands Basin. The structure in Figure 2.25a is therefore more easily explained by sinistral slip rather than dextral slip as Mauffrey and others (1986) have suggested.

Reproduced with permission of the copyright owner. Further reproduction prohibited without permission.

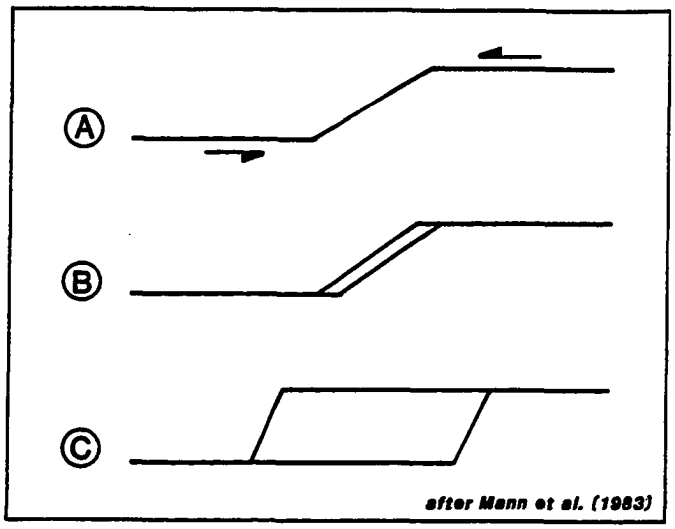

Figure 2.24. Development model for pull-apart basins along a left-stepping, left-lateral fault system.

As additional evidence for right-lateral rifting, Jany and others (1987) show a NW-SE seismic cross section across the St. Croix Basin, to the east of St. Croix island (Fig. 2.25b). Although the seismic traverse shows normal faulting in the basin, the orientation of the block faulting in the NW-SE section could just as easily have been the result of left-lateral slip as right-lateral slip. Furthermore, the structural relationship between the St. Croix Basin and the Anegada Passage/Virgin Island Basin system is not understood. For this reason, these seismic profiles shed no light on the direction of motion in the Virgin Island Basin.

Similarly, in the Virgin Island Basin directly north of St. Croix, Jany and others (in press) use seismic profiles that show "flower structures" - indicating strike-slip faulting - overlying what they interpret as the late Miocene sedimentary surface (Fig. 2.25c). In N-S transects such as these, although strike-slip motion may be a reasonable interpretation, there is no way of accurately assessing the direction of motion. It is therefore difficult to accept or reject either model on the basis of this evidence. In

Reproduced with permission of the copyright owner. Further reproduction prohibited without permission.

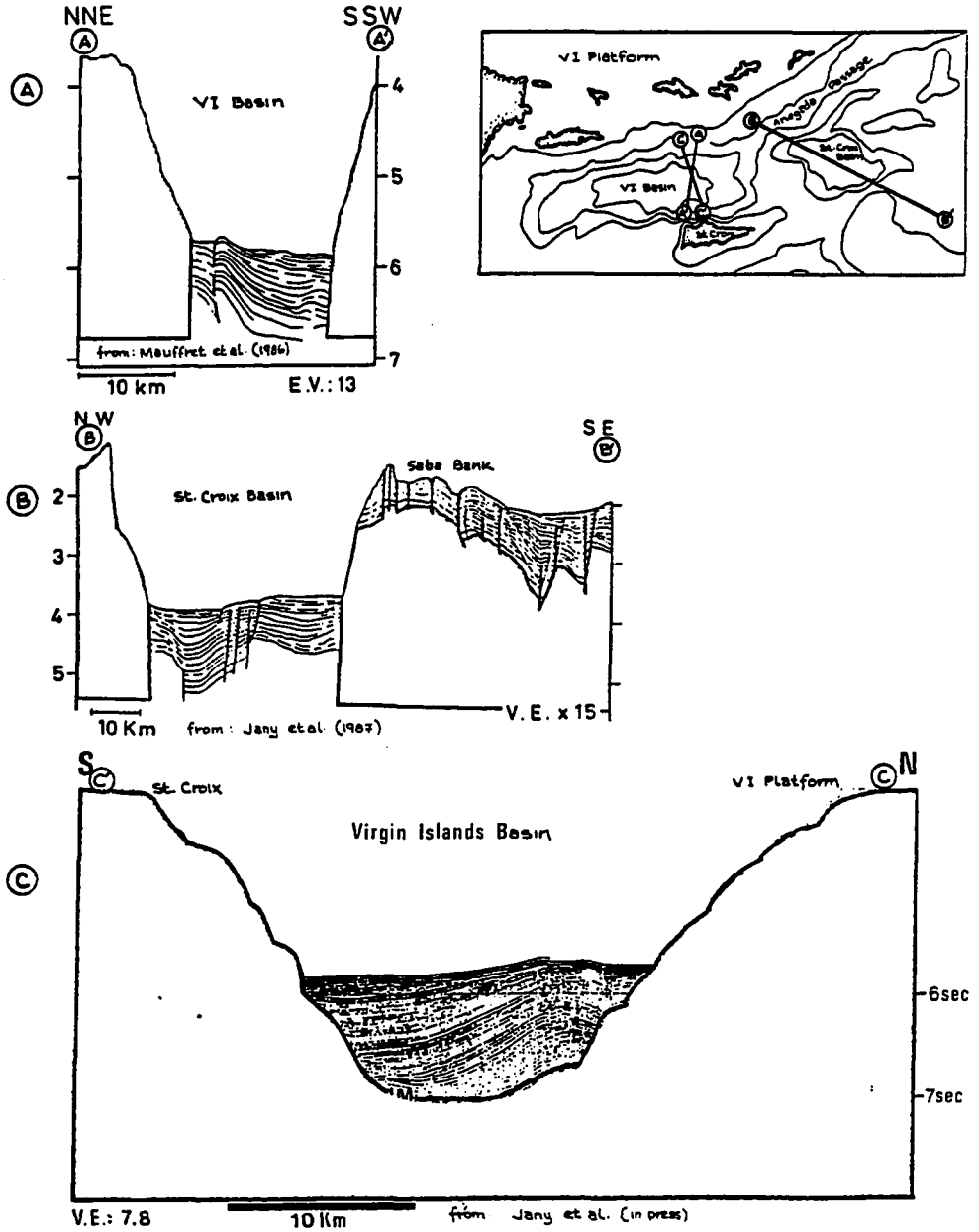

Figure 2.25. Seismic sections in the St. Croix Basin and Virgin Islands Basin.
(A) Seismic section across the V. I. Basin oriented NNE-SSW. The structure illustrated in this section is interpreted by Mauffret and others (1986) as a probable reverse fault formed during right-lateral motion in the V. I. Basin. However, left-lateral faulting would be more likely to form a compressional structure of this orientation.
(B) NE-SW seismic section across St. Croix Basin and Saba Bank, showing extensive normal faulting (Jany and others, 1987).
(C) Seismic section oriented SSE-NNW interpreted by Jany and others (in press) as evidence for strike-slip faulting in the V. I. Basin. However, determining the direction of motion is not possible with this information alone.

Reproduced with permission of the copyright owner. Further reproduction prohibited without permission.

addition, several other seismic traverses published by Houlgatte (1983) similarly document the dominance of normal faulting in the basin, but can not indicate the orientation of transverse faulting, if it exists (Fig. 2.26).

It is my contention that the seismic sections from the Virgin Islands Basin document the dominance of block faulting, but do little to confirm either right- or left-lateral fault models.

Side scan profiling.

Side scan profiles are presented in Jany and others (1987), and Jany and others (in press) in support of the right-lateral slip model. In neither of these papers is there a clear enough presentation of the sidescan data to allow evaluation. Clear sonograms of the Puerto Rico and Virgin Islands area are presented in the recently published Atlas of the Exclusive Economic Zone (EEZ-SCAN 85 Scientific Staff, 1987). In this case submarine features of the Virgin Islands Basin are clearly shown, but there is no clear evidence of the direction of fault displacement. Because the evidence seen to date does not show any trends that are unequivocally tectonic as opposed to sedimentary, it is difficult to use this evidence to support either dextral or sinestral slip.

Seismicity.

As discussed above, the patterns of seismicity in the Virgin Islands Basin prove that the basin is seismically active today, but in the absence of fault-plane solutions, cannot indicate the orientation of faulting.

Reproduced with permission of the copyright owner. Further reproduction prohibited without permission.

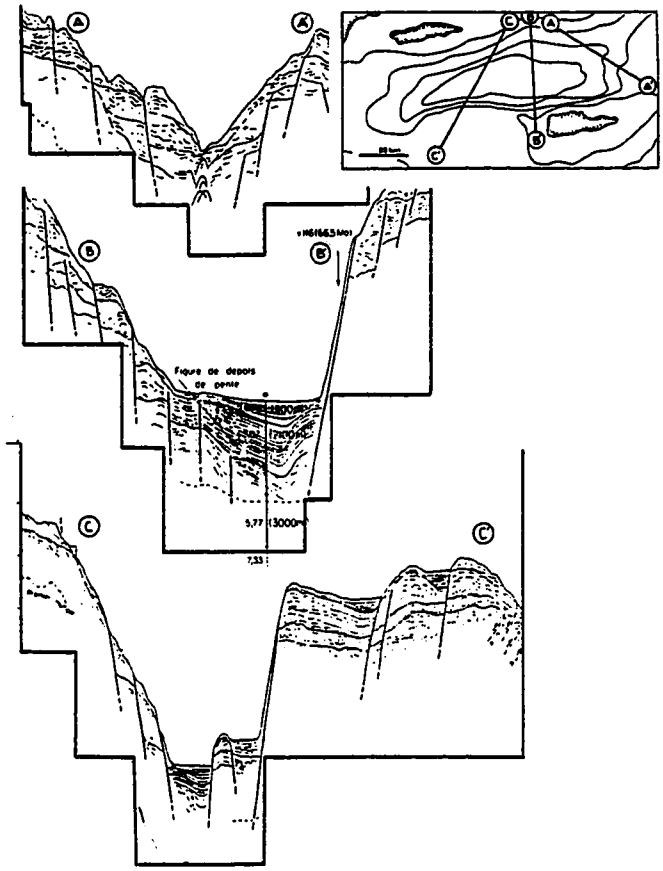

Figure 2.26. Seismic sections of varied orientation, showing the dominance of normal faulting within the Virgin Islands Basin (from Houlgatte, 1983).

Regional tectonic framework and problems with a dextral slip model.

The dextral slip model suffers from several problems when incorporated into a regional model of tectonics. Primary among these is the difficulty in reconciling a dextral strike-slip fault in the Virgin Islands Basin with the compression established along the length of the Muertos Trough (McCann and others, 1987). This would require an extension of the Anegada Passage/Virgin Islands Basin fault zone westward of its present termination, and there is no seismic or bathymetric evidence to support this. Jany and others (in press) suggest a triple point junction south of Puerto Rico to

Reproduced with permission of the copyright owner. Further reproduction prohibited without permission.

accomodate right lateral plate movements (Fig. 2.23). There is no seismic evidence, however, to support this.

Dextral motion along the Anegada fault zone would also require Puerto Rico to move eastward faster than the Caribbean Plate, and a driving mechanism for this movement is difficult to visualize. Similarly, it is difficult to reconcile right-lateral motion in the Anegada Passage with:

1) established left-lateral motion for the Puerto Rico trench and plate boundary zone;
2) mapped left-lateral displacement in terrestrial faults on Puerto Rico and the northern Virgin Islands;
3) the NE-SW normal faults on St. Croix and on the St. Croix Ridge.

If dextral faulting is occurring in the Anegada fault zone, it must postdate the faulting on the Puerto Rico /Virgin Islands Platform and on St. Croix. Changing to right-lateral slip in the latest Neogene or Quaternary would require a major reversal of plate motion in the northeastern Caribbean. It is difficult to understand the mechanism that would reverse the motion along an established Tertiary fault zone, but such a process would presumably require a major change in motion along several sides of Puerto Rico and perhaps Hispaniola as well. If such a reversal did occur, it apparently left no trace in the rocks exposed on St. Croix which record deposition and faulting through at least the lower Pliocene.

Reproduced with permission of the copyright owner. Further reproduction prohibited without permission.

Rotating Platelet Model for Puerto Rico

A third, related model for the northeastern Caribbean suggests that Puerto Rico exists as a separate platelet that is rotating counterclockwise with a pole of rotation south of Puerto Rico at the juncture between the St. Croix ridge and the Muertos Trough (Fig. 2.27; Scanlon and Masson, 1988). This model is based primarily on seismic profiling and GLORIA sidescan work done by the USGS (EEZSCAN 85 Scientific Staff, 1987) in 1985. The Scanlon and Masson model (1988) is superficially compatible with the conclusions of McCann and others (1987) and Lithgow and others (1987) in that it requires the presence of a separate Puerto Rico microplate, but does not address relative motion between the microplate and the boundaries of the Caribbean plate, the North American plate and Hispaniola. This model does not specifically preclude either dextral or sinistral slip in the Anegada Passage and is therefore not of major concern to this discussion. However, intuitively, if The Puerto Rico Platform rotated counterclockwise relative to a fixed Caribbean plate, this motion would most likely produce right-lateral slip in the Anegada fault zone (Fig. 2.27).

In addition, with a pole of rotation situated southwest of St. Croix, counterclockwise rotation of a separate Puerto Rico platelet would produce a zone of extension in the Anegada fault zone that widens to the northeast (Fig. 2.27). In fact, the Anegada Passage is quite narrow along its entire length until it empties into the Virgin Islands Basin to the southwest and into the Sombrero Basin to the northeast (Fig. 2.22). For this reason, the bathymetry of the region does not support simple rotation alone. If rotation did occur, it must have been coupled with other motion as well.

Reproduced with permission of the copyright owner. Further reproduction prohibited without permission.

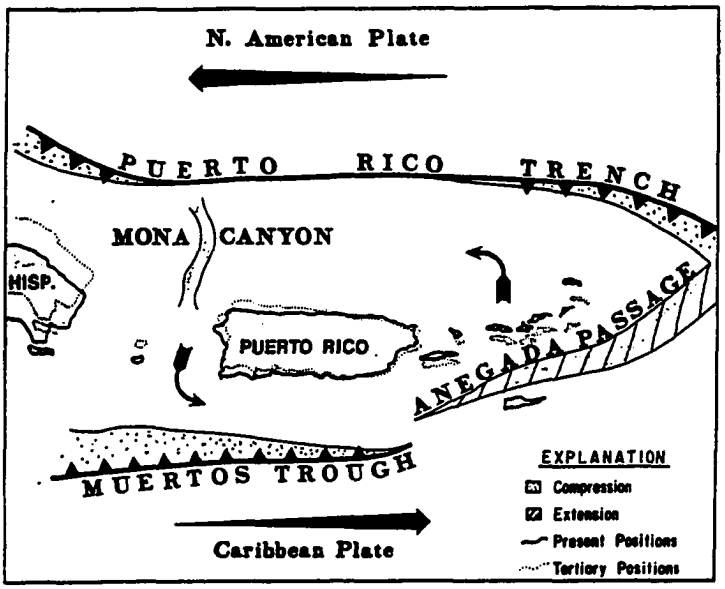

Figure 2.27. Rotating microplate model of Scanlon and Masson (1988). This model does not specifically address whether motion in the V. I. Basin is right- or left-lateral. However, the model apparently calls for the widening of the Anegada Passage to the northeast, which is not supported by bathymetric data.

Summary

A sinistral transtensional model for the Virgin Islands Basin and the Anegada Passage is most consistent with the structural and sedimentological characteristics of St. Croix. Such a model satisfies structural evidence on St. Croix such as the consistent orientation of the normal fault system, as well as the requirement for an extrabasinal source of sediments. In addition, a left-lateral motion is consistent with the position of the fault scarps in the basin, as well as the location of the closest likely sediment source. From a regional standpoint, a sinistral-motion model provides the simplest explanation for the kinematics of the region and is consistent with recent work defining the Puerto Rico microplate (e.g. McCann and others, 1987).

Reproduced with permission of the copyright owner. Further reproduction prohibited without permission.

Dextral slip in the Anegada fault zone is supported by several recent papers, but lacks the support of any structural evidence. In addition, such a model requires several complicating *ad hoc* assumptions to make it fit the known characteristics of the area, including a mechanism for reversing the direction of slip in the fault zone, and some unspecified means of translating compressional stress along the length of the Muertos Trough. While it is certainly possible that a reversal of slip direction has occurred since the Pliocene, such a reversal has not been recorded by deformation in the Tertiary strata of St. Croix.

Our position, from the context of St. Croix geology, is that St. Croix was initially part of the Virgin Islands Platform and that motion along the Anegada Passage was left-lateral and transtensional throughout most of the Tertiary. Whether subsequent motion in the Virgin Islands Basin was right-lateral remains neither proved nor disproved, and proof waits for earthquake fault-plane solutions or better seismic sections. However, from my perspective, a fault-movement reversal without producing compression in the Virgin Islands Basin or on St. Croix is unlikely.

Reproduced with permission of the copyright owner. Further reproduction prohibited without permission.

CONCLUSIONS

1) St. Croix is not a product of vertical tectonic motion alone, and has not remained stationary throughout the Tertiary. Instead, we suggest that St. Croix has been separated from a larger land mass by transtensional faulting. Puerto Rico and the Virgin Islands Platform, as well as Saba Bank and Anguilla are possible source areas for the coarse, shelf-derived clasts in the lower Kingshill Limestone and the Jealousy Formation.

2) The Virgin Islands Basin is a strike-slip structure formed by sinistral faulting that rifted St. Croix away from the mainland along the Anegada Passage. Horizontal rifting rates were between 3 and 21 mm/y, but were probably close to 6 mm/y.

3) The Tertiary Kingshill-Jealousy Basin on St. Croix records bathyal deposition throughout its known sedimentary record until extensive shallowing occurred in the late Miocene to early Pliocene. Vertical uplift rates for St. Croix are estimated at between 0.1 and 0.2 mm/y. The Kingshill-Jealousy Basin was probably not a trough-like seaway until late in the Neogene, if at all.

4) Faulting did not occur in the boundary graben faults until the beginning of the middle Miocene at the earliest, but may have begun by the end of the middle Miocene. The horst blocks of the basin could not have been available as a sediment source for the Jealousy Formation, and an external source for these sediments was required.

5) The Jealousy Formation, which includes the majority of the sampled Tertiary section, is a Miocene unit that does not outcrop. The Jealousy Formation may extend into the

Reproduced with permission of the copyright owner. Further reproduction prohibited without permission.

Oligocene or earlier due to its thickness, but no Jealousy Formation samples older than the Miocene have been documented.

6) The Jealousy Formation is composed dominantly of deep-water planktonic foram tests and was deposited in water depths between 600 and 800 m. The Jealousy is not a shallow, estuarine unit.

7) The transition between the Jealousy Formation and the Kingshill Limestone is abrupt and distinct, but is time-transgressive and does not indicate any major bathymetric or other environmental change. There is no apparent paleontological or lithological difference between the lower Kingshill Limestone and the Jealousy Formation.

8) Recently suggested dextral strike-slip faulting for the origin of the Virgin Islands Basin, if it occurred, is not supported by structural or sedimentological evidence on St. Croix.

9) St. Croix had acquired its present shoreline configuration by the Pliocene, and an extensive reef and lagoon tract had established itself along the present western and southern shorelines.

10) Structural control of the coastline in the form of a subsidiary graben or demi-graben allowed the accumulation and preservation of reef and platform Pliocene sediments. Normal faulting has continued on St. Croix at least into the Pliocene.

Reproduced with permission of the copyright owner. Further reproduction prohibited without permission.

CHAPTER 3.

INSULAR DOLOMITIZATION ON ST. CROIX, U.S.V.I.: THE CRUZAN DOLOMITIZATION MODEL

Reproduced with permission of the copyright owner. Further reproduction prohibited without permission.

ABSTRACT

Current thinking on mechanisms of dolomitization centers around several models, based on the geological, hydrological and chemical requirements of the dolomitization process. Some of the commonly cited models for dolomitization involve mixing of marine and groundwaters, evaporation of marine brines, and the removal of kinetic inhibitors such as sulfate ions. None of the models successfully explains all occurrences of sedimentary dolomite, and it has become apparent that a wide variety of water types and hydrologic settings can in time produce dolomite.

This project concentrates on a regionally restricted location of dolomite, and utilizes the chemistry of the modern groundwater, as well as the chemistry, distribution and petrologic aspects of the dolomite, to test possible models. The rock samples for this project are derived from twenty two test holes drilled to a maximum depth of 91 m subsurface, and from rock exposures representing the carbonate section through the Miocene. Water samples were collected from public and private well sites on St. Croix representing a range of environments.

Dolomite on St. Croix exists in a highly localized region of outcrops and subsurface occurrences in a Pliocene reef tract. Bioclasts in the dolomitic strata often show surprisingly good preservation of microstructure, particularly in large benthic forams and coralline algal clasts. The dolomite is stoichiometrically calcium rich, and exists as euhedral rhombs ranging from 2 to 30 μm in diameter and as a replacement mineral in dolomitized bioclasts.

Reproduced with permission of the copyright owner. Further reproduction prohibited without permission.

The dolomite presently in strata above the water table occurs in reef, lagoonal and platform facies that rim the pre-development shoreline of Krause Lagoon. Below the present water table, dolomitized rock follows the lithified undersurface of the same lagoon. Despite the existence of similar facies elsewhere on St. Croix, the dolomite is found nowhere else. This spatial distribution suggests that the formation of the dolomite was genetically related to hydrologic conditions found in Krause Lagoon.

The $^{87}Sr/^{86}Sr$ isotopic composition of the dolomite is 0.70887 (±0.00002), which corresponds to the $^{87}Sr/^{86}Sr$ ratio of Miocene seawater. However, the dolomite resides in Pliocene strata, making a Miocene dolomitization event unsupportable and requiring a significant external source of non-radiogenic strontium. St. Croix groundwater $^{87}Sr/^{86}Sr$ ranges from 0.7076 to 0.7085, well below the ratio of both modern seawater and the dolomites.

Mixing calculations show that St. Croix groundwater could be a significant source of non-radiogenic strontium in a dolomite formed from a two-component groundwater-seawater mix. The groundwater component in the St. Croix dolomites may have ranged from 40 to 80% of the dolomitizing fluids. For this reason, groundwater effects on the strontium isotopic ratio cannot be neglected *a priori*, even in systems containing a significant seawater component. The dating of carbonate phases from similar geologic environments should be approached with this in mind.

Stable isotopic values for the dolomite ranges from +0.7 to +3.8 ‰ $\delta^{18}O$ and from +0.6 to +2.4 ‰ $\delta^{13}C$ relative to PDB, with an enrichment trend from the margins to the center of the lagoon. The maximum oxygen isotopic values reached in these dolomites are too enriched in ^{18}O to be formed from groundwater or seawater even

Reproduced with permission of the copyright owner. Further reproduction prohibited without permission.

accounting for ice-volume effects. These data imply that dolomite precipitated from fluids enriched in ^{18}O, probably as a result of evaporation.

In order to account for the geochemistry and geologic distribution of the dolomites we suggest that dolomitization took place from fluids that were produced from a mixture of evaporated seawater and groundwater. Calculations show that such a scenario is possible, and may be more common than one would suspect. The dolomitization was confined to a fault-bounded lagoon, and affected reef, lagoonal and platform carbonates. Block faulting of the lagoon area may have provided a stable hydrologic regime for a long enough time for dolomite to form, despite island uplift in the late Tertiary.

Reproduced with permission of the copyright owner. Further reproduction prohibited without permission.

INTRODUCTION

The island of St. Croix is partly composed of a carbonate rock section that includes basinal to reefal deposits, and ranges in age from early Miocene to Recent. The Pliocene part of the carbonate section has been locally dolomitized, and thus offers an opportunity to study the process of dolomitization before continued diagenesis has obliterated clues of its origin.

This study attempts to constrain the timing, distribution and geochemistry of a late Cenozoic dolomite. Because dolomitization must be closely tied to hydrologic effects, it is important not only to understand the stratigraphic, petrographic, and geochemical characteristics of the dolomitic rock, but the chemistry of the modern groundwater system as well. The groundwater system is important to understand in order to decide whether, or to what extent, the island aquifer system is involved with the dolomitization. I propose that the modern St. Croix groundwater system is a reasonable analog for the hydrologic system operative at the time of dolomitization -- or at least that the modern system provides first-order guidelines to the types and magnitudes of geochemical processes that existed during dolomitization.

This chapter attempts to eliminate several competing dolomitization hypotheses on the basis of hydrologic, stratigraphic and geochemical evidence. Throughout the text, it is recognized that dolomite may undergo subsequent rearrangement and stabilization similar to metastable carbonates, and the term "dolomitizing fluid" could also be interpreted as "dolomite resetting fluid". In order to be as accurate and clear as possible, estate names and place names in the text are taken from the original Danish estate names

Reproduced with permission of the copyright owner. Further reproduction prohibited without permission.

for St. Croix, whereas the names of hydrographic features such as Krause Lagoon are taken from the U.S. Geological Survey topographic maps for the area.

Reproduced with permission of the copyright owner. Further reproduction prohibited without permission.

GEOLOGIC SETTING

St. Croix lies at the northwestern edge of the Lesser Antilles arc, approximately 176 km southeast of San Juan, Puerto Rico (Fig. 3.1). St. Croix is 39 km long, 9 km wide and is tectonically and geologically distinct from the majority of the primarily igneous islands of the Lesser Antilles.

The central plain of the island consists of deposits of alluvium and exposures of Tertiary carbonate rocks (Fig. 3.2), and lies between the mountainous Eastend and Northside Ranges composed of Cretaceous resedimented volcaniclastic and intrusive rocks of the Mt. Eagle Group. The Tertiary carbonates are contained within a graben that we will refer to as the *Kingshill-Jealousy Basin* (Chapt. 2, this dissertation). The Tertiary carbonates and Quaternary alluvium compose the bulk of the aquifer system on St. Croix.

The rock units dealt with in this paper are (Fig. 3.3):

1) the Cretaceous *Mt. Eagle Group* that brackets the basin to the east and west, and presumably floors the graben.
2) the Miocene *Jealousy Formation*, consisting of grey-blue, planktonic foram-rich basinal carbonates and clays;
3) the Miocene *Kingshill Limestone*; consisting of hemipelagic limestones, carbonate debris flows, terrigenous material and chalks;
4) The Blessing Formation and Mannings Bay Member of the Kingshill Limestone. These carbonate units overlie the lower Kingshill Limestone along the southern coast and will be referred to collectively here as the *post-Kingshill limestones*. These units have been locally dolomitized, and are the focus of this paper (Fig. 3.3).

Reproduced with permission of the copyright owner. Further reproduction prohibited without permission.

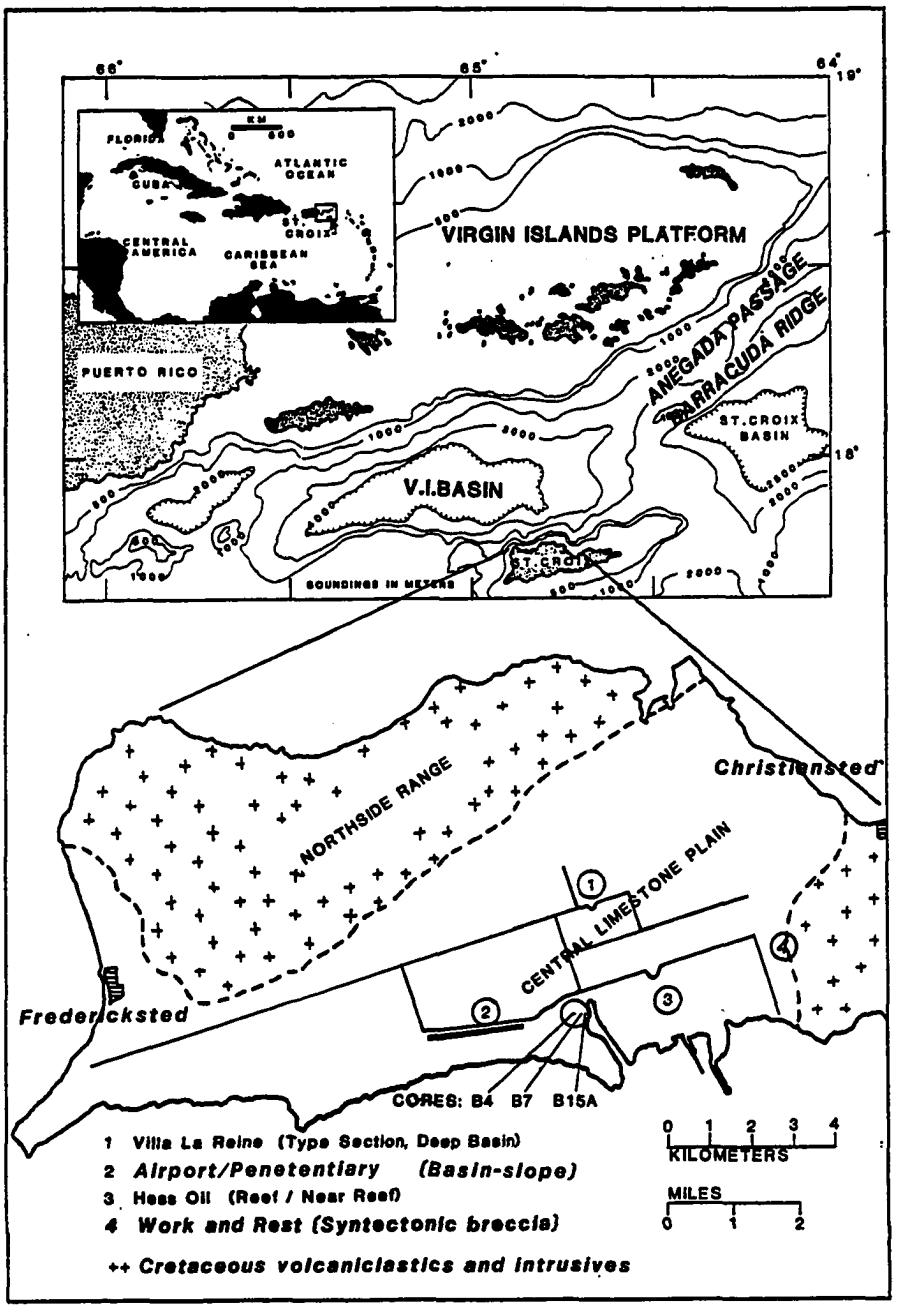

Figure 3.1. Location map and study area.

The maximum known thickness of the Kingshill Limestone is close to 140 m in the carbonate highlands along the north coast of St. Croix. The total thickness of the combined Kingshill Limestone and post-Kingshill carbonate section in the south coast

Reproduced with permission of the copyright owner. Further reproduction prohibited without permission.

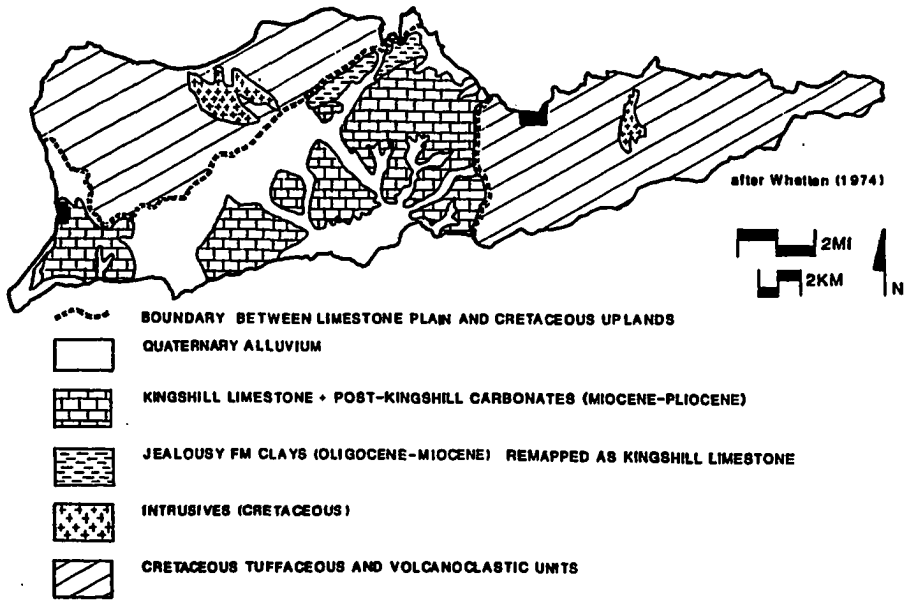

Figure 3.2. Generalized geologic map of St. Croix, modified after Whetten (1966).

area is unknown, but exceeds 90 m, the maximum drilling penetration for this project. The underlying Jealousy Formation sediments are at least 427 m thick as proven by drilling completed in 1939 (Cederstrom, 1950), and are estimated to be as much as 2000 m thick on the basis of gravity-anomaly surveys (Shurbet and others, 1956).

In this study we use the modern aquifer system, described above, as an analog for the groundwater system in place at the time of dolomitization. We believe that the modern system approximates late Neogene-Quaternary conditions for the following reasons:

1) The Pliocene reef trend clearly outlines the position and extent of the late Neogene coastline, which was little different than the coastline of St. Croix today. Based on this and structural evidence (Gill and Hubbard, 1987; Chapt. 2, this dissertation), I propose

Reproduced with permission of the copyright owner. Further reproduction prohibited without permission.

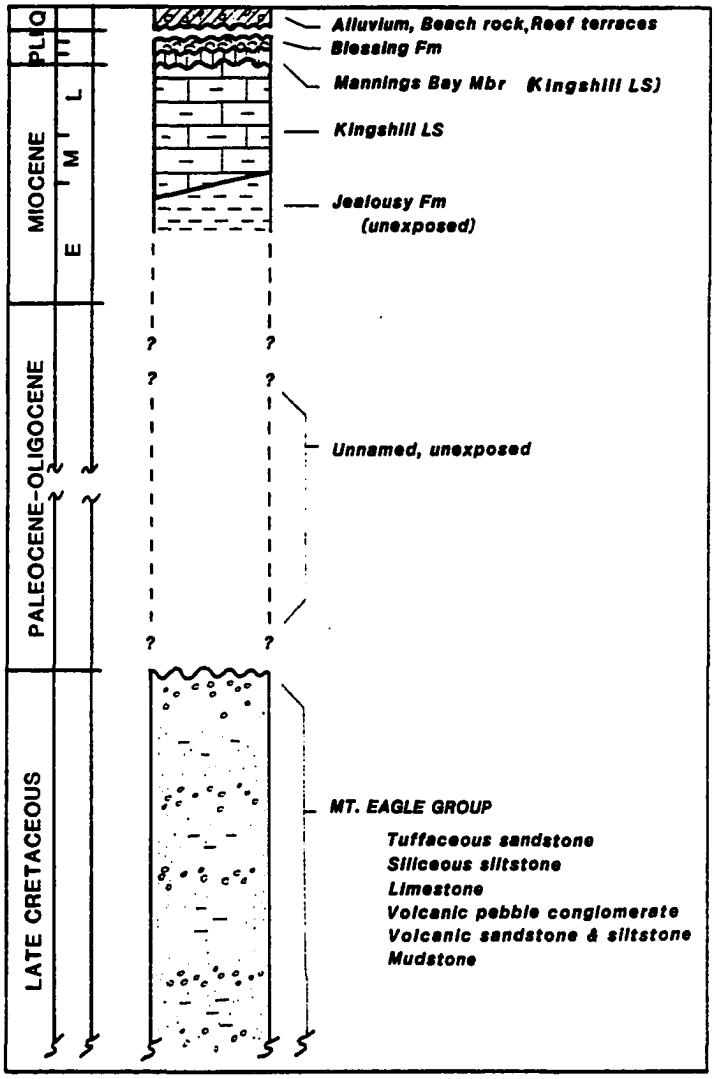

Figure 3.3. Generalized stratigraphic column. All units listed are exposed in outcrop except the Jealousy Formation (see the discussion in Chapt. 2, this dissertation). Intrusives not shown.

that the shape and size of the carbonate aquifer system during the Pliocene was similar to the modern system, and that the groundwater system may have been similar as well.

2) The Miocene Kingshill Limestone and Jealousy Formation which underlie the dolomitized Pliocene strata are part of a continuous, basinal deposition system that may extend to depths as great as 2000 m. These strata, along with weathered Cretaceous

Reproduced with permission of the copyright owner. Further reproduction prohibited without permission.

rock, compose the bulk of the aquifer system today, and probably did so in the Pliocene and early Quaternary as well (Chapt. 2, this dissertation). Therefore, the aquifer material that came in contact with the groundwater in the Pliocene was most likely mineralogically similar to that of the aquifer material today, with the obvious exception of mineral stabilization, particularly within the carbonate section.

3) The dolomitized strata are shallow marine, and have been uplifted at most several tens of meters. Again, the magnitude of change in conditions has not been so large as to remove the usefulness of the modern system as an analog.

Reproduced with permission of the copyright owner. Further reproduction prohibited without permission.

METHODS

Sampling

Fourteen test holes were drilled with a rotary drilling rig capable of sampling to a depth of 100 m; cumulative drilling for the project exceeds 580 m. Friable or unconsolidated sediments were sampled at 1.5 or 3 m (5 or 10 ft) intervals with a split-spoon sampler; well-lithified material was collected with a diamond-bit core barrel. Core material from preexisting test holes provides additional data on the carbonate units underlying the southeastern portion of the central plain.

Unconsolidated sediments were sieved into gravel-, sand- and mud- size fractions. Further size analyses were not undertaken due to significant diagenetic alteration and aggregation of carbonate grains. Whole-grain counts and mineralogical analysis by X-ray diffraction provided data on grain origin and composition. Thin sections were prepared from consolidated material and loose grain mounts, and were used for mineralogical and facies analysis.

Stratigraphy and Sedimentology

The biostratigraphic and sedimentological framework of this study is based on the work of Multer and others (1977), Gerhard and others (1978), Lidz (1982), and Andreieff and others (1986). Revisions to the planktonic foraminiferal biostratigraphy is detailed in Chapt. 1 (this dissertation). Revisions of the sedimentology and basin evolution can be found in Gill and Hubbard (1985, 1986, 1987) and Chapt. 2 (this dissertation).

Reproduced with permission of the copyright owner. Further reproduction prohibited without permission.

Carbonate geochemistry

Stable isotopic analyses followed standard extraction and mass spectrometric procedures, and were carried out in the Louisiana State University stable isotope laboratory, Coastal Science Laboratories, Austin, and the Unocal Laboratory, La Brea. Dolomitic samples were prepared by repetitive leaching in 0.25N Acetic acid for 10-20 minutes at room temperature followed by distilled water dilution and centrifugation. The complete removal of calcite was confirmed by x-ray diffraction, and repetitive leaching did not cause measurable shifts in ordering or isotopic composition.

Strontium isotopic analyses were carried out by standard ion separation and mass spectrometry at Mobil Research and Development Laboratory in Dallas. Strontium isotopic results in this dissertation are therefore best compared to analyses made on the same equipment, such as the carbonate and seawater analyses by Burke and others (1982) and Koepnick and others (1985). Trace elements in carbonates were analyzed by microprobe on polished samples and by inductively coupled plasma spectrophotometer (ICP) on crushed, samples digested in dilute HCl.

Groundwater chemistry

Well Selection.-- Twenty-seven public and private wells were sampled for this project (Fig. 3.4). Public wells were steel-cased and equipped with oil-lubricated pumps. Private wells were equipped with submersible pumps and PVC casing.

Reproduced with permission of the copyright owner. Further reproduction prohibited without permission.

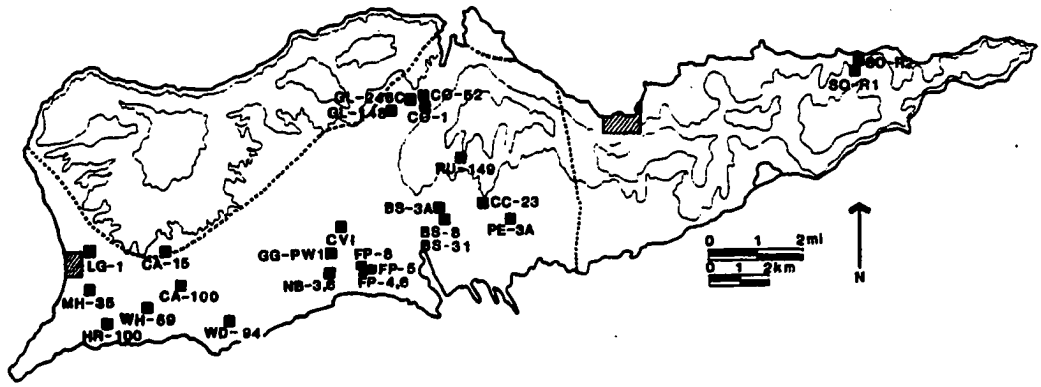

Figure 3.4. Water sampling locations. Samples were taken from existing public and private wells throughout the Central Plain carbonate areas, as well as from several wells in non-carbonate aquifers.

Water-Sample Collection and Treatment.-- Samples were collected from wells only after the water chemistry had stabilized as indicated by repetitive tests for temperature, pH and specific conductivity (Claasen, 1982). Buffers for pH determination were kept at ambient groundwater temperature with a water flow bath. All samples were taken as close as possible to the well head, and were collected through inert plastic tubing and fittings (Wood, 1976). All samples were filtered through 0.45 micron filters and preserved for subsequent analysis.

Aliquots for major and trace elements were acidified and stored in sealed, tightly capped polyethylene bottles. Aliquots for sulfate and nitrate analysis were preserved with mercuric chloride in polyethylene bottles. Aliquots for alkalinity and stable isotope analysis were stored in sealed glass jars. All storage and delivery vessels were chemically cleaned and dried in the laboratory, and repeatedly rinsed with the sampled water before final collection.

Analysis.-- Temperature to the nearest 0.1 ^{o}C, pH to the nearest 0.01 unit and specific conductivity to the nearest 10 micromhos/cm^2 were determined in the field.

Reproduced with permission of the copyright owner. Further reproduction prohibited without permission.

Specific conductivity was measured at ambient water temperature, and was not temperature compensated. Salinity was determined in the field by a temperature-compensating specific conductance/salinity meter. Specific conductivity corrected to 25 ^{o}C and the sum of dissolved constituents were calculated later and are listed in Table 3.1.

Major and minor elements were analyzed on an inductively coupled spectrophotometer (ICP). Chlorides were determined titrimetrically by the Mohr procedure, or on a laboratory chloridometer. Sulfate was measured turbidimetrically or by ion chromatography and the results were double checked by analysis for total sulfur on the ICP. Alkalinity was analyzed in the field or within 24 hours of collection after storage in tightly sealed glass bottles. Wet chemical techniques generally followed Skougstad and others (1979) or American Public Health Association (1971).

Alkalinity titrations followed the Gran technique of Gieskes and Rogers (1973). End points for this titration were determined by a linear regression of the Gran plot. Data points for the linear regression were selected objectively by a simple numerical technique, that eliminates those points that occur prior to where the function becomes linear (Fig. 3.5). Quality control procedures for analytical data followed guidelines set forth in Skougstad and others (1979) and Friedman and Erdmann (1982).

Speciation Modeling.-- Data sets selected on the basis of electrical neutrality were numerically modeled for thermodynamic speciation by the PHREEQE computer model (Parkhurst and others 1980). A *pe* of 12 was used in all calculations. We assume mildly oxidizing and near-neutral pH conditions in the groundwater.

Reproduced with permission of the copyright owner. Further reproduction prohibited without permission.

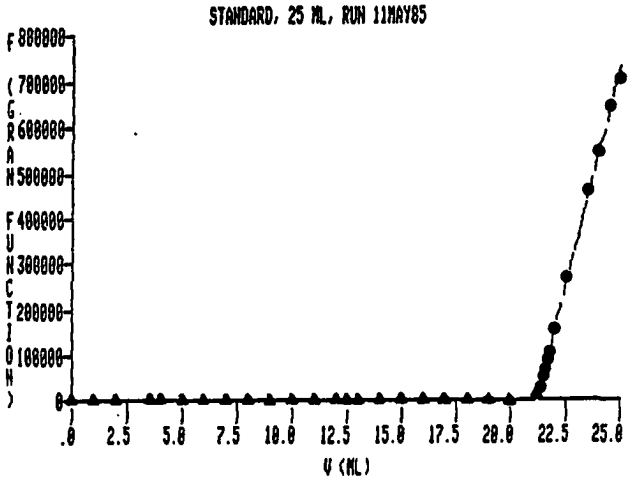

Figure 3.5. Sample Gran plot of an alkalinity titration. Data points indicated by circles are included in the linear regression for the determination of the end point.

Reproduced with permission of the copyright owner. Further reproduction prohibited without permission.

RESULTS

Stratigraphy and Timing of Dolomitization

Dolomitized strata occur both in the surface and subsurface of the southeastern industrial section of St. Croix's central plain (Fig. 3.6). Biostratigraphic work by Andreieff and others (1986) assigns the dolomitic strata in the Hess Cut outcrop (Outcrop 3, Fig. 3.1; Well M3, Fig. 3.7) to the early Pliocene *Globorotalia margaritae* zone. The maximum age for the dolomite is therefore early Pliocene, with the dolomitizing process occurring sometime between the early Pliocene and the present, a span of some five million years.

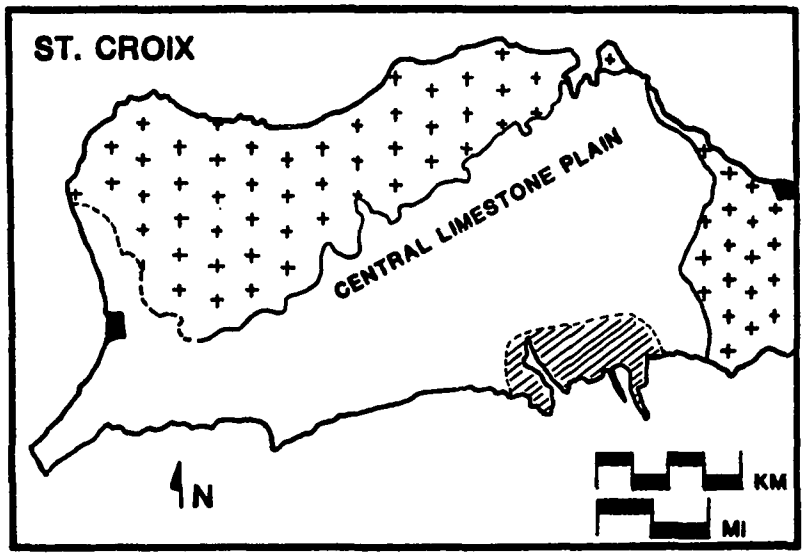

Figure 3.6. Location of dolomitized St. Croix strata. Dolomite is found only within the hatchured region in the southeastern portion of the Central Plain.

The post-Kingshill limestones in which the dolomitization has taken place are distributed along the southern shoreline of the Central Plain region of St. Croix. The thickest preserved strata of the post-Kingshill carbonates lie within a subsidiary graben or

Reproduced with permission of the copyright owner. Further reproduction prohibited without permission.

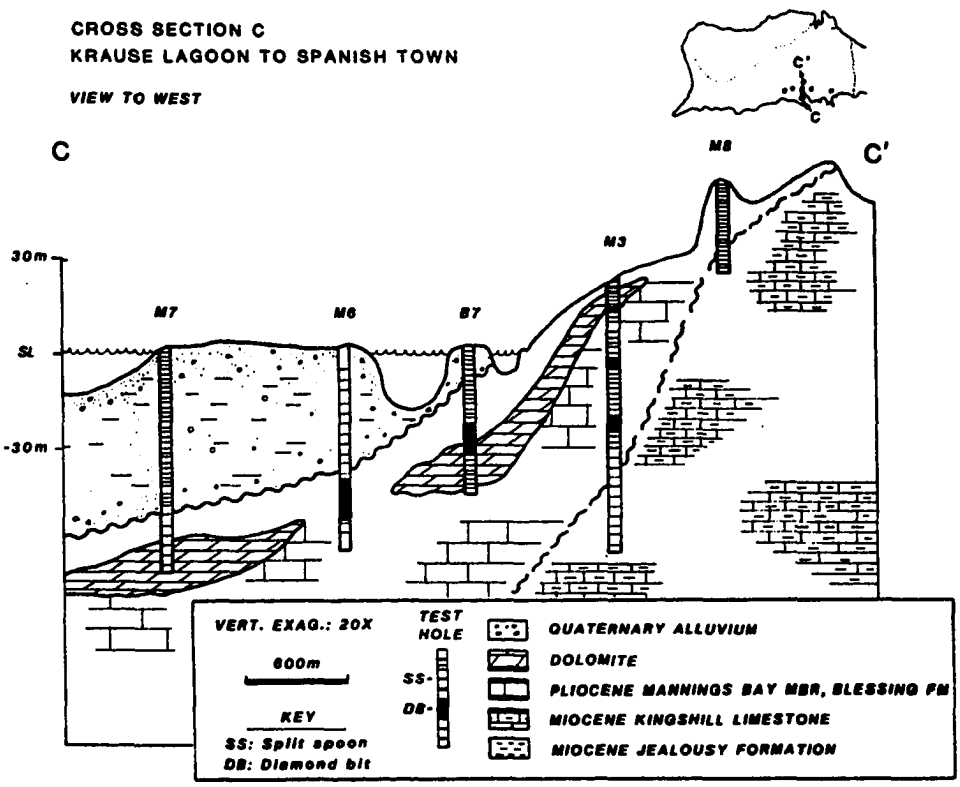

Figure 3.7. Cross section C-C' through the southeastern Central Plain: Krause Lagoon to Spanish Town. Interpreted zones of dolomitization are shown following the upper contact of the post-Kingshill limestone and the lower boundary of Krause Lagoon sediments. Depths of split-spoon samples and cored intervals are shown for each well. Cored intervals represent areas of well-indurated limestone. In friable or unconsolidated rock, split spoon samples were taken.

demi-graben that shows evidence of faulting at least as recently as the Pliocene (Gill and Hubbard, 1987; Chapt. 2, this dissertation).

Dolomitization has taken place within algal-foraminiferal grainstones and wackestones of the Mannings Bay Formation as well as reefal and lagoonal limestones of the Blessing Formation. There does not appear to be any lithological or facies-related control on the distribution of the dolomite within the post-Kingshill limestones.

Reproduced with permission of the copyright owner. Further reproduction prohibited without permission.

Dolomite Petrography and Texture

Dolomite in the St. Croix carbonate section exists both as euhedral rhombic cement in intergranular pores (Fig. 3.8), and as a replacement mineral of originally calcitic bioclasts (Fig. 3.9). The euhedral rhombs range from 1 to 75 microns in size (very fine- to medium-crystalline), with an average size of approximately 30 microns (finely crystalline). Dolomite crystals within bioclasts range from submicron-size within coralline algal fragments and dolomitic peloids, to millimeter-size replacements of echinoid fragments with unit extinction.

Skeletal clasts such as echinoid plates and coralline algae that were originally high-magnesian calcite are preserved in surprising detail, with the cellular structure and organic layering in coralline algae, as well as the unit extinction and porous plate structure in echinoid fragments preserved (Fig. 3.10.). This is in contrast to the complete obliteration of biogenic texture often observed in coarse-grained ancient dolomites.

Selective dissolution of skeletal clasts is common, with wholesale removal of planktonic and larger benthic forams occurring during or after dolomitization as indicated by the moldic porosity produced by their still-recognizable test shapes in a rhombic dolomitic matrix (Fig. 3.11). Other less-stable grains originally composed of aragonite and magnesian calcite seem to have been dissolved or recrystallized prior to dolomitization, with the resulting pore space now apparently occupied by dolomite.

Pervasive dolomite abruptly underlies calcitic limestone strata in continuous core samples taken from the industrial area on St. Croix, with the transition from calcite to dolomite taking place over a few centimeters. In less completely dolomitized sections,

Reproduced with permission of the copyright owner. Further reproduction prohibited without permission.

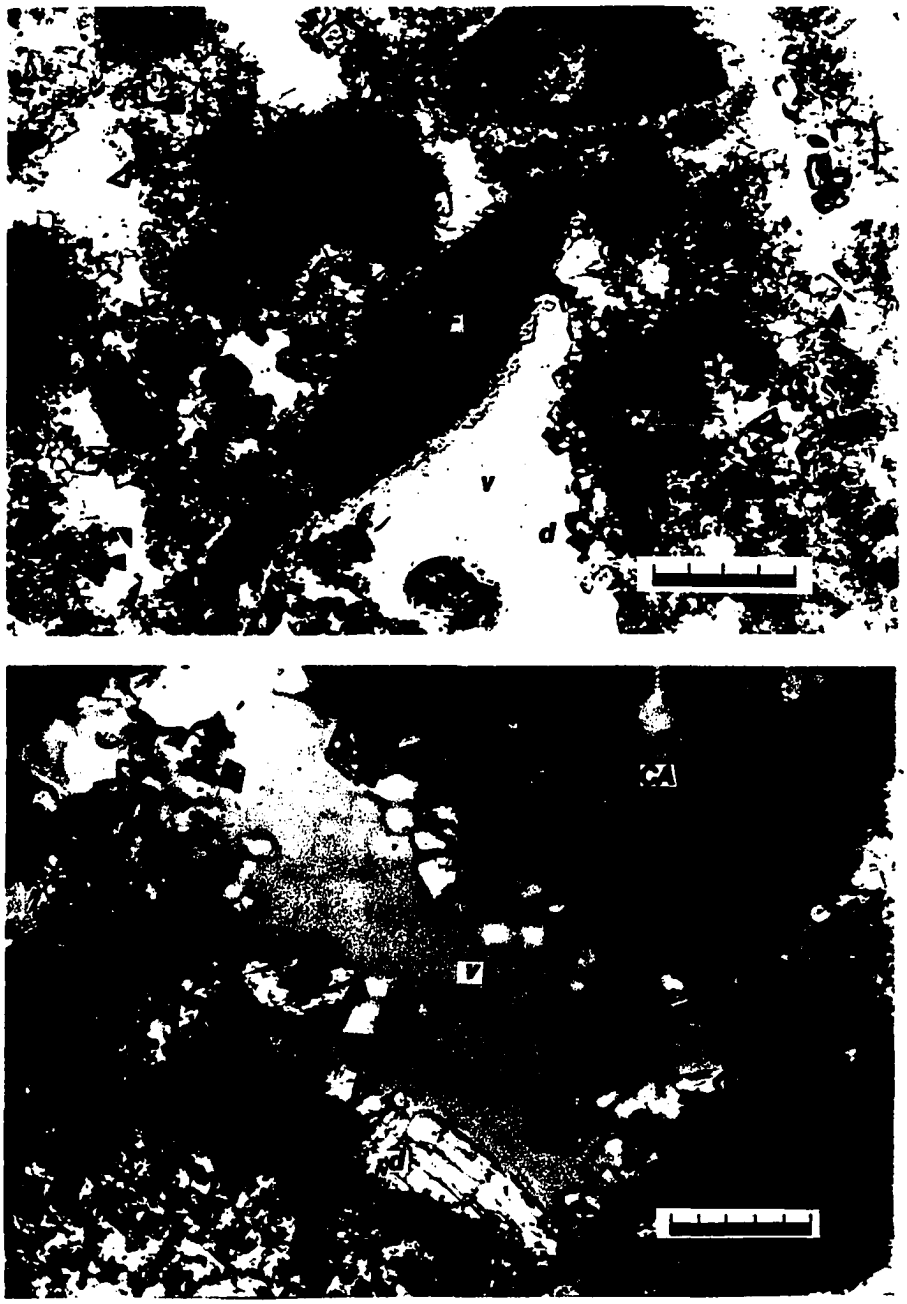

Figure 3.8. Photomicrographs of pervasively dolomitized material. Sample B7/5/10.
Upper photo: Dolomitized benthic foramininiferan (BF) and coralline algal fragment (CA) surrounded by dolomite rhombs (d) and void space (v). Scale bar = 0.2 mm; plane polarized light.
Lower photo: Dolomitized coralline algal fragment (CA) with preserved microstructure. Rhombic dolomite (d) rims void space (v). Scale bar = 0.1 mm; plane polarized light.

Reproduced with permission of the copyright owner. Further reproduction prohibited without permission.

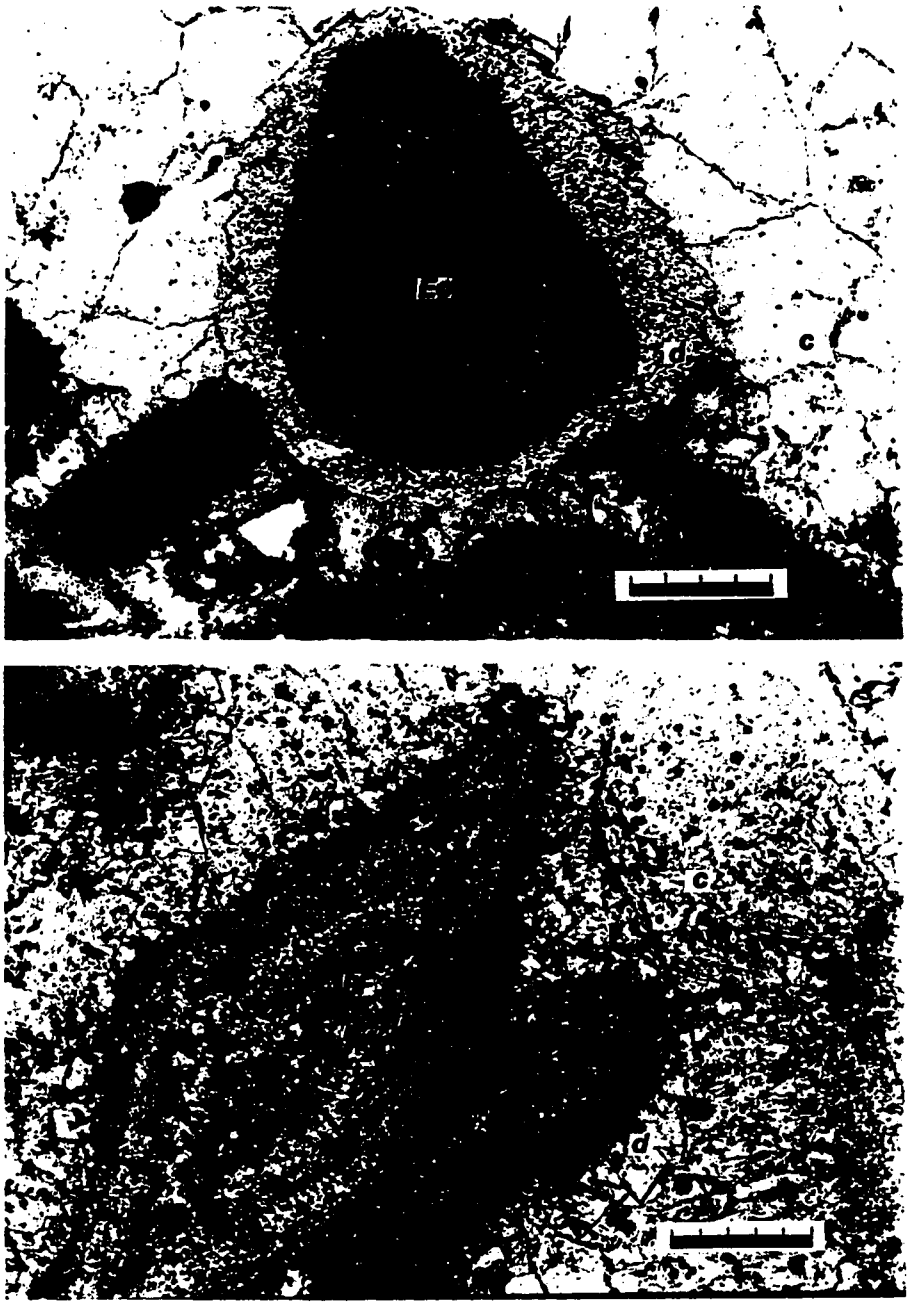

Figure 3.9. Photomicrographs of dolomitized bioclasts; sample B4/4/2.
Upper photo: Dolomitized echinoderm fragment (Ec) with syntaxial dolomite overgrowth (d) and enveloping calcite spar (c). Scale bar = 0.2 mm; plane polarized light.
Bottom photo: Dolomitized benthic foraminiferan (BF) with rim of rhombic dolomitic cement (d) enclosed in poikilitic calcite (c). Scale bar = 0.1 mm; plane polarized light.

Reproduced with permission of the copyright owner. Further reproduction prohibited without permission.

Figure 3.10. Photomicrograph of dolomitized coralline algal fragment (CA) retaining microstructural detail. Bioclasts are rimmed with dolomite (d). Sample B4/4/8. Scale bar = 0.2 mm, Plane polarized light.

Figure 3.11. Thin section photomicrograph showing complete dolomitization of bioclasts and moldic porosity of planktonic foraminifera (PF(v)). Sample B15A/5/6. Scale bar = 1.0 mm, Plane polarized light.

Reproduced with permission of the copyright owner. Further reproduction prohibited without permission.

the dolomite forms pore linings and isopachous fringes that are engulfed by calcite mosaic pore fillings (Fig. 3.12). This strongly suggests that dolomite formation preceded the precipitation of calcite spar.

Cathodoluminescence reveals that the dolomite exhibits different crystal zonation patterns depending on its stratigraphic position. Dolomite presently below the water table is strongly luminescent, with the euhedral dolomite rhombs and overgrowths ornately zoned (Fig. 3.13). Bioclasts that have been dolomitized are strongly luminescent, but are generally not zoned.

In contrast, dolomite presently in the vadose zone, such as that exposed in outcrop, has luminescence that varies from very weak to moderately bright, and is generally unzoned. Euhedral rhombs showing luminescent zonation in vadose strata generally have homogeneously dull interiors with a brightly luminescent rim (Fig. 3.14). Two possible interpretations are that the dolomites within the present vadose zone (1) have been recrystallized, or (2) were formed under chemically different conditions than the dolomites presently below the water table. Some support for these hypotheses is found in the stable isotopic chemistry of the dolomites, as well as the stratigraphic distribution of the dolomitic rock, which is discussed in the following section.

Reproduced with permission of the copyright owner. Further reproduction prohibited without permission.

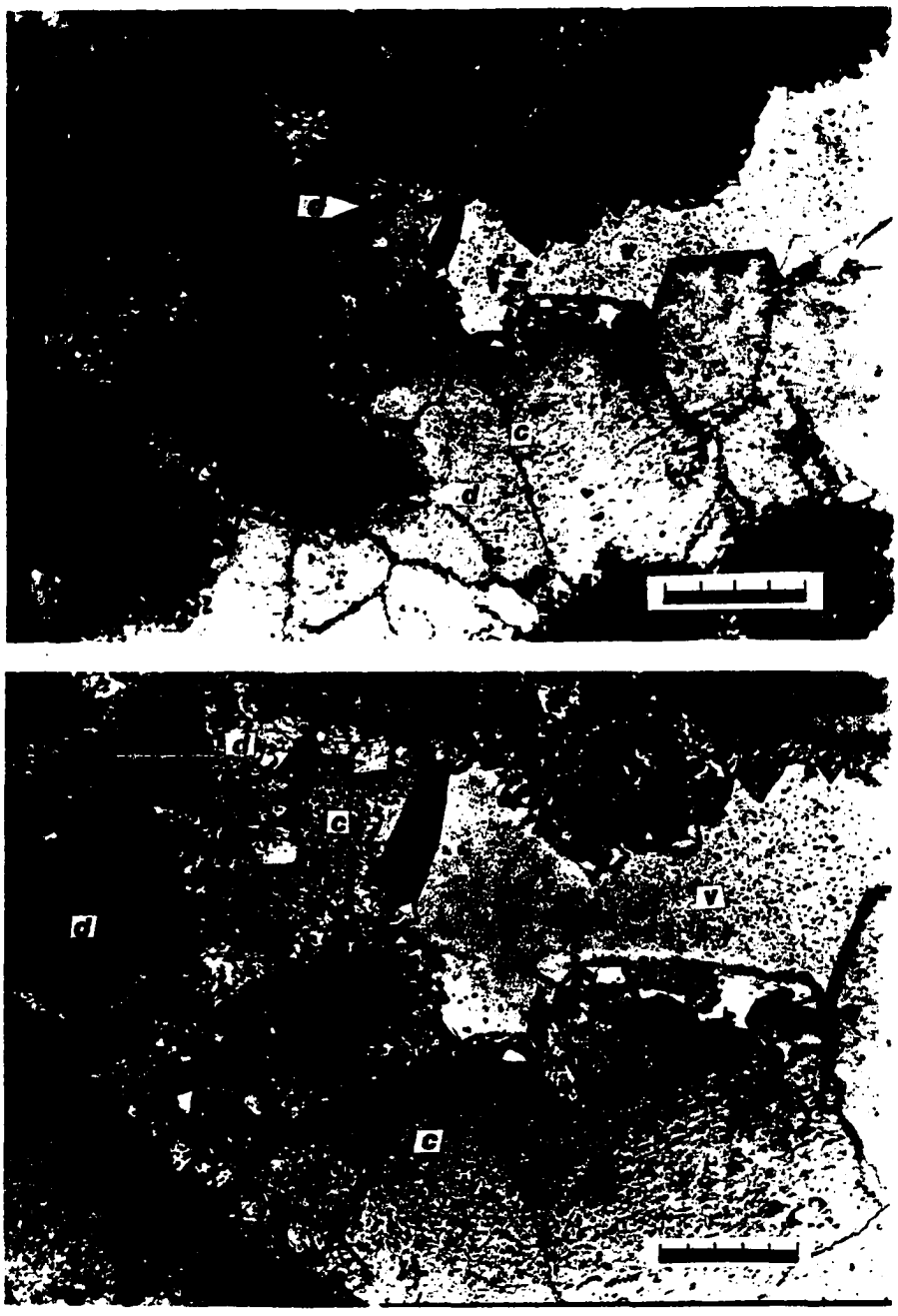

Figure 3.12. Photomicrographs showing rhombic dolomite grain-fringing cement followed by coarse calcite mosaic. Sample B4/4/2, stained with Alizarin-Red/K-Ferricyanide.
Upper Photo: scale bar = 0.2 mm, Plane polarized light.
Lower Photo: scale bar = 0.1 mm, Plane polarized light.

Reproduced with permission of the copyright owner. Further reproduction prohibited without permission.

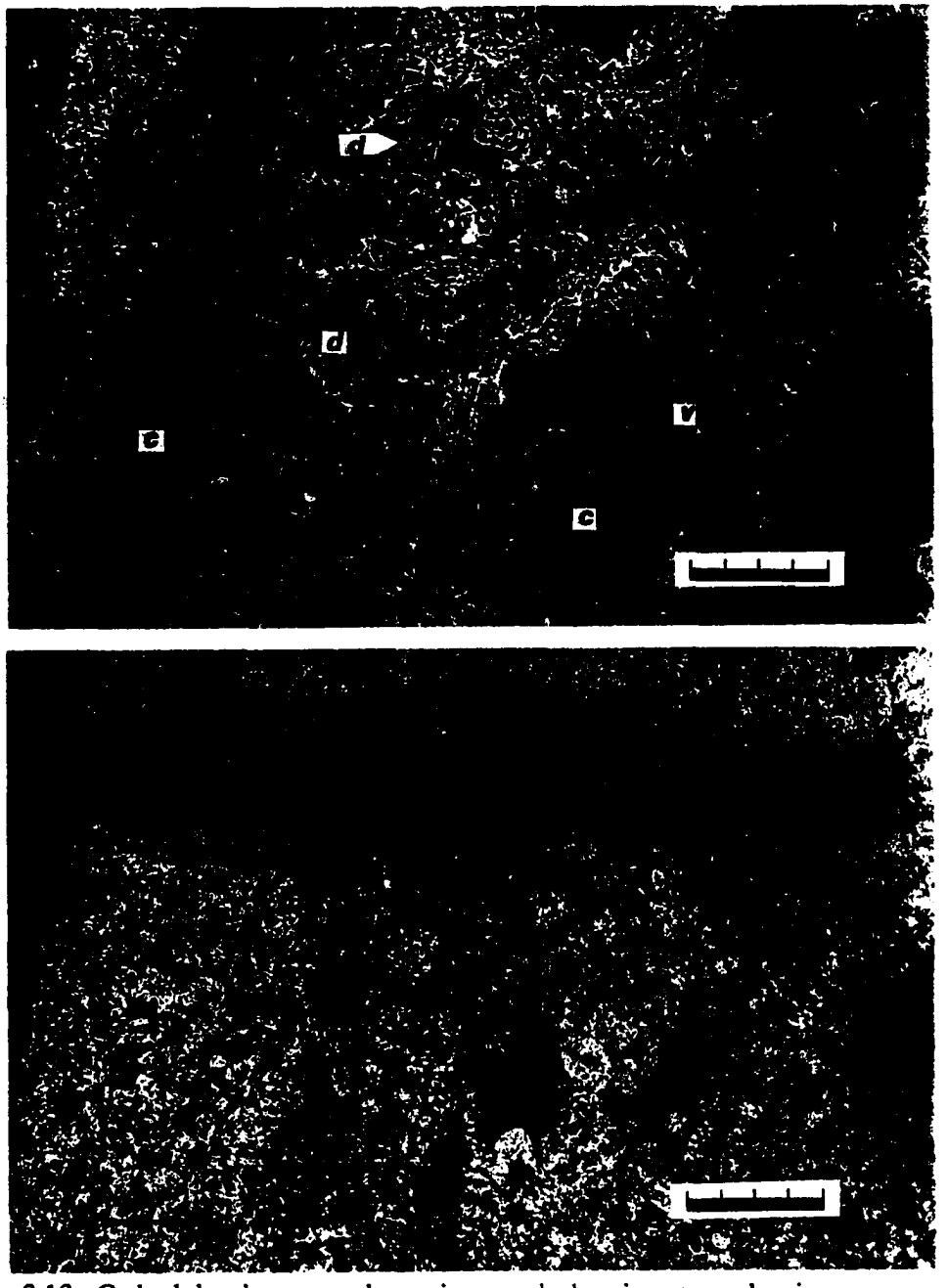

Figure 3.13. Cathodoluminesence photomicrograph showing strong luminescence and detailed zonation of St. Croix dolomites below the water table. Sample B4/5/4. Scale bar = 0.2 mm for both photos.
Upper Photo: Cathodoluminescence. Dolomite (d), calcite spar (c), void space (v).
Lower Photo: Plane polarized light; same frame as the upper photo.

Reproduced with permission of the copyright owner. Further reproduction prohibited without permission.

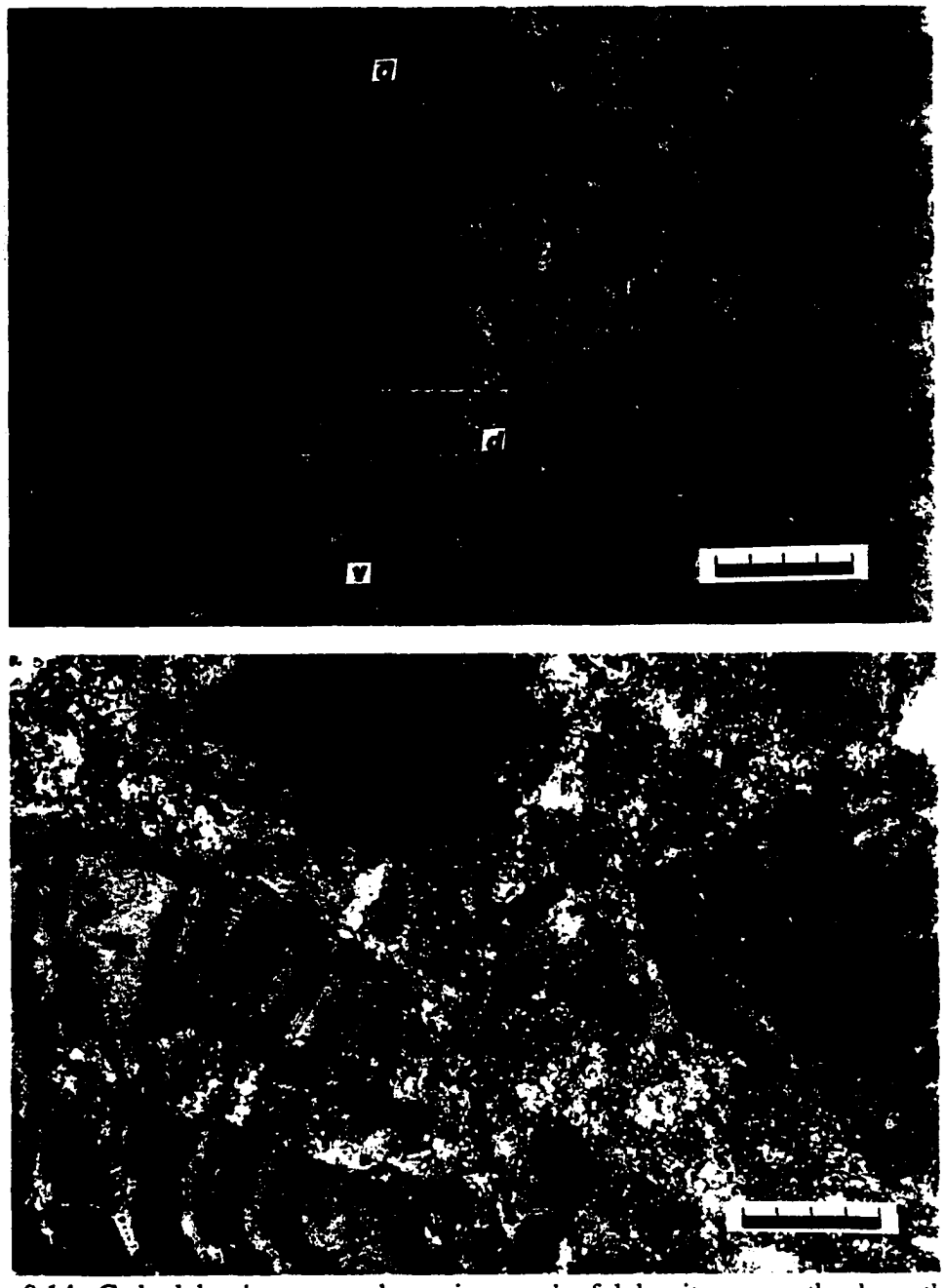

Figure 3.14. Cathodoluminescence photomicrograph of dolomites presently above the water table. Note duller luminescence and single luminescent zone around rim of dolomite rhombs. Sample VII 26E. Scale bar = 0.2 mm for both photos.
Upper photo: cathodoluminescence; dolomite (d), void space (v).
Lower photo: plane polarized light; same frame as the upper photo.

Reproduced with permission of the copyright owner. Further reproduction prohibited without permission.

Geographic and Stratigraphic Distribution of St. Croix Dolomite

Seen in cross section, the St. Croix dolomite closely follows the overlying contact with unconsolidated carbonates and siliciclastic alluvium (Figs. 3.7, 3.15). Unconsolidated sediments in Krause Lagoon represent a mixed carbonate and siliciclastic assemblage comprised of *in-situ* mangrove- lagoon carbonates and alluvium eroded off exposed island strata. Krause Lagoon has traditionally served as a drainage basin for the southeastern central coast, and as a collection area for stream-transported alluvium (Fig. 3.16).

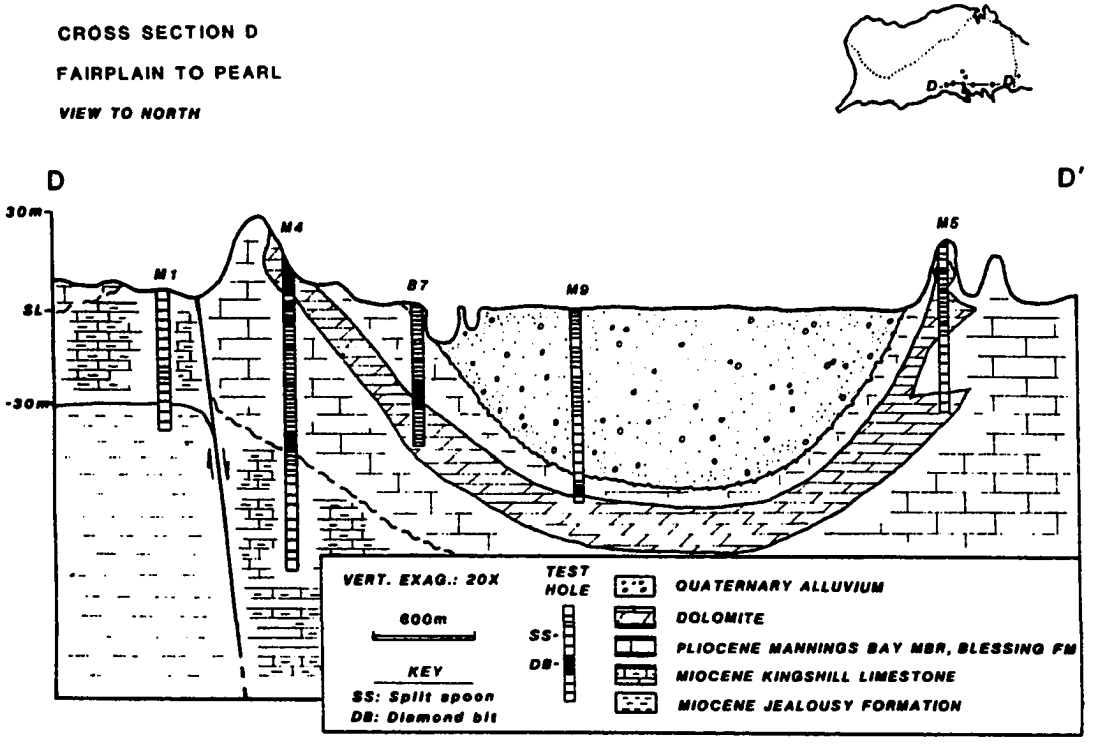

Figure 3.15. Cross section D-D' through the southeastern Central Plain: Fairplain to Pearl. Interpreted zone of dolomitization follows the base of Krause Lagoon and the upper contact of the post-Kingshill limestones. Depth locations of split-spoon samples and cored intervals are shown for each well, with split-spoon samples taken in friable or unconsolidated material.

Reproduced with permission of the copyright owner. Further reproduction prohibited without permission.

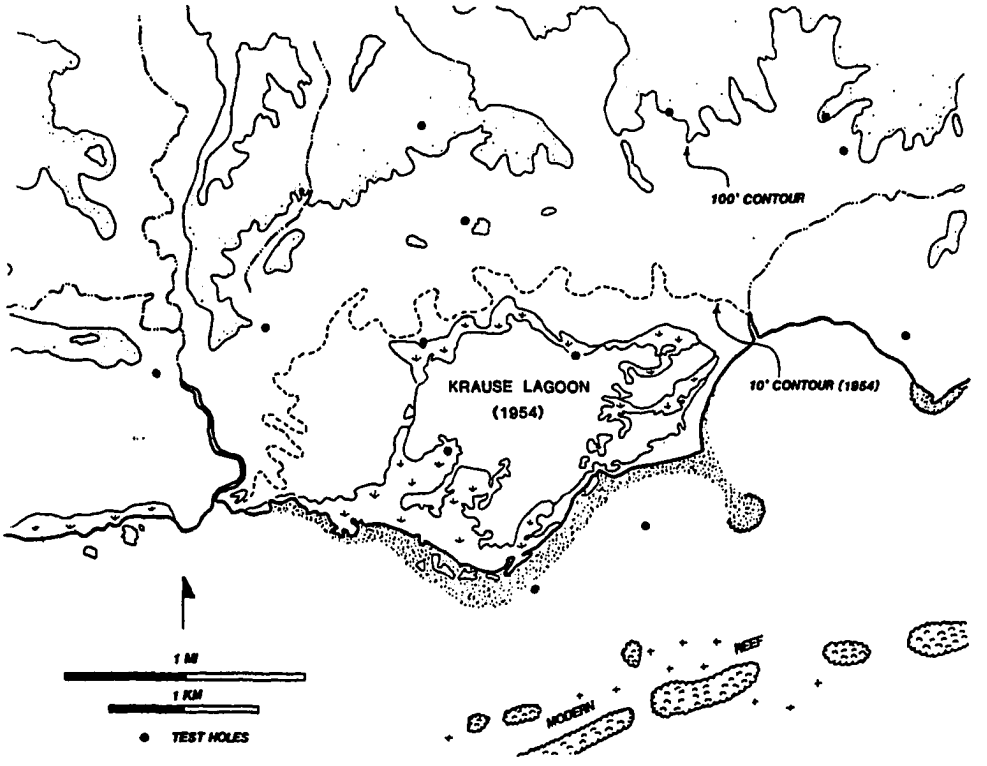

Figure 3.16. Natural drainage and morphology of the Krause Lagoon area. The 10 ft contour represents the approximate pre-industrial development shoreline. The 100 ft contour may mark an earlier shoreline or structural feature. Topographic data from the1958 Christiansted topographic quadrangle map.

Seen in map view, surficially exposed dolomite forms an arcuate pattern that closely coincides with the St. Croix natural shoreline and the trend of the Pliocene reef tract (Fig. 3.17). The subsurface dolomite occurs offshore of the Pliocene reef-tract, within the confines of the pre-industrial development Krause Lagoon and within deposits of shelf and fore-reef carbonates. The pre-industrial development shoreline used here was taken from the 1954 USGS Christiansted quadrangle topographic map. The present (post-industrial development) coastline of St. Croix (Fig. 3.18) does not coincide with the dolomite distribution pattern due to the extensive dredge and fill operations that have accompanied industrial development on the island since the late 1950s.

Reproduced with permission of the copyright owner. Further reproduction prohibited without permission.

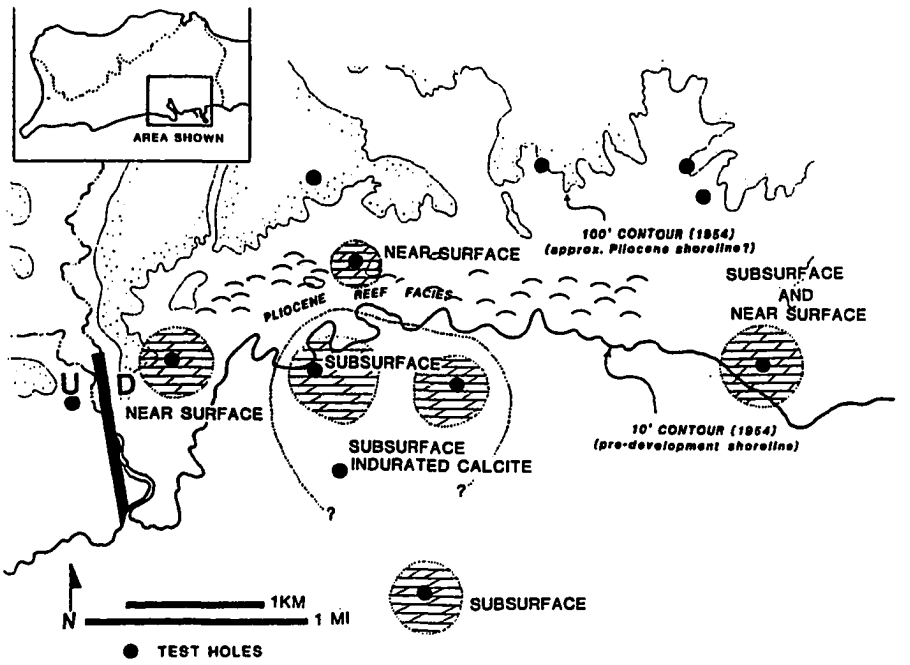

Figure 3.17. Dolomite distribution relative to the natural (pre-development) island shoreline and local structure (from 1958 topographic quadrangle map). Dolomite presently exposed or above the water table is found within a patchy, arcuate zone that mimics the Pliocene reef trend and the natural shoreline. Dolomite presently below the water table is found in platform sedimentary facies in Krause Lagoon.

Dolomite was not found in any other geographic location on St. Croix, nor does it occur within any sedimentary facies other than the shelf and reefal carbonates of the post-Kingshill limestones within Krause Lagoon. The spatial distribution of the dolomite, both laterally as well as stratigraphically, closely follows the boundaries of Krause Lagoon and the sedimentary facies contained within it. This distribution pattern implies a genetic relationship between the formation of the dolomite and the presence of Krause Lagoon.

The location of Krause Lagoon itself is apparently controlled by faulting that cuts through Pliocene strata, and the faulting therefore has been active at least as recently as the Pliocene. The western border of the lagoon is bounded by a normal fault of greater than 80 m (260 ft) displacement (Fig. 3.18, 3.15), and faulting along this boundary was

Reproduced with permission of the copyright owner. Further reproduction prohibited without permission.

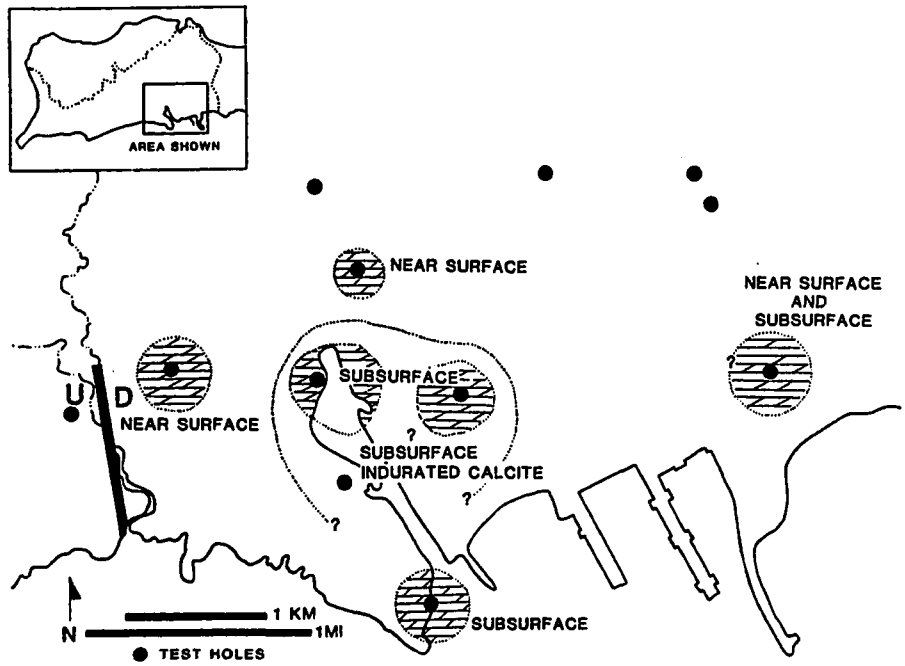

Figure 3.18. Dolomite distribution relative to the 1988 shoreline and local structure. The geographic distribution of the dolomite does not correspond to the shoreline produced by recent industrial development.

probably responsible for the deposition and preservation of the great thickness of Kingshill and post-Kingshill sediments in the area (Gill and Hubbard, 1987; Chapt. 2, this dissertation). I suggest that Krause Lagoon is a relict feature that existed in the Pliocene. Processes restricted to its borders apparently effected the formation of dolomite.

Groundwater

Due to the close connection between groundwater flow and several currently accepted models of dolomitization (Land, 1980; Muir and others, 1980) it is reasonable to ask whether the present groundwater system is a reasonable analog for the system that produced the St. Croix dolomite. In particular:

Reproduced with permission of the copyright owner. Further reproduction prohibited without permission.

1) what are the sources of dissolved solids within St. Croix groundwater?

2) can the present groundwater support dolomitization?

3) what carbonate phases are presently stable within the present carbonate aquifer system?

To answer these questions, 34 groundwater samples were analyzed from a variety of locations within the carbonate Central Plain of St. Croix. In addition, water from several locations in non-carbonate regions, rainwater and seawater were similarly analyzed. The groundwater averaged 1730 ppm total dissolved solids, with a range that varied from 250 to 6500 ppm. The groundwater samples were primarily sodium-chloride waters, Na (Ca-Mg) - Cl (HCO_3) grading into sodium- bicarbonate waters Na (Ca+Mg) - HCO_3 (Cl) (Fig. 3.19) according to criteria suggested by Morgan and Winner (1962) and Back (1966) both *in* Freeze and Cherry (1979). Results of the groundwater analyses can be found in Table 3.1.

Geographic Trends.-- In general, the total dissolved solid content and chloride concentrations in groundwater increase markedly near the coastlines, and decrease inland (Fig. 3.20). The concentration pattern of sodium closely follows that of chloride, with sodium concentrations increasing rapidly toward the coast. In a crude sense, these patterns indicate that mixing between groundwater and seawater is probably an important process in producing the chemical composition of St. Croix groundwater today.

Residual salts in the aquifer and interaction with formation waters ("connate waters"; Robison, 1972) from the Kingshill Limestone and Jealousy Formation may also be responsible for the high ionic content of the groundwater. Earlier workers report concentrations of total dissolved solids exceeding 20,000 ppm in groundwater from

Reproduced with permission of the copyright owner. Further reproduction prohibited without permission.

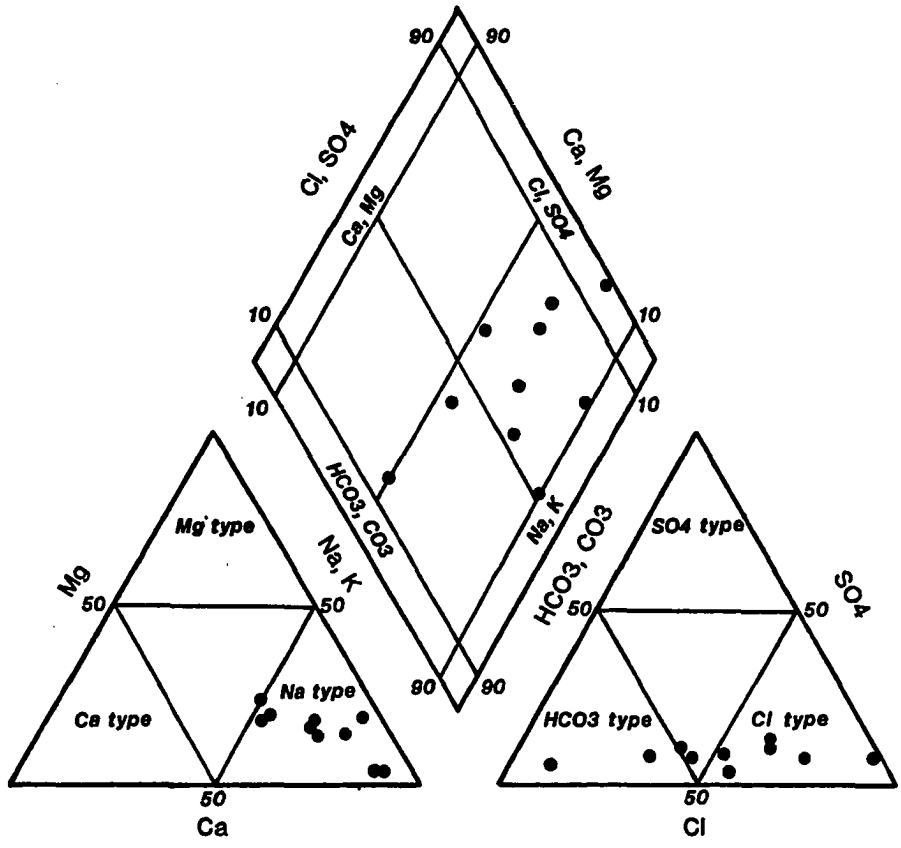

Figure 3.19. Piper diagram showing the chemical range of ionic distribution in St. Croix groundwaters.

inland portions of the Central Plain region (Robison, 1972; Jordan, 1975). With the possibility of 2000 m of compactable sediments in the underlying Jealousy Formation, it is certainly possible that formation-derived waters and salts affect the Tertiary plain groundwaters. A residual salt source for the dissolved solids would also explain why the groundwater samples tested all showed a meteoric isotopic signature (Fig. 3.21). However, the anomalously high dissolved solids levels were not detected by more recent studies (Geraghty and Miller, 1983; Gill and Hubbard, 1986), and these waters were therefore unavailable for testing.

Regardless of the source of the bulk of the dissolved solids, the ratio of sodium to chloride (Na:Cl) in groundwater increases rapidly away from the coastline (Fig. 3.22).

Reproduced with permission of the copyright owner. Further reproduction prohibited without permission.

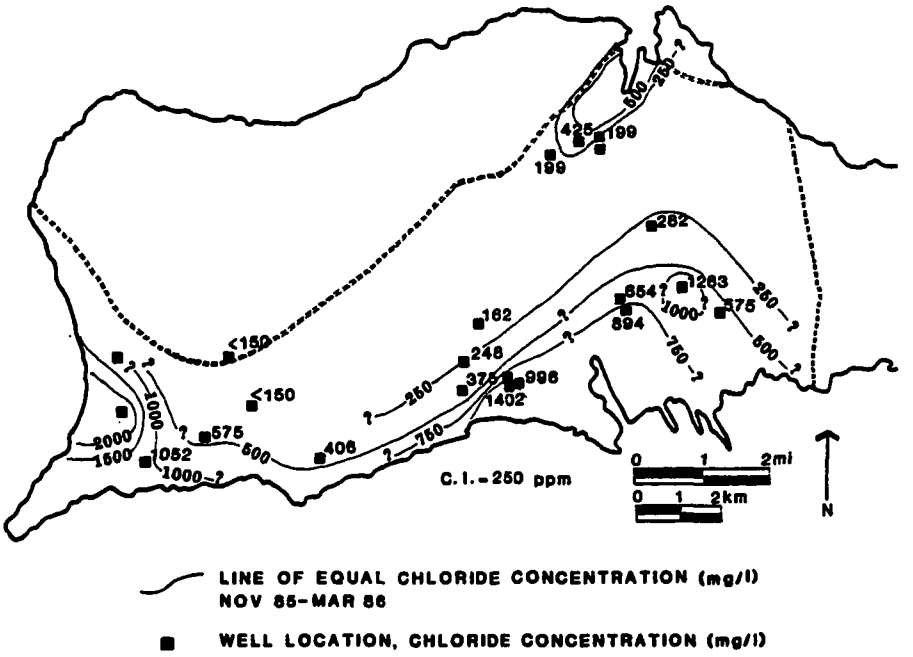

Figure 3.20. Groundwater chloride concentration isopleth map. Groundwater chloride concentation increases sharply toward the coastline, particularly in areas of permeable linestone or high withdrawal. Water wells are generally screened from the water table to the bottom of the well, and the contours therefore must be interpreted as averages over a wide depth range.

This relation cannot be explained by mixing processes alone as shown in the section below. Thus, although the mixing of fresh groundwater and seawater, as implied by the geographical distribution of chloride, is an important control on the groundwater chemistry, other processes must be responsible for the distribution of elements in the groundwater. Since the source of dissolved solids in the groundwater is relevant to the formation of dolomite, the following section investigates this point in more detail.

Mixing Curves.-- In order to test whether the solutes in St. Croix groundwater are the result of mixing alone, mixing curves have been plotted for several elements using values for rainwater and seawater as the end members of the curve. Chloride is used as the independent variable, and is assumed to behave conservatively.

Reproduced with permission of the copyright owner. Further reproduction prohibited without permission.

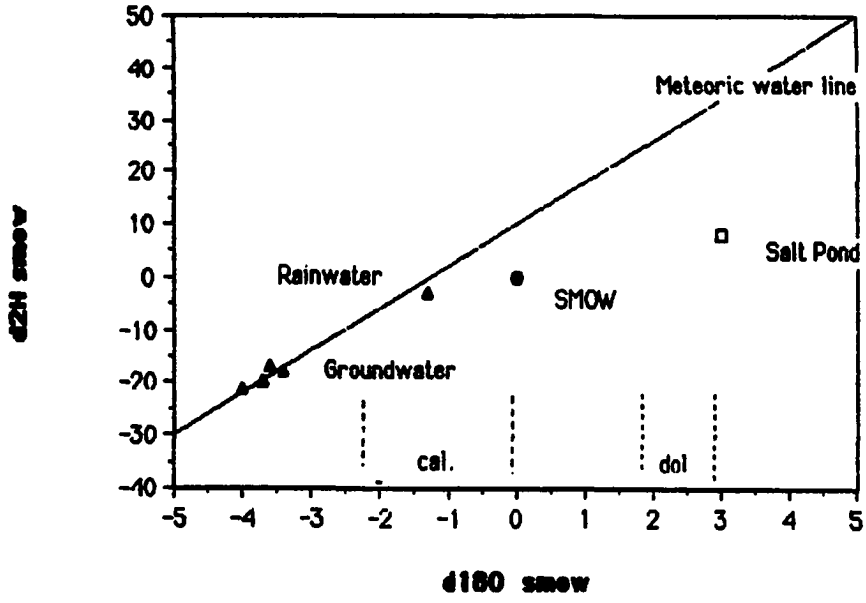

Figure 3.21. Stable isotopic cross plot for St. Croix groundwaters, rainwater and water from West End Salt Pond on St. Croix. Waters in oxygen isotopic equilibrium with St. Croix calcitic limestones and dolomites are shown in the fields marked "cal." and "dol." respectively. Equilibrium calculations assume 25 ^{o}C and the dolomite fractionation factor of Fritz and Smith (1970).

Mixing line calculations are based on literature values of seawater (Drever, 1982) and Virgin Islands rainwater (Jordan, 1975).

Sodium plots consistently in excess of values expected if the chemistry of the groundwater were a simple function of mixing fresh water and seawater (Fig. 3.23). The excess sodium averages more than 100 ppm greater than would be predicted for a mixed water of comparable chloride content. Similarly, total dissolved solids plots consistently in excess of the mixing curve, with a high correlation with total chloride content (Fig. 3.24). This suggests a net contribution of dissolved constituents to the groundwater through interaction with aquifer materials, formation water or some other source (Jordan, 1975).

Reproduced with permission of the copyright owner. Further reproduction prohibited without permission.

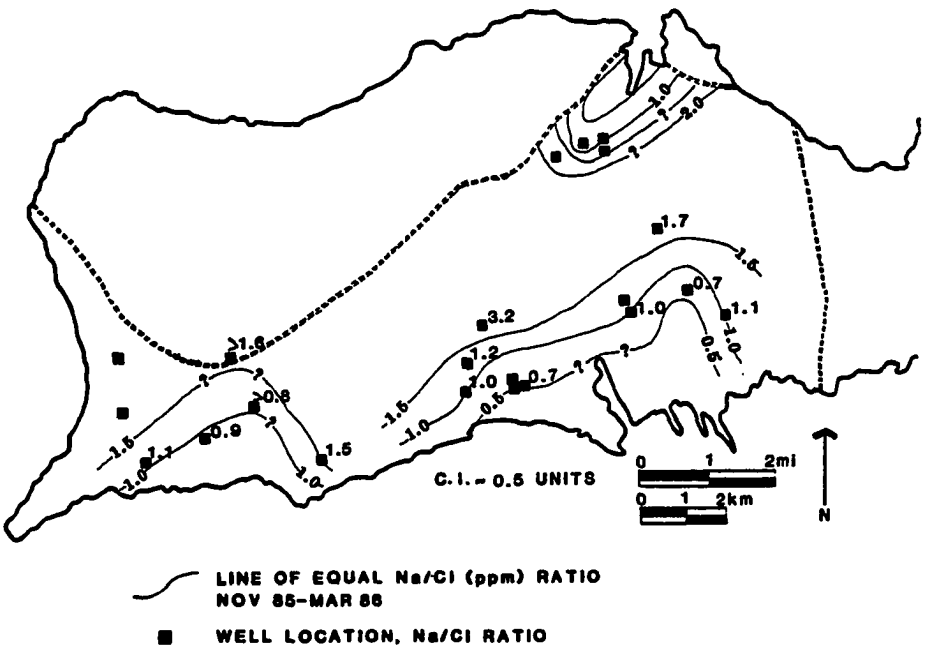

Figure 3.22. Groundwater sodium: chloride ratio isopleth map. The ratio of sodium to chloride (in ppm) increases inland, deviating sharply from the seawater ratios measured in wells near the coastline.

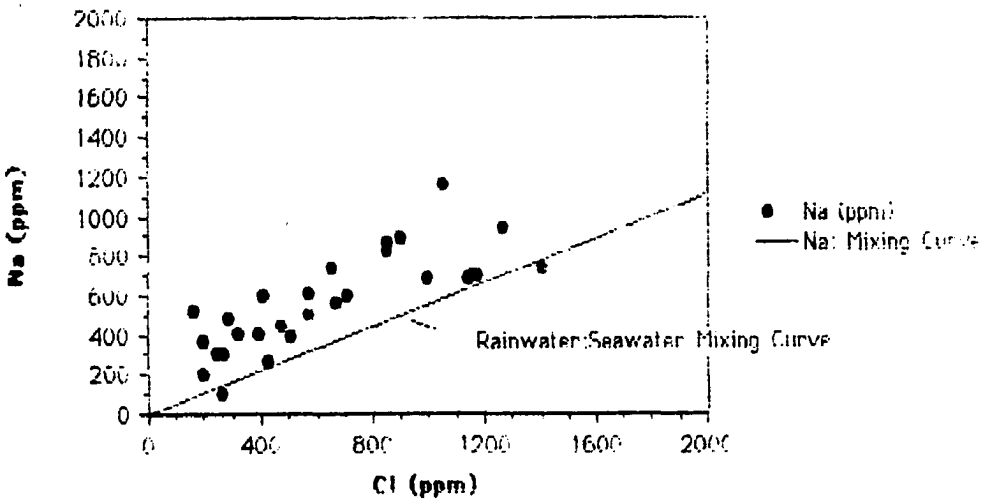

Figure 3.23. Rainwater:seawater mixing curve for sodium. Data points show, with few exceptions, that sodium is found in excess of values expected if only rainwater:seawater mixing were responsible for the sodium content in groundwater.

Reproduced with permission of the copyright owner. Further reproduction prohibited without permission.

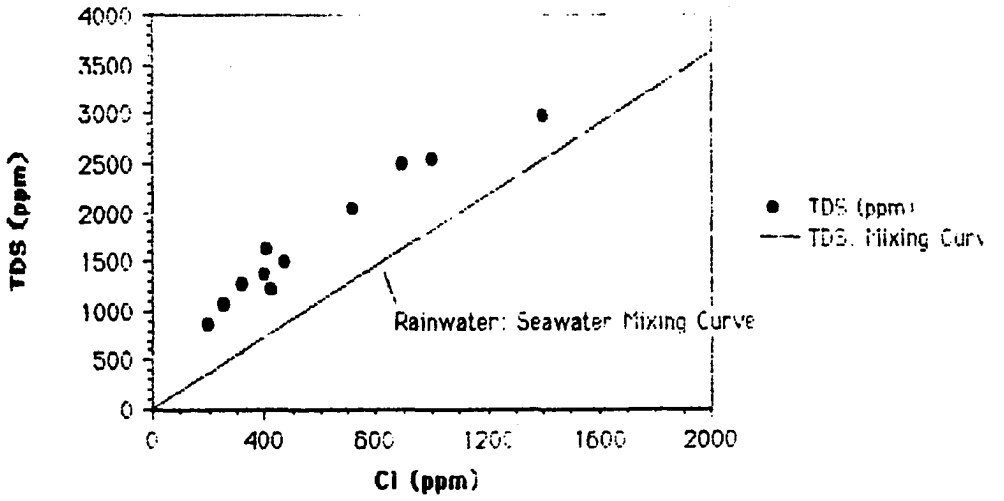

Figure 3.24. Rainwater:seawater mixing curve for total dissolved solids. Data points show that material is being added to groundwater by aerosols, dissolution of aquifer materials, or residual salts and formation water within the aquifer.

In contrast, potassium consistently fell below theoretical mixing values when plotted against chloride (Fig. 3.25). Because both sodium and potassium are highly mobile and form extremely soluble minerals during extreme evaporation of water, it is unlikely that concentrations of either element would be modified by evaporative precipitation as in the Hardie-Eugster model (Hardie and Eugster, 1970) or by evaporative precipitation and re-solution of rainwater.

Both calcium and alkalinity concentrations are well in excess of a rainwater/seawater mixing curve, which is not surprising in a carbonate aquifer (Figs. 3.26; 3.27). Similarly, the concentration of strontium is consistently in excess of values to be expected from the mixing of rainwater and seawater (Fig. 3.28). In contrast, magnesium values form a scatter plot when plotted against chloride, and are not consistently above or below a seawater/freshwater mixing line (Fig. 3.29).

Reproduced with permission of the copyright owner. Further reproduction prohibited without permission.

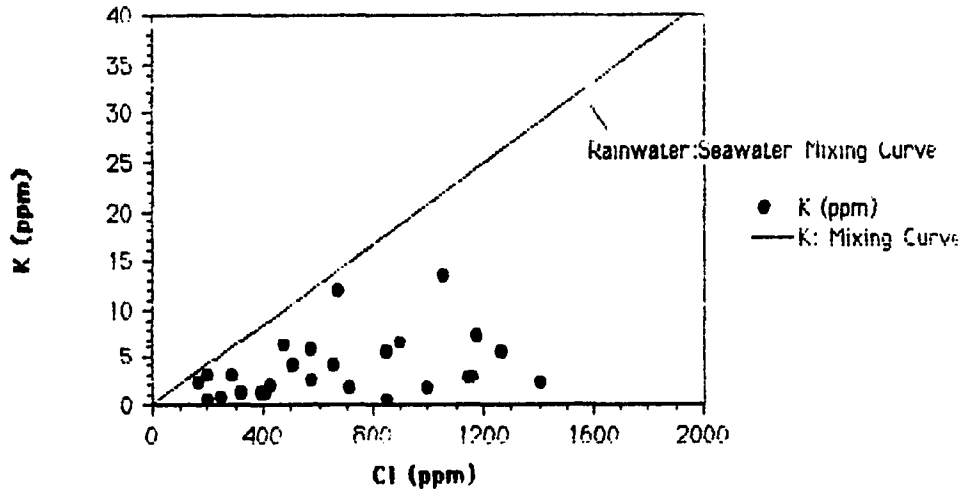

Figure 3.25. Rainwater:seawater mixing curve for potassium. Potassium is depleted in St. Croix groundwater relative to a rainwater: seawater mixing curve, implying either diagenetic interaction with the groundwater such as ion-exchange, or a potassium-depleted source for the dissolved solids.

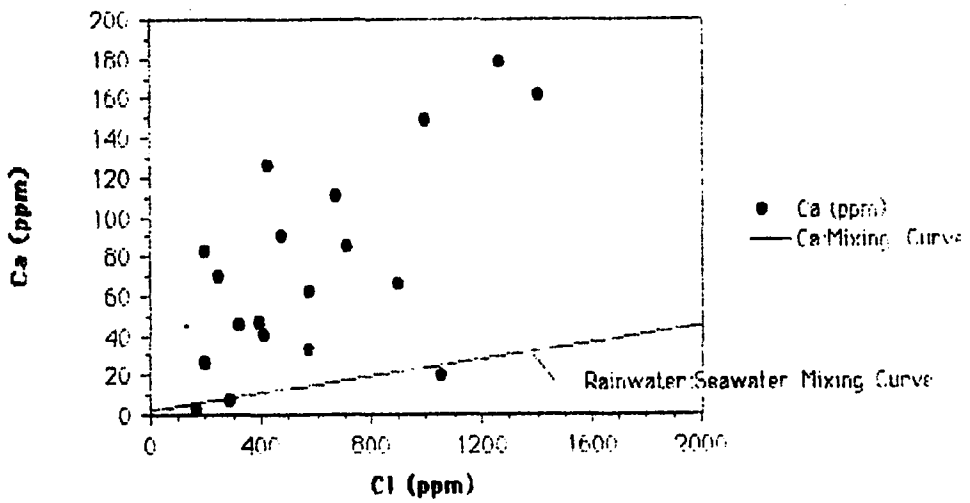

Figure 3.26. Rainwater:seawater mixing curve for calcium.

In general, the mixing curves show that a significant proportion of the dissolved solids in St. Croix groundwater cannot be explained by the mixing of meteoric water and marine water alone. The relatively large proportion of sodium and calcium, in particular, must be derived from a source other than seawater. Dissolution of carbonates in the aquifer system is an obvious source for the calcium, but does not explain the distribution

Reproduced with permission of the copyright owner. Further reproduction prohibited without permission.

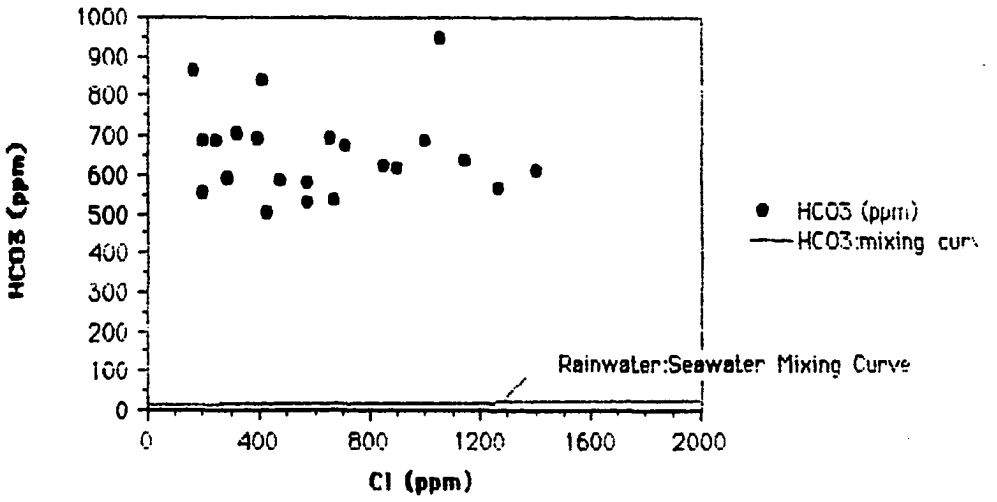

Figure 3.27. Rainwater:seawater mixing curve for bicarbonate. Total alkalinity in this carbonate aquifer system is in excess of the rainwater:seawater mixing curve.

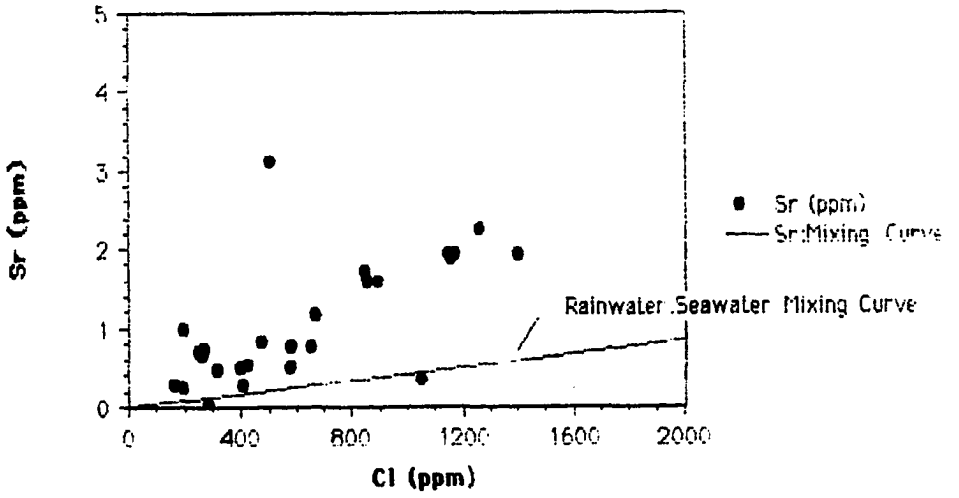

Figure 3.28. Rainwater:seawater mixing curve for strontium showing that strontium is generally in excess of a rainwater:seawater mixing curve.

of the alkali metals. The excess sodium as well as the deficiency of potassium in the groundwater cannot result from interaction with carbonates alone, and must instead be due to interaction with siliciclastics, the contribution of aerosols and rainwater, and the contribution of formation waters and residual salts within the aquifer (Jordan, 1975).

Reproduced with permission of the copyright owner. Further reproduction prohibited without permission.

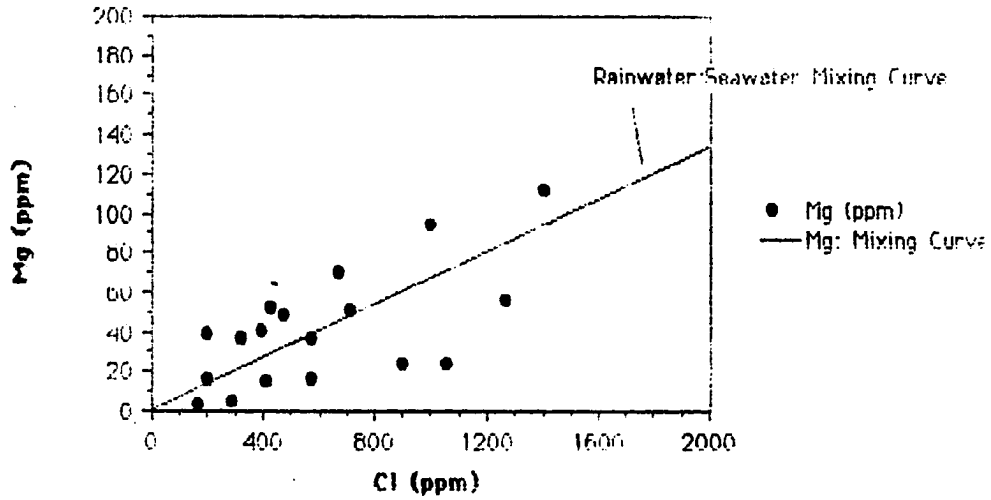

Figure 3.29. Rainwater:seawater mixing curve for magnesium.

Because the quantity of dissolved solids increases markedly with well depth (Robison, 1972; Gill and Hubbard, 1986), surficial processes such as evaporation and concentration of rainwater and aerosol-derived salts cannot explain the bulk of the groundwater chemistry. In addition, the average groundwater composition in the Tertiary carbonates is several times higher than that in alluvial and Mt. Eagle rocks (Jordan, 1975), also indicating that surficial processes alone do not explain the high salt content of the Tertiary carbonate aquifer system.

The distribution of the ions in the groundwater is at least in part due to interaction with siliciclastic aquifer materials, a conclusion supported by the $^{87}Sr/^{86}Sr$ ratio of the groundwater, discussed below. The extent of siliciclastic interaction is surprising in this predominantly carbonate aquifer, and it is important to understand whether the interaction with siliciclastics results in saturation conditions for carbonate minerals.

Chemical Modeling.-- In order to judge the state of saturation of carbonate minerals in St. Croix groundwater, saturation calculations were performed on seven

Reproduced with permission of the copyright owner. Further reproduction prohibited without permission.

samples by the PHREEQE program (Parkhurst and others, 1980). The results of the saturation calculations are shown on Table 3.2, and indicate that St. Croix groundwater is saturated with respect to calcite and dolomite only in locations close to the coastline and in samples of fairly high total dissolved solids content. We attribute the supersaturation close to the coast primarily to the contribution of seawater.

These results indicate that carbonate saturation in the present aquifer system is only achieved close to the coastline, and that at present, the groundwater conditions are not sufficient to allow precipitation of dolomite (or calcite for that matter) in inland areas. Because the dolomite is distributed only along a portion of the island shoreline, the evidence from the saturation modeling supports the hypothesis that some coastal process was required to induce dolomitization. The chemistry of the dolomite itself may also reflect the nature of the dolomitizing process, and is discussed in the following sections.

Stable Isotopic Composition of the St. Croix Dolomite

Because stable isotopes in carbonates are controlled by the composition of the precipitating medium, as well as the temperature of formation, they can be used to constrain the possible chemical conditions of diagenesis. The usefulness of stable isotopes is complicated by the uncertainties of the fractionaltion factors for dolomite (and non-stoichiometric dolomite in particular) as well as the difficulties in separating temperature effects from the effects of fluid isotopic composition. These difficulties are discussed in more detail by Land (1980). Unless stated otherwise, stable isotopic values are listed without correction for the phosphoric acid fractionation factor, following Land (1980).

Reproduced with permission of the copyright owner. Further reproduction prohibited without permission.

There is a wide variation in the stable carbon and oxygen isotopic composition of the St. Croix dolomites, with a mean $\delta^{18}O$ of +3.0 (±0.7) ‰ and an average $\delta^{13}C$ of +1.6 (±0.7) ‰, both measured relative to PDB. The stable isotopic composition of St. Croix dolomites range from +0.7 to +3.8 ‰ $\delta^{18}O$ and from +0.6 to +2.4 ‰ $\delta^{13}C$, relative to PDB (Table 3.3).

In general, a clear positive correlation exists between the the stable oxygen and carbon isotopic composition of the dolomites (Fig. 3.30). This correlation appears either to be geographically controlled, or controlled by the location of the dolomites relative to the water table. The dolomites presently below water table have higher $\delta^{13}C$ values by +1.0 ‰ and higher $\delta^{18}O$ values by +1.1 ‰ on average, relative to the dolomites presently in the vadose zone. However, because the isotopically heavier dolomites are also located downdip and seaward of the isotopically lighter dolomites, the same trend could be interpreted as stemming from geographic factors, with the isotopically lighter phases reflecting more intense meteoric water influence.

Although it is not possible at this point to separate the potential pene-contemporaneous geographical controls from post-dolomitization water table effects, it is important to accept the possibility of groundwater influence. The most isotopically light dolomite, sample VII 26K, is from a caliche layer on the perimeter of the Pliocene reef zone. The extreme depletion of this sample with respect to ^{18}O and ^{13}C ($\delta^{18}O$=0.7, $\delta^{13}C$=-1.4 ‰) even compared to samples from the same outcrop (VII 26A, VII 26E, $\delta^{18}O$=+2.6, $\delta^{13}C$=+1.0 ‰, Table 3.3) suggests that recrystallization of dolomite may have occurred.

Reproduced with permission of the copyright owner. Further reproduction prohibited without permission.

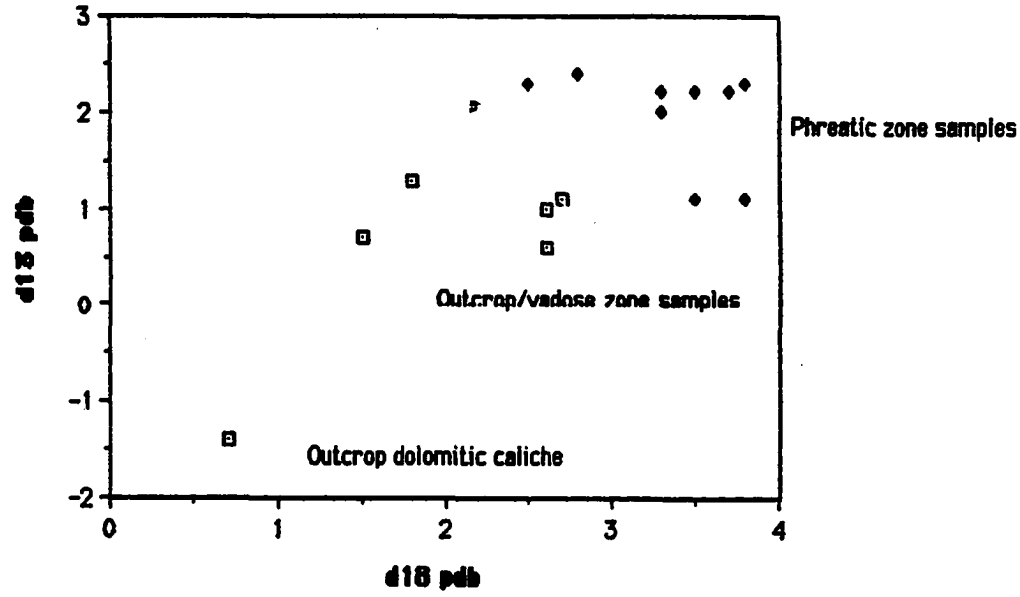

Figure 3.30. Stable isotopic composition of St. Croix dolomites. The dolomites become depleted in both ^{18}O and ^{13}C as one moves from the phreatic zone in the center of Krause Lagoon to the vadose zone at the edges. The trend of depletion may be controlled by chemical gradients during dolomitization, or by subsequent recrystallization, or both. The caliche dolomite is substantially depleted even relative to samples within the same outcrop, which suggests subsequent meteoric alteration of the isotopic signature.

There is also a significant correlation between the stable oxygen composition and the mole fraction of magnesium in the dolomite lattice (Fig. 3.31). This effect may be due to a change in the isotopic fractionation factor correlated to the stoichiometry of the dolomite. Such an effect has been documented for magnesian calcites by Tarutani and others (1969), and has been suggested for dolomites by Land (1983b) and Vahrencamp (pers. comm.,1987) and for coexisting magnesites and dolomites by Aharon (1988).

Dolomite equilibrium calculations. Using a commonly accepted oxygen isotopic fractionation factor for dolomite (10^3 ln alpha = $3.2 \cdot 10^6 T^{-2} - 3.3$, Sheppard and Schwarcz, 1970, *in* Land, 1983b) and assuming precipitation at 25°C, water in equilibrium with the isotopically heaviest St. Croix dolomites would have required an

Reproduced with permission of the copyright owner. Further reproduction prohibited without permission.

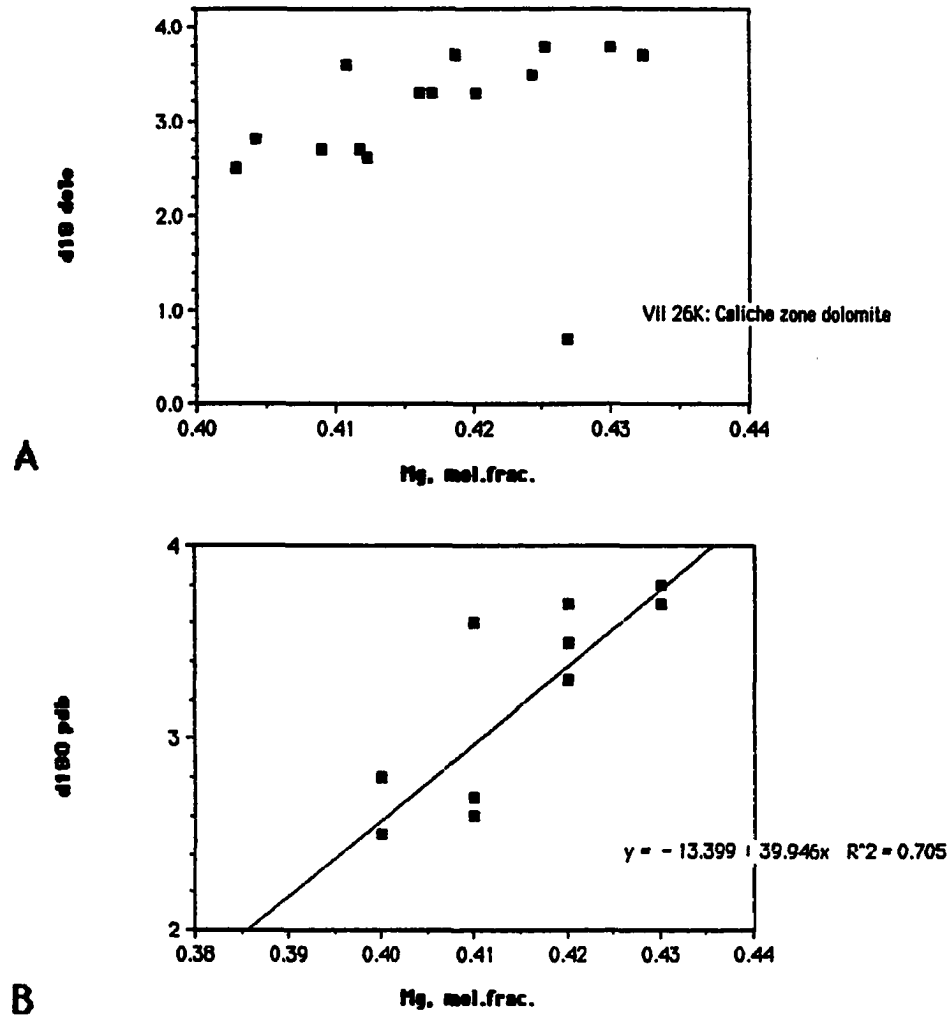

Figure 3.31. *Upper diagram:* Plot of $\delta^{18}O_{PDB}$ vs. magnesium mole fraction in St. Croix dolomites. Note that the dolomite sample from the caliche zone does not plot along the same trend as the rest of the samples.

Lower diagram: Plot of $\delta^{18}O_{PDB}$ vs. magnesium mole fraction with the caliche sample removed. The data suggest a 1 ‰ increase in $\delta^{18}O_{PDB}$ for every 3% increase in the magnesium molar concentration of the dolomites.

isotopic composition of +1.5 ‰ $\delta^{18}O$ relative to SMOW (Fig. 3.32). Making the same assumptions but using the fractionation factors for 'protodolomite' (10^3 ln alpha = $2.78 \cdot 10^6 T^{-2} - 0.11$, Fritz and Smith, 1970), water in equilibrium with the dolomite would have had an isotopic ratio of +2.8 ‰ $\delta^{18}O_{SMOW}$.

Reproduced with permission of the copyright owner. Further reproduction prohibited without permission.

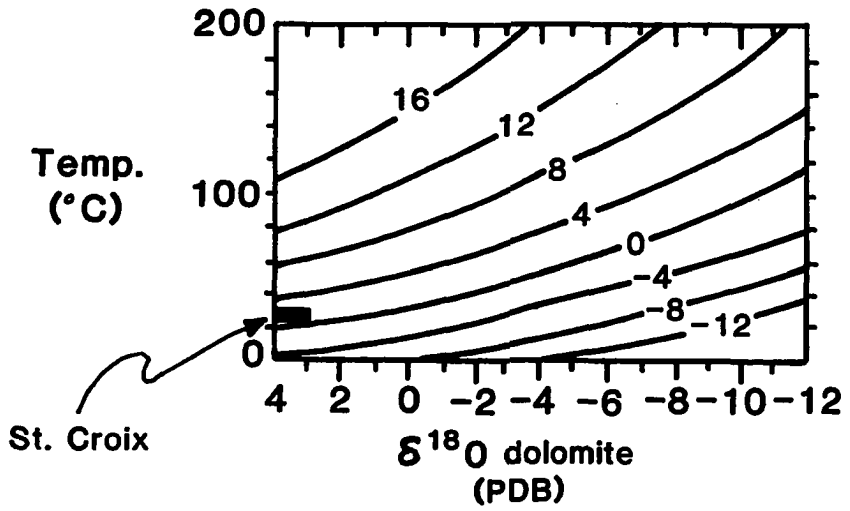

Figure 3.32. $\delta^{18}O_{dolomite}$ vs. temperature scale for a range of water compositions. $\delta^{18}O_{dolomite}$ given relative to PDB; $\delta^{18}H_2O$ given relative to SMOW. Fractionation equation used: $10^3 \ln \alpha_{dolo\text{-}water} = 3.2 \times 10^6 T^{-2} - 3.3$. From Land (1983b).

The 'protodolomite' of Fritz and Smith (1970) is closest in composition to the calcium-rich St. Croix dolomites (Table 3.4), and their fractionation factors are therefore most applicable to this case. In either case, the average St. Croix dolomite would have required a fluid with oxygen composition significantly enriched in ^{18}O relative to modern seawater, making unaltered modern seawater an unlikely candidate as a potential dolomitizing fluid.

However, it cannot be assumed that the stable isotopic composition of ocean water has remained constant over time, and therefore modern seawater may not be an appropriate standard to use with St. Croix dolomite. The stable isotopic composition of the world ocean has varied through time primarily as a function of withdrawal and release of isotopically light water from the polar ice caps, the "ice-volume effect" (Shackleton, 1967; Shackleton and Opdyke, 1973; Matthews and Poore, 1980; among others). This variation in the isotopic composition of oceanic water is recorded in the tests of oceanic

Reproduced with permission of the copyright owner. Further reproduction prohibited without permission.

microfossils along with a sympathetic variation in the isotopic signal caused by oceanic temperature changes.

Because the relative contributions of temperature versus the isotopic composition of seawater cannot easily be determined, we make the assumption that the variation in oxygen isotopic composition is *entirely* due to changes in oceanic water composition. In so doing, we arrive at an estimate of the *maximum* possible variation in oceanic water chemistry. This variation is most reasonably compared with an *average* value for Pleistocene seawater (ca. +0.8 ‰ SMOW), rather than the isotopically light value of modern seawater (Matthews and Poore, 1980).

Using data from oceanic foraminiferal calcite, the maximum recorded variation in oceanic ^{18}O composition from the end of the middle Miocene to the present is less than 2.0 ‰ (data from Emiliani, 1966 in Shackleton and Opdyke, 1973; Shackleton and Opdyke, 1973; Ruddiman and McIntyre, 1979; Savin and others, 1975; Shackleton and Kennett, 1975; Shackleton and Cita, 1979; Savin and others, 1985; Kennett, 1985). Assuming that one half of the seawater variation, or 1.0 ‰, was greater than a Pleistocene seawater average of +0.8 ‰, the *maximum* possible value for late Tertiary through Holocene seawater is about +1.8 ‰ SMOW. This value is well in excess of most estimates for the total variation in oceanic isotopic composition, which range from 0.8 to a maximum of 1.3 ‰ (Savin and Yeh, 1981 in Anderson and Arthur, 1983; Shackleton and Opdyke, 1977) and I therefore feel comfortable assuming that actual seawater composition could not have exceeded +1.8 ‰ SMOW since the late Miocene.

Because this value for Tertiary seawater is not isotopically heavy enough to produce much of the St. Croix dolomite, the dolomitizing fluids must either have been

Reproduced with permission of the copyright owner. Further reproduction prohibited without permission.

enriched by evaporation, or the dolomite must have formed at lower temperatures. However, because climatic modeling suggests that tropical ocean surface temperatures have remained relatively constant even during glacial periods (Matthews and Poore, 1980), the St. Croix dolomites must have formed from waters locally enriched in ^{18}O by evaporation.

On the basis of isotopic evidence alone, however, it is not possible to infer the salinity of the dolomitizing fluid or the extent to which it underwent mixing with other fluids. The strontium isotopic composition of the dolomite as well as the groundwater chemistry indicate that some mixing has taken place. This is discussed in the next sections.

Reproduced with permission of the copyright owner. Further reproduction prohibited without permission.

$^{87}Sr/^{86}Sr$ Composition of the Dolomites

The relatively recent interest in strontium isotopic systematics in carbonates stems in part from the improvement in measurement technology that has allowed the construction of a secular curve for oceanic strontium-isotopic ratios (Burke and others, 1982). Strontium 87 is the product of the beta decay of rubidium-87, an element commonly found in potassium-bearing minerals such as micas, K-feldspars and some clay minerals (Faure, 1977). Due to its association with potassium-bearing minerals, rubidium is found in highest concentrations in granitic rocks and other elements of the continental crust, and is found in far lower concentrations in mafic and ultramafic rocks. The ratio of strontium-87 to strontium-86 ($^{87}Sr/^{86}Sr$) is therefore both a function of the original concentration of rubidium-87, and a function of time, with the highest $^{87}Sr/^{86}Sr$ ratios found in old rock of the continental crust.

For this discussion, we are primarily interested in the characteristics of carbonates precipitated from seawater. The primary controls on the strontium isotopic composition of the oceans are the relative contribution of each of the major sources of strontium in the crust: young volcanic rocks such as ridge basalts, older sialic rocks from continental weathering and marine carbonates (Faure, 1977). The ratio of strontium-87 to strontium-86 in the modern ocean appears to be homogeneous, but has varied through time as a function of terrestrial weathering, the flux of fluvial systems and magmatic production rate, among other factors (Peterman, 1970; Faure 1977; Burke and others, 1982). The empirical temporal curves produced by this fluctuation (e.g. Burke and others, 1982; Koepnick and others, 1985; Fig. 3.33) allow the dating of carbonate phases precipitated from seawater, particularly in the late Tertiary where the slope of the curve is quite high.

Reproduced with permission of the copyright owner. Further reproduction prohibited without permission.

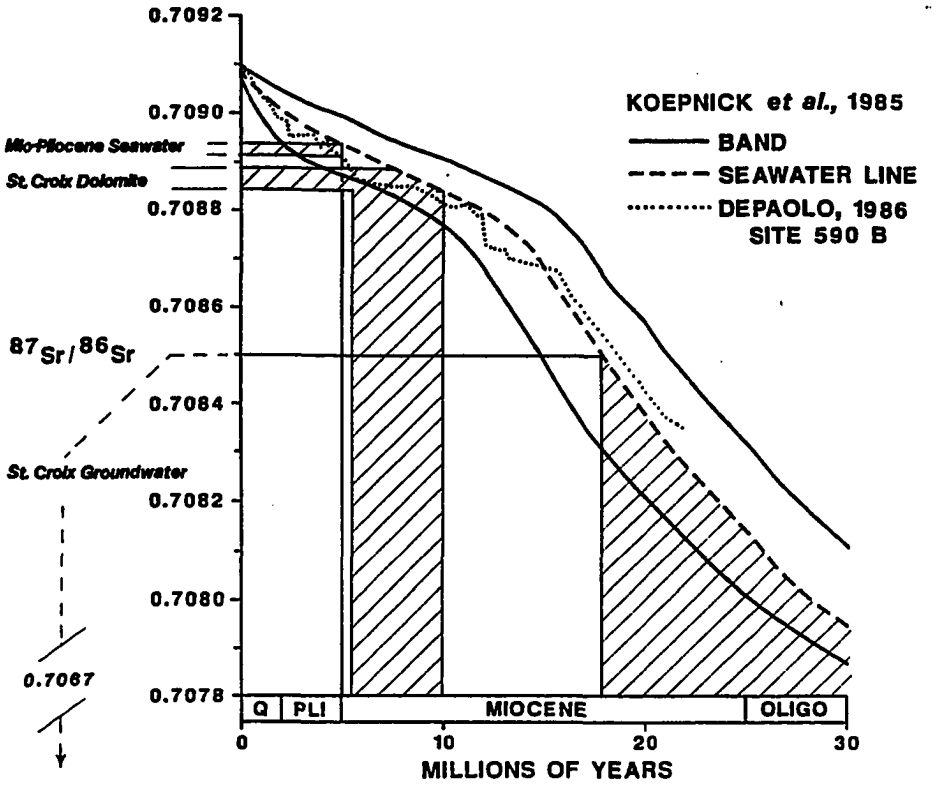

Figure 3.33. Seawater $^{87}Sr/^{86}Sr$ ratio in the middle to late Tertiary from Koepnick and others, 1985. Isotopic compositions of Mio-Pliocene seawater, St. Croix dolomites, and the maximum measured ratio of St. Croix groundwater are marked. The measured $^{87}Sr/^{86}Sr$ ratios in St. Croix groundwater range from 0.7067 to 0.7085.

The assumptions made in assigning ages to carbonate rocks on the basis of their strontium isotopic ratios are the following:

1) the carbonates are precipitated from seawater, and the seawater is isotopically homogeneous;

2) there is no isotopic fractionation during precipitation;

3) the carbonates have not been altered since precipitation.

Regarding the first assumption, studies of modern seawater and ancient carbonates indicate that the post-Paleozoic ocean has been homogeneous with respect to

Reproduced with permission of the copyright owner. Further reproduction prohibited without permission.

strontium isotopes, probably due to the rapid rate of mixing in the ocean relative to strontium residence times (Faure, 1977). Regarding the second assumption, the close similarities in relative mass between the isotopes of strontium would indicate that isotopic fractionation during precipitation is unlikely, a conclusion confirmed by experimental work (Peterman and others, 1970).

Thus, marine carbonates can potentially be dated using strontium isotopic techniques, providing they have not been subjected to diagenetic alteration (assumption 3, above). In dating carbonate rocks with potential contamination from diagenetic strontium, most workers assume that diagenetic alteration would cause the $^{87}Sr/^{86}Sr$ to rise since modern marine water and continental groundwater both contain high isotopic ratios of strontium.

Samples of St. Croix dolomite contain essentially identical ratios of $^{87}Sr/^{86}Sr$, with a mean value of 0.70887 ($\pm$ 0.00002; Table 3.5). Assuming that the dolomite is precipitated from seawater, this value would correspond to middle to late Miocene seawater (Figs. 3.33, 3.34), (Koepnick and others, 1985; DePaolo, 1986). However, the dolomites on St. Croix are clearly within Pliocene strata (Andreieff, 1983; Andreieff and others, 1986; Gill and Hubbard, 1987). Since the dolomites would apparently predate their host-rock, the application of a strontium "date" to these dolomites becomes untenable.

Assuming that the Pliocene depositional age assignment is correct, the St. Croix dolomites must have been subjected to fluids depleted in strontium-87 relative to both modern and Pliocene seawater. We therefore suggest that either the dolomitizing fluids

Reproduced with permission of the copyright owner. Further reproduction prohibited without permission.

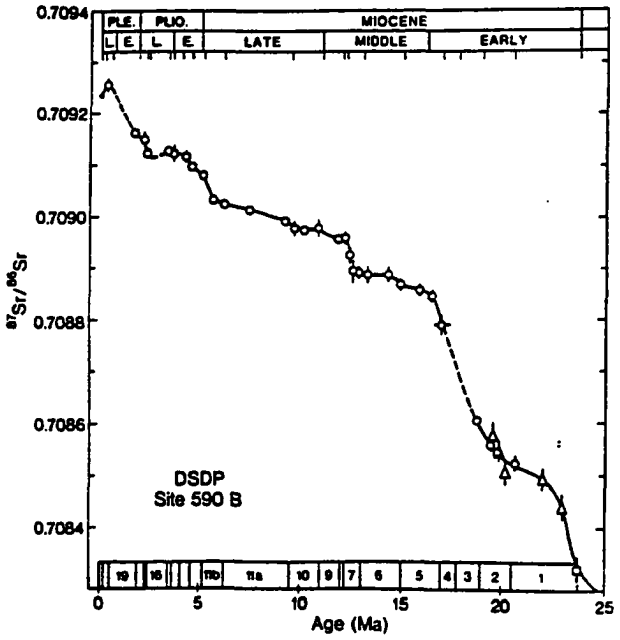

Figure 3.34. Seawater $^{87}Sr/^{86}Sr$ curve for the Neogene according to DePaolo (1986).

contained an end-member other than seawater, or that the seawater had been locally modified by significant quantities of ^{86}Sr.

In most discussions of strontium isotopes, the usual sources of contamination are from sialic crustal rocks or marine waters younger than the diagenetic phase in question. Either of these two sources would serve to elevate the strontium isotopic ratio of a diagenetic phase rather than depress it. We suggest that the weathered basic igneous rocks of tectonically active areas like the northeastern Caribbean, as well as the groundwaters that come into contact with them, are potential strontium sources that cannot be ignored.

Reproduced with permission of the copyright owner. Further reproduction prohibited without permission.

Strontium in the Modern St. Croix Groundwater System

The modern St. Croix groundwater system shows chemical patterns that imply sources of dissolved solids other than simple fresh water/sea water mixing and simple dissolution of carbonate rocks. The chemical patterns in the groundwater system suggest either that extensive reaction with non-carbonate components is taking place, or that the meteoric waters are mixing with altered formation waters (see Groundwater section) One such pattern is the pronounced depletion of St. Croix groundwater with respect to ^{87}Sr.

St. Croix groundwater has an average $^{87}Sr/^{86}Sr$ ratio of 0.7077, but ranges from 0.7067 to 0.7085 (n=4, Table 3.5). These ratios are not only significantly lower than Modern or Pliocene seawater values, they are considerably lower than the strontium isotopic ratios of the St. Croix dolomites.

The source of strontium in St. Croix groundwater is speculative, but due to the absence of aragonite in the carbonate section, and the indications of siliciclastic rock-water interactions mentioned earlier, the source of the non-radiogenic strontium is most likely the terrigenous material and weathering products contained both in the Cretaceous section of the island as well as within the Kinghill Limestone itself. For example, sample MW-4, from siliciclastic alluvium in the Cretaceous highlands, has the lowest $^{87}Sr/^{86}Sr$ ratio of the four aliquots analyzed, 0.7067, despite being isolated from the Tertiary carbonate system (Table 3.5). This $^{87}Sr/^{86}Sr$ ratio is comparable to ratios in geosynclinal 'melange' sediments and in altered oceanic basalts (Hawkesworth, 1982).

The other major potential source for groundwater strontium is the marine carbonate in Kingshill Limestone and Jealousy Formation strata. However, St. Croix

Reproduced with permission of the copyright owner. Further reproduction prohibited without permission.

groundwaters are significantly depleted in ^{87}Sr even relative to late early Miocene seawater, the age of the oldest documented sediments in the Tertiary section (Chapt. 1, this dissertation). For this reason, the Kingshill Limestone and Jealousy Formation carbonates cannot be significant strontium contributors to the present groundwater system.

Regardless of the source of strontium in the modern aquifer system, groundwater with extremely low $^{87}Sr/^{86}Sr$ ratios cannot be ignored as a potential supplier of non-radiogenic strontium during diagenesis. The question here is whether a groundwater can significantly affect the strontium ratio of a diagenetic phase such as dolomite, and if so, what proportions of groundwater are required to produce a dolomite with the $^{87}Sr/^{86}Sr$ ratios measured on St. Croix? This question is numerically testable, and is the subject of the next section.

Strontium-Isotopic Mixing Calculations

The question of whether or not a groundwater end-member could have a significant effect on the strontium isotopic composition of a diagenetic phase depends on:

1) the isotopic composition of the strontium in the marine and groundwater end members;
2) the strontium concentration of the groundwater and seawater; and
3) the relative proportions of each end member in the mix.

Reproduced with permission of the copyright owner. Further reproduction prohibited without permission.

Conventional wisdom has it that seawater strontium concentrations are several orders of magnitude higher than those of groundwaters, and that strontium isotopic contributions from groundwaters are therefore negligible in mixing systems. In this case, the actual compositions of the seawater and groundwater are known or can be estimated, and the effects of mixing the two end members can be calculated, providing that:

1) we are dealing with a two end-member system;
2) the strontium-isotopic ratios are not affected by reactions that take place during or after the mixing process (Faure, 1977);

Strontium isotopic mixing relations can be calculated as a linear function by assuming that the abundance of ^{86}Sr is identical in each end-member, and that the atomic weight of Sr is identical in each end-member (Faure, 1977). The relation between $^{87}Sr/^{86}Sr$ and [Sr] is hyperbolic, but can be transformed into a linear function by inverting the strontium concentrations (Faure, 1977; Langmuir and others, 1978).

Mixing calculations using strontium values from modern St. Croix groundwater and Pliocene seawater from Koepnick and others (1985) suggest that groundwater can have a significant effect on the strontium- isotopic ratio of the mixed fluid, and therefore cannot be discounted as a source of strontium in diagenetic phases formed from seawater mixtures. In this specific case, three of the four groundwater samples analysed had sufficiently low $^{87}Sr/^{86}Sr$ ratios and sufficiently high dissolved strontium concentrations to reduce the strontium isotopic composition of a seawater mix to match the isotopic ratio of St. Croix dolomites. Of the four groundwater samples analyzed, only one had a strontium concentration more than two orders of magnitude below that of seawater (Table 3.5). Mixtures of modern groundwater and Pliocene seawater containing between about

Reproduced with permission of the copyright owner. Further reproduction prohibited without permission.

35% and 80% groundwater would have a strontium isotopic ratio equal to the St. Croix dolomites (Fig. 3.35, Table 3.6).

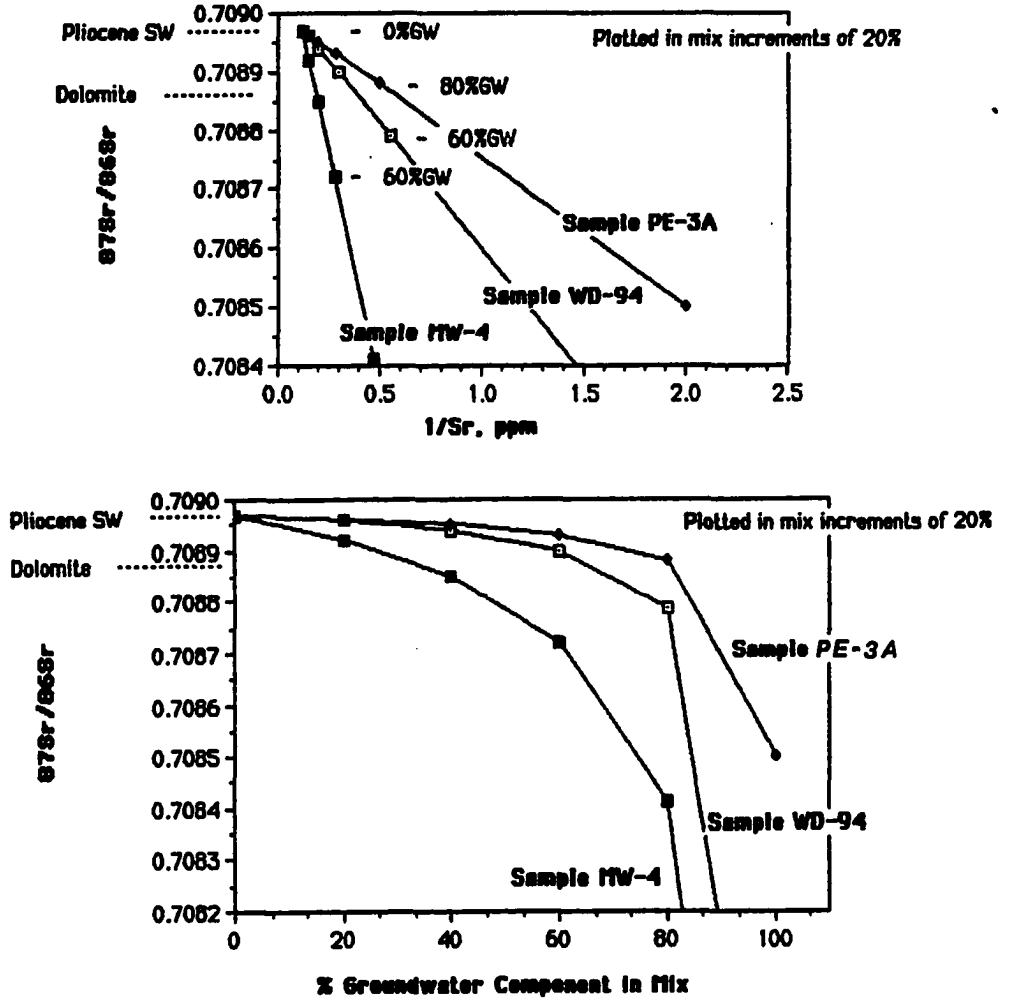

Figure 3.35. Strontium isotopic mixing curves for Pliocene seawater and St. Croix groundwater, plotted in mixing increments of 20%. The isotopic composition of the St. Croix dolomites is shown on the vertical axis.

Upper diagram:: Strontium isotopic ratio plotted versus the inverse concentration of strontium. The $^{87}Sr/^{86}Sr$ ratio of unmixed sample MW-4 = 0.7067, below the range of the diagram.

Lower diagram:: Strontium isotopic composition plotted versus the percentage of the groundwater component in the mix. Pure end members of both MW-4 and WD-94 plot below the range of the diagram.

Reproduced with permission of the copyright owner. Further reproduction prohibited without permission.

It can therefore be shown that the strontium composition of present St. Croix groundwaters is significant in mixing relations, even with fluids as saline as seawater. For this reason, the mixing of meteoric and marine waters is one plausible explanation for the strontium isotopic composition of St. Croix dolomites. Strontium contributions from volcanoclastics and intrusives similar to those on St. Croix could be common in areas close to destructive plate margins. In addition, although it can be ruled out in the case of St. Croix, the contribution of older marine carbonates can not always be assumed to be minimal.

It has already been shown that the *stable* isotopic composition of the dolomites cannot be explained by dolomitization from either a mixed meteoric fluid or seawater alone. Therefore, the question that needs to be answered is whether a combination of meteoric and evaporitic waters could physically be responsible for dolomitization, given the chemical constraints that we have established for the dolomitizing fluids. This question is testable, and will be explored in the next section.

Evaporation of Mixed Marine and Meteoric Waters

In order for dolomitization to occur, sufficient water flow is necessary to supply the requisite magnesium to a calcitic host rock. Even assuming that seawater is the dolomitizing agent, at least 600 to 800 pore volumes of seawater are necessary to dolomitize a cubic meter of sediment (Land, 1983a). Substantially more water is required for mixed meteoric/marine waters, which emphasizes the importance of the hydrologic system. The question that arises is, what type of environment would create a mixture of evaporated seawater and meteoric water, and still provide the hydrologic drive necessary for dolomitization?

Reproduced with permission of the copyright owner. Further reproduction prohibited without permission.

Given the chemical constraints on the dolomitizing fluid, and the geographic constraint limiting the dolomitization to Krause Lagoon, the following are two possible models for the production of the dolomitizing fluid, provided that some source of reflux is required:

1) *Mix first, then evaporate:* Groundwater and marine water mix subaerially in a coastal pond, and then evaporates. Hydrologic drive is provided by the density difference between the evaporated mixture and seawater.

2) *Evaporate first, then mix:* The dolomitizing fluid starts as seawater which evaporates to the point where the evaporated fluid displaces underlying less dense seawater. Mixing with meteoric water occurs within the strata following the sinking of the marine brine.

These two models represent simplified end members of the mixing and evaporative sequence to allow the testing of the feasibility of a conventional reflux dolomitization process involving meteoric water. Simultaneous mixing and evaporation, as well as non-reflux models are certainly possible.

In the first model, if a meteoric fluid first mixes with seawater and the resulting mixture then evaporates:

1) Will it be able to reach the stable isotopic composition representing equilibrium with the dolomite?

Reproduced with permission of the copyright owner. Further reproduction prohibited without permission.

2) If fluid density is to provide the hydrologic drive, will the mixed, evaporated fluid achieve sufficient density to displace seawater?

In the second model, where evaporated seawater alone mixes in the subsurface with meteoric water:

1) What stable isotopic composition will the evaporated marine end-member have to achieve, such that later mixing with isotopically light groundwater leaves the mixture with a composition consistent with the dolomite?
2) Can the brine theoretically reach the isotopic composition discussed above?
3) What would the density of the resulting evaporated fluid be?

In either case, the final fluid would have to have an oxygen isotopic composition between +2.0 and +2.8 ‰ $_{SMOW}$, and would have to represent a meteoric/marine mixture composed of about 60% meteoric water in order to be compatible with the isotopic composition of St. Croix dolomites (Table 3.6).

The isotopic composition of an evaporating brine follows a curve controlled by 1) the isotopic composition of the atmosphere, 2) the relative humidity, 3) the ambient temperature, 4) the activity of water in the evaporating solution, and 5) the isotopic fractionation between the fluid and the waters of hydration, which is in turn dependent on the dominant ions in solution (Sofer and Gat, 1975; Gonfiantini, 1986). The $\delta^{18}O$ composition of a sodium-chloride brine with an initial molality close to seawater follows a hook-shaped trajectory such as that shown in Figure 3.36 during evaporation. In general, both 1) raising the relative humidity, and 2) reducing the difference in isotopic composition between the evaporating fluid and the atmosphere, effectively reduce the

Reproduced with permission of the copyright owner. Further reproduction prohibited without permission.

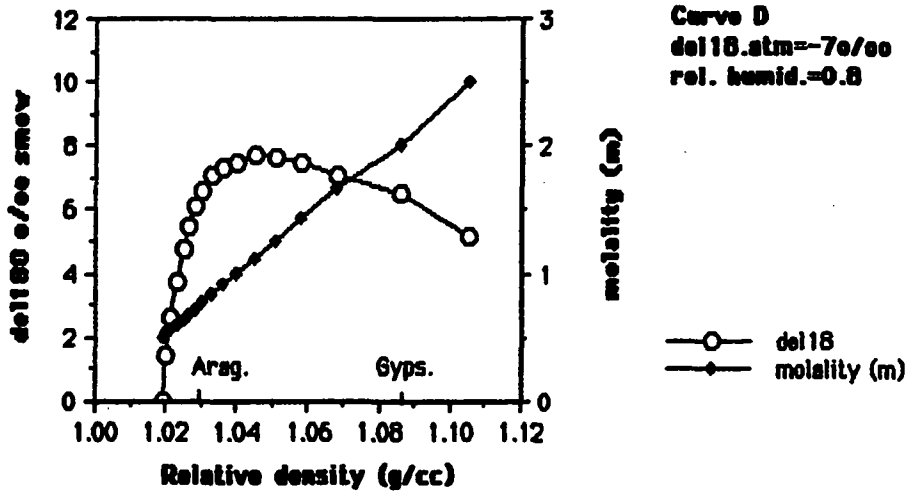

Figure 3.36. Evaporation curve for 0.5m NaCl brine (approximately seawater molality). Ambient conditions: δ^{18}Oatm = -7%, relative humidity =0.8. Isotopic data from Sofer and Gat (1975).

maximum isotopic enrichment of the brine. Figure 3.37 shows the evaporation curve resulting from a decrease in both the relative humidity and the δ^{18}O of atmospheric water wapor of an NaCl solution with the same molality as that in Figure 3.36, above.).

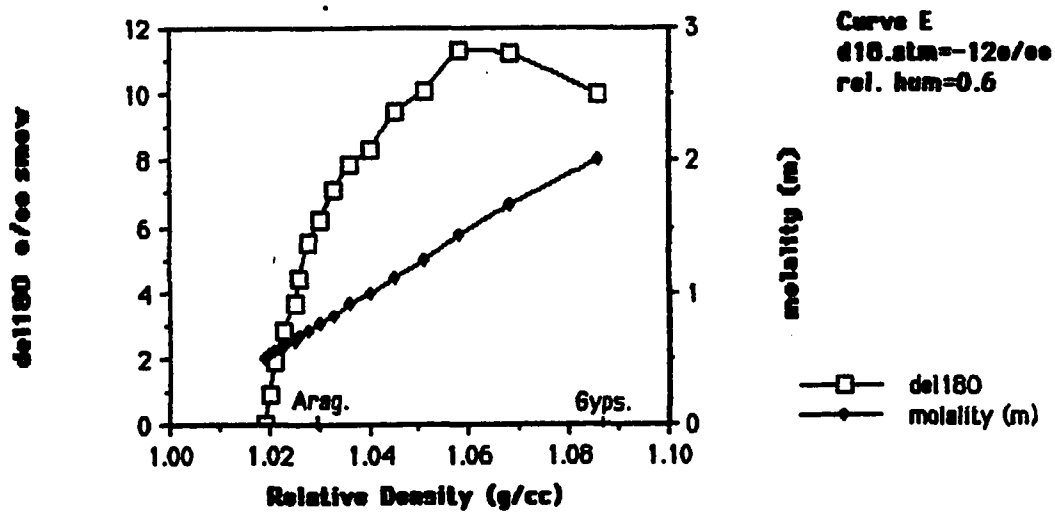

Figure 3.37. Evaporation curve for 0.5m NaCl brine. Ambient conditions: δ^{18}Oatm = -12%, relative humidity = 0.6. Isotopic data from Sofer and Gat (1975).

Reproduced with permission of the copyright owner. Further reproduction prohibited without permission.

Both the *mix-first then evaporate* and the *evaporate then mix*t models mentioned previously have been modeled in order to see whether either could achieve the isotopic composition and presumed density characteristics of the dolomitizing fluids. Initial atmospheric and fluid composition conditions for both models are from Lloyd (1966) for the island of Inagua in the Bahamas, and Sofer and Gat (1975). The solutions were modeled as NaCl brines using the numerical model of Gonfiantini (1986) with end-member compositions taken from St. Croix data or using presumed Pliocene values (Fig. 3.38).

The case of the *mix first, then evaporate* model is illustrated in Figure 3.38, using a 50:50 mix of Pliocene seawater and St. Croix groundwater. If such a mixture were allowed to evaporate, it would reach the isotopic water-mineral equilibrium value for dolomite at a relative density of 1.017 g/cm^3, still less than the density of seawater (1.02 g/cm^3). Such a mixture would be unable to displace seawater, and would therefore be incapable of dolomitization by a conventional reflux mechanism.

In the *evaporate first, then mix* sequence (Fig. 3.39), seawater must reach an oxygen isotopic value of +7.5 ‰ SMOW in order for a subsequent 50:50 mix to have an isotopic ratio in equilibrium with the dolomite. Seawater reaches this value after evaporating to a relative density of approximately 1.05, significantly more dense than seawater. It is interesting that +7.5 ‰ is very close to the maximum isotopic enrichment attained by Sofer and Gat (1975) using less-depleted atmospheric vapor (Fig. 3.37).

In either case, seawater could reach isotopic values compatible with the St. Croix dolomites at densities that would allow refluxion (cf. Simms, 1984). The molality of the

Reproduced with permission of the copyright owner. Further reproduction prohibited without permission.

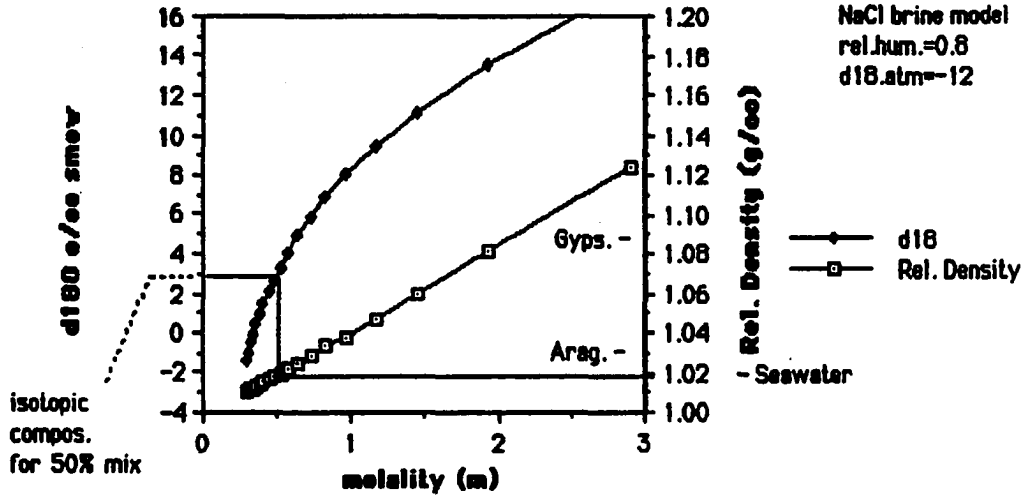

Figure 3.38. Evaporation curve for a 50:50 mix of Pliocene seawater and average St. Croix groundwater, under ambient St. Croix conditions. Note that the evaporated mix, in oxygen isotopic equilibrium with St. Croix dolomite, is still less dense than seawater.

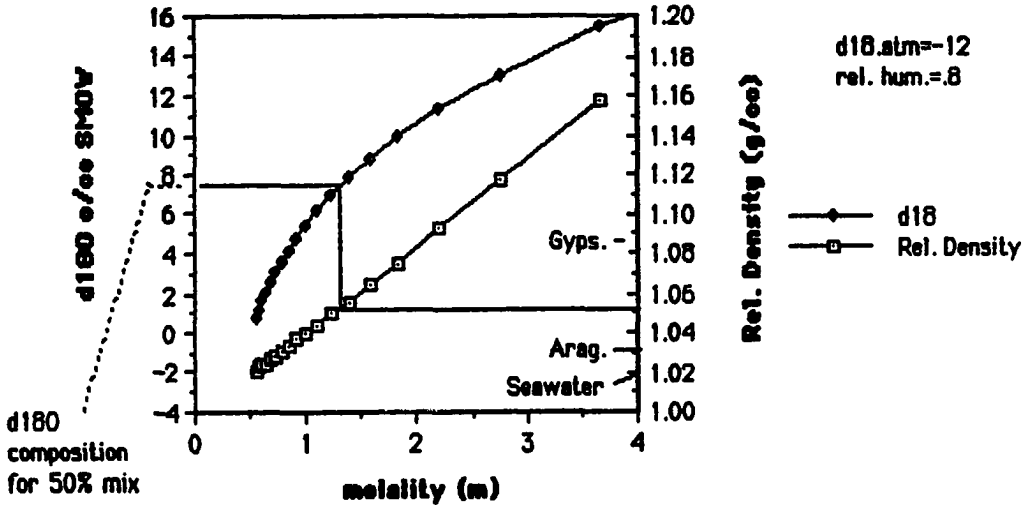

Figure 3.39. Evaporation curve for Pliocene seawater under ambient conditions similar to St. Croix, modeled as an NaCl brine. Note that the brine reaches oxygen isotopic equilibrium with St. Croix dolomite between the aragonite and gypsum saturation points.

solution in the cases discussed above is still below gypsum precipitation values in marine brines (Deffeyes and others, 1965; Butler, 1969, 1973). On the basis of the preceding

Reproduced with permission of the copyright owner. Further reproduction prohibited without permission.

discussion, marine evaporation followed by mixing with meteoric water is consistent with the isotopic chemistry and geographic distribution of the St. Croix dolomites, and would be compatible with a brine refluxion mechanism. Mixing of meteoric water *prior* to evaporation, however, would not allow the formation of a fluid dense enough to displace seawater even if the quantity of meteoric water did not exceed 25% of the mixture.

In the models outlined above, the isotopic chemistry of the dolomites (carbon, oxygen and strontium) is consistent with a model of mixed evaporated seawater and groundwater. However, it is worth considering whether the various models are consistent with the trace-element chemistry of the dolomites as well, which (as you feared) will be discussed in the next section.

Elemental Concentrations in St. Croix Dolomites

Trace elemental concentrations in carbonates have been the subject of a substantial amount of attention, and have become a traditional, though not necessarily fruitful, approach to carbonate diagenesis. The trace-element approach is based on experimental work showing that the distribution of trace elements within carbonate minerals is proportional to the trace element distribution of the fluid from which the mineral formed. Lacking accurate thermodynamic activity coefficients, most distribution coefficients are determined empirically and are therefore expressed simply by molal ratios (Land, 1980).

The distribution coefficient, D in this paper, is a coefficient of proportionality between the solid phase and the liquid phase, and is specific both to the ion and to the mineral in question:

Reproduced with permission of the copyright owner. Further reproduction prohibited without permission.

$$\frac{(Me)}{(Ca)_{xtal}} = D^{Me} \frac{(Me^{2+})}{(Ca^{2+})_{fluid}}$$

where Me and Ca are the molal concentrations of the cation and calcium in the crystal, D^{Me} is the distribution coefficient for the cation in the mineral being considered, and Me^{2+} and Ca^{2+} are the molal concentrations of the cation and calcium in solution.

A distribution coefficient of 1 implies that the molar ratio of the cation will be incorporated into the mineral lattice in the same proportion that it is found within the precipitating fluid. Similarly, a distribution coefficient of less than 1 means that the cation will be excluded from the crystal lattice, and the mineral will contain a *lower* molar ratio of the cation in the mineral than exists in the fluid. A distribution coefficient of greater than 1 implies that the mineral will contain a *higher* proportion of the cation than exists in the precipitating fluid.

Ideally, distribution coefficients could be used to distinguish between several different potential diagenetic fluids. In the case of St. Croix dolomitization, it is theoretically possible to distinguish marine from meteoric waters provided that the ionic compositions of the waters were sufficiently distinct. It would also be theoretically possible to distinguish waters below the saturation state for gypsum from those that have altered ionic proportions due to gypsum precipitation.

Unfortunately, there are several major complications with this approach. First, due to the reluctance of dolomite to precipitate in the laboratory at low temperatures, no

Reproduced with permission of the copyright owner. Further reproduction prohibited without permission.

direct experimental evidence exists as to the value of the distribution coefficient in dolomite at earth-surface conditions. Dolomite studies have attempted to circumvent this problem by reasoning that Sr, due to its large ionic radius, should preferentially substitute for Ca rather than magnesium in the dolomite lattice (Behrens and Land, 1972; Kretz, 1982 *in* Veizer, 1983). By this reasoning, dolomite should allow roughly one-half as much strontium into its lattice as does calcite, a mineral for which laboratory data are available. Stated another way, the distribution coefficient for strontium in dolomite should be close to one-half that for strontium in calcite.

Other uncertainties in the use of distribution coefficients involve the documented effect of reaction rate on trace-element partitioning (Lorens, 1981) and the difficulty in establishing the existence of open-system conditions. The former effect, that of reaction rate, has been shown to cause variation in the measured distribution coefficient by close to an order of magnitude (Lorens, 1981). In the latter case, if open system conditions do not apply, the precipitation of the solid phase would cause a corresponding change in the chemistry of fluid, and distribution coefficients would be invalid. These problems are discussed in detail in Land (1980) and Veizer (1983), and are denounced along with mixing zone models and other carnal sins by Hardie (1987).

However, the distribution coefficients of Sr in calcite have been experimentally determined for calcite precipitation from a number of precursors. Recent work by Baker (1982) and Delaney and Kastner (1984) has confirmed earlier work by Katz and others (1972) on the value of the strontium distribution coefficient in calcite. Ranges of these distribution coefficients are compiled in Veizer (1983). Using the possible values for the distribution coefficient of strontium, Figure 3.40 shows the range of strontium in St. Croix dolomites relative to the molality of calcium in the dolomite. Also plotted are the

Reproduced with permission of the copyright owner. Further reproduction prohibited without permission.

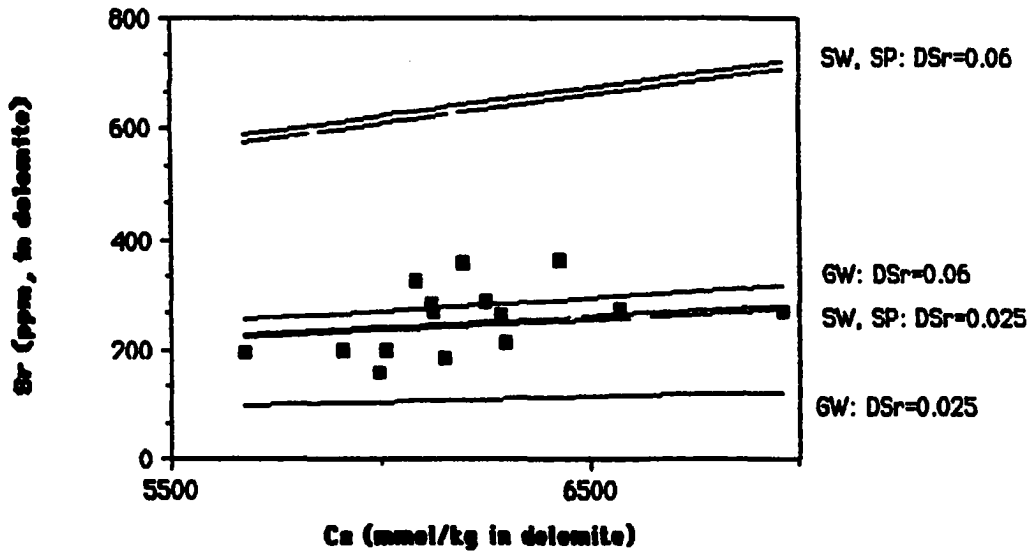

Figure 3.40. Strontium concentrations in actual St. Croix dolomites (scatter plot) plotted relative to the theoretical Sr concentrations (lines) calculated for dolomites precipitated from seawater (SW), St. Croix groundwater (GW) and Salt Pond Water (SP). Distribution coefficient values used for the calculations are shown for each data set (D_{Sr} = 0.025 or 0.06).

theoretical concentrations of strontium in dolomites precipitated at equilibrium with the average composition of St. Croix groundwater, seawater and saltpond water.

The St. Croix dolomites loosely cluster around values compatible with seawater or St. Croix saltpond water assuming a distribution coefficient D^{Sr}dolo of 0.025 (Veizer, 1983; Baker, 1982). However these values are also compatible with a D^{Sr}dolo of 0.06 or greater (Land, 1980) providing that the precipitating fluid was composed almost entirely of groundwater.

In either case, it is apparent that it is not possible to distinguish between a groundwater, saltpond or seawater source for the dolomitizing fluid given the uncertainty in the value of the distribution coefficient. For the same reasons, it is also not possible to

Reproduced with permission of the copyright owner. Further reproduction prohibited without permission.

resolve waters that are below the saturation state of gypsum from those that have had their Sr/Ca ratios increased due to gypsum precipitation.

The distribution coefficient data, given the present state of knowledge, do not eliminate any of the potential dolomitizing mechanisms, and are therefore of little use to us here. They may be more useful in cases such as brines, where the diagenetic waters have chemistries that are far more distinct than seawater and groundwater. In these cases an order of magnitude estimate of the distribution coefficient may be sufficient. Use of distribution coefficients in a relative sense, showing geographic gradients, has been successfully used by Land (1983b) and Land, Salem and Morrow (1975) among others. In the case of St. Croix, similar gradients can be shown for stable isotopes and magnesium contents, and indicate a strong geographic control on dolomite chemistry (see stable isotopes section). It is not clear whether this geographic gradient is a product of recrystallization or of original hydrology.

Reproduced with permission of the copyright owner. Further reproduction prohibited without permission.

DISCUSSION

The approach taken for this dissertation is based on the assumption that converting original skeletal mineralogies to dolomite is both a chemical and hydrologic process. For this reason, the present groundwater system on St. Croix is used as a model in order to understand the nature and magnitude of the chemical processes that occurred in the ancient groundwater system. There are obvious dangers to this approach, but modern groundwater data are felt to offer a reasonable first approximation of earlier groundwater conditions. The goal here is to present a model that is most consistent with multiple lines of geologic evidence, after elimination of those models that are not supportable.

Model for the formation of dolomite on St. Croix

Assessing the available information, there are several factors which must be included in any model proposed for the formation of the St. Croix dolomites:

1) The dolomite is spatially restricted to a small area corresponding to what was probably a Tertiary lagoon or embayment.
2) The dolomite is stratigraphically restricted to Pliocene strata, requiring that dolomitization take place no earlier than the Pliocene.
3) The dolomite is significantly enriched in ^{18}O over both seawater and groundwater values, implying significant evaporation providing that the commonly used dolomite fractionation factors are correct.

Reproduced with permission of the copyright owner. Further reproduction prohibited without permission.

4) The $^{87}Sr/^{86}Sr$ values in the dolomite are lower than could be produced by direct precipitation from Pliocene or younger seawater alone. Instead, the dolomitizing fluid must have been exposed to a significant source of strontium depleted in ^{87}Sr.

On the basis of this evidence, we suggest that the dolomite was formed from a mixture of seawater and meteoric waters that had been evaporated prior to dolomitization. Although this process is more complex than simple mixing or evaporation alone, the combination of both evaporation and mixing allows for a diagenetic phase that is more enriched in ^{18}O than either seawater or meteoric water, with a $^{87}Sr/^{86}Sr$ composition lower than would be possible from unaltered marine waters. Neither mixing alone nor evaporative concentration alone can account for the geochemical characteristics of the dolomite.

The dolomite must be genetically related to a lagoon or restricted embayment on the basis of its facies relationships and geographic distribution. This lagoon, situated at the present location of Krause Lagoon, would have had to allow both:

1) mixing of marine and fresh waters; and

2) evaporation.

Such environments exist today on St. Croix, such as Westend Saltpond on the western tip of the island (Fig. 3.41), and Great Pond on the southeastern coastline. The stable isotopic composition of waters from Westend Saltpond exceed those required to produce the isotopic signature in the St. Croix dolomites, and salinities there can reach two to three times seawater values (Fig. 3.21, Table 3.7).

Similar environments of dolomitization involving the evaporation of continentally derived waters have been documented in Australia (von der Borch and others, 1975;

Reproduced with permission of the copyright owner. Further reproduction prohibited without permission.

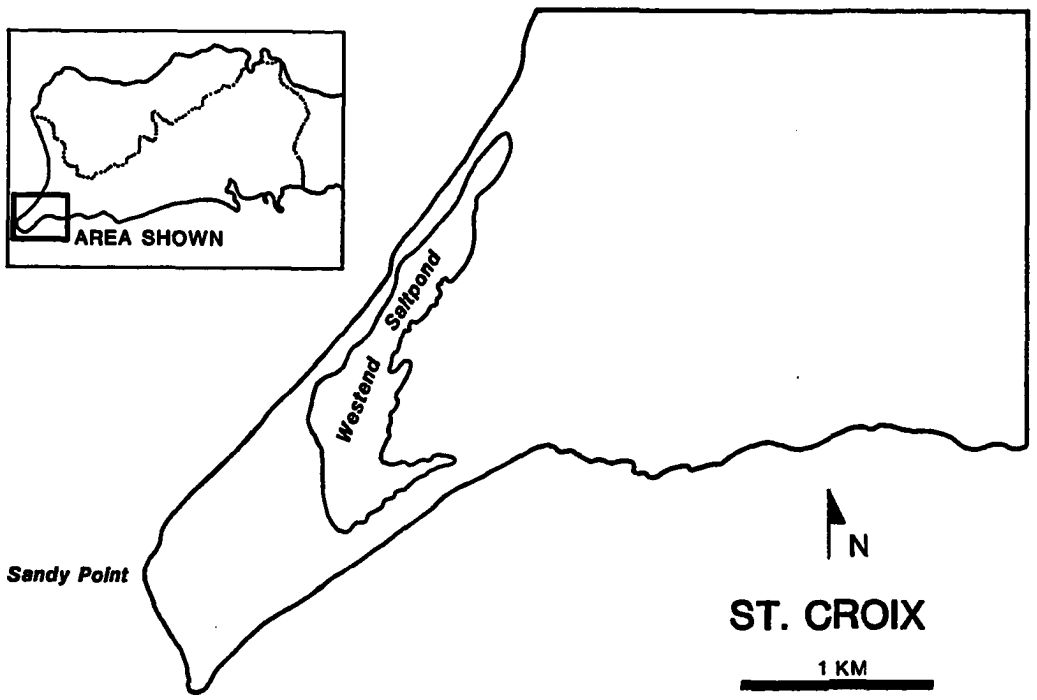

Figure 3.41. Location map for West End Salt Pond, a hypersaline pond on the westernmost tip of St. Croix.

Muir and others, 1980), or suggested on the basis of geologic evidence (e.g. Sibley, 1980; Knauth and Beeunas, 1986). We suggest that the evaporation of meteoric water and meteoric/marine water mixtures may be common in geologic environments, and may occur even in relatively humid environments such as tropical coastal systems on St. Croix.

The mixing-zone hypothesis for dolomitization has been justifiably criticized on thermodynamic grounds, and for the uncertainties of the stable-isotopic and geochemical data used as evidence (Hardie, 1987). In the case of St. Croix, the most compelling evidence for mixing stems from the strontium isotopic composition of the dolomites. The strontium isotopic system does not share the uncertainties of the oxygen and carbon

Reproduced with permission of the copyright owner. Further reproduction prohibited without permission.

systems, in that strontium isotopes do not fractionate during precipitation, and are not affected by evaporation.

Regarding the thermodynamic problems with mixing, Hardie (1987) raises the objection that most mixing zone models utilize data from stoichiometric dolomites rather than from the calcium-rich dolomites common in younger sediments and rocks. When equilibrium conditions are calculated using less ordered, calcium-rich dolomites, the "Dorag zone" --where the fluid is simultaneously supersaturated with respect to dolomite and undersaturated with respect to calcite -- shrinks to a very small window between 60 and 70% meteoric water (Fig. 3.42) (Hardie, 1987).

It is fortuitous (and no doubt coincidental!) that this recalculated "Dorag zone" corresponds closely to the proportions of meteoric water required by the strontium isotopic composition of the St. Croix dolomites. Obviously, the exact location of the saturation window, and whether there even is one, is dependent on the chemical conditions and composition of the end-member waters. I require simply that the St. Croix dolomitizing fluids were supersaturated with respect to dolomite, but can not prove that the fluids were also undersaturated with respect to calcite.

Other Dolomitization Models

Stabilization of a dolomite precursor.-- Due to the depleted ^{18}O content of many ancient dolomites relative to their supposed modern precursors, as well as the relative instability of most geologically young dolomites, it has been suggested that many dolomites have undergone recrystallization (Land, 1980; 1983b). This stabilization results in a change from a non-stoichiometric mineral, to a more stable, stoichiometric

Reproduced with permission of the copyright owner. Further reproduction prohibited without permission.

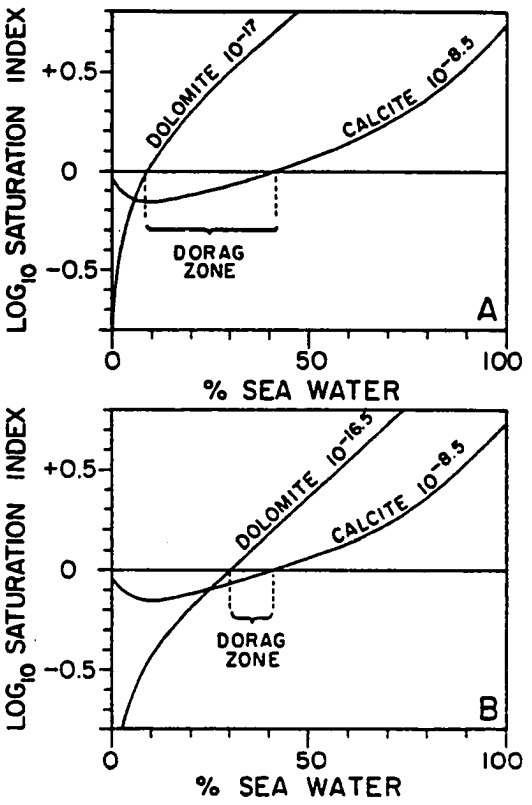

Figure 3.42. Saturation relations between dolomite and calcite in seawater-meteoric water mixtures for both ordered and disordered dolomites.
Upper diagram: saturation relations for ordered dolomite, $K_{sp}=10^{-17}$ and calcite.
Lower diagram: saturation relations for disordered dolomite, $K_{sp}=10^{-16.5}$. Note the decrease in size of the "dorag zone", where the mixed water is simultaneously supersaturated with respect to dolomite and undersaturated with respect to calcite; from Hardie (1987).

form with trace-element and stable isotopic chemistry derived from the recrystallizing fluid. The process is analogous to the stabilization of skeletal carbonates.

The problem in this case remains the source of fluids enriched in ^{18}O and depleted in ^{87}Sr relative to seawater. With the exception of mixed evaporitic waters, which have already been discussed, the available alternative is water altered by passage through aquifer carbonates, i.e. the Kingshill Limestone. A major problem here is that

Reproduced with permission of the copyright owner. Further reproduction prohibited without permission.

many platform carbonate constituents, scleractinians and many calcareous algae for example, are substantially depleted in ^{18}O relative to equilibrium with seawater (data from Milliman, 1974). Modern St. Croix reef and platform sediments have a bulk isotopic composition ranging from $\delta^{18}O$ -1.8 ‰ to -2.9 ‰ relative to PDB (Saller, unpubl. data). Since most reef and platform assemblages would be similar to these figures, it is apparent that platform carbonates are incapable of producing a pore water significantly more enriched in ^{18}O than seawater.

However, another possibility is a carbonate substantially enriched in ^{18}O, such as a chalk. Water equilibrated with an unaltered, recently uplifted chalk could obtain a $\delta^{18}O$ signature subtantially higher than that of seawater, and could theoretically "reset" the isotopic signature in a previously precipitated dolomite. Such a model has been suggested for the Hope Gate dolomites on Jamaica which were previously interpreted as a mixing zone product (Land, 1973; Land, pers. comm., 1989).

This hypothesis is certainly possible, however, there are several problems that should be considered:

1) The Kingshill Limestone is not a pure chalk and contains not only substantial amounts of terrigenous material, but also significant admixtures of platform and reef-derived sediment. Platform-derived sediments not only are depleted in ^{18}O, but are dominated by reactive polymorphs such as Mg-calcite and aragonite.
2) Reef and platform-derived carbonates in the Kingshill Limestone are often concentrated in coarse-grained sediment-gravity flow layers that have become cemented with diagenetic calcite. These once-permeable layers, rather than the ^{18}O-enriched chalk layers, probably acted as conduits for groundwater.

Reproduced with permission of the copyright owner. Further reproduction prohibited without permission.

3) Water contributes four orders of magnitude more oxygen to a given volume of calcite-saturated water than does calcite, and it is therefore difficult to alter the oxygen isotopic content of water without extremely high rock:water ratios (Veizer, 1983). Water moving along a lengthy flow-path through highly reactive chalk could perhaps exchange enough ^{18}O with the calcite to obtain the isotopic signature of the chalk. However, the isotopic exchange would leave the rock incapable of any subsequent ^{18}O-enrichment of water. Any dolomitization by meteoric water produced by this process would therefore have to be (1) a single, short-term event, and (2) would have to take place immediately after the uplift of the chalks, before meteoric stabilization.

4) The dolomitic rocks on St. Croix are separated from the Kingshill Limestone by an unconformity (Chapt. 2, this dissertation). In at least one place this unconformity is marked by the presence of a paleosol (Frost, pers. comm., 1986). Assuming that the unconformity represents exposure and erosion of the underlying strata, the Miocene Kingshill Limestone was exposed to meteoric weathering prior to the deposition of the Pliocene reef tract as well as prior to their alteration to dolomite. The extensive exposure history of the Kingshill Limestone makes it rather unlikely that water derived from fresh, unaltered chalks ever came in contact with the Pliocene reef tract.

5) The isotopic composition of sea-floor chalks is highly dependent on the length of burial. Most chalks undergo substantial redistribution of carbonate during burial on the seafloor, and the result is a chalk significantly depleted in ^{18}O without any exposure to meteoric water (Scholle, 1977, Land, 1980). Although this objection is probably not relevant to St. Croix due to the length of time that this transformation takes, it does reduce the general applicability of the model.

6) The distribution of the dolomitic strata within Krause Lagoon is not explained by this model alone. Regardless of whether or not the dolomites on St. Croix have been

Reproduced with permission of the copyright owner. Further reproduction prohibited without permission.

geochemically "reset", the process of dolomitization was still apparently restricted to Krause Lagoon.

I conclude that this model cannot be entirely eliminated on the basis of the present evidence, but that it does not satisfactorily explain the geographic distribution of the dolomite. This model also requires a large number of complicating assumptions, and is difficult to support with the known exposure history of St. Croix.

Mixing model.-- Dolomite formation via meteoric water/seawater mixing has gained substantial popularity as an explanation for dolomites found in non-evaporitic environments (Land, 1973; Badiozamani, 1973; Folk and Land, 1975; among others). The thermodynamic reasoning behind the mixing zone hypothesis is explored by Plummer (1975) and is discussed critically by Hardie (1987), and will not be discussed in detail here.

Despite its popularity as a model for coastal dolomites, there are several reasons why we reject fresh/seawater mixing *alone* as an explanation for the St. Croix dolomites. Firstly, such a mechanism would presumably be active throughout the coastal mixing zones on St. Croix. Fresh water discharge has been documented historically and by our drilling along substantial portions of the southern coastline. In spite of these observations, dolomite is highly localized on St. Croix, and is restricted to the area surrounding Krause Lagoon. The mixing model does not explain the highly localized distribution of the dolomitization.

Reproduced with permission of the copyright owner. Further reproduction prohibited without permission.

Secondly, the oxygen isotopic composition of the dolomites is significantly enriched over the isotopic composition of seawater, and even more enriched in ^{18}O over a fresh water/seawater mixture. The stable isotopic composition of the dolomites requires that local evaporation or some other process produce fluids with elevated isotopic ratios.

Evaporative Model.-- Evaporation of seawater is a well documented mechanism for the formation of dolomite in both recent and ancient environments. However, evaporative processes do not alter the strontium isotopic ratio of a fluid or an authigenic phase:

1) Pliocene and younger seawater would produce dolomite with far higher $^{87}Sr/^{86}Sr$ ratios than measured St. Croix dolomite values.
2) Dolomitization from St. Croix groundwater alone would produce dolomites with substantially reduced $^{87}Sr/^{86}Sr$ ratios than measured values.

Evaporation alone could be responsible for the elevated oxygen isotopic ratios in the St. Croix dolomites, but can not account for the strontium isotopic composition.

Alteration of seawater via refluxion through the siliciclastic alluvium.-- An alternative of the evaporative mixing hypothesis would be the argument that alteration of the seawater strontium isotopic content occurred through interaction with lagoonal siliciclastics rather than through mixing with St. Croix meteoric waters. This mechanism would account for both the stable isotopic and strontium isotopic characteristics of the dolomite, but would require fluid transport of brine through the mud-rich Holocene alluvial and lagoonal sediments that overlie the dolomites.

Reproduced with permission of the copyright owner. Further reproduction prohibited without permission.

This hypothesis cannot be rejected on the basis of present evidence, but there are several problems that make it less likely:

1) The lagoonal sediments presently overlying the dolomitized limestones are lithologically variable, but are fine grained and relatively impermeable. Extensive reflux through these sediments is not likely.
2) The path length for waters in contact with the lagoonal sediments is far shorter than that for groundwater flow, allowing for less exposure of the evaporative fluid to reactive mineral phases.
3) Siliciclastics in the lagoonal alluvium would probably be far less reactive in an evaporated seawater than the same minerals would be in meteoric water. Breakdown of feldspars to clays, for instance, occurs more readily in solutions of high acidity and low concentrations of sodium and potassium (Garrels and Christ, 1965). Seawater contains several orders of magnitude higher concentrations of sodium, and is more alkaline than St. Croix rainwater.
4) The dolomitized strata exist several meters below the carbonate/alluvium contact, and represent an abrupt lithologic break below the calcite-cemented limestones. This stratigraphic relationship would be difficult to produce if the dolomitizing fluids were transported vertically to the calcite host rock.

Moving altered seawater upward through strata.-- Circulation of seawater upward through carbonate strata via convective flow has been suggested as a possible mechanism for diagenetic alteration within carbonate platforms and atolls (Kohout, 1965; Simms, 1984; Aharon and others, 1987). Alteration of the strontium isotopic ratio of seawater would be possible via this mechanism if seawater reacted with aquifer materials. However, we reject this possibility for the following reasons:

Reproduced with permission of the copyright owner. Further reproduction prohibited without permission.

1) The sediments underlying the post-Kingshill carbonates have very low permeabilities.
2) There is no evidence of sufficient heat flow to provide a driving mechanism for convective circulation.
3) This mechanism does not account for the oxygen isotopic ratios of the dolomites.

Deep Marine.-- Dolomitization via circulation of cold, deep marine waters has been convincingly argued as a mechanism for the dolomitization of Tertiary strata in Enewetak atoll (Saller, 1983; 1984). The hydrologic drive for seawater circulation could be provided by tidal circulation or convective flow. This mechanism is unlikely on St. Croix due to the problems mentioned above with relatively impermeable underlying sediments and the lack of a suitable heat source. In addition, the geologic setting of the St. Croix dolomites are not compatible with this model:

1) The dolomitized strata represent reef and near-reef environments; they have never been deeply buried, and show ample evidence of meteoric exposure.
2) The tectonic setting of St. Croix is one of uplift, rather than subsidence. There is no reasonable mechanism for the deep submergence of the the St. Croix carbonate strata for long periods of time, nor any evidence that this occurred.

Reproduced with permission of the copyright owner. Further reproduction prohibited without permission.

CONCLUSIONS

On the basis of this study, we suggest the following for the St. Croix dolomites:

1. The dolomite formed in a basin shaped by Tertiary or later faulting.
2. The dolomitizing fluids were depleted in ^{87}Sr and enriched in ^{18}O.
3. The dolomitization was accomplished by an evaporative mix of both meteoric and marine waters.
4. Significant groundwater influence on the $^{87}Sr/^{86}Sr$ ratio of diagenetic carbonates cannot be neglected *a priori,* even in cases with extensive seawater contribution.
5. The formation of brines and diagenetic minerals from evaporated meteoric and meteoric/marine mixtures may be more common a geologic process than is currently acknowledged.

Although it is difficult to prove that a particular mechanism was responsible for a particular geologic product, we feel confident that several competing hypotheses can effectively be eliminated in this case, and that a slightly more complex mixing and evaporation mechanism must be considered.

However, the results of this study are not necessarily confined to St. Croix. The geological environments and aquifer lithologies encountered on St. Croix are not unusual, and there is no reason to believe that the processes discussed in this paper could not occur elsewhere. I do not pretend that the mechanism suggested in this chapter explains all occurrences of sedimentary dolomite. However, a limited, well-considered example such as the dolomite on St. Croix adds detail to the knowledge of general dolomitization processes. In this case, it is important to show both the feasability of this

Reproduced with permission of the copyright owner. Further reproduction prohibited without permission.

mechanism, as well as the potential significance of groundwater strontium effects in diagenesis, regardless of the general applicability of the model.

Reproduced with permission of the copyright owner. Further reproduction prohibited without permission.

TABLES

Reproduced with permission of the copyright owner. Further reproduction prohibited without permission.

Reproduced with permission of the copyright owner. Further reproduction prohibited without permission.

Table 3.1. Groundwater geochemistry data.

WELL NAME	COLL. DATE	LOCATION	OWNER	SOURCE
EPA M. P. C.*	--	--	--	Freeze and Cherry (1979)
EPA R. C. L.**	--	--	--	
Detection Limit	--	--	--	--
BS-31	Nov 25 85	Barren Spot wellfield, #31	VI Govt	--
BS-31	May 19 85	Barren Spot wellfield, #31	VI Govt	--
BS-3A	May 19 85	Barren Spot wellfield, #3A	VI Govt	--
BS-8	Apr 4 84	Barren Spot wellfield, #8	VI Govt	--
CA-109	Mar 8 86	Carlton, Plot 109	J. Stout	--
CA-15	Mar 12 86	Carlton, Plot 15	B. Rezende	--
CC-23	Mar 21 86	Castle Coakley, Plot 23	L. Satomayor	--
CO-1	Apr 4 84	Concordia wellfield, #1	VI Govt	--
CO-52	Mar 14 86	Concordia, Plot 52	F. Malloy	--
CVI	Mar 12 86	College of the VI	CVI	--
FP-4	Nov 27 85	Fairplain wellfield, #4	VI Govt	--
FP-5	Nov 27 85	Fairplain wellfield, #5	VI Govt	--
FP-6	Apr 4 84	Fairplain wellfield, #6	VI Govt	--
FP-6	May 15 85	Fairplain wellfield, #6	VI Govt	--
FP-6	May 19 85	Fairplain wellfield, #6	VI Govt	--
FP-6	Nov 26 85	Fairplain wellfield, #6	VI Govt	--
FP-8	Nov 27 85	Fairplain wellfield, #8	VI Govt	--
GG-PW1	Apr 4 84	Golden Grove wellfield, #PW1	VI Govt	--
GG-PW1	Dec 9 85	Golden Grove wellfield, #PW1	VI Govt	--
GL-148	Mar 20 86	Glynn, Plot 148	L. Williams	--
GL-246C	Mar 14 86	Glynn, Plot 246C	Dr. Williams	--
HR-100	Mar 10 86	Hannahs Rest, Plot 100	C. George	--
LG-1	Apr 4 84	La Grange wellfield, #1	VI Govt	--
MH-35	Mar 10 86	Mars Hill, Plot 35	Tony's Laundromat	--
MW-4	Dec 6 86	Mt. Washington, Plot 4		--
NB-3	Nov 29 85	Negro Bay wellfield, #3	VI Govt	--
NB-6	Dec 7 85	Negro Bay wellfield, #6	VI Govt	--
PE-3A	Mar 18 86	Pearl, Plot 3A	M. Maneilly	--
Rainwater	Mar 13 86	East End, St. Croix	--	--
RU-149	Mar 18 86	Ruby, Plot 149	S. Smith	--
Seawater	Mar 86	Tague Bay, St. Croix	--	--
Seawater-avg.	--	--	--	Drever (1982)
SO-R1	Mar 16 86	Solitude Remainder, Well 1	R. Roebuck	--
SO-R2	Mar 16 86	Solitude Remainder, Well 2	R. Roebuck	--
WD-94	Mar 7 86	Williams Delight, Plot 94	D. McLean	--
WH-59	Mar 12 86	Whim, Plot 59	R. Jackson Jr.	--

* Maximum Permissible Concentration, US EPA
** Recommended Concentration Limit, US EPA

Reproduced with permission of the copyright owner. Further reproduction prohibited without permission.

Table 3.1. (Cont.)

WELL NAME	COLL. DATE	TEMP (C)	pH	(amb.temp) (umho/cm) SPEC COND	(conduct.) (ppm) SALINITY	(sum, ppm) SOLIDS	as CaCO3 (ppm) HARDNESS
EPA M. P. C.*	--	--	--	--	--	--	--
EPA R. C. L.**	--	--	--	--	500	500	--
Detection Limit	--	--	--	--	--	--	--
BS-31	Nov 25 85	26.7	7.13	4110	2200	2492	266
BS-31	May 19 85	27.4	7.05	4150	2100	--	--
BS-3A	May 19 85	27.5	7.27	3330	1900	--	--
BS-8	Apr 4 84	--	--	--	--	--	--
CA-109	Mar 8 86	29.1	6.95	822	250	--	265
CA-15	Mar 12 86	27.3	7.20	1327	1270	--	175
CC-23	Mar 21 86	27.3	6.80	5500	2900	--	679
CO-1	Apr 4 84	--	--	--	--	--	--
CO-52	Mar 14 86	32.3	6.91	1558	650	856	367
CVI	Mar 12 86	29.0	7.97	2110	1000	--	22
FP-4	Nov 27 85	28.0	7.01	4610	2200	2547	763
FP-5	Nov 27 85	29.0	6.96	3550	1800	2027	421
FP-6	Apr 4 84	--	--	--	--	--	--
FP-6	May 15 85	28.2	6.87	4690	--	--	--
FP-6	May 19 85	27.3	6.88	4650	2500	--	--
FP-6	Nov 26 85	28.1	6.96	5100	2750	2969	866
FP-8	Nov 27 85	27.4	7.06	3280	--	--	407
GG-PW1	Apr 4 84	--	--	--	--	--	--
GG-PW1	Dec 9 85	27.3	6.67	1903	800	1082	175
GL-148	Mar 20 86	27.4	7.20	1805	800	--	138
GL-246C	Mar 14 86	27.4	6.72	2102	1000	1211	531
HR-100	Mar 10 86	27.5	7.38	5100	2700	--	150
LG-1	Apr 4 84	--	--	--	--	--	--
MH-35	Mar 10 86	30.8	7.32	12750	6500	--	600
MW-4	Dec 6 86	27.7	6.65	1300	500	--	--
NB-3	Nov 29 85	27.3	7.05	2203	1000	1376	285
NB-6	Dec 7 85	27.1	6.99	2103	967	1285	266
PE-3A	Mar 18 86	30.4	7.12	3075	1500	--	150
Rainwater	Mar 13 86	--	5.13	--	--	--	2
RU-149	Mar 18 86	26.8	7.68	2107	1033	--	37
Seawater	Mar 86	--	--	--	--	--	6657
Seawater-avg.	--	--	8.15	--	--	35016	6322
SO-R1	Mar 16 86	28.4	6.76	2655	1250	1504	426
SO-R2	Mar 16 86	28.2	6.71	3420	1700	--	564
WD-94	Mar 7 86	28.2	7.09	2300	1100	1636	162
WH-59	Mar 12 86	29.6	7.16	2997	1450	--	309

* Maximum Permissible Concentration, US EPA
** Recommended Concentration Limit, US EPA

Table 3.1. (Cont.)

WELL NAME	COLL. DATE	Cl (mg/l)	Na (ppm)	SO4 (mg/l)	S (as SO4) (mg/L)	Mg (ppm)	Ca (ppm)	K (ppm)
EPA M. P. C.*	--	--	--	--	--	--	--	--
EPA R. C. L.**	--	250	--	250	--	--	--	--
Detection Limit	--	--	.25	--	--	.002	.002	1.0
BS-31	Nov 25 85	894	896	272	286	23.9	66.7	6.7
BS-31	May 19 85	853	825	266		--	--	5.6
BS-3A	May 19 85	654	739	208		--	--	4.0
BS-8	Apr 14 84	846	860	268		--	--	.5
CA-109	Mar 8 86	<150	121	37	33	30.6	55.6	.8
CA-15	Mar 12 86	<150	235	61	60	15.1	45.2	<DL
CC-23	Mar 21 86	1263	937	--	480	56.6	178.0	5.6
CO-1	Apr 4 84	507	401	155		--	--	4.2
CO-52	Mar 14 86	199	201	59	63	39.0	82.7	3.0
CVI	Mar 12 86	162	522	--	107	3.7	2.7	2.4
FP-4	Nov 27 85	996	683	248	271	94.9	149.5	1.7
FP-5	Nov 27 85	714	598	207	207	50.5	85.5	1.9
FP-6	Apr 4 84	1173	703	180		--	--	7.4
FP-6	May 15 85	1146	689	254		--	--	2.7
FP-6	May 19 85	1157	697	228		--	--	2.7
FP-6	Nov 26 85	1402	744	208	220	112.1	162.0	2.3
FP-8	Nov 27 85	--	604	211	222	49.8	80.9	2.0
GG-PW1	Apr 4 84	269	302	102		--	--	<DL
GG-PW1	Dec 9 85	248	304	99	104	>RNG	69.6	.8
GL-148	Mar 20 86	199	367	--	56	17.1	27.0	.6
GL-246C	Mar 14 86	425	271	50	54	52.6	126.1	2.1
HR-100	Mar 10 86	1052	1165	--	265	24.2	20.2	13.6
LG-1	Apr 4 84	259	99	--		--	--	<DL
MH-35	Mar 10 86	--	2445	--	633	104.2	68.6	51.0
MW-4	Dec 6 86	126	79	--	53.4	32.9	174.7	--
NB-3	Nov 29 85	395	403	103	106	40.4	47.7	1.4
NB-6	Dec 7 85	319	413	78	92	36.8	45.9	1.3
PE-3A	Mar 18 86	575	610	--	127	16.1	33.6	5.8
Rainwater	Mar 13 86	--	<DL	--	2.4	.4	<DL	<DL
RU-149	Mar 18 86	282	486	--	101	4.6	7.4	3.0
Seawater	Mar	--	12029	--	2885	1370.0	414.0	402.0
Seawater-avg.		19350	10760	2710		1290.0	411.0	399.0
SO-R1	Mar 16 86	470	447	119	123	48.4	90.8	6.4
SO-R2	Mar 16 86	669	560	--	201	69.7	110.9	12.1
WD-94	Mar 7 86	406	599	154	140	14.9	40.2	1.3
WH-59	Mar 12 86	575	510	--	137	37.3	62.2	2.6

* Maximum Permissible Conctration, US EPA
** Recommended Concentrati Limit, US EPA

Reproduced with permission of the copyright owner. Further reproduction prohibited without permission.

Table 3.1. (Cont.)

Alkalinity

WELL NAME	COLL. DATE	HCO3 (ppm)	CO3 (ppm)	Sr (ppm)	Si (ppm)	SiO2 (ppm)
EPA M. P. C.*	--	--	--	--	--	--
EPA R. C. L.**	--	--	--	--	--	--
Detection Limit	--	--	--	.0025	.14	.096
BS-31	Nov 25 85	617	--	1.58	12.9	27.6
BS-31	May 19 85	626	--	1.59	--	--
BS-3A	May 19 85	693	--	.77	--	--
BS-8	Apr 4 84	--	--	1.72	--	--
CA-109	Mar 8 86	532	--	.43	>RNG	>RNG
CA-15	Mar 12 86	534	--	.22	17.0	36.4
CC-23	Mar 21 86	567	--	2.26	11.4	24.4
CO-1	Apr 4 84	--	--	3.12	--	--
CO-52	Mar 14 86	551	--	1.00	>RNG	>RNG
CVI	Mar 12 86	866	--	.28	19.8	42.4
FP-4	Nov 27 85	690	--	--	15.8	33.8
FP-5	Nov 27 85	676	--	--	17.3	37.0
FP-6	Apr 4 84	--	--	1.94	--	--
FP-6	May 15 85	636	--	1.93	--	--
FP-6	May 19 85	--	--	1.87	--	--
FP-6	Nov 26 85	609	--	1.95	17.3	37.0
FP-8	Nov 27 85	828	--	1.17	20.0	42.8
GG-PW1	Apr 4 84	--	--	.73	--	--
GG-PW1	Dec 9 85	690	--	.69	9.2	19.7
GL-148	Mar 20 86	688	--	.25	>RNG	>RNG
GL-246C	Mar 14 86	504	--	.54	16.2	34.7
HR-100	Mar 10 86	949	--	.36	13.5	28.9
LG-1	Apr 4 84	--	--	.68	--	--
MH-35	Mar 10 86	--	--	1.12	13.0	27.8
MW-4	Dec 6 86	--	--	.65	14.6	--
NB-3	Nov 29 85	693	--	.51	20.1	43.0
NB-6	Dec 7 85	710	--	.48	19.1	40.9
PE-3A	Mar 18 86	582	--	.50	9.6	20.5
Rainwater	Mar 13 86	<DL	--	<DL	.2	<DL
RU-149	Mar 18 86	595	--	.01	9.1	19.5
Seawater	Mar 86	--	--	6.75	--	--
Seawater-avg.	--	142	18	8.00	--	--
SO-R1	Mar 16 86	586	--	.83	15.4	32.9
SO-R2	Mar 16 86	535	--	1.18	15.0	32.1
WD-94	Mar 7 86	841	--	.28	3.0	6.4
WH-59	Mar 12 86	528	--	.77	14.6	31.2

* Maximum Permissible Concentration, US EPA
** Recommended Concentration Limit, US EPA

Reproduced with permission of the copyright owner. Further reproduction prohibited without permission.

Table 3.1. (Cont.)

WELL NAME	COLL. DATE	Al (ppm)	Ba (ppm)	Cd (ppm)	Co (ppm)	Cr (ppm)	Cu (ppm)
EPA M. P. C.*	--	--	1.00	.01	--	.05	--
EPA R. C. L.**	--	--	--	--	--	--	1
Detection Limit	--	.1	.001	.01	.03	.025	.01
BS-31	Nov 25 85	<DL	.048	<DL	<DL	<DL	<DL
BS-31	May 19 85	--	--	--	--	--	--
BS-3A	May 19 85	--	--	--	--	--	--
BS-8	Apr 4 84	--	--	--	--	--	--
CA-109	Mar 8 86	<DL	.035	<DL	<DL	<DL	<DL
CA-15	Mar 12 86	<DL	<DL	<DL	<DL	<DL	<DL
CC-23	Mar 21 86	<DL	.036	<DL	<DL	<DL	<DL
CO-1	Apr 4 84	--	--	--	--	--	--
CO-52	Mar 14 86	<DL	.042	<DL	<DL	<DL	<DL
CVI	Mar 12 86	<DL	<DL	<DL	<DL	<DL	<DL
FP-4	Nov 27 85	<DL	.067	<DL	<DL	<DL	<DL
FP-5	Nov 27 85	<DL	.050	<DL	<DL	<DL	<DL
FP-6	Apr 4 84	--	--	--	--	--	--
FP-6	May 15 85	--	--	--	--	--	--
FP-6	May 19 85	--	--	--	--	--	--
FP-6	Nov 26 85	<DL	.064	<DL	<DL	<DL	<DL
FP-8	Nov 27 85	<DL	.042	<DL	<DL	<DL	<DL
GG-PW1	Apr 4 84	--	--	--	--	--	--
GG-PW1	Dec 9 85	<DL	.044	<DL	<DL	<DL	<DL
GL-148	Mar 20 86	<DL	.040	<DL	<DL	<DL	<DL
GL-246C	Mar 14 86	<DL	.038	<DL	<DL	<DL	<DL
HR-100	Mar 10 86	<DL	.033	<DL	<DL	<DL	<DL
LG-1	Apr 4 84	--	--	--	--	--	--
MH-35	Mar 10 86	.1	.038	<DL	<DL	<DL	.064
MW-4	Dec 6 86	--	--	--	--	--	--
NB-3	Nov 29 85	<DL	.041	<DL	<DL	<DL	<DL
NB-6	Dec 7 85	<DL	.037	<DL	<DL	<DL	<DL
PE-3A	Mar 18 86	<DL	.040	<DL	<DL	<DL	<DL
Rainwater	Mar 13 86	<DL	<DL	<DL	<DL	<DL	<DL
RU-149	Mar 18 86	<DL	.031	<DL	<DL	<DL	<DL
Seawater	Mar 86	--	<DL	<DL	<DL	<DL	<DL
Seawater-avg.	--	.002	.002	0.05	.00005	.0003	.0005
SO-R1	Mar 16 86	<DL	.061	<DL	<DL	<DL	<DL
SO-R2	Mar 16 86	<DL	.060	<DL	<DL	<DL	<DL
WD-94	Mar 7 86	<DL	.040	<DL	<DL	<DL	<DL
WH-59	Mar 12 86	<DL	.036	<DL	<DL	<DL	<DL

* Maximum Permissible Concentration, US EPA
** Recommended Concentration Limit, US EPA

Reproduced with permission of the copyright owner. Further reproduction prohibited without permission.

Table 3.1. (Cont.)

WELL NAME	COLL. DATE	Fe (ppm)	Mn (ppm)	Ni (ppm)	V (ppm)	Zn (ppm)	(Cat/An) CHG.BAL.
EPA M. P. C.*	--	--	--	--	--	--	--
EPA R. C. L.**	--	.3	.05	--	--	.5	--
Detection Limit	--	.015	.0025	.05	.025	.005	--
BS-31	Nov 25 85	<DL	.004	<DL	<DL	<DL	1.08
BS-31	May 19 85	<DL	<DL	--	--	--	--
BS-3A	May 19 85	<DL	<DL	--	--	--	--
BS-8	Apr 4 84	<DL	<DL	--	--	--	--
CA-109	Mar 8 86	--	--	<DL	<DL	<DL	--
CA-15	Mar 12 86	<DL	<DL	<DL	<DL	<DL	--
CC-23	Mar 21 86	<DL	.057	<DL	<DL	.009	--
CO-1	Apr 4 84	<DL	<DL	--	--	--	--
CO-52	Mar 14 86	--	--	<DL	<DL	<DL	1.01
CVI	Mar 12 86	<DL	<DL	<DL	.358	<DL	--
FP-4	Nov 27 85	--	--	<DL	<DL	.013	1.00
FP-5	Nov 27 85	--	--	<DL	.028	<DL	.97
FP-6	Apr 4 84	.030	<DL	--	--	--	--
FP-6	May 15 85	.040	<DL	--	--	<DL	--
FP-6	May 19 85	<DL	<DL	--	--	<DL	--
FP-6	Nov 26 85	2.216	.061	<DL	<DL	<DL	.92
FP-8	Nov 27 85	<DL	.010	<DL	.035	<DL	--
GG-PW1	Apr 4 84	<DL	<DL	--	--	--	--
GG-PW1	Dec 9 85	--	--	<DL	<DL	<DL	.81
GL-148	Mar 20 86	<DL	<DL	<DL	<DL	<DL	--
GL-246C	Mar 14 86	<DL	<DL	<DL	<DL	<DL	.95
HR-100	Mar 10 86	<DL	.002	<DL	.070	.025	--
LG-1	Apr 4 84	<DL	<DL	--	--	--	--
MH-35	Mar 10 86	<DL	.016	<DL	<DL	<DL	--
MW-4	Dec 6 86	<DL	.004	<DL	--	--	--
NB-3	Nov 29 85	<DL	<DL	<DL	.033	.007	.93
NB-6	Dec 7 85	.154	.008	<DL	<DL	.051	1.04
PE-3A	Mar 18 86	<DL	<DL	<DL	<DL	<DL	--
Rainwater	Mar 13 86	--	--	<DL	.028	.073	--
RU-149	Mar 18 86	<DL	<DL	<DL	.040	<DL	--
Seawater	Mar 86	<DL	<DL	<DL	<DL	<DL	--
Seawater-avg.	--	.002	.0002	.0005	--	.002	1.00
SO-R1	Mar 16 86	<DL	<DL	<DL	<DL	<DL	1.09
SO-R2	Mar 16 86	<DL	<DL	<DL	<DL	.451	--
WD-94	Mar 7 86	<DL	<DL	<DL	<DL	.007	1.03
WH-59	Mar 12 86	.027	.009	<DL	<DL	<DL	--

* Maximum Permissible Concentration, US EPA
** Recommended Concentration Limit, US EPA

Reproduced with permission of the copyright owner. Further reproduction prohibited without permission.

Table 3.1. (Cont.)

WELL NAME	COLL. DATE	d2H (SMOW)	d18O (SMOW)	d13C (PDB)	87Sr/86Sr
EPA M. P. C.*	--	--	--	--	--
EPA R. C. L.**	--	--	--	--	--
Detection Limit	--	--	--	--	--
BS-31	Nov 25 85	--	--	--	--
BS-31	May 19 85	--	--	--	--
BS-3A	May 19 85	--	--	--	--
BS-8	Apr 4 84	--	--	--	--
CA-109	Mar 8 86	--	--	--	--
CA-15	Mar 12 86	--	--	--	--
CC-23	Mar 21 86	--	--	--	--
CO-1	Apr 4 84	--	--	--	--
CO-52	Mar 14 86	--	--	--	--
CVI	Mar 12 86	--	--	--	--
FP-4	Nov 27 85	--	--	--	--
FP-5	Nov 27 85	--	--	--	--
FP-6	Apr 4 84	--	--	--	--
FP-6	May 15 85	--	--	--	--
FP-6	May 19 85	--	--	--	--
FP-6	Nov 26 85	--	--	--	--
FP-8	Nov 27 85	--	--	--	--
GG-PW1	Apr 4 84	--	--	--	--
GG-PW1	Dec 9 85	--	--	--	--
GL-148	Mar 20 86	--	--	--	--
GL-246C	Mar 14 86	--	--	--	--
HR-100	Mar 10 86	--	--	--	--
LG-1	Apr 4 84	--	--	--	--
MH-35	Mar 10 86	--	--	--	--
MW-4	Dec 6 86	-21	-4	-14.8	.7067
NB-3	Nov 29 85	--	--	--	--
NB-6	Dec 7 85	--	--	--	--
PE-3A	Mar 18 86	-18	-3.4	-9	.7085
Rainwater	Mar 13 86	-3	-1.3	-22.4	--
RU-149	Mar 18 86	-20	-3.7	-8.6	.7082
Seawater	Mar 86	--	--	--	--
Seawater-avg.	--	--	--	--	--
SO-R1	Mar 16 86	--	--	--	--
SO-R2	Mar 16 86	--	--	--	--
WD-94	Mar 7 86	-17	-3.6	-7.8	.7075
WH-59	Mar 12 86	--	--	--	--

* Maximum Permissible Concentration, US EPA
** Recommended Concentration Limit, US EPA

Reproduced with permission of the copyright owner. Further reproduction prohibited without permission.

Table 3.2: Chemical equilibrium modeling results for St. Croix groundwaters.

WELL	COLL. DATE	SUPERSATURATED PHASES
BS-31	11/25/85	CALCITE, BARITE, CHALCEDONY, QUARTZ
CO-52	03/14/86	CALCITE, DOLOMITE, CHALCEDONY, QUARTZ, GIBBSITE, KAOLINITE
FP-6	11/26/85	CALCITE, DOLOMITE, BARITE, CHALCEDONY, QUARTZ, HEMATITE, GOETHITE, Fe(OH)3
GL-148	03/20/86	CHALCEDONY, QUARTZ, GIBBSITE, KAOLINITE
NB-6	12/07/85	DOLOMITE, CHALCEDONY, QUARTZ, HEMATITE, GOETHITE, Fe(OH)3
PE-3A	03/18/86	QUARTZ, GIBBSITE, KAOLINITE
SO-R1	03/16/86	CHALCEDONY, QUARTZ

Reproduced with permission of the copyright owner. Further reproduction prohibited without permission.

Table 3.3. Stable isotopic data for St. Croix dolomites.

(all values relative to the PDB standard, uncorrected for phosphoric acid fractionation)

Sample ID	Trtmt	$\delta^{13}C$	$\delta^{18}O$	Position rel. to WT*
B4/5/4	L2	+2.0	+2.5	below WT
B7/5/10	L2	+2.2	+3.5	"
B7/5/4	LCH	+2.4	+3.8	"
B7/6/3	LCH	+2.3	+3.8	"
B15A/6/1	L2	+2.4	+3.3	"
B15A/6/4	LCH	+2.2	+3.5	"
B15A/6/9A	L2	+2.2	+3.7	"
M5/25	L2	+1.5	+2.8	"
M7/38	L1	+1.4	+3.8	"
M9/34	L3	+0.6	+3.3	"
M3/7/25'	L2, LCH	+0.6	+2.6	above WT
M4/1/3/25'	L4	+0.7	+1.5	"
M4/3/1	L3	+1.3	+1.8	"
VII26A	LCH	+1.0	+2.6	"
VII26E	L1	+1.1	+2.7	"

* Position relative to present water table

Reproduced with permission of the copyright owner. Further reproduction prohibited without permission.

Reproduced with permission of the copyright owner. Further reproduction prohibited without permission.

Table 3.4. Wet chemical analysis of St. Croix carbonates. Elemental values refer to ICP analyses of the soluble rock fraction.

BOTTLE #	SAMPLE NO		(g) Net Wt RAW SPL	% INSOL RES	Ca ppm	Mg ppm	Na ppm
#36	B15A/5/6	(L1)	.1095	3.5%	252477.3	106738.4	470.5
#21	B15A/6/1	(L2)	.1229	5.6%	227332.3	99918.9	437.8
#38	B15A/6/1	(L1)	.0991	3.3%	236632.0	102661.9	448.3
#4	B15A/6/4	(BLK)	.5206	4.5%	239050.4	112119.9*	820.9*
#12	B15A/6/4	(BLK)	.1830	5.2%	256522.3	118492.9	807.4
#8	B15A/6/9	(L1)	.1563	4.9%	240871.6	111233.1	452.7
#16	B15A/6/9	(L1)	.1448	5.0%	245320.5	107178.9	426.1
#24	B4/5/4	(L2)	.0626	22.8%	243757.4	99711.4	621.0
#28	B4/5/4	(BLK)	.2629	2.1%	571857.0	55179.2	538.6
#34	B4/5/4	(BLK)	.0538	23.4%	157880.8	100220.0	683.7
#20	B7/5/10	(L2)	.1614	5.9%	251846.2	112583.8	447.2
#42	B7/5/10	(BLK)	.1933	4.9%	242495.4	111443.3	899.3
#5	B7/6/3	(L2)	.2245	3.2%	246493.3	112779.8	439.1
#13	B7/6/3	(L2)	.1495	4.3%	263440.8	118164.7	450.0
#26	B7/6/3	(BLK)	.1650	2.6%	258358.9	100790.8	539.2
#7	BLANK		0.0000	0.0%	0.0	0.0	0.0
#15	BLANK		0.0000	0.0%	0.0	0.0	0.0
#30	BLANK		0.0000	0.0%	0.0	0.0	0.0
#39	BLANK		0.0000	0.0%	0.0	0.0	0.0
#22	EH.HTS/1	Forams,unlchd	.2228	1.7%	412299.9	1297.2	81.5
#19	GFS-400	(BLK)	.1463	1.6%	220352.7	133286.5	324.7
#23	GFS-400	(BLK STD)	.1449	.3%	210737.1	128409.9	361.1
#41	GFS-400	(STD)	.1433	0.0%	212462.8	128540.0	375.0

* Average of analyses from two dilutions.

Reproduced with permission of the copyright owner. Further reproduction prohibited without permission.

Table 3.4. (Cont.)

Table 3.4.

BOTTLE #	SAMPLE NO	(g) Net Wt RAW SPL	% INSOL RES	Ca ppm	Mg ppm	Na ppm
#43	HC280/13.0 (BLK)	.1725	.9%	407091.2	2852.7	NA
#35	HC280/4.0 (BLK)	.1411	2.8%	409954.0	2822.7	NA
#25	HC280/4.85 (BLK)	.2837	3.1%	257045.9	108885.6	491.0
#45	HTS.EH/1 forams,cld,lch	.1312	1.1%	412290.7	1371.4	NA
#18	LPG-1 (BLK)	.1648	.4%	431905.1	3406.4	182.1
#11	M1/13 (BLK)	.1491	49.1%	357422.2	3158.9	3059.2
#10	M1/13 (SND)	.0796	14.4%	412830.3	1137.8	1556.7
#2	M1/13/115 (SND)	.1995	13.2%	405349.9	1337.5	1470.1
#3	M1/13/115 (BLK)	.2296	47.2%	360415.1	4153.8	2577.7*
#40	M1/16 (BLK)	.1018	50.8%	341844.1	5742.6	4030.6
#44	M2/24.4 (BLK)	.0980	30.1%	365540.0	3182.2	4095.6
#37	M5/25 (L2)	.1404	19.2%	248200.9	102135.7	518.0
#27	M7/38 (BLK)	.1278	6.4%	234046.2	99270.4	540.4
#33	M7/38 (BLK)	.1825	11.7%	268433.6	119040.4	1378.0
#29	M9/34 (L3)	.1131	65.2%	240222.8	103826.7	820.3
#31	VII 26A (L1)	.1677	3.2%	250417.5	106531.2	417.0
#6	VII 26E (BLK)	.2548	1.1%	251051.4	110973.7	477.9
#9	VII 26E (L1)	.1585	1.1%	245130.7	104060.8	473.0
#14	VII 26E (BLK)	.1767	1.8%	258167.8	107155.5	473.2
#17	VII 26E (L1)	.1505	1.3%	257621.8	108096.4	474.8
#32	VII 26K (L2)	.0823	19.1%	279084.9	125999.1	800.6

* Average of analyses from two dilutions.

Reproduced with permission of the copyright owner. Further reproduction prohibited without permission.

Table 3.4. (Cont.)

Table 3.4 (Cont.)

BOTTLE #	SAMPLE NO	Sr ppm	Fe ppm	Mn ppm	Si ppm
#36	B15A/5/6 (L1)	212.3	1118.7	86.9	429.6
#21	B15A/6/1 (L2)	192.6	1213.8	96.3	417.6
#38	B15A/6/1 (L1)	200.4	1048.5	116.6	400.9
#4	B15A/6/4 (BLK)	205.3	783.0	90.0	176.9
#12	B15A/6/4 (BLK)	268.4	785.7	129.3	38.0
#8	B15A/6/9 (L1)	200.4	1244.4	81.7	764.6
#16	B15A/6/9 (L1)	267.5	934.8	93.5	0.0
#24	B4/5/4 (L2)	324.1	2272.6	104.8	1455.6
#28	B4/5/4 (BLK)	604.9	947.2	81.8	297.2
#34	B4/5/4 (BLK)	319.8	2073.1	110.1	1622.3
#20	B7/5/10 (L2)	262.0	1253.9	78.9	0.0
#42	B7/5/10 (BLK)	NA	1415.1	106.3	454.6
#5	B7/6/3 (L2)	185.0	887.1	67.8	443.0
#13	B7/6/3 (L2)	272.0	690.6	87.9	0.0
#26	B7/6/3 (BLK)	174.4	741.6	101.3	179.0
#7	BLANK	0.0	0.0	0.0	0.0
#15	BLANK	0.0	0.0	0.0	0.0
#30	BLANK	0.0	0.0	0.0	0.0
#39	BLANK	0.0	0.0	0.0	0.0
#22	EH.HTS/1 Forams,unlchd	178.3	315.8	103.1	63.8
#19	GFS-400 (BLK)	655.7	157.0	43.3	0.0
#23	GFS-400 (BLK STD)	556.7	173.9	36.6	0.0
#41	GFS-400 (STD)	NA	154.2	39.1	0.0

* Average of analys from two dilutions.

Reproduced with permission of the copyright owner. Further reproduction prohibited without permission.

Table 3.4 (Cont.)

BOTTLE #	SAMPLE NO	Sr ppm	Fe ppm	Mn ppm	Si ppm
#43	HC280/13.(BLK)	NA	149.1	11.3	67.0
#35	HC280/4.0(BLK)	242.2	194.9	29.6	114.4
#25	HC280/4.8(BLK)	330.6*	438.8	38.5	343.7
#45	HTS.EH/1 forams,cld,lch	NA	311.9	103.4	0.0
#18	LPG-1 (BLK)	700.3*	798.9	215.5	0.0
#11	M1/13 (BLK)	1172.8	952.6	1116.1	827.1
#10	M1/13 (SND)	1063.0	608.2	707.5	51.7
#2	M1/13/115(SND)	993.9	1213.3	487.4	1061.8
#3	M1/13/115(BLK)	1088.2	3950.6	923.8	5983.6
#40	M1/16 (BLK)	1338.3*	5523.1	1079.8	5931.3
#44	M2/24.4 (BLK)	NA	3307.3	566.3	2720.8
#37	M5/25 (L2)	356.6	3294.7	111.8	1619.5
#27	M7/38 (BLK)	208.6	1260.8	147.1	588.2
#33	M7/38 (BLK)	230.5	1299.5	164.4	546.5
#29	M9/34 (L3)	157.9	5306.7	376.1	4984.0
#31	VII 26A (L1)	286.8	335.5	26.4	338.3
#6	VII 26E (BLK)	265.4*	494.5	24.1	424.1
#9	VII 26E (L1)	279.9	484.7	24.3	329.8
#14	VII 26E (BLK)	371.2	475.0	27.1	0.0
#17	VII 26E (L1)	359.8	468.1	27.2	0.0
#32	VII 26K (L2)	267.4	699.7	80.1	208.2

* Average of analys from two dilutions.

Reproduced with permission of the copyright owner. Further reproduction prohibited without permission.

Table 3.4 (Cont.)

BOTTLE #	SAMPLE NO		CaCO3 mmol/kg	MgCO3 mmol/kg	SrCO3 mmol/kg	FeCO3 mmol/kg	MnCO3 mmol/kg
#36	B15A/5/6	(L1)	6299	4392	2	20	2
#21	B15A/6/1	(L2)	5672	4111	2	22	--
#38	B15A/6/1	(L1)	5904	4224	2	19	2
#4	B15A/6/4	(BLK)	5964	4613*	2	14	--
#12	B15A/6/4	(BLK)	6400	4875	3	14	--
#8	B15A/6/9	(L1)	6010	4577	2	22	--
#16	B15A/6/9	(L1)	6121	4410	3	17	--
#24	B4/5/4	(L2)	6082	4103	4	41	2
#28	B4/5/4	(BLK)	14268	2270	7	17	1
#34	B4/5/4	(BLK)	3939	4123	4	37	2
#20	B7/5/10	(L2)	6284	4632	3	22	--
#42	B7/5/10	(BLK)	6050	4585	NA	25	2
#5	B7/6/3	(L2)	6150	4640	2	16	--
#13	B7/6/3	(L2)	6573	4862	3	12	--
#26	B7/6/3	(BLK)	6446	4147	2	13	2
#7	BLANK		0	0	0	0	--
#15	BLANK		0	0	0	0	--
#30	BLANK		0	0	0	0	0
#39	BLANK		0	0	0	0	0
#22	EH.HTS/1	Forams,unlchd	10287	53	2	6	--
#19	GFS-400	(BLK)	5498	5484	7	3	--
#23	GFS-400	(BLK STD)	5258	5283	6	3	--
#41	GFS-400	(STD)	5301	5289	NA	3	1

* Average of analyses from two dilutions.

Table 3.4. (Cont.)

Reproduced with permission of the copyright owner. Further reproduction prohibited without permission.

Table 3.4 (Cont.)

BOTTLE #	SAMPLE NO	CaCO3 mmol/kg	MgCO3 mmol/kg	SrCO3 mmol/kg	FeCO3 mmol/kg	MnCO3 mmol/kg
#43	HC280/13.0 (BLK)	10157	117	NA	3	0
#35	HC280/4.0 (BLK)	10228	116	3	3	1
#25	HC280/4.85 (BLK)	6413	4480	4*	8	1
#45	HTS.EH/1 forams,cld,lch	10287	56	NA	6	2
#18	LPG-1 (BLK)	10776	140	8*	14	--
#11	M1/13 (BLK)	8918	130	13	17	--
#10	M1/13 (SND)	10300	47	12	11	--
#2	M1/13/115 (SND)	10114	55	11	22	--
#3	M1/13/115 (BLK)	8992	171	12	71	--
#40	M1/16 (BLK)	8529	236	15*	99	20
#44	M2/24.4 (BLK)	9120	131	NA	59	10
#37	M5/25 (L2)	6193	4202	4	59	2
#27	M7/38 (BLK)	5839	4084	2	23	3
#33	M7/38 (BLK)	6697	4898	3	23	3
#29	M9/34 (L3)	5994	4272	2	95	7
#31	VII 26A (L1)	6248	4383	3	6	0
#6	VII 26E (BLK)	6264	4566	3	9	--
#9	VII 26E (L1)	6116	4281	3	9	--
#14	VII 26E (BLK)	6441	4409	4	9	--
#17	VII 26E (L1)	6428	4447	4	8	--
#32	VII 26K (L2)	6963	5184	3	13	1

* Average of analyses from two dilutions.

Table 3.4. (Cont.)

Table 3.4. (Cont.)

Table 3.4 (Cont.)

BOTTLE #	SAMPLE NO		CaCO3 mol.frac	MgCO3 mol.frac
#36	B15A/5/6	(L1)	.59	.41
#21	B15A/6/1	(L2)	.58	.42
#38	B15A/6/1	(L1)	.58	.42
#4	B15A/6/4	(BLK)	.56	.44
#12	B15A/6/4	(BLK)	.57	.43
#8	B15A/6/9	(L1)	.57	.43
#16	B15A/6/9	(L1)	.58	.42
#24	B4/5/4	(L2)	.59	.40
#28	B4/5/4	(BLK)	.86	.14
#34	B4/5/4	(BLK)	.49	.51
#20	B7/5/10	(L2)	.58	.42
#42	B7/5/10	(BLK)	.57	.43
#5	B7/6/3	(L2)	.57	.43
#13	B7/6/3	(L2)	.57	.43
#26	B7/6/3	(BLK)	.61	.39
#7	BLANK		0.00	0.00
#15	BLANK		0.00	0.00
#30	BLANK		0.00	0.00
#39	BLANK		0.00	0.00
#22	EH.HTS/1	Forams,unlchd	.99	.01
#19	GFS-400	(BLK)	.50	.50
#23	GFS-400	(BLK STD)	.50	.50
#41	GFS-400	(STD)	.50	.50

* Average of analyses from two dilutions.

Reproduced with permission of the copyright owner. Further reproduction prohibited without permission.

Table 3.4. (Cont.)

Table 3.4 (Cont.)

BOTTLE #	SAMPLE NO	CaCO3 mol.frac	MgCO3 mol.frac
#43	HC280/13.0 (BLK)	.99	.01
#35	HC280/4.0 (BLK)	.99	.01
#25	HC280/4.85 (BLK)	.59	.41
#45	HTS.EH/1 forams,cld,lch	.99	.01
#18	LPG-1 (BLK)	.99	.01
#11	M1/13 (BLK)	.98	.01
#10	M1/13 (SND)	.99	.01
#2	M1/13/115 (SND)	.99	.01
#3	M1/13/115 (BLK)	.97	.02
#40	M1/16 (BLK)	.96	.03
#44	M2/24.4 (BLK)	.93	.01
#37	M5/25 (L2)	.60	.40
#27	M7/38 (BLK)	.59	.41
#33	M7/38 (BLK)	.58	.42
#29	M9/34 (L3)	.58	.41
#31	VII 26A (L1)	.59	.41
#6	VII 26E (BLK)	.58	.42
#9	VII 26E (L1)	.59	.41
#14	VII 26E (BLK)	.59	.41
#17	VII 26E (L1)	.59	.41
#32	VII 26K (L2)	.57	.43

* Average of analyses from two dilutions.

Reproduced with permission of the copyright owner. Further reproduction prohibited without permission.

Table 3.5. Strontium isotopic data for St. Croix dolomites and groundwaters.

Sample Identification	Sample Type	87Sr/86Sr	Std.Dev.
PE-3A	Groundwater	0.7085	0.0001
WD-94	Groundwater	0.7075	0.0001
RU-149	Groundwater	0.7082	0.0001
MW-4	Groundwater	0.7067	0.0001
B15a/6/9a	Dolomite	0.70889	0.00002
B15a/6/4	Dolomite	0.70884	0.00001
B7/6/3	Dolomite	0.70888	0.00002

Reproduced with permission of the copyright owner. Further reproduction prohibited without permission.

Table 3.6. Strontium isotopic mixing relations between seawater and St. Croix groundwaters.

COMPONENT A			COMPONENT B			Mixture of Components		
87/86	[Sr]	Fraction	87/86	[Sr]	Fraction	[Sr]	1/[Sr]	87/86
Modern SW			Sample WD-94					
.70910	8.00	0.00	.70750	.28	1.00	.28	3.571	.70750
.70910	8.00	.20	.70750	.28	.80	1.82	.548	.70890
.70910	8.00	.40	.70750	.28	.60	3.37	.297	.70902
.70910	8.00	.60	.70750	.28	.40	4.91	.204	.70906
.70910	8.00	.80	.70750	.28	.20	6.46	.155	.70909
.70910	8.00	1.00	.70750	.28	0.00	8.00	.125	.70910
Mod SW			RU-149					
.70910	8.00	0.00	.70820	.01	1.00	.01	100.000	.70820
.70910	8.00	.20	.70820	.01	.80	1.61	.622	.70910
.70910	8.00	.40	.70820	.01	.60	3.21	.312	.70910
.70910	8.00	.60	.70820	.01	.40	4.80	.208	.70910
.70910	8.00	.80	.70820	.01	.20	6.40	.156	.70910
.70910	8.00	1.00	.70820	.01	0.00	8.00	.125	.70910
Mod SW			MW-4					
.70910	8.00	0.00	.70670	.65	1.00	.65	1.538	.70670
.70910	8.00	.20	.70670	.65	.80	2.12	.472	.70851
.70910	8.00	.40	.70670	.65	.60	3.59	.279	.70884
.70910	8.00	.60	.70670	.65	.40	5.06	.198	.70898
.70910	8.00	.80	.70670	.65	.20	6.53	.153	.70905
.70910	8.00	1.00	.70670	.65	0.00	8.00	.125	.70910
Mod SW			PE-3A					
.70910	8.00	0.00	.70850	.50	1.00	.50	2.000	.70850
.70910	8.00	.20	.70850	.50	.80	2.00	.500	.70898
.70910	8.00	.40	.70850	.50	.60	3.50	.286	.70905
.70910	8.00	.60	.70850	.50	.40	5.00	.200	.70908
.70910	8.00	.80	.70850	.50	.20	6.50	.154	.70909
.70910	8.00	1.00	.70850	.50	0.00	8.00	.125	.70910
Mid Pliocene Seawater			Sample WD-94					
.70897	8.00	0.00	.70750	.28	1.00	.28	3.571	.70750
.70897	8.00	.20	.70750	.28	.80	1.82	.548	.70879
.70897	8.00	.40	.70750	.28	.60	3.37	.297	.70890
.70897	8.00	.60	.70750	.28	.40	4.91	.204	.70894
.70897	8.00	.80	.70750	.28	.20	6.46	.155	.70896
.70897	8.00	1.00	.70750	.28	0.00	8.00	.125	.70897
Mid Plio			RU-149					
.70897	8.00	0.00	.70820	.01	1.00	.01	100.000	.70820
.70897	8.00	.20	.70820	.01	.80	1.61	.622	.70897
.70897	8.00	.40	.70820	.01	.60	3.21	.312	.70897
.70897	8.00	.60	.70820	.01	.40	4.80	.208	.70897
.70897	8.00	.80	.70820	.01	.20	6.40	.156	.70897
.70897	8.00	1.00	.70820	.01	0.00	8.00	.125	.70897
Mid Plio SW			PE-3A					
.70897	8.00	0.00	.70850	.50	1.00	.50	2.000	.70850
.70897	8.00	.20	.70850	.50	.80	2.00	.500	.70888
.70897	8.00	.40	.70850	.50	.60	3.50	.286	.70893
.70897	8.00	.60	.70850	.50	.40	5.00	.200	.70895
.70897	8.00	.80	.70850	.50	.20	6.50	.154	.70896
.70897	8.00	1.00	.70850	.50	0.00	8.00	.125	.70897
Mid Plio SW			MW-4					
.70897	8.00	0.00	.70670	.65	1.00	.65	1.538	.70670
.70897	8.00	.20	.70670	.65	.80	2.12	.472	.70841
.70897	8.00	.40	.70670	.65	.60	3.59	.279	.70872
.70897	8.00	.60	.70670	.65	.40	5.06	.198	.70885
.70897	8.00	.80	.70670	.65	.20	6.53	.153	.70892
.70897	8.00	1.00	.70670	.65	0.00	8.00	.125	.70897

Reproduced with permission of the copyright owner. Further reproduction prohibited without permission.

Reproduced with permission of the copyright owner. Further reproduction prohibited without permission.

Table 3.7. Chemical analyses of Virgin Island Salt Pond waters.

		Ca		Mg	
Sample	Location/Description	ppm	mmol/kg	ppm	mmol/kg
84/01	St. John Salt Pond	663.5	16.6	3580.3	147.3
84/02	St. John Salt Pond	704.7	17.6	3605.4	148.3
84/3	Boiler Bay, pond	395.7	9.9	1235.1	50.8
84/4	Small salt pond, S. side E. end	740.5	18.5	491.9	20.3
84/5	Great Pond	577.5	14.4	1759.0	72.4
84/6	SE corner, Westend Salt Pond	1054.8	26.3	3835.1	157.8
84/7	Greenish Pond, SE of WESP	462.7	11.5	1482.4	61.0
84/8	Small pond SE of WESP	1117.9	27.9	3794.7	156.1
84/9	Westend Salt Pond (W. central)	752.3	18.8	2578.5	106.1
84/10	Westend Salt Pond (north end)	822.0	20.5	2643.7	108.8
MW-4	Groundwater, Mt. Washington	174.7	4.4	32.9	1.4

Table 3.7. (Cont.)

Sample	Na		Sr		Fe		Mn	
	ppm	mmol/kg	ppm	mmol/kg	ppm	mmol/kg	ppm	mmol/kg
84/01	29919	1301	16.75	.19	.02	.000	0.00	0.000
84/02	30561	1329	16.88	.19	.03	.000	0.00	0.000
84/3	9462	412	7.27	.08	.97	.017	.53	.010
84/4	4265	186	11.47	.13	3.66	.066	.13	.002
84/5	16264	707	10.76	.12	1.14	.020	.03	.001
84/6	32458	1412	19.67	.22	.23	.004	.05	.001
84/7	13234	576	9.63	.11	.17	.003	.03	.001
84/8	34656	1508	23.65	.27	.10	.002	.03	.001
84/9	23893	1039	14.35	.16	.08	.001	.03	.001
84/10	24829	1080	14.48	.17	.11	.002	.02	.000
MW-4	79	3	.65	.01	0.00	0.000	.00	.000

Reproduced with permission of the copyright owner. Further reproduction prohibited without permission.

Table 3.7. (Cont.)

Sample	Si		S (total), as SO4		Cl		TDS	
	ppm	mmol/kg	ppm	mmol/kg	mEq/L	ppm	o/oo	(refract) o/oo
84/01	0.0	0.0	6557.4	68.3	1664	58989	106.0	104
84/02	0.0	0.0	6631.1	69.0	1660	58837	106.5	105
84/3	4.6	.2	2865.1	29.8	533	18884	36.6	36
84/4	7.8	.3	2262.7	23.6	199	7066	17.7	16
84/5	3.9	.1	4585.2	47.7	875	31029	57.8	57
84/6	6.1	.2	8938.1	93.0	1724	61120	113.7	131
84/7	1.0	0.0	3435.6	35.8	717	25421	48.0	50
84/8	.5	.0	8938.5	93.1	1873	66403	122.6	125
84/9	4.3	.2	6522.1	67.9	1257	44571	84.0	92
84/10	4.5	.2	6695.3	69.7	1315	46622	87.1	96
MW-4	14.6	.5	53.4	.6	4	126	NA	NA

Reproduced with permission of the copyright owner. Further reproduction prohibited without permission.

REFERENCES

Reproduced with permission of the copyright owner. Further reproduction prohibited without permission.

Chapter 1

Andreieff, P.A., Bouysse, P., et Westercamp, D., 1987. Geologie de l'arc insulaire des Petites Antilles, et évolution géodynamique de l'est-Caraibe. Thèse de Doctorat d'État Ès Sciences, Universitée de Bordeaux I, 465 p.

----------, Mascle, A., Mathieu, Y., and Müller, C., 1986. Les carbonates Néogènes de Sainte Croix (Iles Vierges): Étude stratigraphique et pétrophysique. Revue de l'Institit Français du Pétrole, v. 41, no. 3, p.335-350.

Bandy, O.L., and Arnal, R.E., 1957. Distribution of Recent foraminifera off the west coast of Central America: American Association of Petroleum Geologists Bulletin, v. 41, no. 9, p. 2037-2053.

Bandy, O. L., and Rodolfo, K. S., 1964. Distribution of foraminifera and sediments, Peru-Chile trench area: Deep Sea Research, v.11, p. 817-837.

Banner, F. T. and Blow, W.H., 1965, Progress in the planktonic foraminiferal biostratigraphy of the Neogene: Nature, v. 208, no. 5016, p. 1164-1166.

Bé, A.W.H., 1977. An ecological, zoogeographic and taxonomic review of recent planktonic foraminifera in Ramsey, A.T.S., ed., Oceanic Micropaleontology, Volume 1. Academic Press, London, p. 1-88.

Behrens, G.K., 1976. Stratigraphy, sedimentology, and paleoecology of a Pliocene reef tract: St. Croix, U.S. Virgin Islands. Unpubl. MS thesis, Northern Illinois University, 93 p..

Berggren, W.A. and Haq, B.L, 1976. The Andalusian Stage (Late Miocene): Biostratigraphy, biochronology, and paleoecology: Paleogeography, Paleoclimatology, Paleoecology, v. 20, p. 67-129.

Berggren, W.A., Benson, R.H., Haq, B.U., Riedel, W.R., Sanfilippo, A., Schrader, H.-J., and Tjalsma, R.C., 1976. The El Cuervo section (Andalusia, Spain): Micropaleontologic anatomy of an early Late Miocene lower bathyal deposit: Marine Micropaleontology, v. 1, p. 195-247.

Blow, W.A., 1969. Late Middle Eocene to Recent planktonic foraminiferal biostratigraphy. Proceedings First International Conference on Planktonic Microfossils Geneva, 1967. 1, p. 199-142.

----------, 1979. The Cainozoic Globigerinida. E.J. Brill, Leiden (3 vols.), 1413 pp.

Bold, W.A. van den, 1970. Ostracoda of the lower and middle Miocene of St. Croix, St. Martin, and Anguilla: Caribbean Journal of Science, v. 10, p.35-61.

----------, 1972. Ostrácodos del Post-Eoceno de Venezuela y regiones vecinas. Congr. Geol. Venezolano, v. 2 (Mem. IV, Spec. Publ. No. 5), p. 999-1063.

Reproduced with permission of the copyright owner. Further reproduction prohibited without permission.

Bolli, H.M. and Saunders, J.B., 1985. Oligocene to Holocene low latitude planktic foraminifera in Bolli, H.M., Saunders, J.B., and Perch-Nielsen, K., eds., Plankton Stratigraphy. Cambridge University Press, p. 155-262.

Boltovskoy, E., and Wright, R., 1976. Recent foraminifera. Dr. W. Junk, The Hague, 515p.

Cederstrom, D.J., 1950. Geology and groundwater resources of St. Croix, Virgin Islands: U.S. Geological Survey, Water Supply Paper 1067, p. 1-117.

Cushman, J.A., 1946. Tertiary foraminifera from St. Croix, Virgin Islands: U.S. Geological Survey, Professional Paper 210-A, p.1-17.

Gerhard, L.C., Frost, S.H., and Curth, P.J., 1978. Stratigraphy and depositional setting, Kingshill Limestone, Miocene, St. Croix, U.S. Virgin Islands. American Association of Petroleum Geologists Bulletin, v. 62, no. 3, p. 413-418.

Gill, I.P., and Hubbard, D.K., 1986. Subsurface geology of the St. Croix subsurface rock system. College of the Virgin Islands, St. Thomas, Water Resources Research Center, Technical Report 26, 86 p.

----------, 1987.Subsurface geology of the St. Croix subsurface rock system. Phase II. University of the Virgin Islands, St. Thomas, Water Resources Research Center, Technical Report 28, 66 p.

Hasegawa, S., 1984. Notes on the taxonomy and paleoecology of Melonis pompilioides and its allied taxa from Japan in Oetrli, H.J., ed., Benthos '83, Second International Symposium on Benthic Foraminifera, Pau, 1983: Elf-Aquitaine, Esso REP, and Total CFP, Pau and Bordeaux, p. 299-304.

Jordan, D.G., 1975. A survey of the water resources of St. Croix, Virgin Islands. U.S. Geol. Survey Open File Report, Caribbean Dist., San Juan, 51 p..

Keller, G., 1985. Depth statification of planktonic foraminifers in the Miocene ocean. in Kennett, J.P., ed., The Miocene Ocean: Paleoceanography and biogeography. Geological Society of America Memoir 163, p. 177-193.

Kemp, J.F., 1926. Introduction and review of the literature on the geology of the Virgin Islands: New York Academy of Science, Scientific Survey of Porto Rico and the Virgin Islands, v. 4, pt. 1, p. 3-69.

Kennett, J.P. and Srinivasan, M.S., 1983. Neogene Planktonic Foraminifera. A phylogenetic atlas. Hutchinson Ross, Stroudsburg PA, 265 p.

Lidz, B.H., 1982. Biostratigraphy and paleoenvironment of Miocene-Pliocene hemipelagic limestone: Kingshill Seaway, St. Croix, U.S. Virgin Islands. Journal of Foraminiferal Research, v. 12, no. 3, p. 205-233.

----------, 1988. Upper Cretaceous (Campanian) and Cenozoic stratigraphic sequence, northeast Caribbean (St. Croix, U.S. Virgin Islands). Geological Society of America Bulletin, v.100, p.282-298.

Reproduced with permission of the copyright owner. Further reproduction prohibited without permission.

McLaughlin, P.P., 1989. Neogene planktonic foraminiferal biostratigraphy of the Azua Basin, southwestern Dominican Republic. Journal of Foraminiferal Research (in press).

Morkhoven, F.P.C.M. van, Berggren,W.A., Edwards, E., and collaborators, 1986. Cenozoic Cosmopolitan Deep-water Benthic Foraminifera: Pau, Bulletins de Centres de Recherche Exploration-Production Elf-Aquitaine, Mem. 11, 421 p.

Multer, H.G., Frost, S.H., and Gerhard, L.C., 1977. Miocene "Kingshill Seaway" - a dynamic carbonate basin and shelf model, St. Croix, U.S. Virgin Islands in Frost, S.H., Weiss, M.P., and Saunders, J.B., eds., Reefs and related carbonates - Ecology and sedimentology: American Association of Petroleum Geologists Studies in Geology No. 4, p.329-352.

Natland, 1933. The temperature and depth distribution of some recent and fossil foraminifera in the southern California region: Scripps Institute of Oceanography, Bulletin, Technical Series, v. 3, no. 10, p. 225-230.

Parker, F.L., 1954. Distribution of the foraminifera in the northwestern Gulf of Mexico: Bulletin of the Museum of Comparative Zoology, v. 110, no. 10, p. 453-588.

Pflum, C.E., and Frerichs, W.E., 1976. Gulf of Mexico deep-water foraminifers: Cushman Foundation for Foraminiferal Research, Special Publication 14, p. 7-125.

Phleger, F.B., 1951. Ecology of foraminifera, northwest Gulf of Mexico; Part 1 - Foraminifera distribution: Geological Society of America, Memoir 46, v.1, p. 1-88.

Phleger, F.B., Parker, F.L., and Peirson, J.F., 1953. North Atlantic foraminifera: Reports of the Swedish Deep-Sea Expedition, 1947-1948, v. 7, no.1, p. 3-122.

Phleger, F.B., and Soutar, A., 1973. Production of benthic foraminifera in three east Pacific oxygen minima: Micropaleontology, v.19, p.110-115.

Savin, S. M., Douglas, R. G. and Stehli, F. G., 1975, Tertiary marine paleotemperatures: Geol. Soc. Amer. Bull., v. 86, p. 1499-1510.

Schnitker, D., 1980, Quaternary deep-sea benthic foraminifera and bottom water masses: Ann. Rev., Earth and Planetary Sci., v. 8, p. 343-370.

Sen Gupta, B.K., Lee, R.F., and May, M.S., 1981. Upwelling and an unusual assemblage of benthic foraminifera on the northern Florida continental slope. Journal of Paleontology, v. 55: 853-857.

Shurbet, G.L., Wurzel, J.L., and Ewing, M., 1956. Gravity measurements in the Virgin Islands. Geol. Soc. Amer. Bull., v 67, p. 1529-1536.

Smith, 1964. Ecology of benthonic species in Recent foraminifera off Central America: U.S. Geological Survey Professional Paper 429-B, p. 1-27.

Reproduced with permission of the copyright owner. Further reproduction prohibited without permission.

Speed, R.C., Gerhard, L.C., and McKee, E.H., 1979. Ages of deposition, deformation, and intrusion of Cretaceous rocks, eastern St. Croix, Virgin Islands. Geol. Soc. Amer. Bull., v. 90, p. 629-632.

Stainforth, R.M., Lamb, J.L., Luterbacher, H., Beard, J.H., and Jeffords, R.M., 1975. Cenozoic planktonic foraminiferal zonation and characteristic index forms. Univ. Kansas Paleontol. Contrib., Article 62, 162 p.

Steineck, P., 1981. Upper Eocene to Middle Miocene ostracode faunas and paleo-oceanography of the north Coastal Belt, Jamaica, West Indies. Mar. Micropaleont., v. 6, p. 339-366.

Todd, R., and Low, D., 1976. Smaller foraminifera from deep wells on Puerto Rico and St. Croix: U.S. Geological Survey Professional Paper 863, p. 1-57.

Vaughan, T.W., 1923. Stratigraphy of the Virgin Islands of the United States and of Culebra and Vieques islands, and notes on eastern Porto Rico: Washington Academy of Sciences Journal, v.13, p.303-317.

Whetten, J. T., 1966. The geology of St. Croix, U.S. Virgin Islands. GSA Mem. 98, p.177-239.

Chapter 2

Andreieff, P., Mascle, A., Mathieu, Y. and Muller, C., 1986, Les carbonates neogenes de Sainte Croix (Iles Vierges) etude stratigraphique et petrophysique: Revue de L'Institut Francais du Petrole, v. 41, no. 3, p. 336-350.

Behrens, G. K., 1976, Stratigraphy, sedimentology and paleoecology of a Pliocene reef tract: St. Croix, U.S. Virgin Islands: unpubl. Masters thesis, Northern Illinois University, 93pp.

Blow, W. A., 1979. The Cainozoic Globigerinida. E.J. Brill, Leiden (3 vols.), 1413 p.

Bold, van den, W. A., 1970, Ostracoda of the Lower and Middle Miocene of St. Croix, p. 35-61.

Bolli, H.M. and Saunders, J. B., 1985. Oligocene to Holocene low latitude planktic foraminifera IN Bolli, H.M., Saunders, J.B., and Perch-Nielsen, K., eds., Plankton Stratigraphy. Cambridge University Press: p. 155-262.

Burke, K., Cooper, C., Dewey, J. F., Mann, P., and Pindell, J. L., 1984, Caribbean Tectonics and relative plate motions, *in* Bonini, W. E, Hargraves, R. B. and Shagam, R. (eds), Geological Society of America Memoir 162, Boulder, CO, p. 31-63.

Case J. E., Holcombe, T. L., Martin, R. G., 1984, Map of geologic provinces in the Caribbean region, *in* Bonini, W. E, Hargraves, R. B. and Shagam, R. (eds), Geological Society of America Memoir 162: Geol. Soc. Amer., Boulder, CO, p. 1-30.

Reproduced with permission of the copyright owner. Further reproduction prohibited without permission.

Cederstrom, D. J., 1950, Geology and groundwater resources of St. Croix, U. S. Virgin Islands: U. S. Geological Survey Water Supply Paper 1067, 117 pp.

Cushman, J. A., 1946, Tertiary foraminifera from St. Croix, Virgin Islands: U.S. Geological Survey Professional Paper 210-A, 17 pp.

Dill, R. F., 1977, Deep water erosional feature, bedrock of St. Croix, U.S. Virgin Islands, as seen from the research submersible Alvin, in Abstracts, VIII Caribbean Geological Conference, Addendum, Geologisch Institute (Amsterdam), Curacao, Dutch West Indies.

Donnelly, T. W., 1966, Geology of St. Thomas and St. John, U. S. Virgin Islands, *in* Hess, H. H., (ed.), Caribbean Geological Investigations, Geological Society of America Memoir 98: Geol. Soc. Amer., New York, NY, p. 85-176.

EEZ Scan Scientific Staff, 1987, Atlas of the U. S. Exclusive Econonic Zone, Gulf of Mexico and Eastern Caribbean Areas: U. S. Geological Survey Misc. Inves. Series I-1864-A, B, Washington, D. C., 171 pp.

Frankel , A., McCann, W. R. and Murphy, A. J., 1980, Observations from a seismic network in the Virgin Islands Region: tectonic structures and earthquake swarms: J. Geophys. Res., v. 85, no. B5, p. 2669-2678.

Frost, S. H. and Bakos, N. A., 1977, Miocene pelagic biogenic sediment production and diagenesis, St. Croix, U. S. Virgin Islands: Palaeogeography, Palaeoclimatology, Palaeoecology, v. 22, p. 137-171.

Gerhard, L. C., Frost, S. H., and Curth, P. J., 1978, Stratigraphy and depositional setting, Kingshill Limestone, Miocene, St. Croix, U. S. Virgin Islands: Amer. Assoc. Petrol. Geol. Bull., v. 62, no. 3, p. 403-418.

Gill, I. P., 1983, The sedimentological controls on organic carbon in the Virgin Islands Trough, U. S. Virgin Islands: unpubl. MS thesis, Univ. of Rochester, 70 pp.

Gill, I. P. and Hubbard, D. K., 1985, Subsurface sedimentology of the Miocene-Pliocene Kingshill Limestone, St. Croix, U.S.V.I., in P. D. Crevello and P. M. Harris, eds., Deep Water Carbonates: Buildups, Turbidites, Debris Flows and Chalks, Tulsa, OK: Soc. Econ. Paleon. Mineral. Core Workshop No. 6, p. 431-460.

----------, 1986, Subsurface geology of the St. Croix carbonate rock system: Caribbean Research Institute Technical Report 26, College of the Virgin Islands, 86 pp.

----------, 1987, Subsurface geology of the St. Croix carbonate rock system, phase II: Technical Report No. 28, Water Resources Research Center, College of the Virgin Islands, St. Thomas, U. S. Virgin Islands, 79 pp.

Golumbek, M., 1987, GPS measurements in the Caribbean: Eos, v. 68, no. 46, p. 1593.

Reproduced with permission of the copyright owner. Further reproduction prohibited without permission.

Hasegawa, S., 1984. Notes on the taxonomy and paleoecology of Melonis pompilioides and its allied taxa from Japan in Oetrli, H.J., ed., Benthos '83, Second International Symposium on Benthic Foraminifera, Pau, 1983: Elf-Aquitaine, Esso REP, and Total CFP, Pau and Bordeaux, p. 299-304.

Hess, H. H, 1933, Interpretation of geological and geophysical observations: U. S.Hydrological Office Navy-Priceton gravity expedition to the West Indies in 1932, p. 27-54.

Hess, H. H., 1966, Caribbean research project, 1965, and bathymetric chart, *in* Hess, H. H.(ed.), Caribbean Geological Investigations: Geological Society of America Memoir 98, New York, NY, p. 1-10.

Holcombe, T.L., 1977, Geomorphology and subsurface geology west of St. Croix, U. S. Virgin Islands: Amer. Assoc. of Petrol. Geol. Memoir 29, p. 353-362.

Houlgatte, E., 1983, Etude d'une partie de la frontiere nord-est de la plaque Caraibe: unpubl. Masters thesis, L'Universite de Bretagne Occidentale, 69 pp.

Hubbard, D. K., Suchanek, T. H., Gill, I. P., Cowper, S., Ogden, J. C., Westerfield, J. R. and Bayes, J., 1981, Preliminary studies of the fate of shallow-water detritus in the basin north of St. Croix, USVI: Proceedings of the Fourth International Coral Reef Symposium, v. 1, Manila, Phillipines, P. 383-387.

Jany, I., Mauffret, A., Bouysse, P., Mascle, A., Mercier de Lepiany, B., Renard, V., andStephan, F., 1987, Releve bathymetrique Seabeam et tectonique en decrochements au sud des Iles Vierges (Nord-Est Caraibes): C. R. Acad. Sc. Paris, t. 304, Serie II, no. 10, p. 527-532.

Jany, I., Scanlon, K. M. and Mauffret, A., in prep., Geological interpretation of combined Seabeam, GLORIA and seismic data from Anegada Passage (Virgin Islands, North Caribbean).

Kemp, J. F., 1926, Introduction and review of the literature on the Geology of the Virgin Islands: New York Acad. Sci., Scientific Survey of Porto Rico and the Virgin Islands, v. 4, pt. 1, p. 3-69; in Cederstrom, D. J., 1950, Ground water resources of the U. S. Virgin Islands: U.S. Geological Survey Water Supply Paper 1067, 117 pp.

Khudoley, K. M. and Meyerhoff, A. A. (1971, Paleogeography and geological history of Greater Antilles, Geological Society of America Memoir 129: Geol. Soc. America, Boulder, CO, 199 pp.

Lidz, B. H., 1982, Biostratigraphy and paleoenvironment of Miocene-Pliocene hemipelagic limestone, Kingshill Seaway, St. Croix, U. S. Virgin Islands: J. Foram. Res., v. 12, p. 205-233.

----------, 1984, Neogene sea-level change and emergence, St. Croix, Virgin Islands: evidence from basinal carbonate accumulations: Geol. Soc. Amer. Bull., v. 95, p. 1268-1279.

----------, 1988, Upper Cretaceous (Campanian) and Cenozoic stratigraphic sequence, northeast Caribbean (St. Croix, U.S. Virgin Islands): v. 100, p. 282-298.

Reproduced with permission of the copyright owner. Further reproduction prohibited without permission.

Lithgow, C., McCann , W. R. and Joyce, J., 1987, Extensional tectonics at the eastern edge of the Puerto Rico Platelet (abs.): Eos, v.68, no. 44, p. 1483.

Mauffret, A., Jany, I., Mercier de Lepinay, B., Bouysse, P., Mascle, A., Renard, V. and Stephan, J.-F., 1986, Releve au sondeur multifaisceaux du bassin des iles Vierges (extremite orientale des Grandes Antilles): role de l'extension et des decrochements: C.R. Acad. Sc. Paris, t. 303, Serie II, no. 10, p.923-928.

Mann, P., Hempton, M. R., Bradley, D. C. and Burke, K., 1983, Development of pull-apart basins: Jour. Geology, v.91, p. 529-554.

Moore, C. H. Jr., Graham, E. A. and Land, L. S., 1976, Sediment transport and dispersal across the deep fore-reef and island slope (-55 to -305 m), Discovery Bay, Jamaica: Jour. Sed. Pet., v. 46, p. 174-187.

Multer, H. G., Frost, S. H. and Gerhard, L. C., 1977, Miocene "Kingshill Seaway" - a dynamic carbonate basin and shelf model, St. Croix, U. S. Virgin Islands: in Frost, S. H., Weiss, M. P. and Saunders, J. B. (eds.), Reefs and Related Carbonates--Ecology and Sedimentology: Amer. Assoc. Petrol. Geol. Studies in Geology No. 4, p. 329-352.

Reid, H. and Tabor, S., 1920, The Virgin Islands earthquakes of 1867-1868, Bull. Seismol. Soc. Amer., v. 10, p. 9-30.

Robison, T. M., 1972, Ground water in central St. Croix, U. S. Virgin Islands: U. S. Geol. Survey Open-File Report, Caribbean District, 18 pp.

Scanlon, K. M. and Masson, D., 1988, Seafloor deformation at the northern Caribbean Plate boundary and rotation of a Puerto Rico microplate (abs): EOS, v.69, no. 16, p.462.

Shurbet, G. L., Worzel, J. L. and Ewing, M., 1956, Gravity measurements in the Virgin Islands: Geol. Soc. Amer. Bull., v. 67, p. 1529-1536.

Stephan, J. F., Blanchet, R. and Mercier de Lepinay, B. ,1986, Northern and southern Caribbean festoons (Panama, Colombia-Venezuela and Hispaniola-Puerto Rico), interpreted as pseudo subductions induced by the east-west shortening of the peri-Caribbean continental frame, *in* Wezel, F.-C.(ed.), The Origin of Arcs: elsevier, Inc., New York, NY, p. 401-422.

Todd, R., and Low, D., 1976, Smaller foraminifera from deep wells on Puerto Rico and St. Croix: Geological Survey Professional Paper 863, 58 pp.

Wilcox, R. E., Harding, T. P. and Seely, D. R., 1973, Basic wrench tectonics: Amer. Assoc. Petrol. Geol. Bull., v. 57, no. 1, p. 96.

Whetten, J. T., 1966, The geology of St. Croix, U. S. Virgin Islands: Geol. Soc. of Amer. Memoir 98, p. 177-239.

----------, 1974, Field guide to the geology of St. Croix in Guidebook to the Geology and Ecology of some Marine and Terrestrial Environments, St. Croix, U. S. Virgin Islands: West Indies Laboratory Special Publication No. 5, p. 129-143.

Reproduced with permission of the copyright owner. Further reproduction prohibited without permission.

Chapter 3

Andreieff, P., 1983, Extension stratigraphique des grands Foraminiferes neogenes del la region caraibe: Paraspiroclypeus chawneri (Palmer) et Operculinoides cojimarensis (Palmer): Bull. Soc. Geol., France, v. 7, no. 6, p. 885-888.

Andreieff, P., Mascle, A., Mathieu, Y. and Muller, C., 1986, Les carbonates neogenes de Sainte Croix (Iles Vierges) etude stratigraphique et petrophysique: Revue de L'Institut Francais du Petrole, v. 41, no. 3, p. 336-350.

Aharon, P., 1988, A stable-isotope study of magnesites from the Rum Jungle Uranium Field, Australia: implications for the origin of strata-bound massive magnesites. Chem. Geol., v. 69, p. 127-145.

Aharon, P., Socki, R. A., and Chan, L. H., 1987, Dolomitization of atolls by sea water convection flow: test of a hypothesis at Niue, South Pacific: Journal of Geology, v. 95, p. 187-203

Anderson, T. F. and Arthur, M. A., 1983, Stable isotopes of oxygen and carbon and their application to sedimentologic and paleoenvironmental problems, *in* Stable Isotopes in Sedimentary Geology, SEPM Short Course Notes No. 10, p. 1-1 -- 1-151.

American Public Health Association, 1971, Standard Methods for the Examination of Water and Wastewater, 13th ed. Washington, D.C., 874 pp.

Back, W., 1966, Hydrochemical facies and ground-water flow patterns in the northern part of Atlantic Coastal Plain: U. S. Geol. Survey Prof. Paper 498-A, 42pp.

Badiozamani, K., 1973. The Dorag dolomitization model -- Application to the Middle Ordovician of Wisconsin: Journal of Sedimentary Petrology, v. 43, p. 965-984.

Baker, P. A., Gieskes, J. M. and Elderfield, H., 1982, Diagenesis of carbonates in deep-sea sediments -- evidence from Sr/Ca ratios and interstitial dissolved Sr^{2+} data: Journal of Sedimentary Petrology: v. 52, no. 1, p. 71-82.

Behrens, E. W. and Land, L. S., 1972, Subtidal Holocene dolomite, Baffin Bay, Texas: Journal of Sedimentary Petrology, v. 42, p. 155-161.

Burke, W. H., Denison, R. E., Hetherington, E. A., Koepnick, R. B., Nelson, H. F. and Otto, J. B., 1982, Variation of seawater $^{87}Sr/^{86}Sr$ throughout Phanerozoic time: Geology, v. 10, p.516-519.

Butler, G. P., 1969, Modern evaporite deposition and geochemistry of coexisting brines, the sabkha, Trucial Coast, Arabian Gulf: Jour. Sed. Petrology, v. 39, p. 70-89.

Butler, G. P., 1973, Strontium geochemistry of modern and ancient calcium sulphate minerals: in Purser, B. H. (ed.), The Persian Gulf, Springer-Verlag, p. 423-452.

Cederstrom, D. J., 1950, Geology and groundwater resources of St. Croix, U. S. Virgin Islands: U. S. Geological Survey Water Supply Paper 1067, 117 pp.

Reproduced with permission of the copyright owner. Further reproduction prohibited without permission.

Claasen, H. C., 1982, Guidelines and techniques to obtain valid groundwater quality samples: U. S. Geological Survey Open File Report 82-1024, 54 pp.

Deffeyes, K. S., Lucia, F. J. and Weyl, P. K., 1965, Dolomitization of recent and Plio-Pleistocene sediments by marine evaporite waters on Bonaire, Netherlands Antilles, in Pray, L. C. and Murray, R. C., eds., Dolomitization and Limestone Diagenesis, A Symposium: SEPM Spec. Publ. No. 13, Soc. Econ. Paleon. and Mineral., Tulsa, p. 71-88.

Delaney, M. L. and Kastner, M., 1984, Aragonite to calcite transformation: the use of oxygen isotope fractionation to investigate the Sr distribution coefficient: EOS, v. 65, no. 45, p. 948.

DePaolo, D. J., 1986, Detailed record of the Neogene Sr isotopic evolution of seawter from DSDP Site 590B: Geology, v. 14, p. 103-106.

Drever, J. I., 1982, The Geochemistry of Natural Waters. Englewood Cliffs, N.J.: Prentice Hall, Inc., 388 pp.

Emiliani, C., 1966, Palaeotemperature analysis of Caribbean cores P 6304-8 and P 6304-9 and a generalized temperature curve for the last 425,000 years: Jour. of Geology, v. 74, p. 109-126.

Faure, G., 1977, Isotope Geology: John Wiley and Sons, Inc., New York, 464 pp.

Folk, R. L. and Land, L. S., 1975, Mg/Ca ratio and salinity: two controls over crystallization of dolomite: Amer. Assoc. Petrol. Geol. Bull., v. 59, p. 60-68.

Freeze, R. A. and Cherry, J. A., 1979, Groundwater. Englewood Cliffs, New Jersey: Prentice Hall, Inc., 604 pp.

Friedman, L. C. and Erdmann, D. E., 1982, Quality Assurance Practices for the Chemical and Biological Analyses of Water and Fluvial Sediments, Techniques of Water Resources Investigations, Bk. 5, Ch. A6. Washington, D. C.: U. S. Geological Survey, 181 pp.

Fritz, P. and Smith, D. C. W., 1970, The isotopic composition of secondary dolomites: Geochim. Cosmochim. Acta., v. 34, p. 1161-1173.

Garrels, R. M. and Christ, C. L., 1965, Solutions, Minerals and Equilibria: Freeman, Cooper and Co., 450 pp.

Geraghty and Miller, Inc, 1983, Report on current groundwater conditions in the U. S. Virgin Islands. Syosset, New York: Geraghty and Miller Inc., 89 pp.

Gerhard, L. C., Frost, S. H., and Curth, P. J., 1978, Stratigraphy and depositional setting, Kingshill Limestone, Miocene, St. Croix, U. S. Virgin Islands: Amer. Assoc. Petrol. Geol. Bull., v. 62, no. 3, p. 403-418.

Gieskes, J. M. and Rogers, W. C., 1973, Alkalinity determination in interstitial waters of marine sediments: Jour. of Sed. Petrol., v. 43, no. 1, p. 272-277.

Reproduced with permission of the copyright owner. Further reproduction prohibited without permission.

Gill, I. P. and Hubbard, D. K., 1985, Subsurface sedimentology of the Miocene-Pliocene Kingshill Limestone, St. Croix, U.S.V.I., in P. D. Crevello and P. M. Harris, eds., Deep Water Carbonates: Buildups, Turbidites, Debris Flows and Chalks, Tulsa, OK: Soc. Econ. Paleon. Mineral. Core Workshop No. 6, p. 431-460.

Gill, I. P. and Hubbard, D. K., 1986, Groundwater geochemistry of the St. Croix carbonate aquifer system: Technical Report No. 27, Water Resources Research Center, College of the Virgin Islands, St. Thomas, U. S. Virgin Islands, 59 pp.

Gill, I. P. and Hubbard, D. K., 1987, Subsurface geology of the St. Croix carbonate rock system: Technical Report No. 28, Water Resources Research Center, College of the Virgin Islands, St. Thomas, U. S. Virgin Islands, 79 pp.

Gonfiantini, R., 1986, Environmental isotopes in lake studies, in Fritz, P. and Fontes, J. Ch., eds., Handbook of Environmental Isotope Geochemistry, v. 1A, The Terrestrial Environment: Elsevier, p. 113-168.

Hardie, L. A., 1987, Dolomitization: a critical view of some current views: Journal of Sedimentary Petrology, v. 57, no. 1, p. 166-183.

Hardie, L. A. and Eugster, H. P., 1970, The evolution of closed-basin brines: Mineral. Soc. Am. Spec. Publ. No. 3, p. 273-290.

Hawkesworth, C. J., 1982. Isotope characteristics of magmas erupted along destructive plate margins, *in* R. S. Thorpe, ed., Andesites, John Wiley and Sons, p. 549-571.

Jordan, D. G., 1975, A survey of the water resources of St. Croix, Virgin Islands: U.S. Geological Survey Open-File Report, Caribbean District, San Juan, 51 pp.

Katz, A., Sass, E., Starinsky, A., and Holland, H. D., 1972, Strontium behavior in the aragonite-calcite transformation: an experimental study at 40-98°C: Geochim. Cosmochim. Acta, v.36, p. 481-496.

Kennett, J. P., 1985, Miocene to early Pliocene oxygen and carbon isotope stratigraphy in the Southwest Pacific, Deep Sea Drilling Project Leg 90: Init. repts. DSDP, v. 90, p. 1383-1411.

Knauth, L. P. and Beeunas, M. A., 1986, Isotope geochemistry of fluid inclusions in Permian halite with implications for the isotopic history of ocean water and the origin of saline formation waters: Geochim. Cosmochim. Acta, v. 50, p. 419-433.

Koepnick, R. B., Burke, W. H., Denison, R. E., Hetherington, E. A., Nelson, H. F., Otto, J. B. and Waite, L. E., 1985, Construction of the seawater $^{87}Sr/^{86}Sr$ curve for the Cenozoic and Cretaceous: supporting data: Chemical Geology (Isotope Geoscience Sect.) v. 58, p. 55-81.

Kohout, F. A., 1960, Cyclic flow of salt water in the Biscayne aquifer of southeastern Florida: J. Geophys. Res., v. 65, p. 2133-2141.

Reproduced with permission of the copyright owner. Further reproduction prohibited without permission.

Kretz, R., 1982, A model for the distribution of trace elements between calcite and dolomite: Geochem. Cosmochim. Acta, v. 46, p. 1979-1981.

Land, L. S., 1973, Contemporaneous dolomitization of Middle Pleistocene reefs by meteoric water, north Jamaica: Bull. Marine Science, v. 23, p. 64-92.

Land, L. S., 1980, The isotopic and trace element geochemistry of dolomite: the state of the art: SEPM Spec. Publ. No. 28, p.87-110.

Land, L. S., 1983a, Dolomitization: AAPG Education Course Note Series No. 24, American Association of Petroleum Geologists, Tulsa, 20 pp.

Land, L. S., 1983b, The application of stable isotopes to studies of the origin of dolomite and to problems of diagenesis of clastic sediments, in Stable Isotopes in Sedimentary Geology, SEPM Short Course No. 10, p. 4-1 -- 4-22.

Land, L. S., Salem, M. R. I., and Morrow, D. W., 1975, Paleohydrology of ancient dolomites: geochemical evidence: Am. Assoc. Petroleum Geol. Bull., v. 59, p. 1602-1625.

Langmuir, C. H., Vocke, R. D. Jr., Hanson, G. N. and Hart, S. R., 1978, A general mixing equation with applications to Icelandic basalts: Earth and Planet. Sci. Lett., v. 37, p. 380-392.

Lidz, B. H., 1982, Biostratigraphy and paleoenvironment of Miocene-Pliocene hemipelagic limestone, Kingshill Seaway, St. Croix, U. S. Virgin Islands: J. Foram. Res., v. 12, p. 205-233.

Lloyd, R. M., 1966, Oxygen isotopic enrichment of seawater by evaporation: Geochim. Cosmochim. Acta, v. 30, p. 801-814.

Lorens, R. B., 1981, Sr, Cd, Mn, and Co distribution coefficients in calcite as a function of calcite precipitation rate: Geochim. Cosmochim. Acta, v. 45, p. 553-561.

Matthews, R. K. and Poore, R. Z., 1980, Tertiary $\delta^{18}O$ record and glacio-eustatic sea-level fluctuations: Geology, v. 8, p. 501-504.

Milliman, J. D., 1974, Marine Carbonates, New York: Springer-Verlag, 375 pp.

Morgan, C. O. and Winner, M. D. Jr., 1962, Hydrochemical facies in the 400 foot and 600 foot sands of the Baton Rouge area, Louisiana: U. S. Geological Surv. Prof. Paper 450-B, p. B120-121.

Muir, M., Lock, D. and von der Borch, C., 1980, The Coorong Model for penecontemporaneous dolomite formation in the Middle Proterozoic McArthur Group, Northern Territory, Australia, *in* Zenger, D., Dunham, J. and Ethington, R., eds., Concepts and Models of Dolomitization, SEPM Spec. Publ. No. 28, SEPM, Tulsa, p. 51-68.

Reproduced with permission of the copyright owner. Further reproduction prohibited without permission.

Multer, H. G., Frost, S. H. and Gerhard, L. C., 1977, Miocene "Kingshill Seaway" - a dynamic carbonate basin and shelf model, St. Croix, U. S. Virgin Islands: in Frost, S. H., Weiss, M. P. and Saunders, J. B. (eds.), Reefs and Related Carbonates--Ecology and Sedimentology: Amer. Assoc. Petrol. Geol. Studies in Geology No. 4, p. 329-352.

Parkhurst, D. L., Thorstenson, D. C. and Plummer, L. N., 1980, PHREEQE - a computer program for geochemical calculations: U S Geological Survey Water Resources Investigations, Report WRI-80-96, 210 pp.

Peterman, Z.E., Hedge, C.E. and Tourtelot, H.A., 1970, Isotopic composition of strontium in sea water throughout Phanerozoic time: Geochim. Cosmochim. Acta, v. 34, p. 105-120.

Plummer, L. N., 1975, Mixing of seawater with calcium carbonate ground water: Geol. Soc. of Amer. Mem. 142, p. 219-236.

Robison, T. M., 1972, Ground water in central St. Croix, U. S. Virgin Islands: U. S. Geol. Survey Open-File Report, Caribbean District, 18 pp.

Ruddiman, W. F. and McIntyre, A., 1979, Warmth of the subpolar North Atlantic Ocean during northern hemisphere ice-sheet growth: Science, v. 204, p. 173-175.

Saller, A. H., 1983, Diagenesis of Cenozoic limestones on Enewetak Atoll: Unpubl. PhD Dissertation, Louisiana State University, 363 pp.

Saller, A. H., 1984, Petrologic and geochemical constraints on the origin of subsurface dolomite, Enewetak Atoll: an example of dolomitization by normal seawater: Geology, v. 12, p. 217-220.

Savin, S. M., Douglas, R. G. and Stehli, F. G., 1975, Tertiary marine paleotemperatures: Geol. Soc. Amer. Bull., v. 86, p. 1499-1510.

Savin, S. M. and Yeh, H. W., 1981, Stable isotopes in ocean sediments, *in* Emiliani, C. (ed.), The Sea, v. 7, The Oceanic Lithosphere: Wiley Interscience, p. 1521-1554.

Scholle, P. A., 1977, Chalk diagenesis and its relation to petroleum exploration: oil from chalks, a modern miracle: Amer. Assoc. Petrol. Geol. Bull., v. 61, no. 7, p. 982-1009.

Shackleton, N., 1967, Oxygen isotope analyses and Pleistocene temperatures re-assessed: Nature, v. 215, p. 15-17.

Shackleton, N. J. and Cita, M. B., 1979, Oxygen and carbon isotope stratigraphy of benthic foraminifers at Site 397: detailed history of climatic change during the late Neogene: Init. Repts. DSDP Proj., v. 47, p. 433-445.

Shackleton, N. J. and Kennett, J. P., 1975, Paleotemperature history of the Cenzoic and the initiation of Antarctic glaciation: oxygen and carbon isotope analyses in DSDP Sites 277, 279, and 281: Init. Repts. DSDP Proj., v. 29, p. 743-755.

Reproduced with permission of the copyright owner. Further reproduction prohibited without permission.

Shackleton, N. J. and Opdyke, N. D., 1973, Oxygen isotope and paleomagnetic stratigraphy of Equatorial Pacific core V28-238: oxygen isotope temperature and ice volumes on a 10^5 year and 10^6 year scale: Quaternary Research, v. 3, p. 39-55.

Shackleton, N. J. and Opdyke, N. D., 1977, Oxygen isotope and palaeomagnetic evidence for early Northern Hemisphere glaciation: Nature, v. 270, p. 216-219.

Sheppard, S. M. F. and Schwarcz, H. P., 1970, Fractionation of carbon and oxygen isotopes and magnesium between metamorphic calcite and dolomite: Contrib. Mineral. and Petrology, v. 26, p. 161-198.

Shurbet, G. L., Worzel, J. L. and Ewing, M., 1956, Gravity measurements in the Virgin Islands: Geological Society of America Bulletin, v. 67, p. 1529-1536.

Sibley, D. F., 1980, Climatic control of dolomitization, Seroe Domi Formation (Pliocene), Bonaire, N.A.: SEPM Spec. Publ. No. 28, p. 247-258.

Simms, M., 1984, Dolomitization by groundwater-flow systems in carbonate platforms: Gulf Coast Assoc. Geol. Societies Trans., v. 34, p. 411-420.

Skougstad, M. W., Fishman, M. J., Friedman, L. C., Erdmann, D. E. and Duncan, S. S., eds., 1979, Methods for Determination of Inorganic Substances in Water and Fluvial Sediments, Techniques of Water Resources Investigations, Bk. 5, Ch. A1. Washington, D. C.: U. S. Geological Survey, 626 pp.

Sofer, Z. and Gat, J. R., 1975, The isotope composition of evaporating brines: effects of the isotopic activity ratio on saline solutions: Earth Planet. Sci. Lett., v. 15, p. 179-186.

Tarutani, T., Clayton, R. N. and Mayeda, T. K., 1969, The effect of polymorphism and magnesium substitution on oxygen isotope fractionation between calcium carbonate and water: Geochim. Cosmochim. Acta, v. 33, p. 987-996.

Veizer, J., 1983, Chemical diagenesis of carbonates: theory and application of trace element technique, *in* Stable Isotopes in Sedimentary Geology, SEPM Short Course No. 10, p. 3-1 -- 3-100.

von der Borch, C. C., Lock, D. E., and Schwebel, D., 1975, Ground-water formation of dolomite in the Coorong region of South Australia: Geology, v. 3, p. 283-285.

Whetten, J. T., 1966, Geology of St. Croix, U. S. Virgin Islands: Geol. Soc. Am. Mem. 98, p. 177-239.

Wood, W. W., 1976, Guidelines for collection and field analysis of groundwater samples for selected unstable constituents: Geologic Survey Techniques of Water Resources Investigations, Report No. TWI 01-D2, 24 pp.

Reproduced with permission of the copyright owner. Further reproduction prohibited without permission.

APPENDIX

Reproduced with permission of the copyright owner. Further reproduction prohibited without permission.

Key to Well Log Abbreviations

Texture (after Folk, 1974)

s, S	=	sandy, Sand
z, Z	=	silty, Silt
g, G	=	gravelly, Gravel
m, M	=	muddy, Mud
c, C	=	clayey, Clay

e.g.: (g)sM = slightly gravelly sandy Mud

e.g.: sG = sandy Gravel

mdst	=	mudstone
wkst	=	wackestone
pkst	=	packstone
grst	=	grainstone

Reproduced with permission of the copyright owner. Further reproduction prohibited without permission.

Sample Designation

(12)	=	sample no. 12
ss	=	split spoon sample
db	=	diamond bit sample
hs	=	hollow stem auger sample
TS	=	thin section made from this sample

Color

bk	=	black
br	=	brown
bu	=	blue
gn	=	green
gy	=	grey
or	=	orange
re	=	red
tn	=	tan
wh	=	white
ye	=	yellow

lt	=	light
dk	=	dark

Reproduced with permission of the copyright owner. Further reproduction prohibited without permission.

Key to Well Log Abbreviations, (continued)

Lithology

b. foram	=	benthic foraminifera
calc	=	calcareous
cmtd	=	cemented
CO3	=	carbonate
frags	=	fragments
lith	=	lithic
LS	=	limestone
Mn	=	Manganese
p. foram	=	planktic foraminifera
rbl	=	rubble
recov	=	recovery (core recovery)
rk	=	rock
skel	=	skeletal
spl	=	sample

Reproduced with permission of the copyright owner. Further reproduction prohibited without permission.

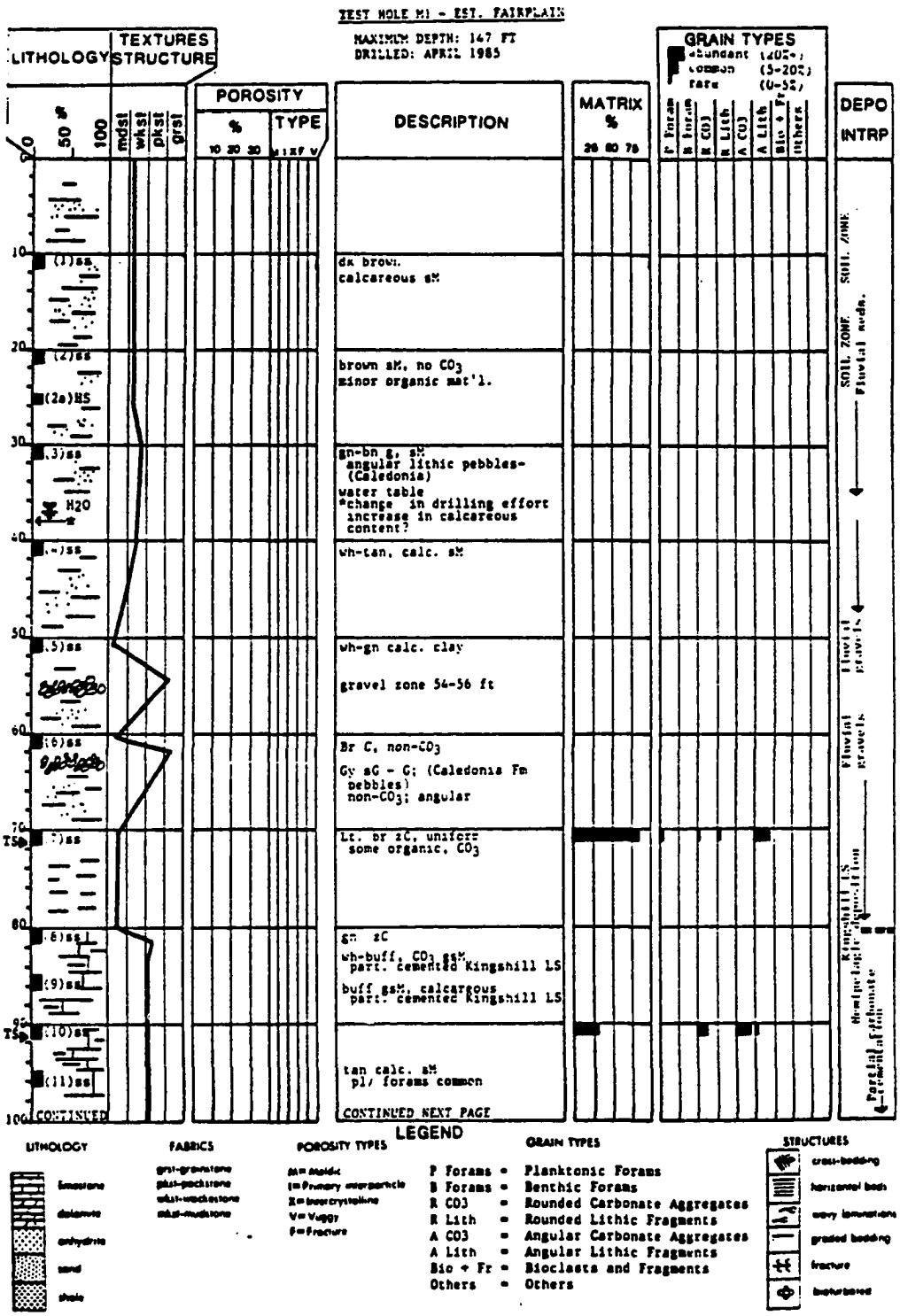

Reproduced with permission of the copyright owner. Further reproduction prohibited without permission.

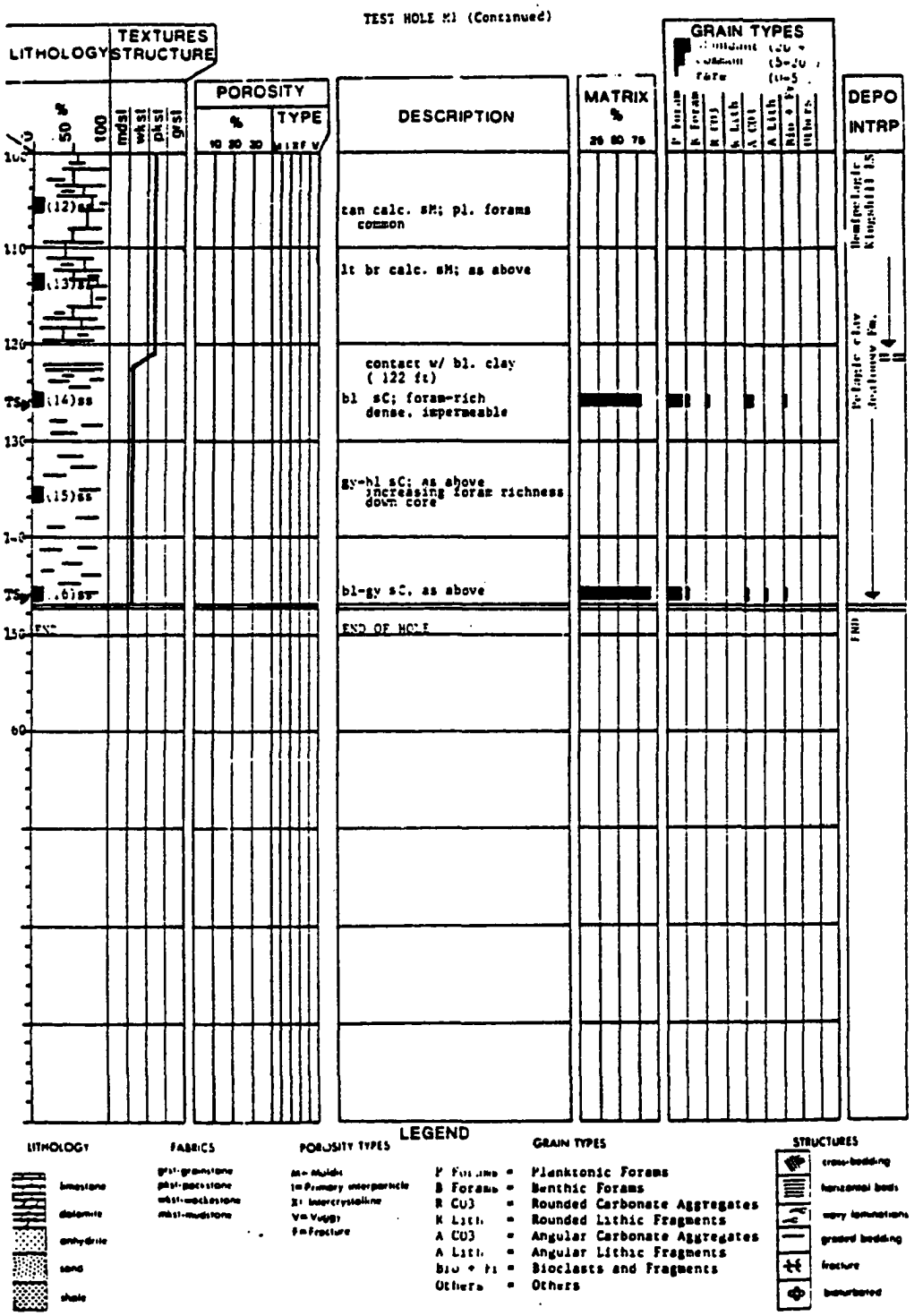

Reproduced with permission of the copyright owner. Further reproduction prohibited without permission.

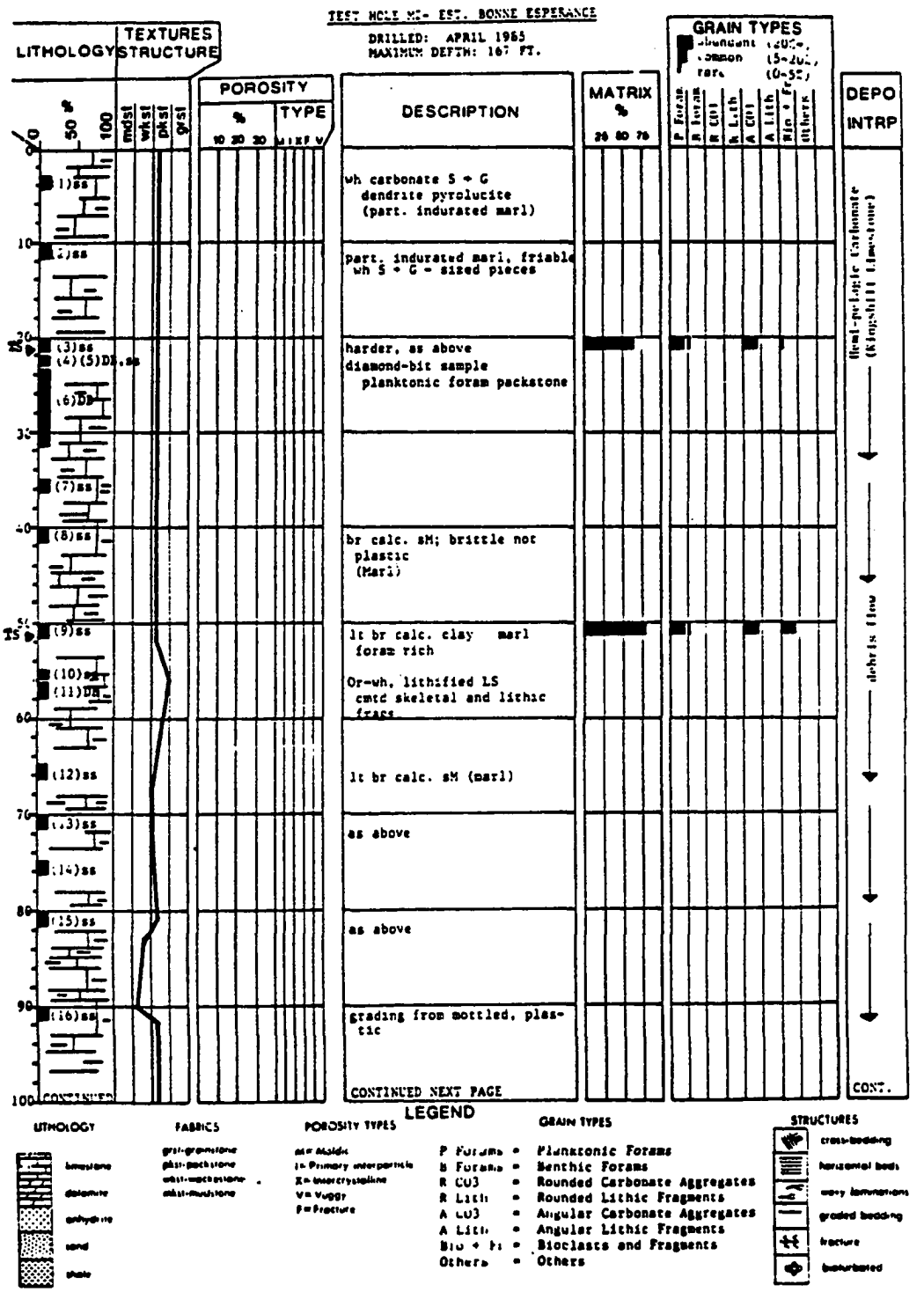

Reproduced with permission of the copyright owner. Further reproduction prohibited without permission.

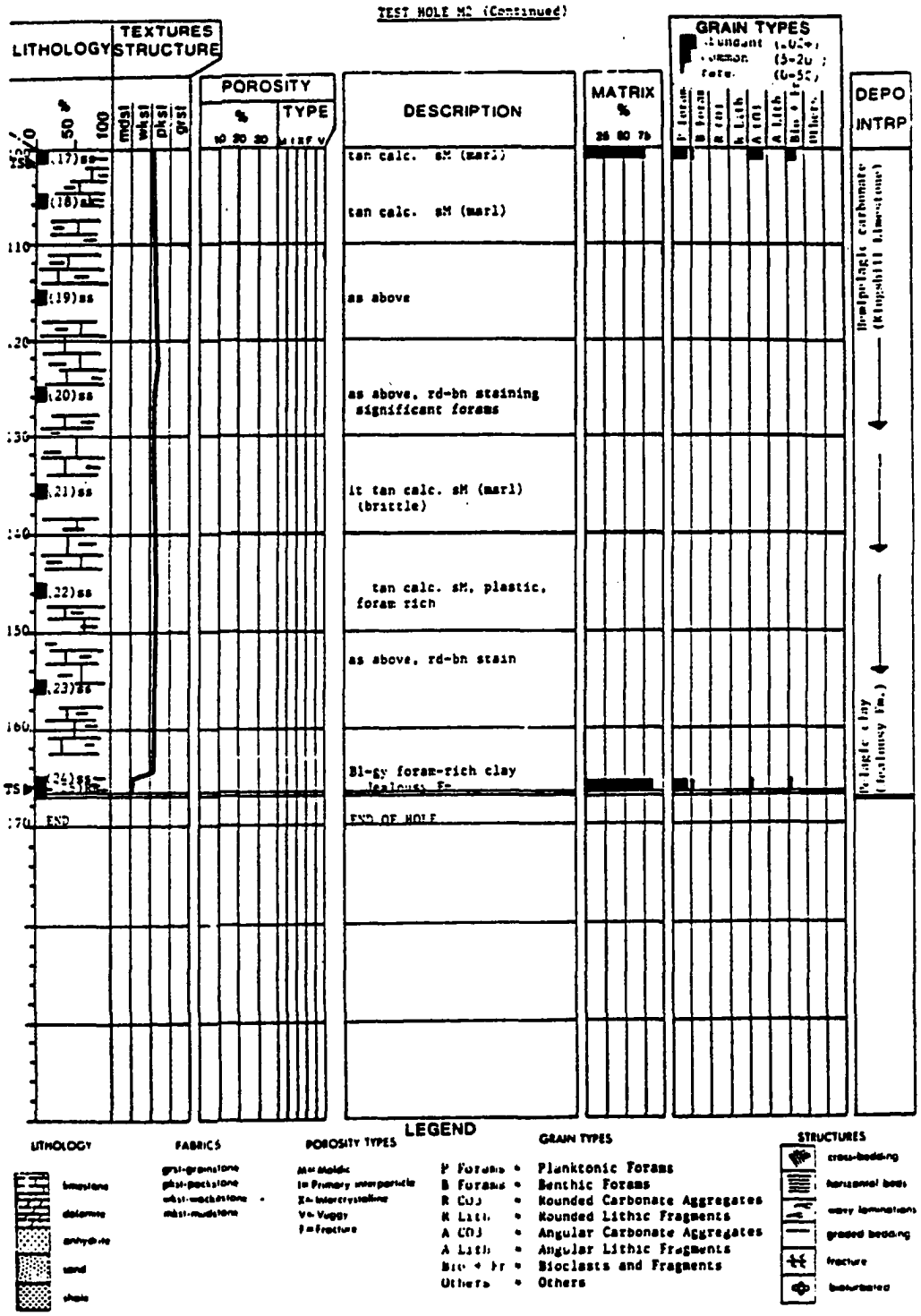

Reproduced with permission of the copyright owner. Further reproduction prohibited without permission.

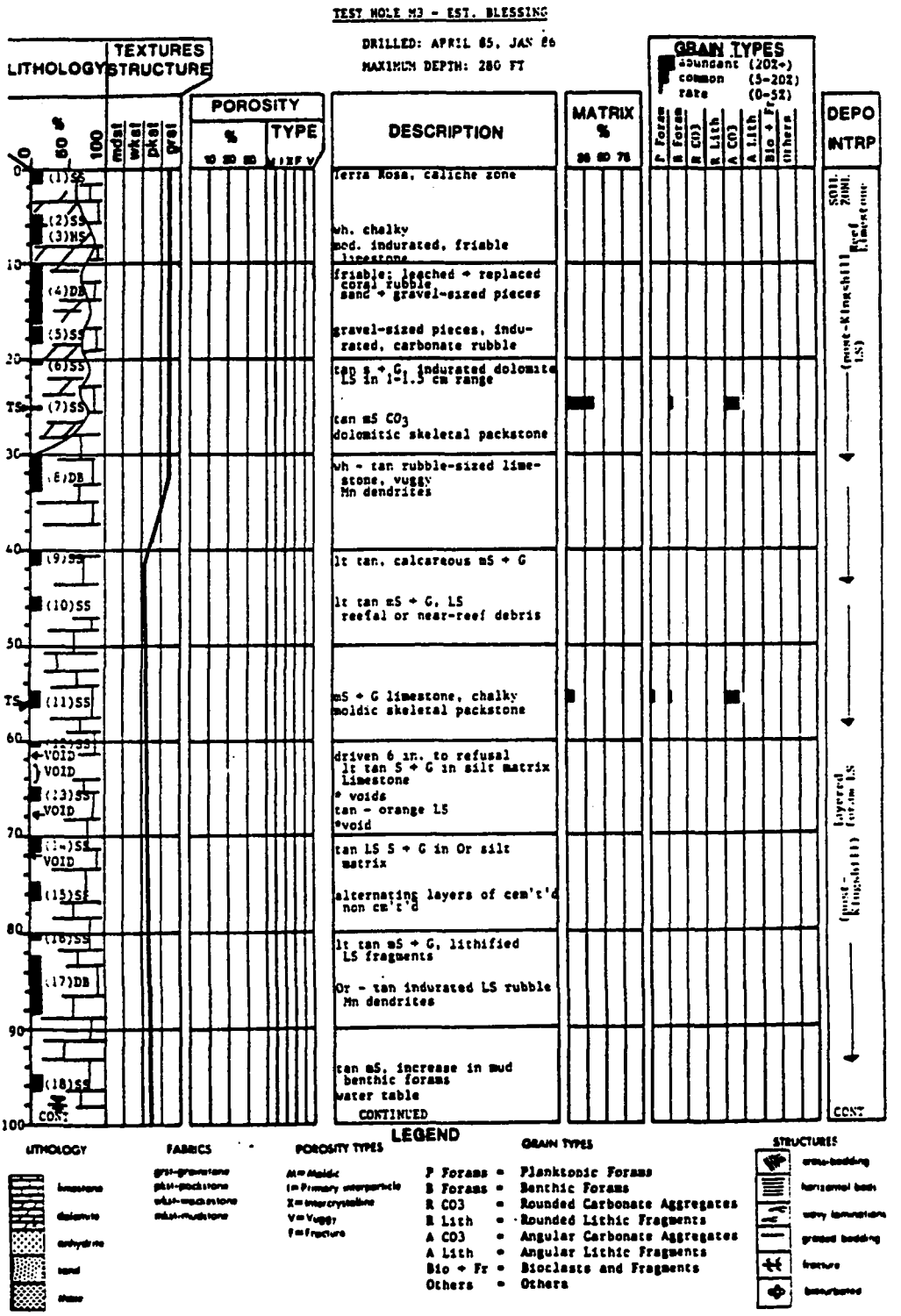

Reproduced with permission of the copyright owner. Further reproduction prohibited without permission.

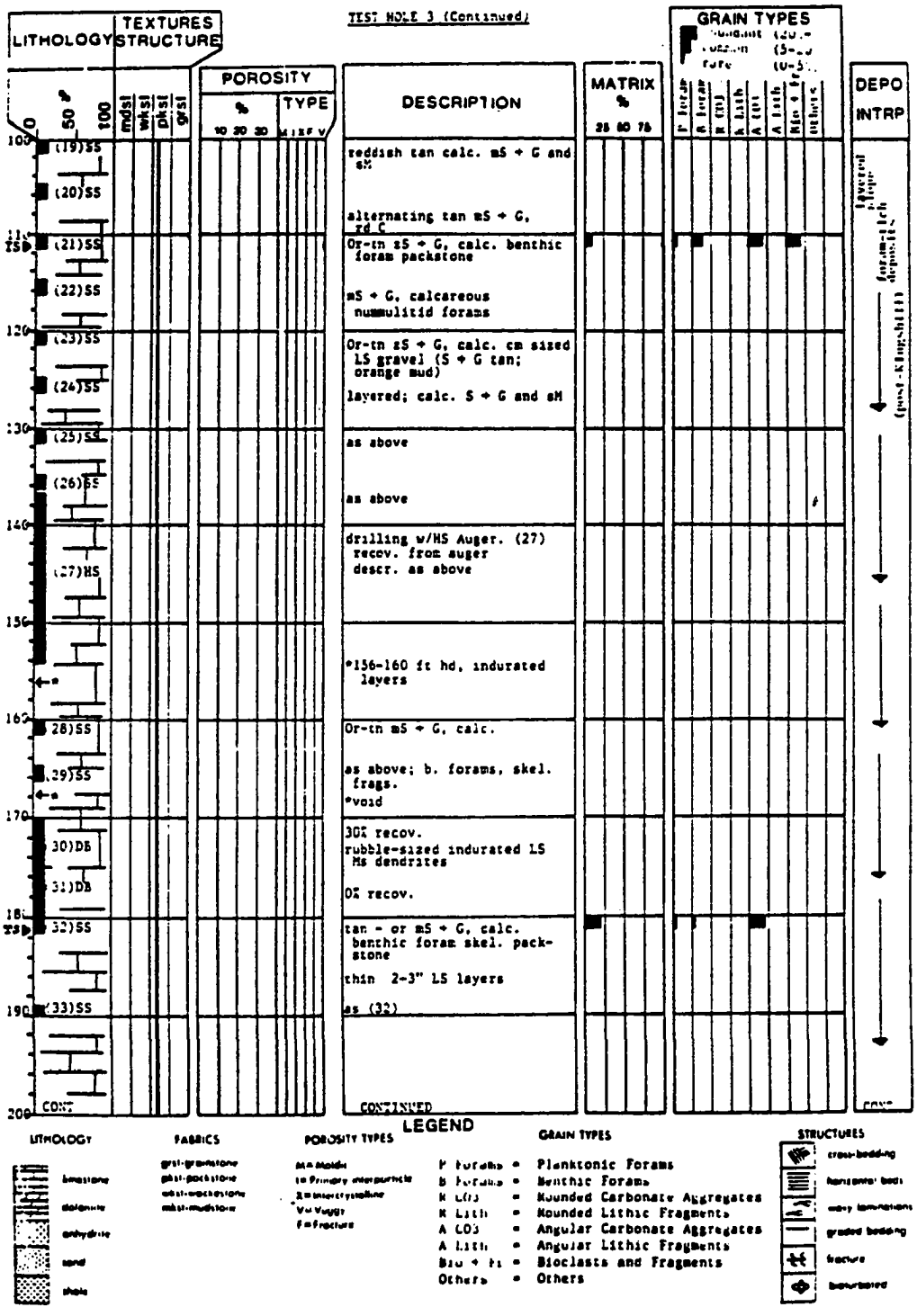

Reproduced with permission of the copyright owner. Further reproduction prohibited without permission.

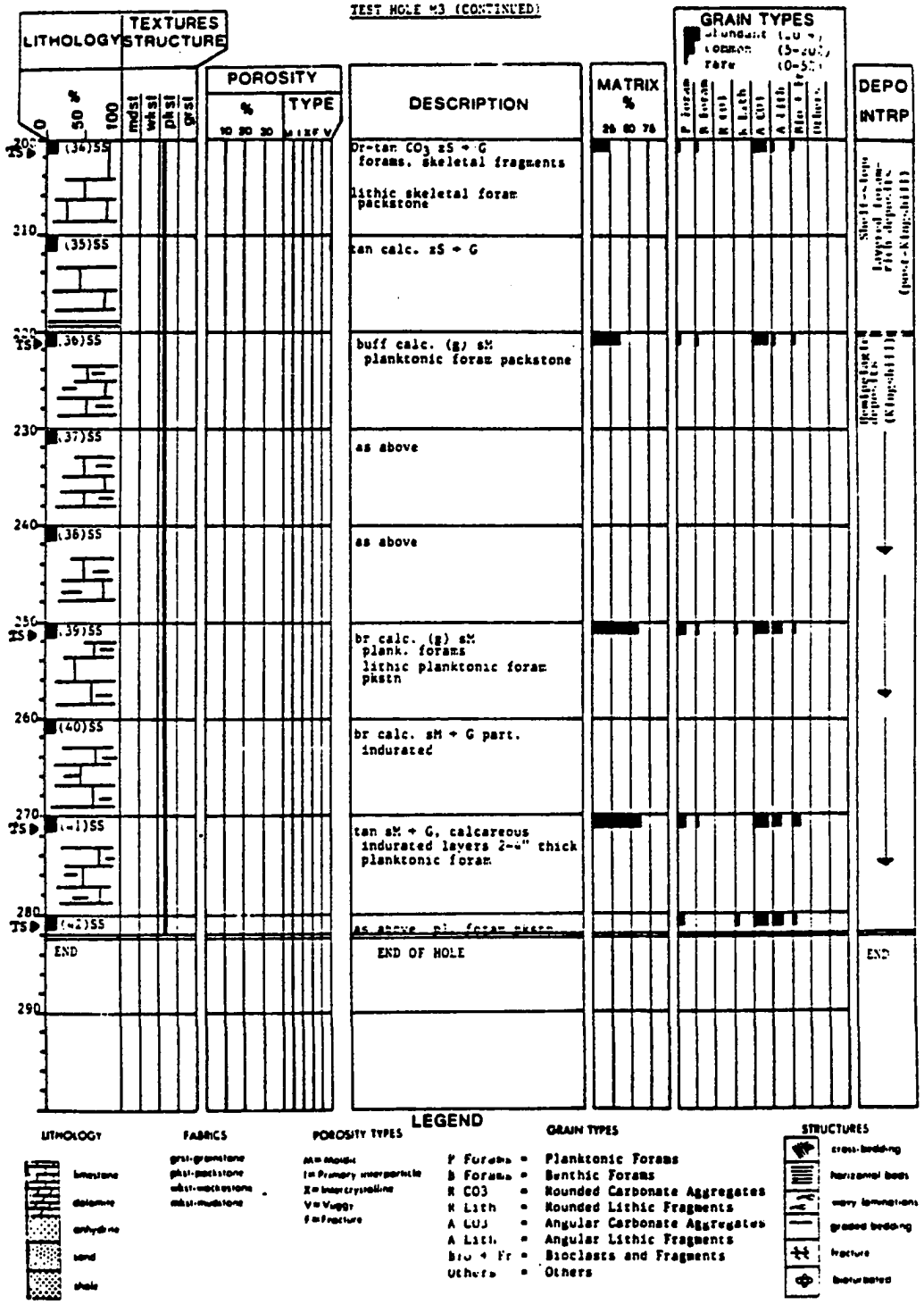

Reproduced with permission of the copyright owner. Further reproduction prohibited without permission.

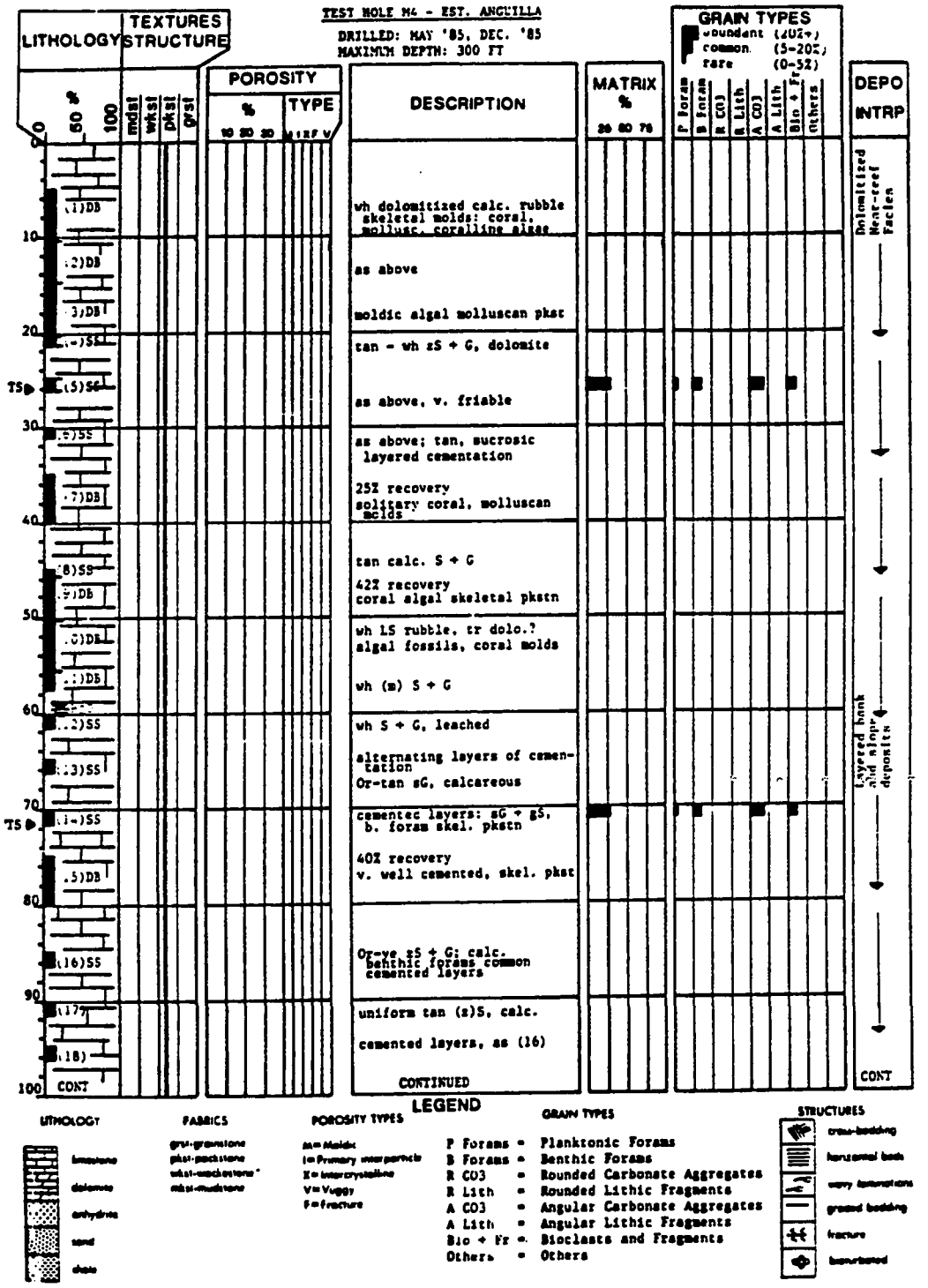

Reproduced with permission of the copyright owner. Further reproduction prohibited without permission.

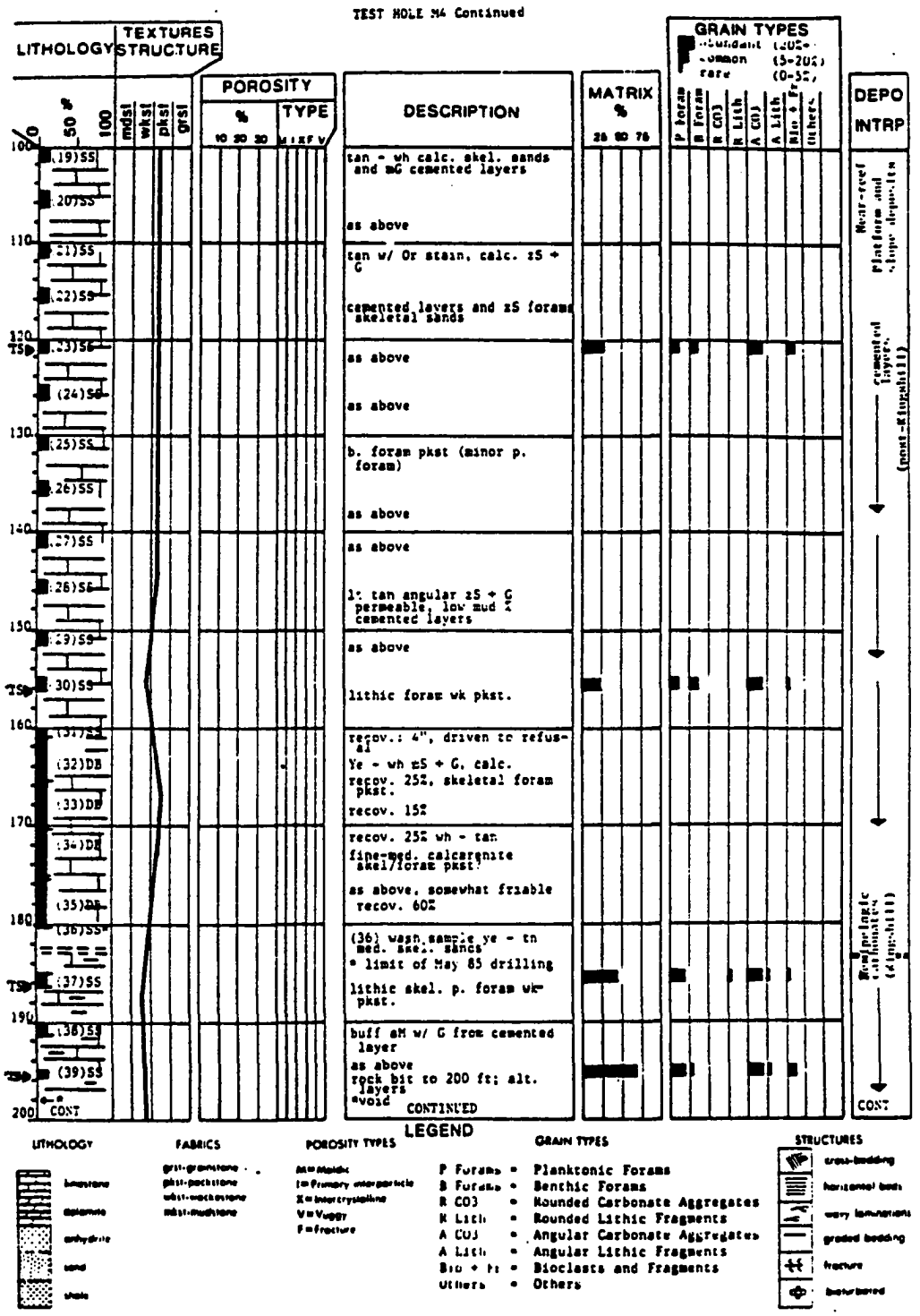

Reproduced with permission of the copyright owner. Further reproduction prohibited without permission.

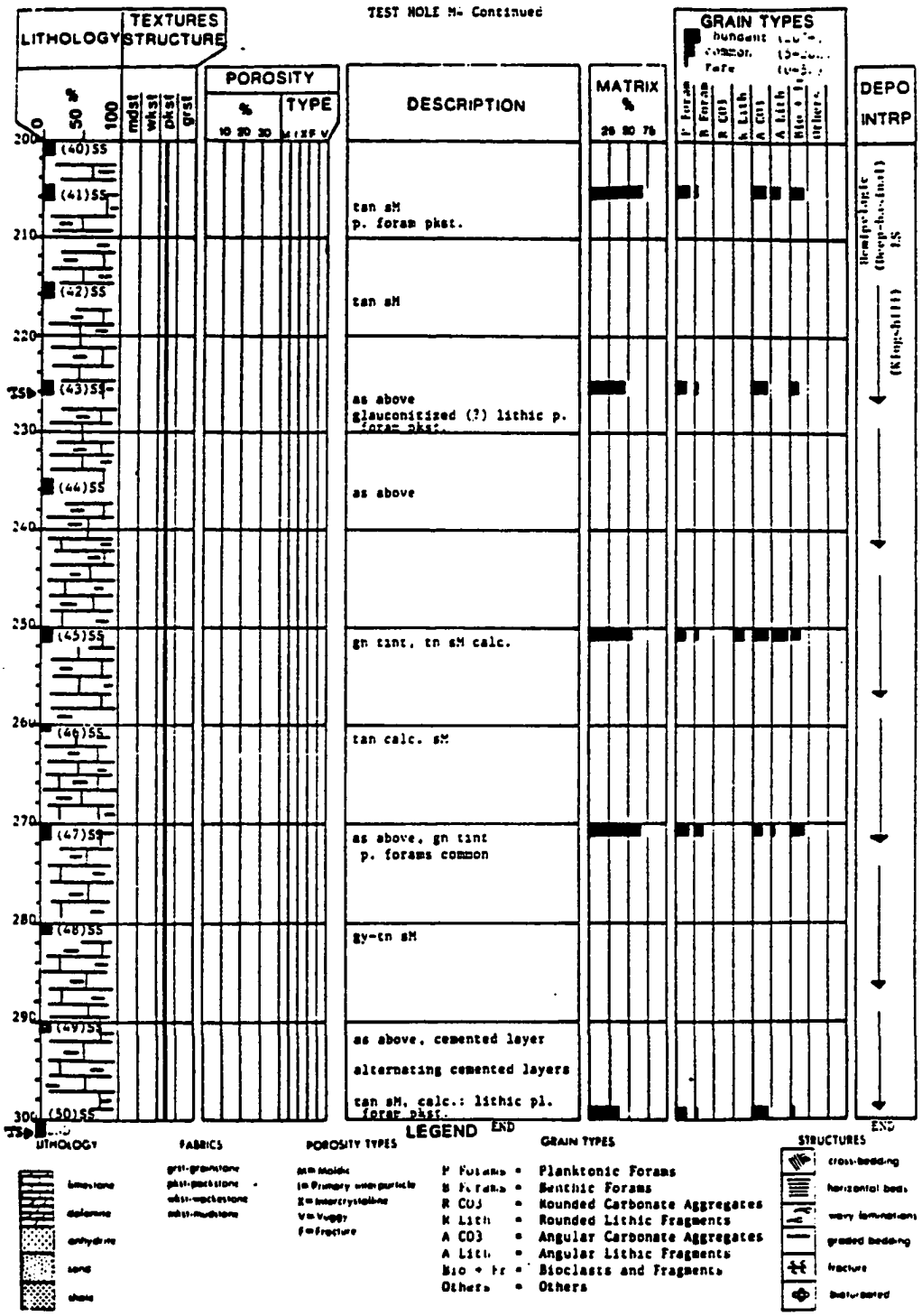

Reproduced with permission of the copyright owner. Further reproduction prohibited without permission.

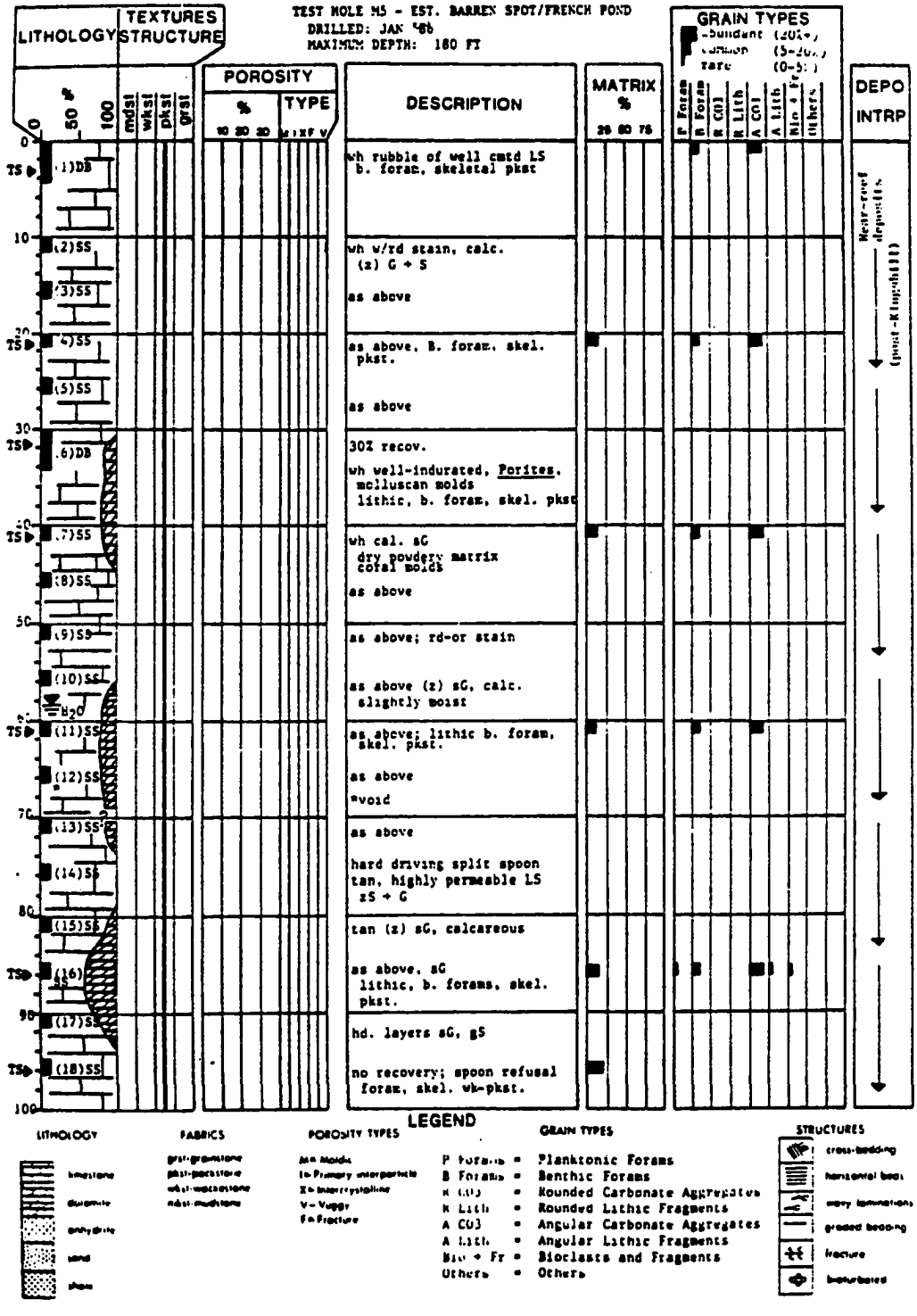

Reproduced with permission of the copyright owner. Further reproduction prohibited without permission.

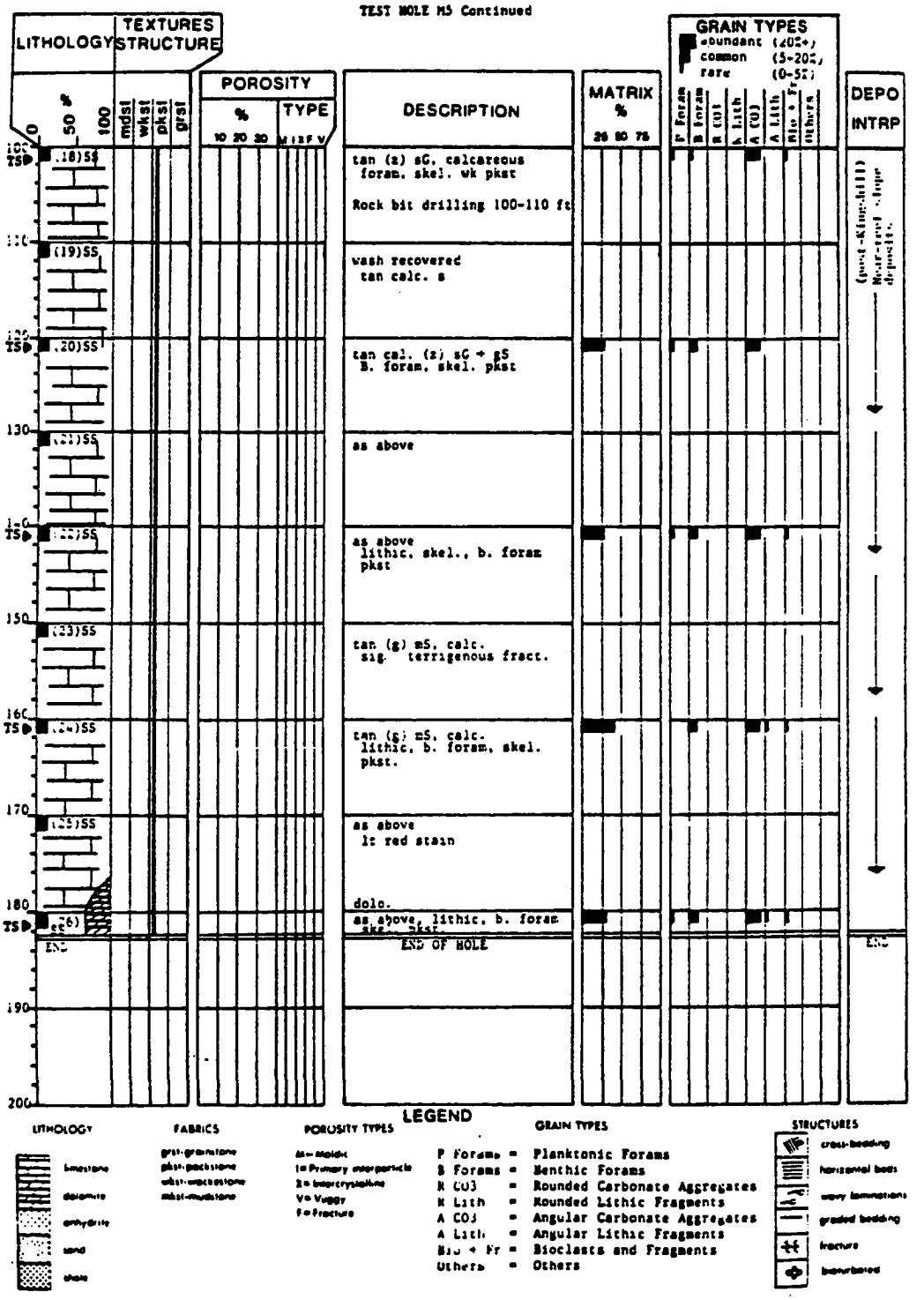

Reproduced with permission of the copyright owner. Further reproduction prohibited without permission.

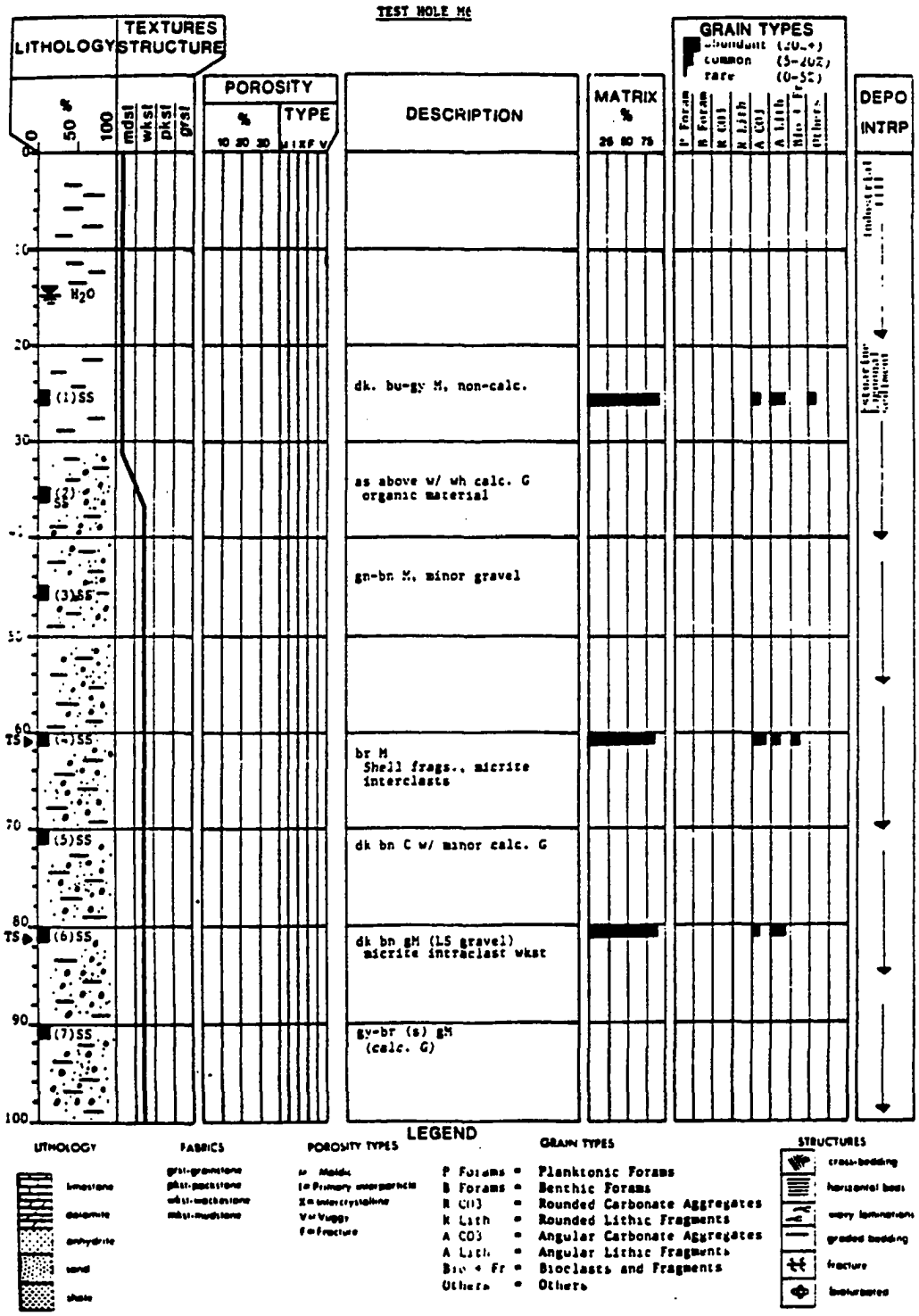

Reproduced with permission of the copyright owner. Further reproduction prohibited without permission.

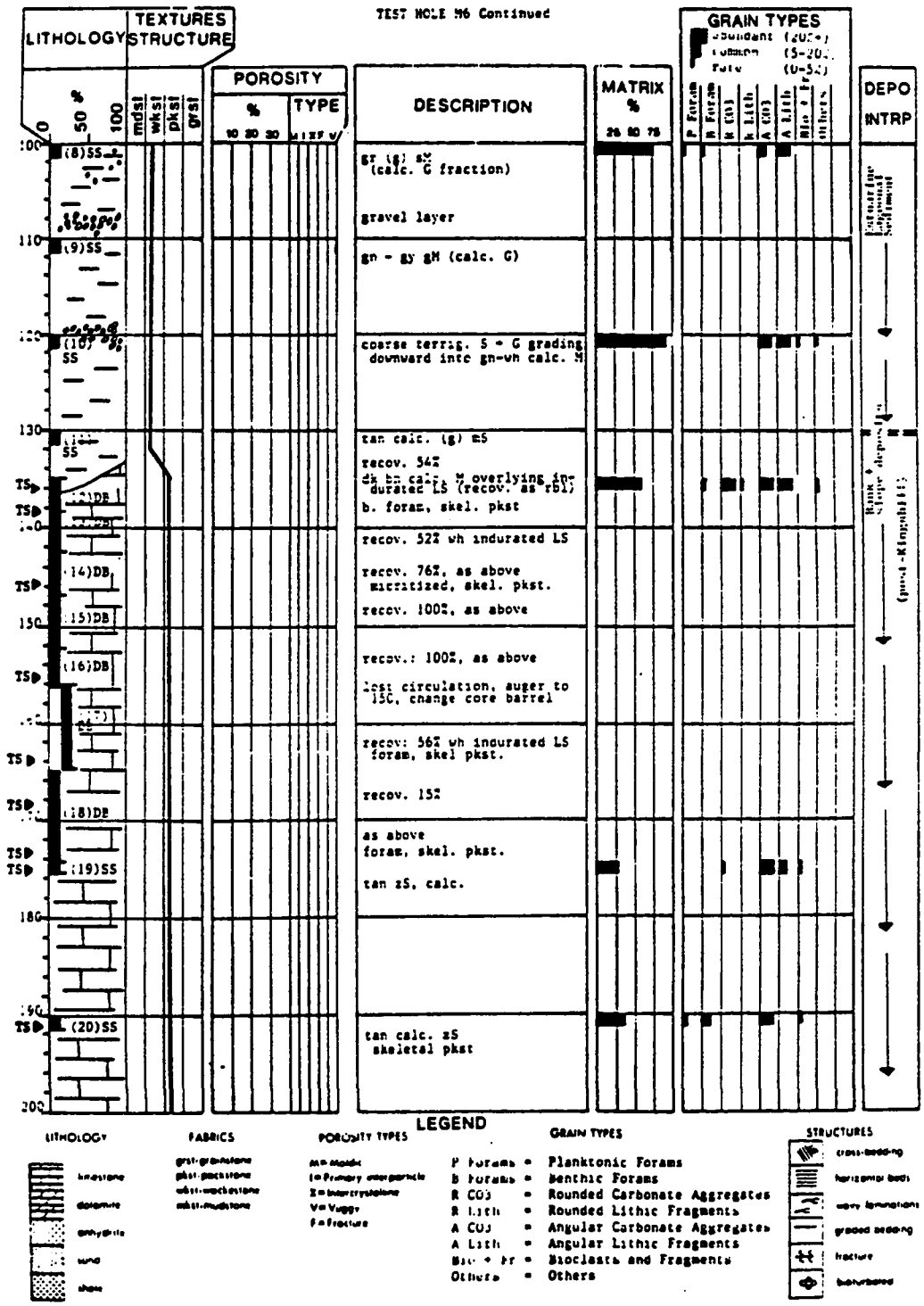

Reproduced with permission of the copyright owner. Further reproduction prohibited without permission.

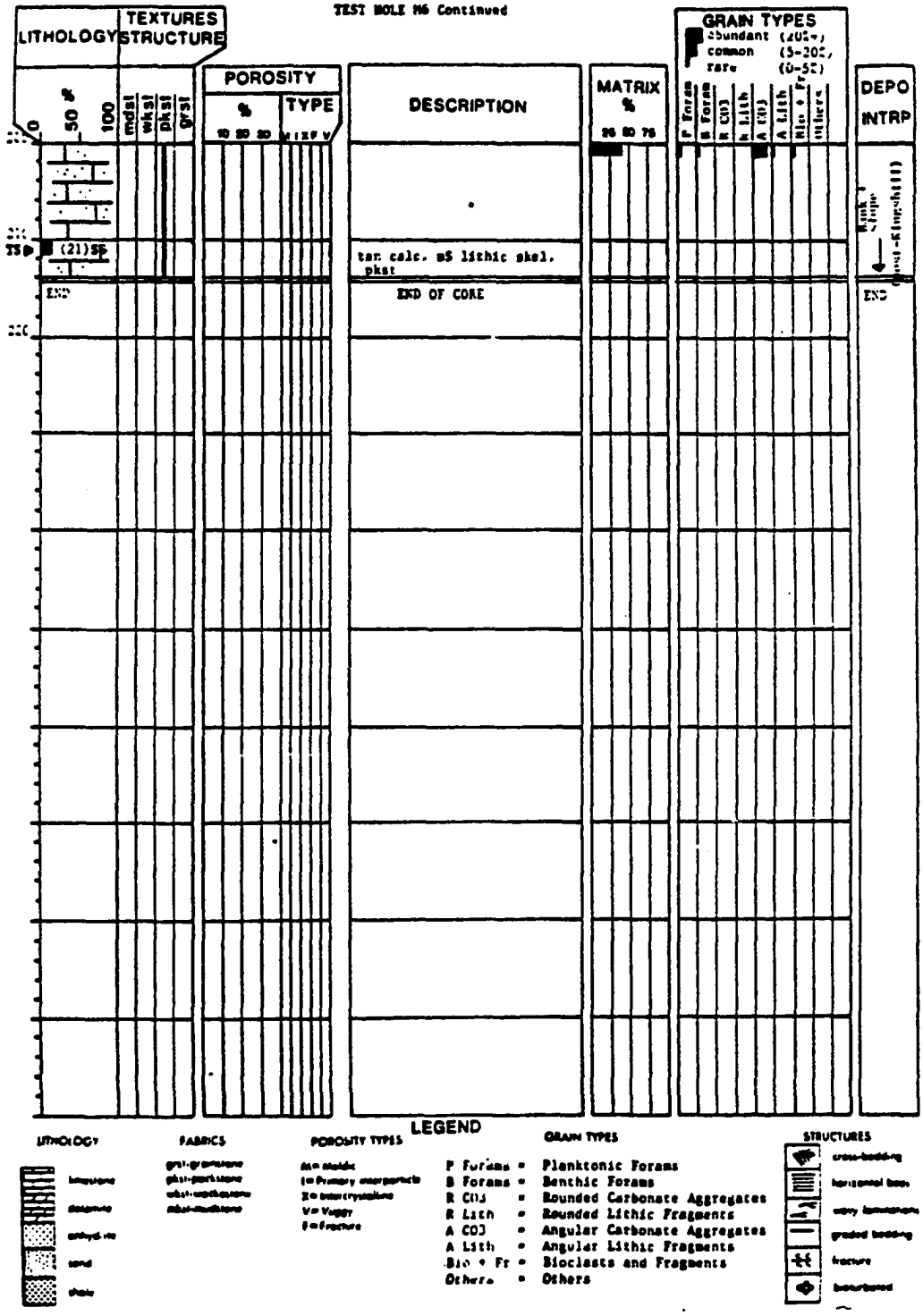

Reproduced with permission of the copyright owner. Further reproduction prohibited without permission.

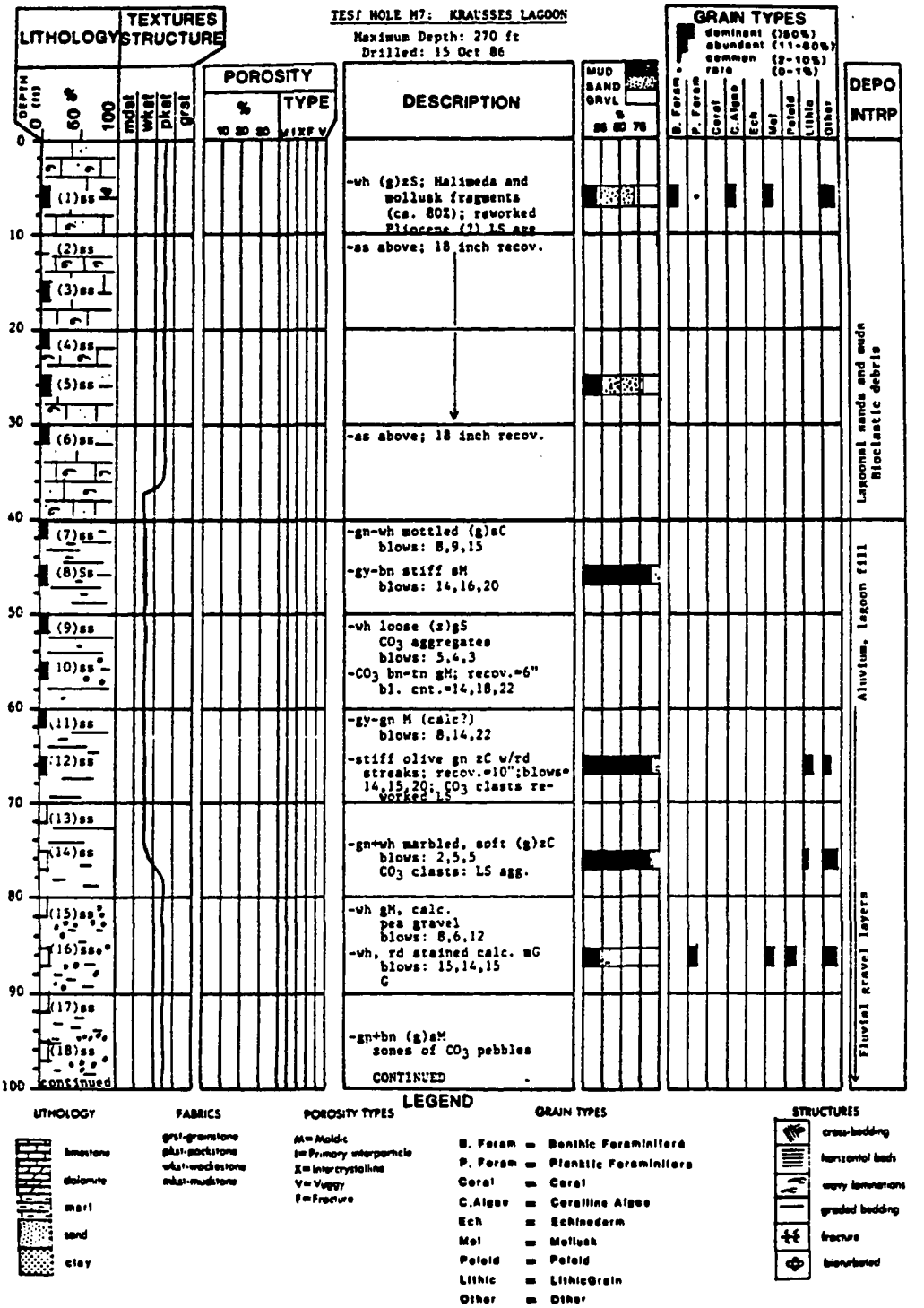

Reproduced with permission of the copyright owner. Further reproduction prohibited without permission.

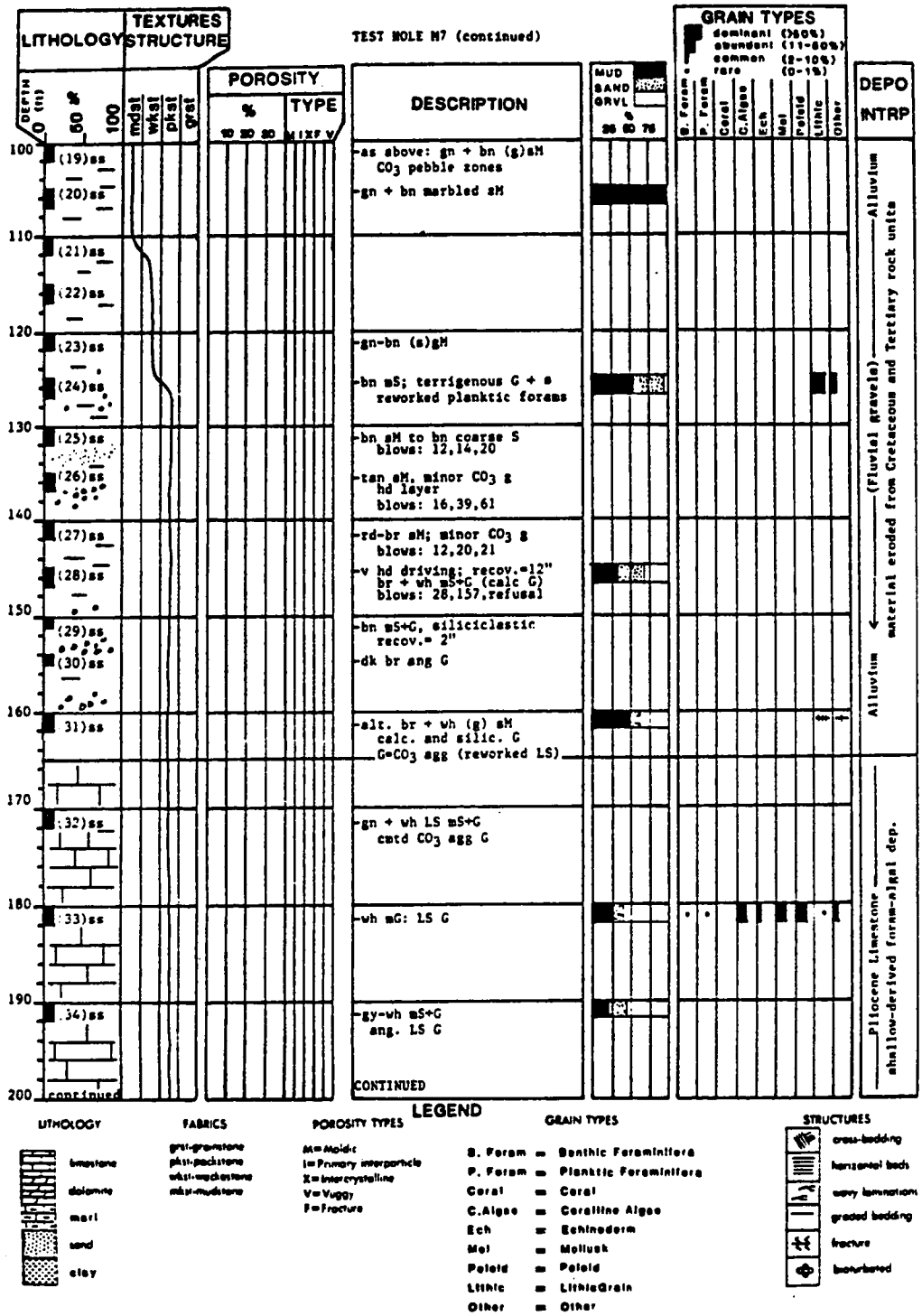

Reproduced with permission of the copyright owner. Further reproduction prohibited without permission.

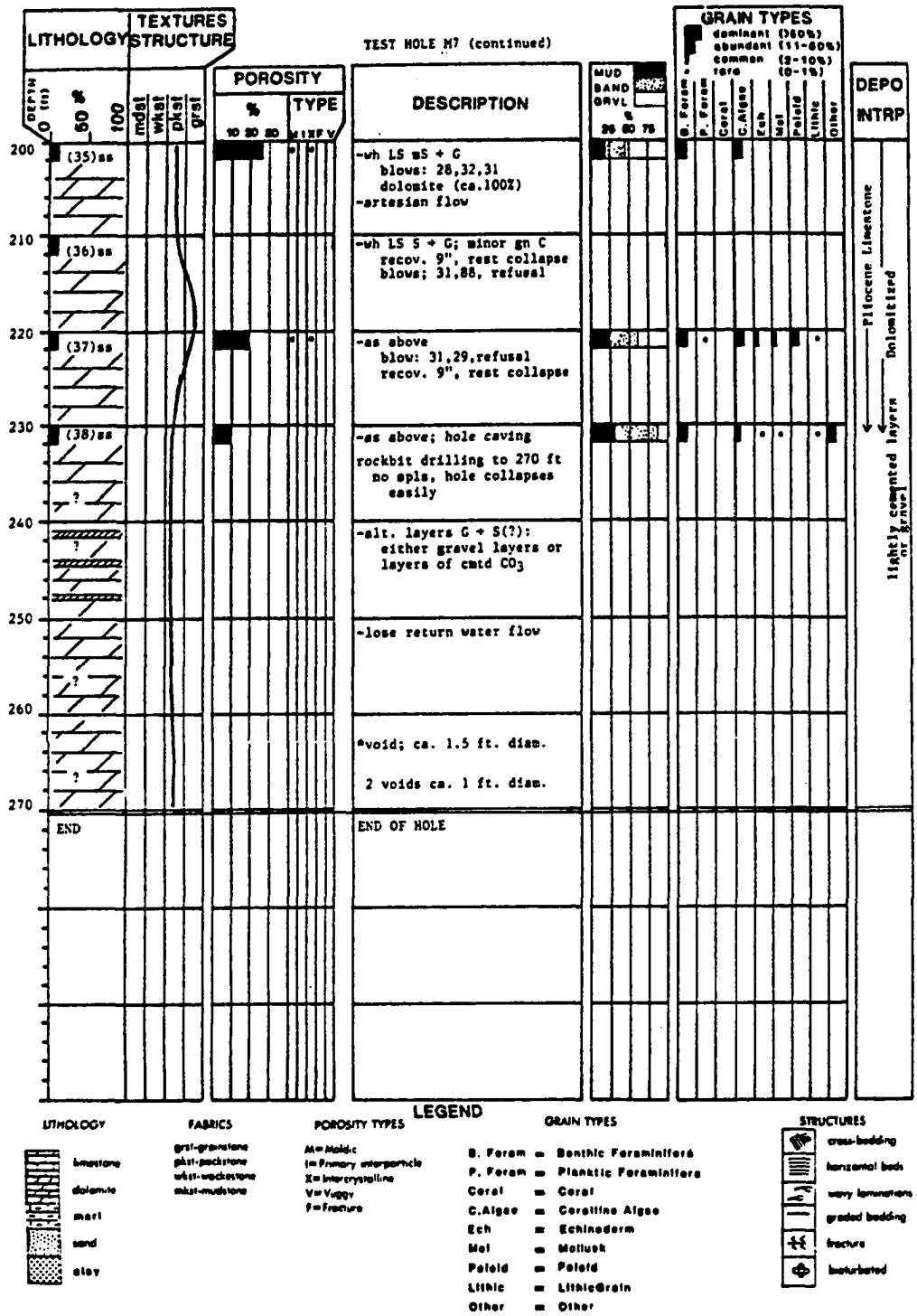

Reproduced with permission of the copyright owner. Further reproduction prohibited without permission.

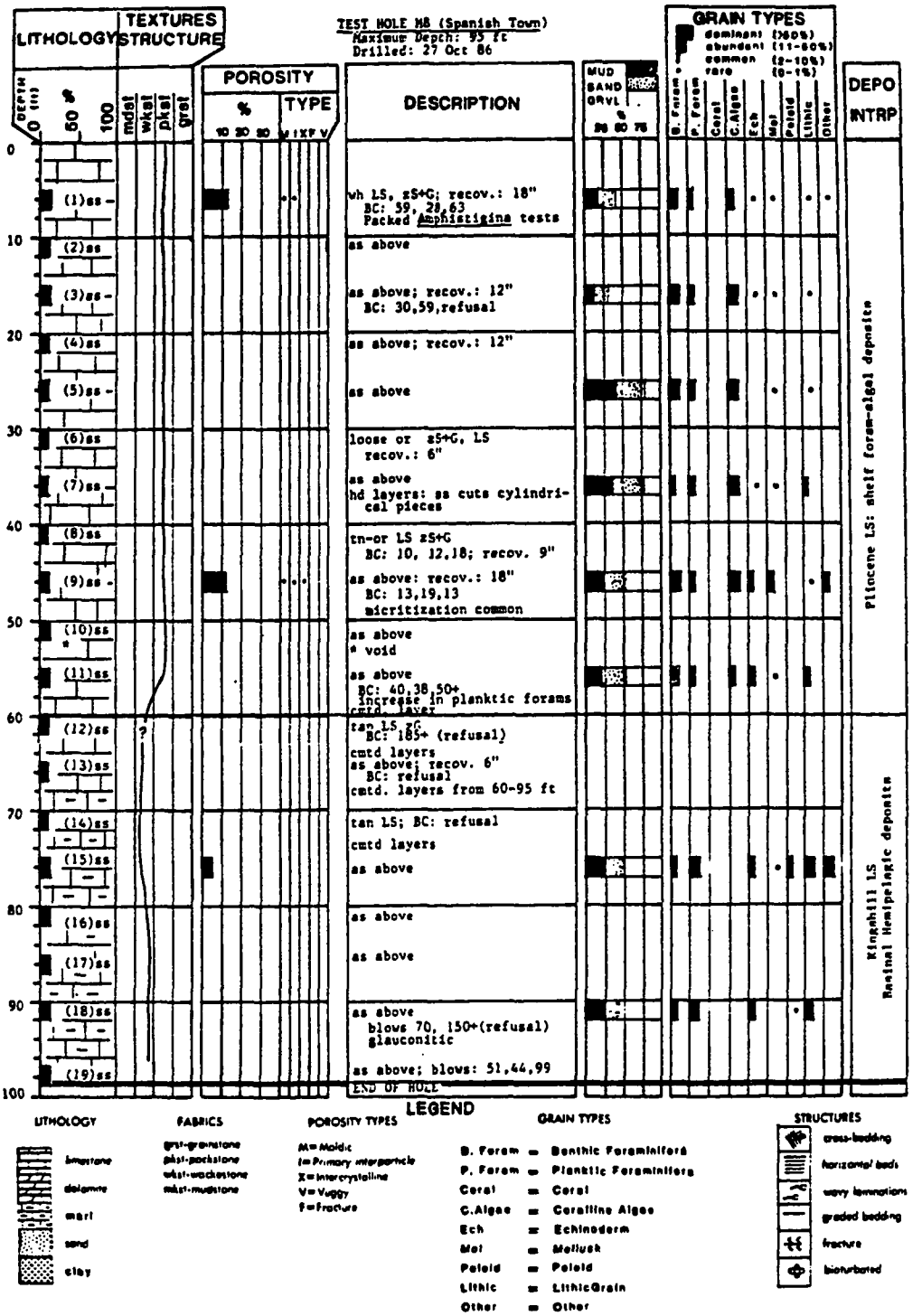

Reproduced with permission of the copyright owner. Further reproduction prohibited without permission.

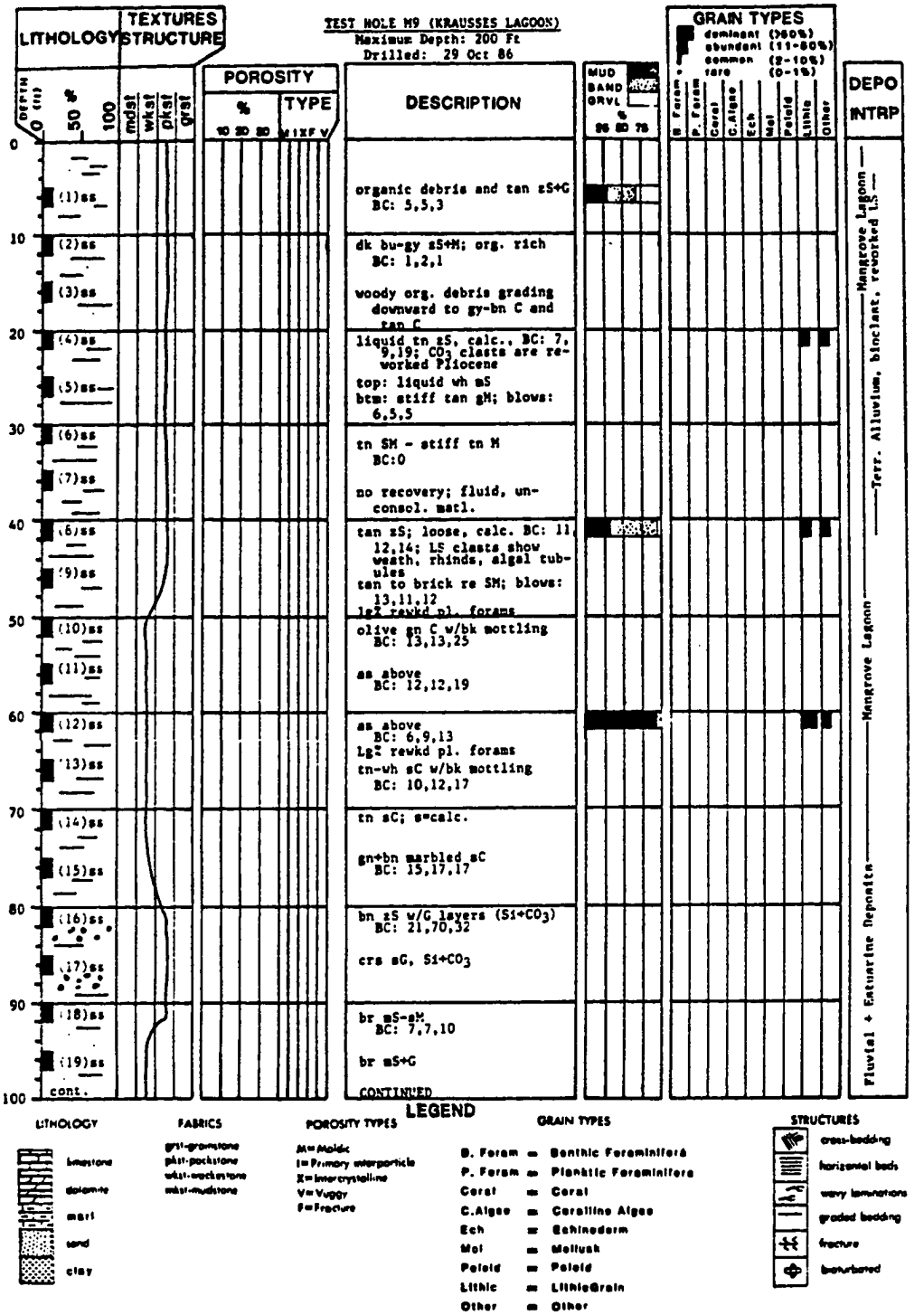

Reproduced with permission of the copyright owner. Further reproduction prohibited without permission.

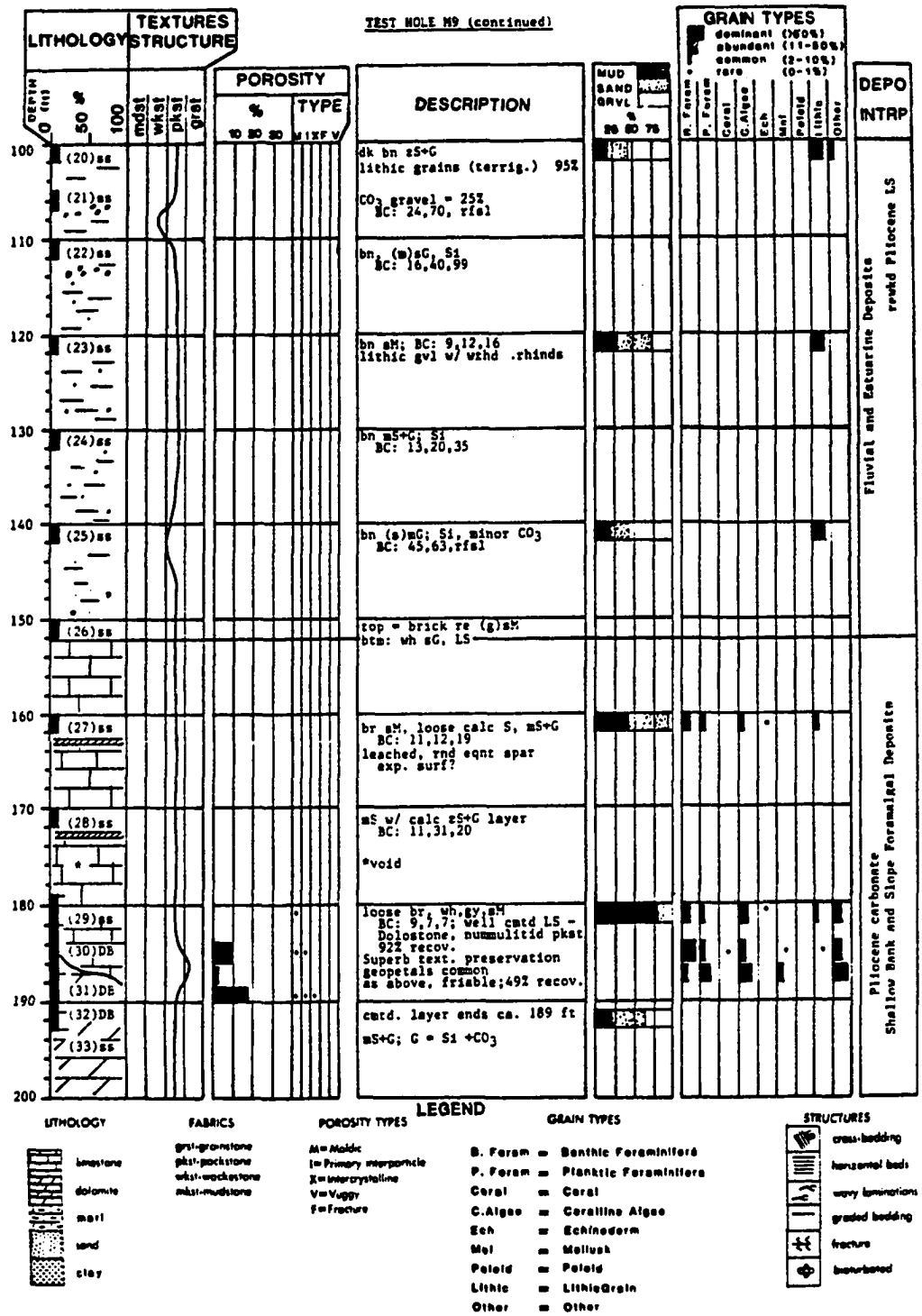

Reproduced with permission of the copyright owner. Further reproduction prohibited without permission.

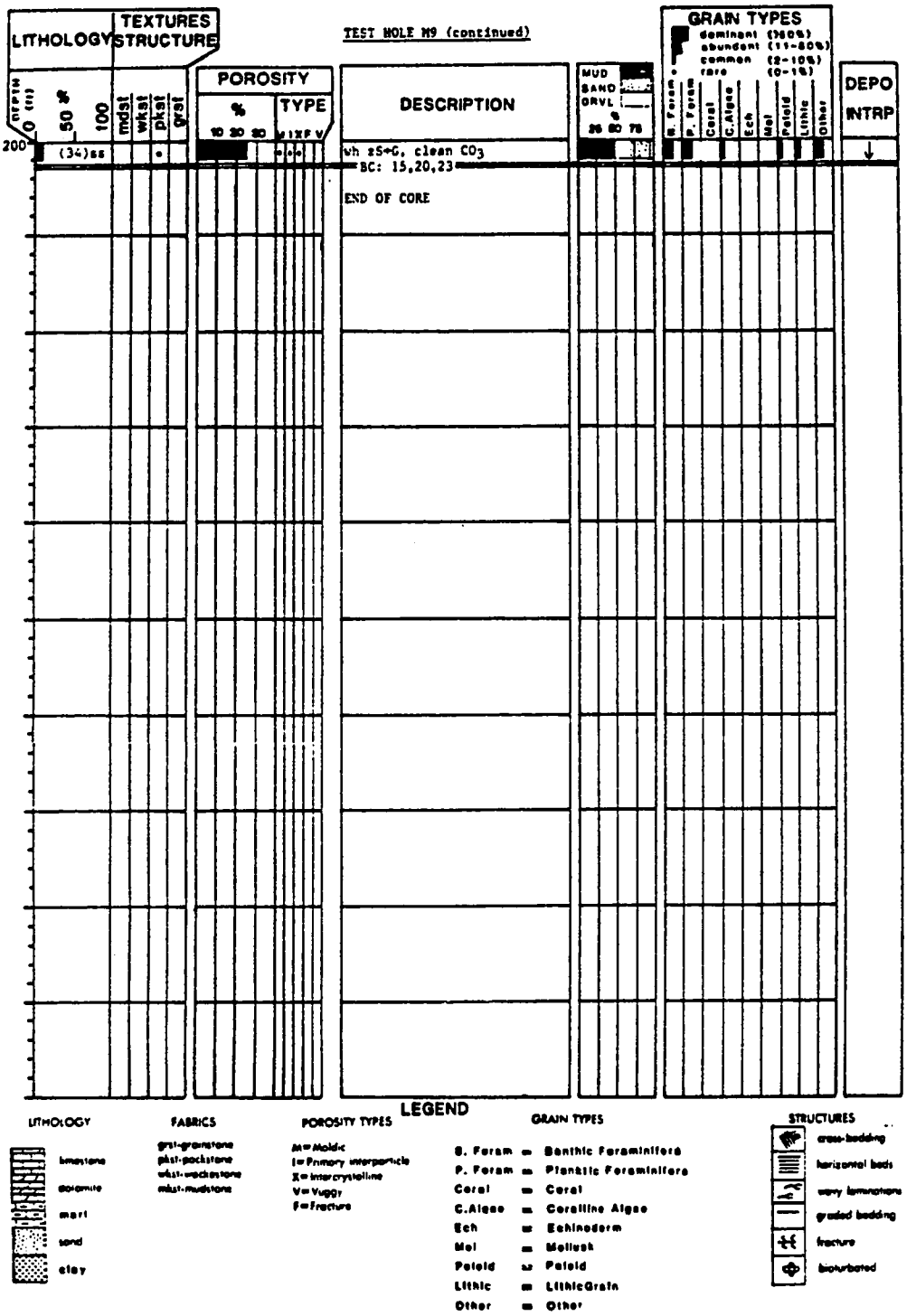

Reproduced with permission of the copyright owner. Further reproduction prohibited without permission.

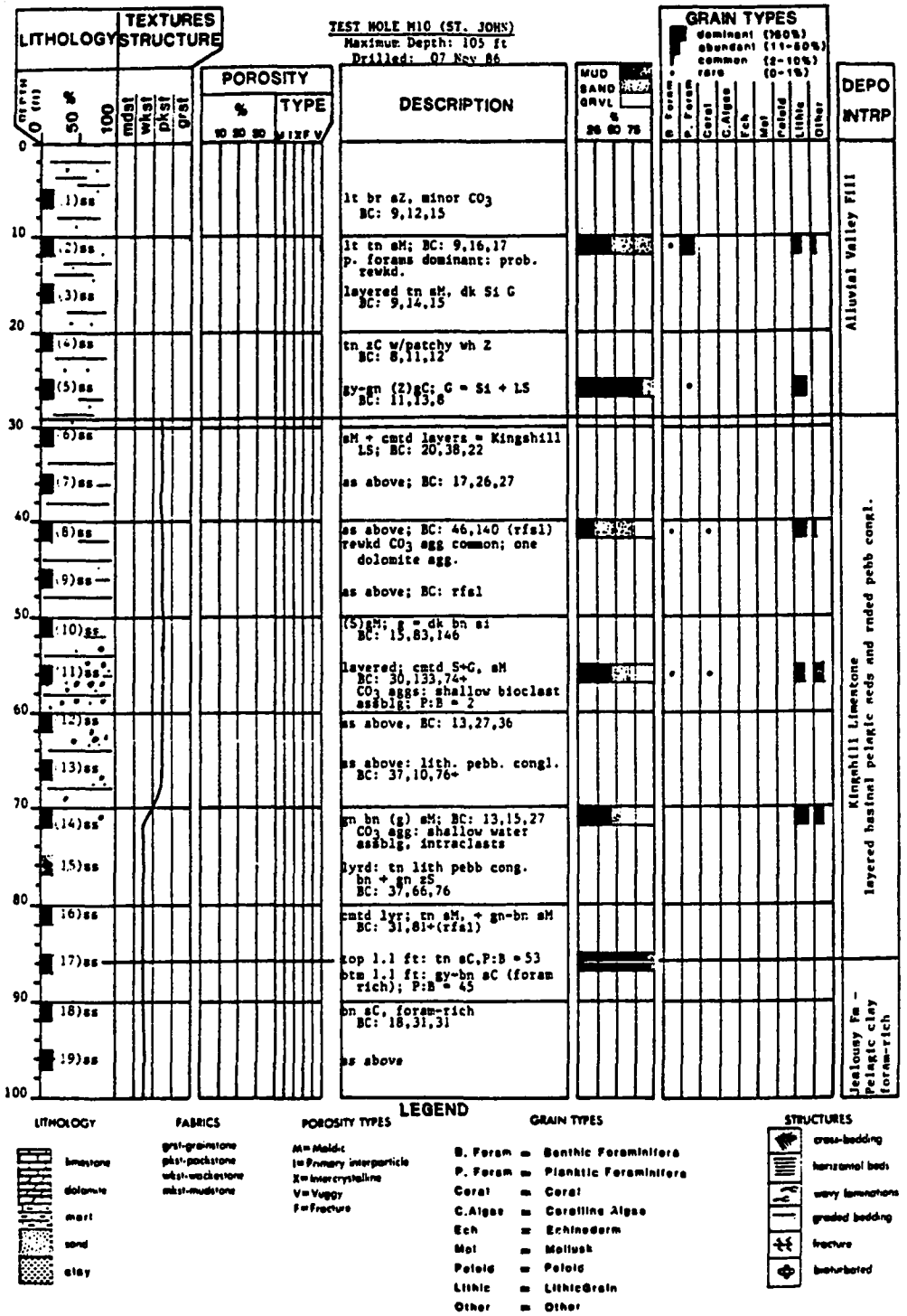

Reproduced with permission of the copyright owner. Further reproduction prohibited without permission.

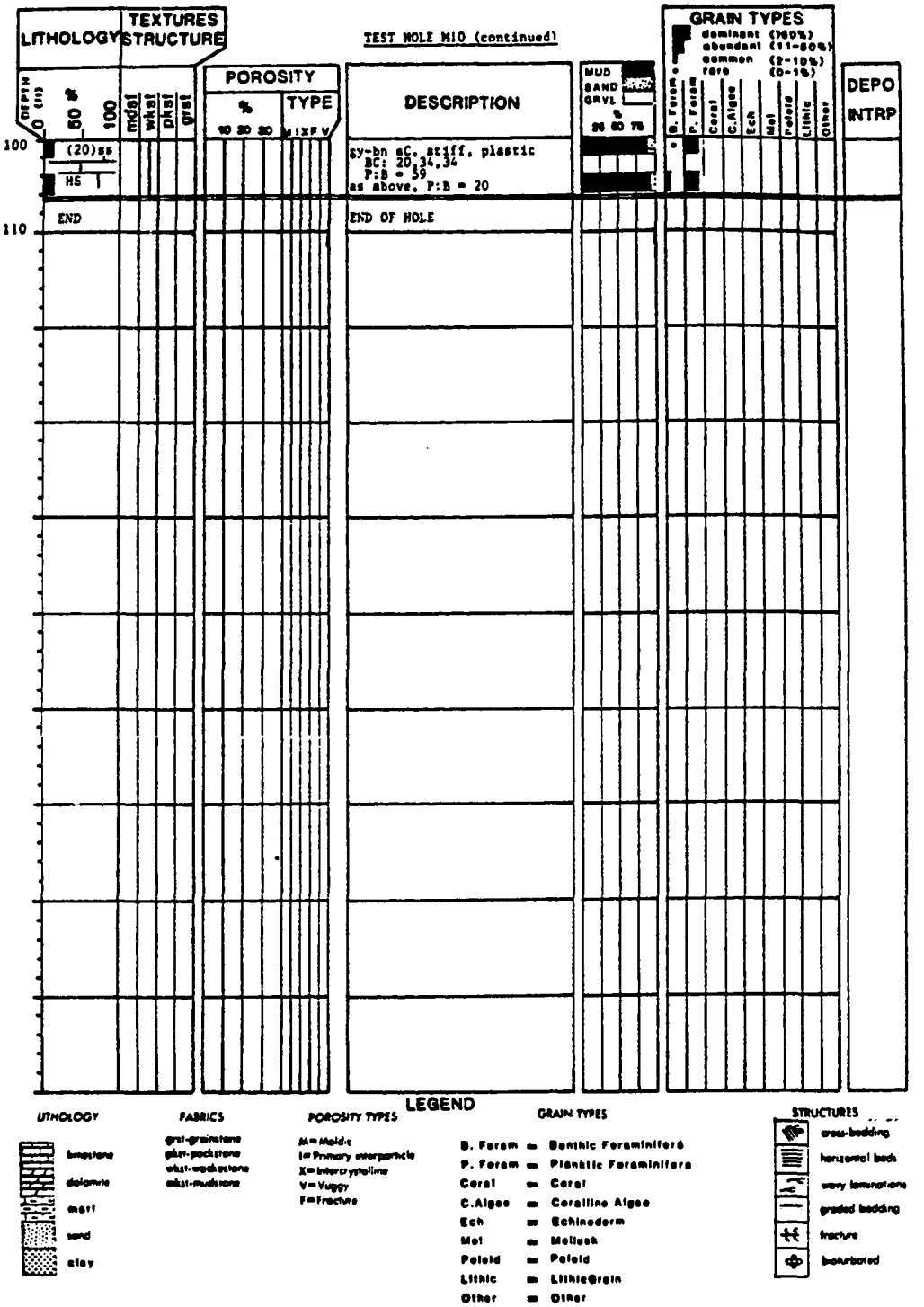

Reproduced with permission of the copyright owner. Further reproduction prohibited without permission.

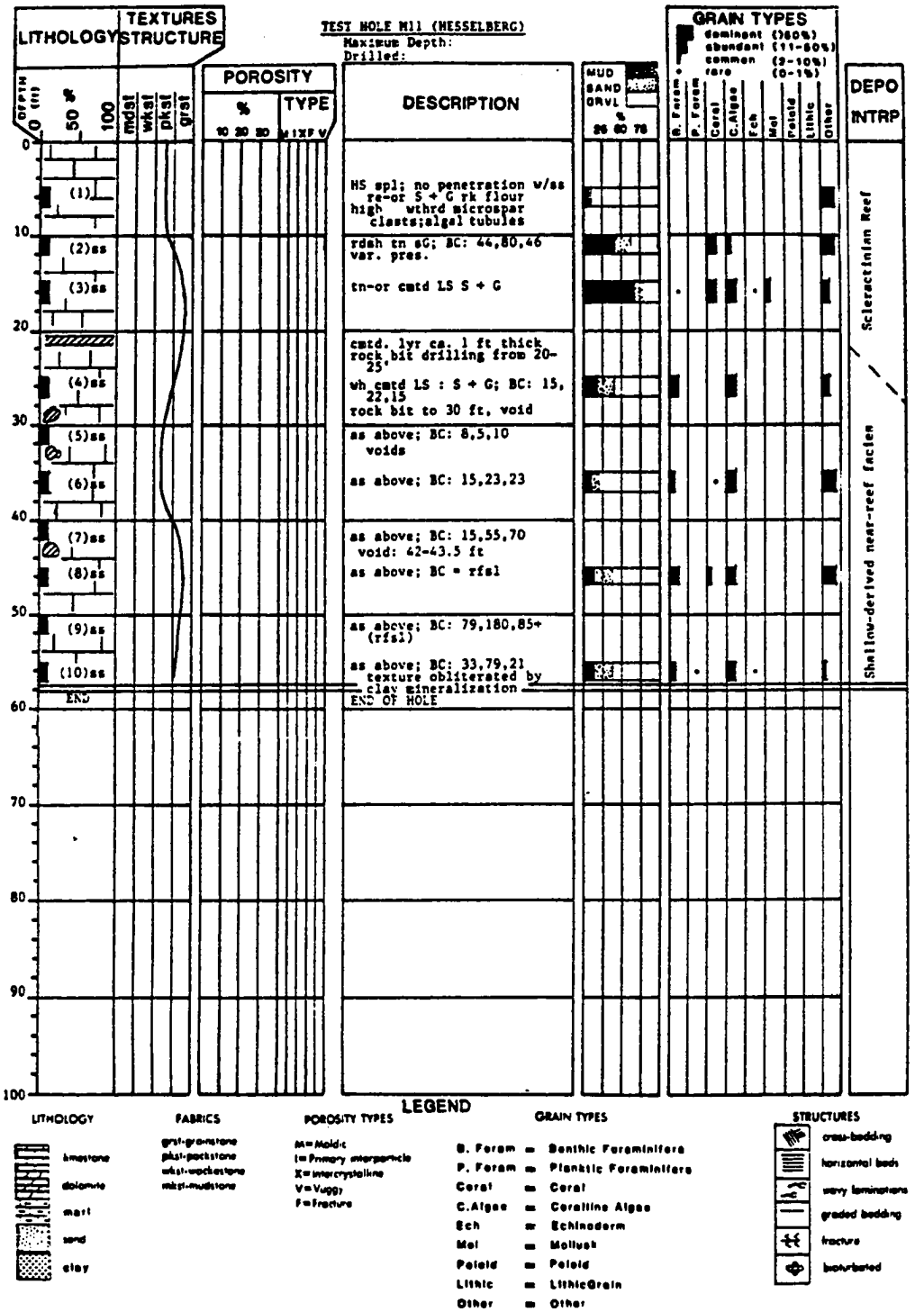

Reproduced with permission of the copyright owner. Further reproduction prohibited without permission.

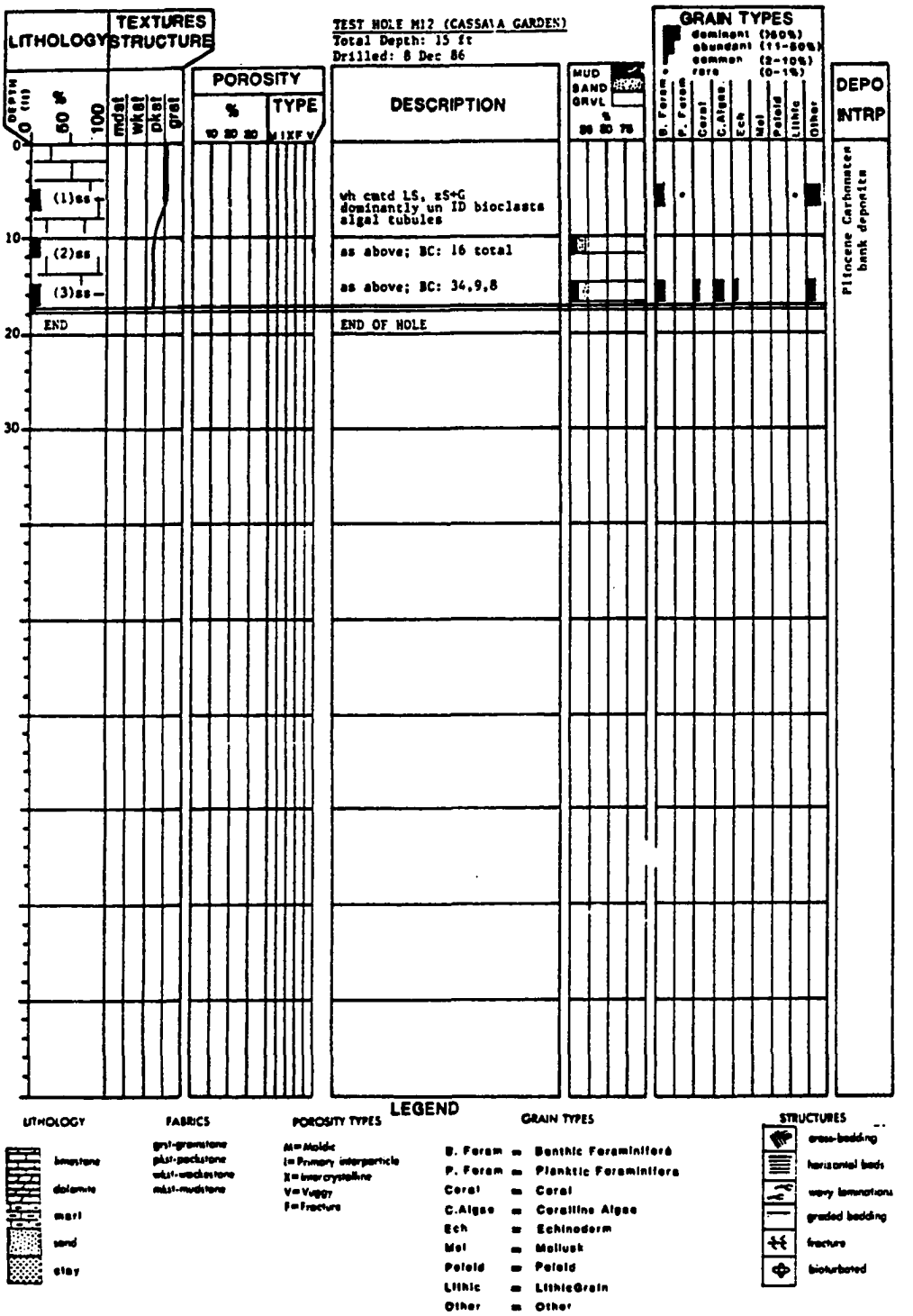

Reproduced with permission of the copyright owner. Further reproduction prohibited without permission.

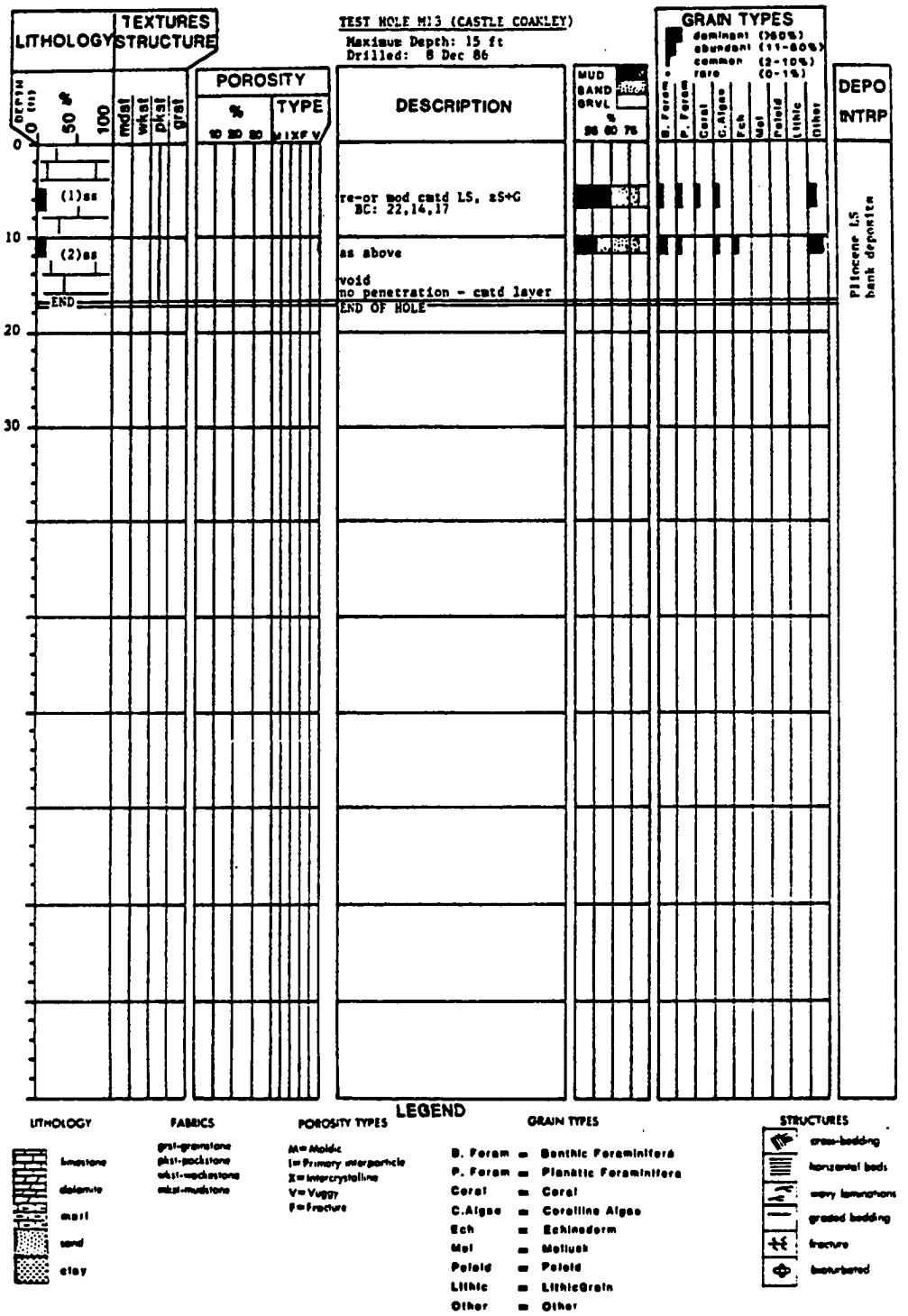

Reproduced with permission of the copyright owner. Further reproduction prohibited without permission.

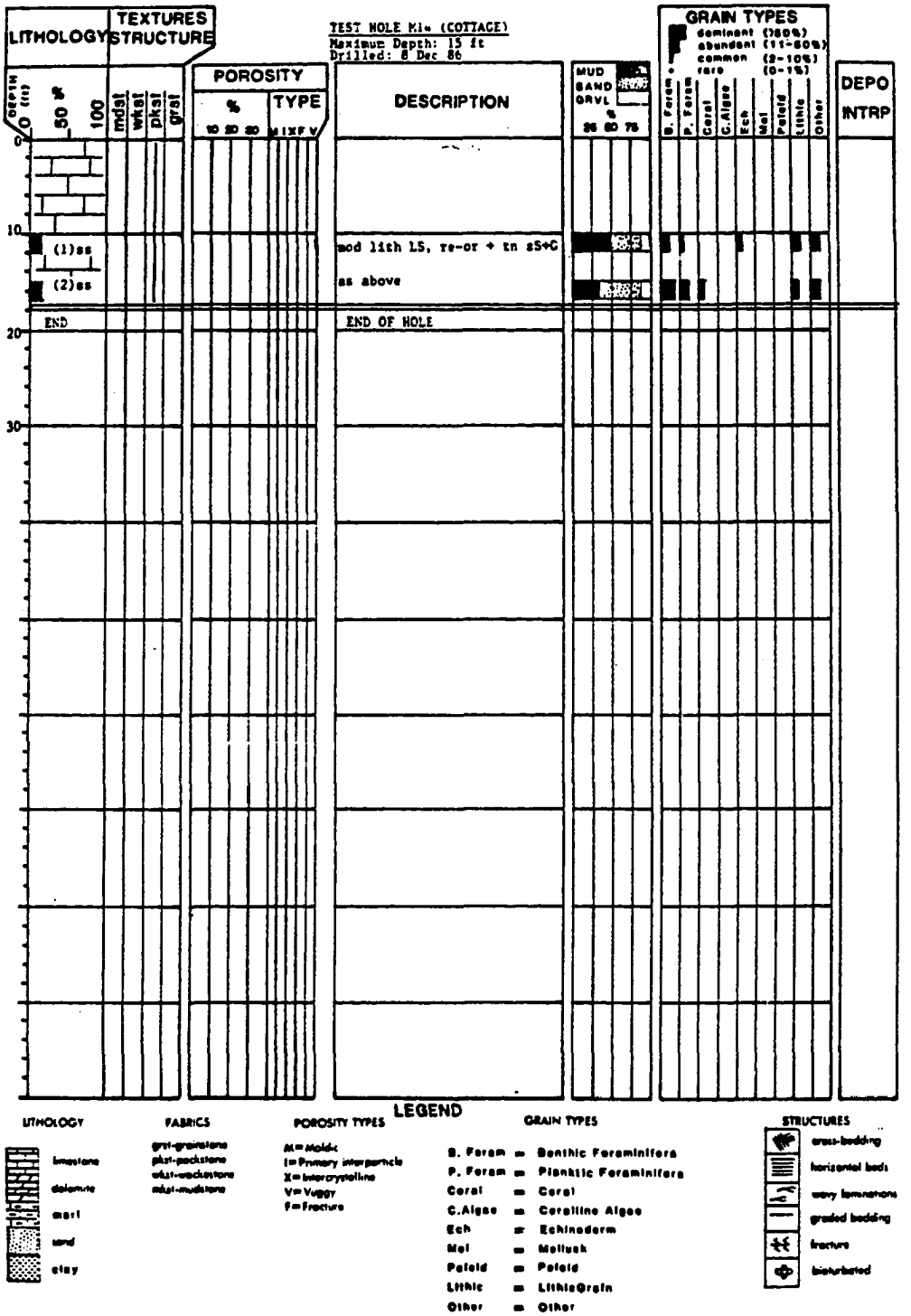

Reproduced with permission of the copyright owner. Further reproduction prohibited without permission.

VITA

Ivan P. Gill was born in Honolulu, in what was then the Territory of Hawaii on November 18, 1956. He attended the public schools in Honolulu, and graduated from University Laboratory School in 1974. Ivan received his bachelors degree in Geology from the University of Rochester in 1979, and his M. S. from the same institution in 1983. His masters thesis dealt with the transport and preservation of organic carbon and carbonate sediment in the Virgin Islands Basin. Field work involved the DSRV *Alvin*, and was partially supported by an assistantship at the West Indies Laboratory on St. Croix.

Ivan began work on a doctorate in Geology at Louisiana State University in September, 1982, and was married to Shelley Choy of Honolulu in December of the same year. Ivan and Shelley live in New Orleans, Louisiana, where Ivan teaches in the Geology Department of Tulane University.

Reproduced with permission of the copyright owner. Further reproduction prohibited without permission.

DOCTORAL EXAMINATION AND DISSERTATION REPORT

Candidate: IVAN P. GILL

Major Field: GEOLOGY

Title of Dissertation: THE EVOLUTION OF TERTIARY ST. CROIX

Approved:

Major Professor and Chairman

Dean of the Graduate School

EXAMINING COMMITTEE:

Date of Examination:

MAY 3, 1989

Reproduced with permission of the copyright owner. Further reproduction prohibited without permission.